R-99-14

Analysis of radionuclide migration from SFL 3-5

Michael Pettersson, Kristina Skagius
Kemakta Konsult AB

Luis Moreno
Department of Chemical Engineering and Technology,
Royal Institute of Technology

December 1999

Svensk Kärnbränslehantering AB
Swedish Nuclear Fuel
and Waste Management Co
Box 5864
SE-102 40 Stockholm Sweden
Tel 08-459 84 00
+46 8 459 84 00
Fax 08-661 57 19
+46 8 661 57 19

ISSN 1402-3091
SKB Report R-99-14

Analysis of radionuclide migration from SFL 3-5

Michael Pettersson, Kristina Skagius
Kemakta Konsult AB

Luis Moreno
Department of Chemical Engineering and Technology,
Royal Institute of Technology

December 1999

Keywords: safety assessment, deep repository, LILW, modelling, radionuclide migration.

Abstract

A preliminary safety assessment has been performed of a deep repository for long-lived low- and intermediate-level waste, SFL 3-5. The main objectives of the assessment is to evaluate the capacity of the facility to act as a barrier to the release of radionuclides and toxic pollutants, and to illustrate the importance of different site characteristics for the safety of the repository. The three hypothetical sites investigated are the same as those used for the safety assessment of a deep repository for spent fuel carried out in parallel to this work.

This report concerns the modelling of the migration of radionuclides and toxic metals from SFL 3-5. The migration in the near field and the geosphere is modelled, and the resulting dose to man is estimated. The main part of this work is based on a reference scenario defined within the safety assessment. In addition, the effect of human activities has been investigated by analysing the consequences of a release of radionuclides and toxic metals to wells.

From the completed study it can be concluded that the radionuclides of importance for the safety are those that are highly mobile and long-lived, e.g. ^{36}Cl and ^{93}Mo. In addition, the site where the repository is built has a significant influence on the safety. Two factors are particularly important: the water flow rate at the depth where the repository is located, and the ecosystem in the areas on the ground surface where releases may take place in the future. High water flow rate in the rock around the repository can be compensated for by better barriers in the near field. However, they must perform satisfactorily over a very long period of time.

Sammanfattning

En preliminär säkerhetsanalys har genomförts av ett djupförvar för långlivat låg- och medelaktivt avfall, SFL 3-5. Syftet med studien är att undersöka konstruktionens förmåga att fungera som en barriär mot uttransport av radionuklider och miljöfarliga ämnen, samt att belysa betydelsen av förvarsplatsens läge. De tre hypotetiska platser som man har valt att studera är de samma som har studerats i den genomförda säkerhetsanalysen av ett djupförvar för använt bränsle.

Denna rapport omfattar modelleringen av migrationen av radionuklider och toxiska metaller från SFL 3-5 Spridningen i närzon och geosfär har modelleras och dos till människan har beräknats. Huvuddelen av detta arbete baseras på ett referensscenario som har definierats inom den preliminära säkerhetsanalysen. Dessutom har påverkan från framtida mänskliga handlingar analyserats genom att beräkna framtida omgivningspåverkan från borrade brunnar i närheten av förvaret.

En slutsats från den genomförda studien är att de radionuklider som är mycket rörliga och har lång livslängd, t ex ^{36}Cl och ^{93}Mo, har störst betydelse vad gäller förvarets säkerhet. Dessutom har förvarsplatsen läge betydelse för säkerheten. Två saker framstår som speciellt viktiga: vattenflödet på det djup i berget där förvaret förläggs och ekosystemet i de områden på markytan där utsläpp kan ske i framtiden. Ett högt vattenflöde i berget omkring förvaret kan kompenseras med bättre barriärer i närområdet. Funktionen måste dock bibehållas under mycket lång tid.

Contents

1 Introduction

1.1 Background

A repository for long-lived low- and intermediate-level waste, SFL 3-5, is foreseen to be constructed in the future. The repository will contain waste for which the content of long-lived radionuclides is too high to be deposited in the present repository for radioactive operational waste, SFR. The present plan is to take SFL 3-5 in operation at approximately the same time as the deep repository for spent fuel. It is possible that SFR is closed at that time, why operational waste from the central interim storage for spent fuel (CLAB) and the encapsulation plant will be deposited in SFL 3-5 as well.

A prestudy of the SFL 3-5 repository was performed 1992 – 1995, in order to evaluate the performance of the constructed barriers (Wiborgh, 1995). The release of radionuclides and toxic metals from the near field was examined. The results were based on a regional water flow of 10^{-4} m^3/m^2, year, which was assumed to be representative for a typical Swedish bedrock at repository depth.

Based on the results from the prestudy, the repository was redesigned. The main modifications of the design are that the SFL 3 and SFL 5 tunnels are identical, and that gravel is used as backfill material instead of bentonite. In addition, an updated estimation of the waste inventory to be deposited in SFL 3-5 has been made (Lindgren *et al.,* 1998). The waste volume and the total activity content at repository closure have not changed, but the reference inventory contains more nuclides.

Based on the new repository design and the updated radionuclide inventory, a preliminary safety assessment of the SFL 3-5 repository has been made (SKB, 1999b). It is assumed that SFL 3-5 will be located in the vicinity of the deep repository for spent fuel. In accordance with the present safety assessment of the latter repository, SR 97 (SKB, 1999a), three different sites are investigated: Äspö, Finnsjön and Gideå. In the following, these sites are denoted Aberg, Beberg and Ceberg, respectively. The sites are different for instance in terms of groundwater composition, specific water flow, and biotopes to which the nuclides are released.

1.2 Objective

This report concerns the modelling of the migration of radionuclides and toxic metals from SFL 3-5 performed within the preliminary safety assessment of SFL 3-5. The main difference between the prestudy and this work is that:

- the repository is based on the new design
- three different sites are investigated
- more nuclides are included in the reference waste inventory
- not only migration in the near field, but also in the geosphere is modelled, and the resulting dose to man is estimated

The analysis is made for a reference scenario describing the expected development of the repository near field assuming that no major changes occur in the thermal, the hydrological, the mechanical or the chemical conditions in the surrounding rock. It is also assumed that no major changes occur in the biosphere. In addition, a scenario where it is assumed that the release is captured in a well is also analysed.

The objectives of this work is to evaluate:

- the new repository design, and
- the importance of different site characteristics for the safety of the repository.

1.3 Structure of report

A brief description of the waste and the repository is given in Chapter 2 and Chapter 3, respectively. The models and input data used for evaluating the migration of radionuclides and toxic metals in the near field, the geosphere and the biosphere are summarised in Chapter 4 and Chapter 5, respectively. In Chapters 6-9, the results of the release calculations for the reference scenario are presented, and in Chapter 10 for the well scenario. Different modifications of the constructed barriers are discussed, and the effect on the near-field release rate is shown in the following chapter. Finally, the results are discussed, and conclusions of this work are drawn in Chapter 12.

2 Description of the waste

In this chapter a description of the waste allocated to SFL 3-5 is given. In comparison to the waste inventory used in the prestudy of SFL 3-5 (Wiborgh, 1995), a more comprehensive radionuclide inventory has been estimated (Lindgren *et al.,* 1998*)*. The total activity content in each repository part is, however, of the same order of magnitude, and waste volumes and amount of materials are similar to those used in the prestudy. A more detailed description of the waste is given in Lindgren *et al.* (1998)

2.1 SFL 3 waste

Long-lived low- and intermediate-level waste conditioned at Studsvik that do not fulfil the present criteria for final deposition in SFR, and low- and intermediate-level operational waste from CLAB and the encapsulation plant is foreseen to be deposited in SFL 3. The waste consists of both organic and inorganic material. Apart from being radioactive, toxic material (lead and cadmium) is also present.

Mainly standard concrete moulds (1.2 × 1.2 × 1.2 m) and 200-litre steel drums are used as packaging in SFL 3. The approximate number of moulds and drums are 2,800 and 4,000, respectively. The total volume of the waste is estimated to be about 5,600 m^3.

2.2 SFL 4 waste

SFL 4 is intended for low-level decommissioning waste from CLAB and the encapsulation plant, and transport casks, transport containers and fuel storage canisters from CLAB. The activity in SFL 4 is dominated by surface contamination on fuel storage canisters. The canisters will probably be decontaminated, and the decontamination solutions will end up in SFL 3. Decommissioning waste and fuel storage canisters will be deposited in some 630 carbon steel cases (2.4 × 2.4 × 2.4 m). Transport cask and transport containers are stored without any additional packaging. To improve the mechanical stability of the waste packages, the void inside the cases may be filled with e.g. gravel or concrete. In this work, it is assumed that concrete is used as filling material. The total volume of the waste is estimated to be about 10,000 m^3, of which about 1,300 m^3 is transport cask and transport containers.

2.3 SFL 5 waste

Operational and decommissioning waste with high specific activity (core components and internal parts) will be deposited in SFL 5. Small volumes of decommissioning waste from Studsvik will be stored in SFL 5 as well. SFL 5 will also contain some toxic material (beryllium and lead). The waste will be packed in long concrete moulds (1.2 × 1.2 × 4.8 m) with an inner steel cassette. Concrete will be injected into the space between the steel cassette and the mould. The approximate number of moulds is 1,400, and the total waste volume is estimated to be about 9,700 m^3.

2.4 Waste inventory

The radionuclide inventory in SFL 3-5 has been estimated based on a combination of measurements, calculations and assumptions. Data from measurements of nuclide activity are available for some nuclides. However, this type of data is missing for the majority of the radionuclides. In that case, the nuclide activity has been estimated using correlations to "key-nuclides". This is described in detail in Lindgren *et al.* (1998). Finally, the radionuclide inventory is recalculated to the time of repository closure (year 2040) taking radioactive decay into account. The estimated radionuclide inventory in SFL 3-5 is summarised in Table 2-1. Radionuclides with a half-life less than approximately two years, and radionuclides being more or less stable and with expected small contents are not included. Data is given for SFL 4 both including and excluding the activity of surface contaminated material (CRUD). The total activity content in SFL 3-5 at the time of repository closure (2040) is estimated to be in the order of 10^{17} Bq. As shown in Figure 2-1, SFL 5 will contain the main part of the activity.

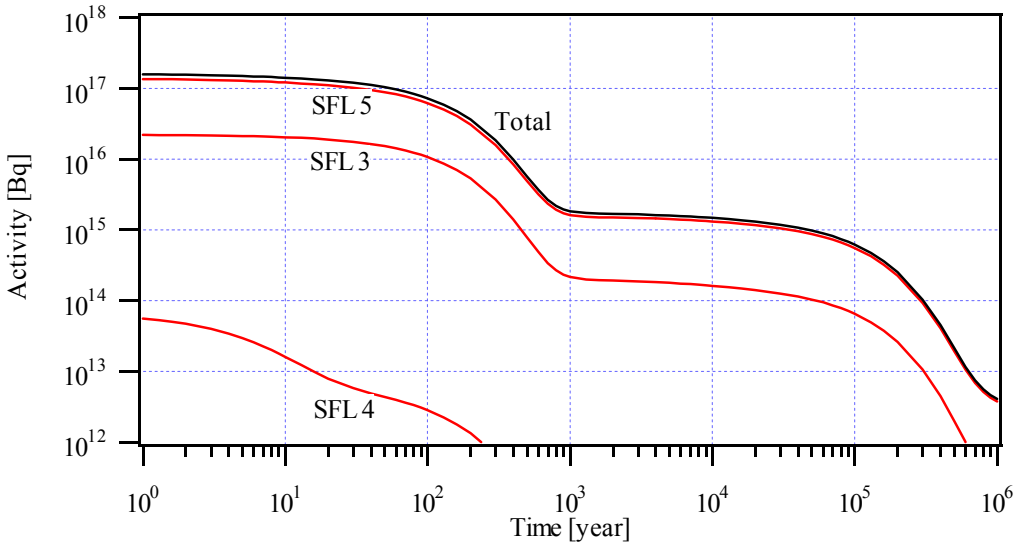

Figure 2-1 Radionuclide inventory in SFL 3-5 as a function of time (time zero corresponds to the year 2040).

Table 2-1 Radionuclide inventory [Bq] in SFL 3-5 at repository closure (2040).

Radionuclide	Half-life [a] [year]	SFL 3	SFL 4 w/o CRUD	SFL 4 with CRUD	SFL 5
^{3}H	12	$3.2\cdot10^{12}$	$1.6\cdot10^{9}$	$4.3\cdot10^{9}$	$2.5\cdot10^{15}$
^{10}Be	$1.5\cdot10^{6}$	$1.2\cdot10^{7}$	12	$1.6\cdot10^{4}$	$1.4\cdot10^{11}$
$^{14}C_{inorganic}$	$5.7\cdot10^{3}$	$3.5\cdot10^{13}$	$3.1\cdot10^{7}$	$2.7\cdot10^{10}$	$1.7\cdot10^{14}$
$^{14}C_{organic}$	$5.7\cdot10^{3}$	$8.2\cdot10^{4}$	-	-	-
^{36}Cl	$3.0\cdot10^{5}$	$2.1\cdot10^{10}$	$2.6\cdot10^{4}$	$1.6\cdot10^{7}$	$2.5\cdot10^{11}$
^{40}K	$1.3\cdot10^{9}$	$1.1\cdot10^{9}$	Not estimated	Not estimated	Not estimated
^{55}Fe	2.7	$9.3\cdot10^{12}$	$3.6\cdot10^{10}$	$2.7\cdot10^{13}$	$9.6\cdot10^{14}$
^{60}Co	5.3	$3.6\cdot10^{14}$	$4.1\cdot10^{10}$	$2.7\cdot10^{13}$	$8.1\cdot10^{15}$
^{59}Ni	$7.6\cdot10^{4}$	$1.6\cdot10^{14}$	$1.2\cdot10^{8}$	$2.7\cdot10^{10}$	$1.4\cdot10^{15}$
^{63}Ni	$1.0\cdot10^{2}$	$2.2\cdot10^{16}$	$1.7\cdot10^{10}$	$5.3\cdot10^{12}$	$1.2\cdot10^{17}$
^{79}Se	$1.1\cdot10^{6}$	$4.6\cdot10^{8}$	$5.0\cdot10^{3}$	$6.4\cdot10^{6}$	$4.5\cdot10^{7}$
^{90}Sr	29	$2.3\cdot10^{12}$	$1.6\cdot10^{8}$	$1.6\cdot10^{11}$	$5.6\cdot10^{11}$
^{93}Zr	$1.5\cdot10^{6}$	$2.1\cdot10^{10}$	$2.1\cdot10^{4}$	$2.7\cdot10^{7}$	$2.2\cdot10^{12}$
^{93m}Nb	16	$6.0\cdot10^{12}$	$2.8\cdot10^{8}$	$2.7\cdot10^{10}$	$8.0\cdot10^{13}$
^{94}Nb	$2.0\cdot10^{4}$	$4.9\cdot10^{11}$	$6.6\cdot10^{6}$	$2.7\cdot10^{8}$	$4.7\cdot10^{12}$
^{93}Mo	$4.0\cdot10^{3}$	$2.4\cdot10^{11}$	$2.0\cdot10^{5}$	$1.3\cdot10^{8}$	$1.8\cdot10^{12}$
^{99}Tc	$2.1\cdot10^{5}$	$5.8\cdot10^{11}$	$6.2\cdot10^{6}$	$8.0\cdot10^{9}$	$3.2\cdot10^{11}$
^{107}Pd	$6.5\cdot10^{6}$	$1.1\cdot10^{8}$	$1.2\cdot10^{3}$	$1.6\cdot10^{6}$	$1.1\cdot10^{7}$
^{108m}Ag	$4.2\cdot10^{2}$	$1.2\cdot10^{12}$	$1.2\cdot10^{6}$	$1.6\cdot10^{9}$	$9.6\cdot10^{9}$
^{113m}Cd	14	$5.7\cdot10^{9}$	$7.4\cdot10^{5}$	$9.6\cdot10^{8}$	$1.5\cdot10^{9}$
^{126}Sn	$1\cdot10^{5}$	$5.7\cdot10^{7}$	$6.2\cdot10^{2}$	$8.0\cdot10^{5}$	$5.6\cdot10^{6}$
^{125}Sb	2.8	$6.6\cdot10^{11}$	$2.1\cdot10^{9}$	$2.7\cdot10^{12}$	$1.4\cdot10^{10}$
^{129}I	$1.6\cdot10^{7}$	$3.4\cdot10^{7}$	$3.7\cdot10^{2}$	$4.8\cdot10^{5}$	$3.4\cdot10^{6}$
^{134}Cs	2.1	$3.9\cdot10^{10}$	$1.2\cdot10^{9}$	$1.6\cdot10^{12}$	$7.9\cdot10^{8}$
^{135}Cs	$2.3\cdot10^{6}$	$5.7\cdot10^{8}$	$6.2\cdot10^{3}$	$8.0\cdot10^{6}$	$5.6\cdot10^{7}$
^{137}Cs	30	$3.4\cdot10^{13}$	$1.2\cdot10^{9}$	$1.6\cdot10^{12}$	$5.7\cdot10^{12}$
^{133}Ba	11	$2.9\cdot10^{10}$	$2.1\cdot10^{5}$	$2.7\cdot10^{8}$	$2.9\cdot10^{8}$
^{147}Pm	2.6	$2.5\cdot10^{10}$	$1.1\cdot10^{9}$	$1.4\cdot10^{12}$	$5.1\cdot10^{9}$
^{151}Sm	90	$2.3\cdot10^{11}$	$3.7\cdot10^{6}$	$4.8\cdot10^{9}$	$2.7\cdot10^{10}$
^{152}Eu	14	$1.5\cdot10^{12}$	$8.7\cdot10^{4}$	$1.1\cdot10^{8}$	$1.7\cdot10^{8}$
^{154}Eu	8.6	$4.8\cdot10^{11}$	$1.2\cdot10^{8}$	$1.6\cdot10^{11}$	$1.1\cdot10^{11}$
^{155}Eu	4.8	$5.2\cdot10^{10}$	$8.7\cdot10^{7}$	$1.1\cdot10^{11}$	$1.4\cdot10^{10}$
^{166m}Ho	$1.2\cdot10^{3}$	$8.3\cdot10^{10}$	$8.2\cdot10^{4}$	$1.1\cdot10^{8}$	$7.3\cdot10^{8}$
^{210}Pb	22	$2.7\cdot10^{11}$	< 1	< 1	< 1
^{226}Ra	$1.6\cdot10^{3}$	$3.8\cdot10^{11}$	< 1	< 1	< 1
^{227}Ac	22	$1.4\cdot10^{6}$	< 1	< 1	4.5
^{229}Th	$7.3\cdot10^{3}$	$1.4\cdot10^{2}$	< 1	< 1	< 1
^{230}Th	$7.5\cdot10^{4}$	$1.8\cdot10^{5}$	< 1	2.4	73
^{232}Th	$1.4\cdot10^{10}$	$1.1\cdot10^{10}$	< 1	< 1	< 1
^{231}Pa	$3.3\cdot10^{4}$	$2.5\cdot10^{6}$	< 1	< 1	7.9
^{232}U	69	$4.4\cdot10^{6}$	< 1	$8.0\cdot10^{2}$	$4.2\cdot10^{3}$
^{233}U	$1.6\cdot10^{5}$	$3.1\cdot10^{4}$	< 1	< 1	13
^{234}U	$2.5\cdot10^{5}$	$7.8\cdot10^{8}$	24	$2.7\cdot10^{4}$	$2.4\cdot10^{5}$
^{235}U	$7.0\cdot10^{8}$	$6.4\cdot10^{9}$	< 1	$5.3\cdot10^{2}$	$3.7\cdot10^{3}$
^{236}U	$2.3\cdot10^{7}$	$8.1\cdot10^{7}$	7.2	$8.0\cdot10^{3}$	$5.6\cdot10^{4}$
^{238}U	$4.5\cdot10^{9}$	$4.6\cdot10^{10}$	9.6	$1.1\cdot10^{4}$	$7.5\cdot10^{4}$
^{237}Np	$2.1\cdot10^{6}$	$1.8\cdot10^{8}$	9.6	$1.1\cdot10^{4}$	$7.9\cdot10^{4}$
^{238}Pu	88	$3.7\cdot10^{11}$	$8.9\cdot10^{4}$	$1.1\cdot10^{8}$	$5.9\cdot10^{8}$
^{239}Pu	$2.4\cdot10^{4}$	$2.3\cdot10^{12}$	$8.5\cdot10^{3}$	$8.9\cdot10^{6}$	$6.2\cdot10^{7}$
^{240}Pu	$6.6\cdot10^{3}$	$1.8\cdot10^{12}$	$1.5\cdot10^{4}$	$1.8\cdot10^{7}$	$1.3\cdot10^{8}$
^{241}Pu	14	$4.4\cdot10^{12}$	$2.3\cdot10^{6}$	$2.7\cdot10^{9}$	$4.6\cdot10^{9}$
^{242}Pu	$3.7\cdot10^{5}$	$1.2\cdot10^{9}$	72	$8.0\cdot10^{4}$	$5.6\cdot10^{5}$
^{244}Pu	$8.1\cdot10^{7}$	$1.8\cdot10^{2}$	< 1	< 1	< 1
^{241}Am	$4.3\cdot10^{2}$	$5.0\cdot10^{12}$	$2.1\cdot10^{4}$	$2.7\cdot10^{7}$	$6.3\cdot10^{8}$
^{242m}Am	$1.4\cdot10^{2}$	$2.0\cdot10^{9}$	$2.4\cdot10^{2}$	$2.7\cdot10^{5}$	$1.6\cdot10^{6}$
^{243}Am	$7.4\cdot10^{3}$	$8.5\cdot10^{9}$	$7.2\cdot10^{2}$	$8.0\cdot10^{5}$	$5.6\cdot10^{6}$
^{243}Cm	29	$1.7\cdot10^{9}$	$4.8\cdot10^{2}$	$5.3\cdot10^{5}$	$1.8\cdot10^{6}$
^{244}Cm	18	$4.4\cdot10^{10}$	$6.3\cdot10^{4}$	$8.0\cdot10^{7}$	$1.9\cdot10^{8}$
^{245}Cm	$8.5\cdot10^{3}$	$7.7\cdot10^{7}$	7.2	$8.0\cdot10^{3}$	$5.6\cdot10^{4}$
^{246}Cm	$4.7\cdot10^{3}$	$2.1\cdot10^{7}$	1.9	$2.1\cdot10^{3}$	$1.5\cdot10^{4}$

a) Firestone (1998)

The waste in SFL 3-5 contains some substances that are hazardous to the environment but not particularly radioactive (see Table 2-2). The consequences of release of the metals beryllium, cadmium and lead is therefore included in this safety analysis.

Table 2-2 Amounts [kg] of toxic materials in SFL 3-5.

Material	SFL 3	SFL 4	SFL 5	Total
Cadmium	990	–	–	990
Lead - waste	3,965	–	–	3,965
Lead - packaging	16,000	–	108,592	124,592
Beryllium	–	–	300	300

3 Description of the repository

The repository SFL 3-5 will be constructed at a depth of 300 – 400 metres below ground level. The repository consists of a system of tunnels. A preliminary layout of the SFL 3-5 repository is shown in Figure 3-1. A transport tunnel (SFL 4) is surrounding two identical, parallel tunnels (SFL 3 and SFL 5).

When the deposition is completed, the access ramp leading to the repository will be sealed with barriers and plugs.

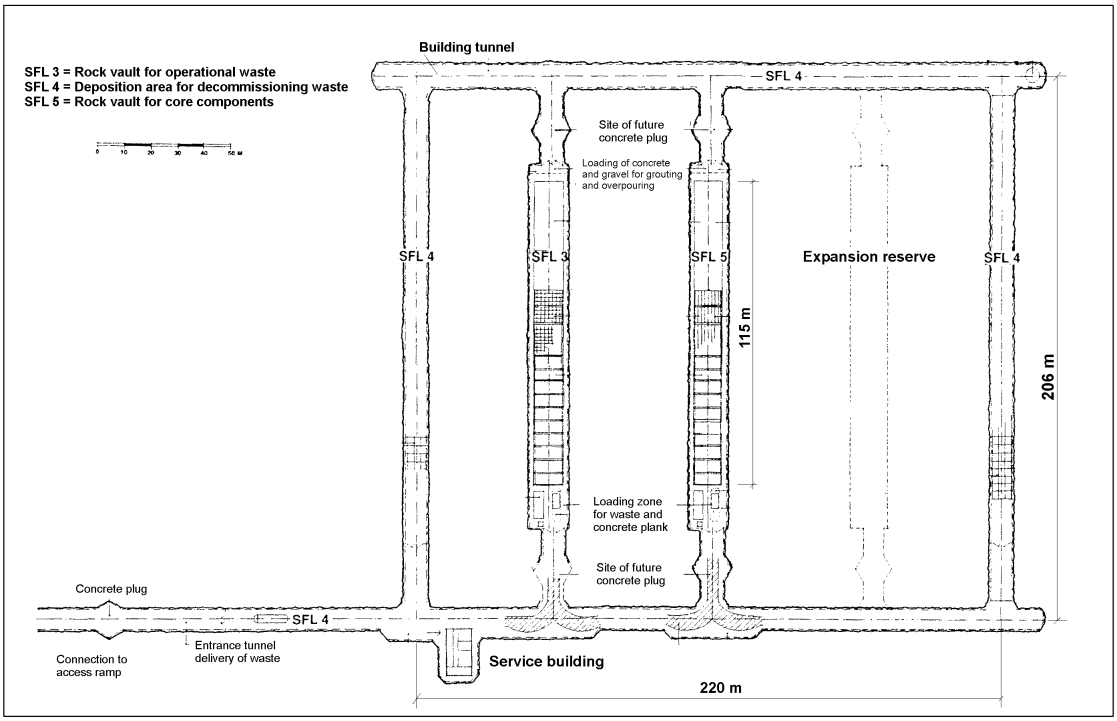

Figure 3-1 Preliminary layout of SFL 3-5.

3.1 SFL 3

The SFL 3 tunnel is 133 m long, 14 m wide and approximately 19 m high. Connecting the ends of SFL 3 with SFL 4 are two, narrower, 30 m long tunnels used as loading zones. This part of the tunnel is foreseen to be filled with crushed rock, and possibly a concrete plug. The walls and the ceiling of SFL 3 will be covered with shotcrete. The bottom of the tunnel will be covered with a 0.5 m thick layer of gravel.

A concrete structure, in which the waste moulds and drums are to be deposited, is built on the gravel. This structure is 114.6 m long, 10.8 m wide and 10.7 m high. It is divided into three sections and each section is divided into seven rooms by transverse concrete walls (0.4 m thick). The inner dimension of the floor area of a room is 10 × 5 m. In a room there is eight layers of moulds, and each layer consists of 8 × 4 moulds. Since some waste is stored in drums, a mould may be replaced by a plate (1.2 × 1.2 m) on which four drums are placed. The height of a drum is somewhat smaller than a mould, why ten plates with four drums each can be piled on top of each other. The void

between moulds and drums will be filled with porous concrete. Figure 3-2 shows an illustration of the concrete structure and of the deposited waste. Based on the approximate number of waste packages given in section 2.1, two thirds of the available volume inside the concrete structure will be filled with waste.

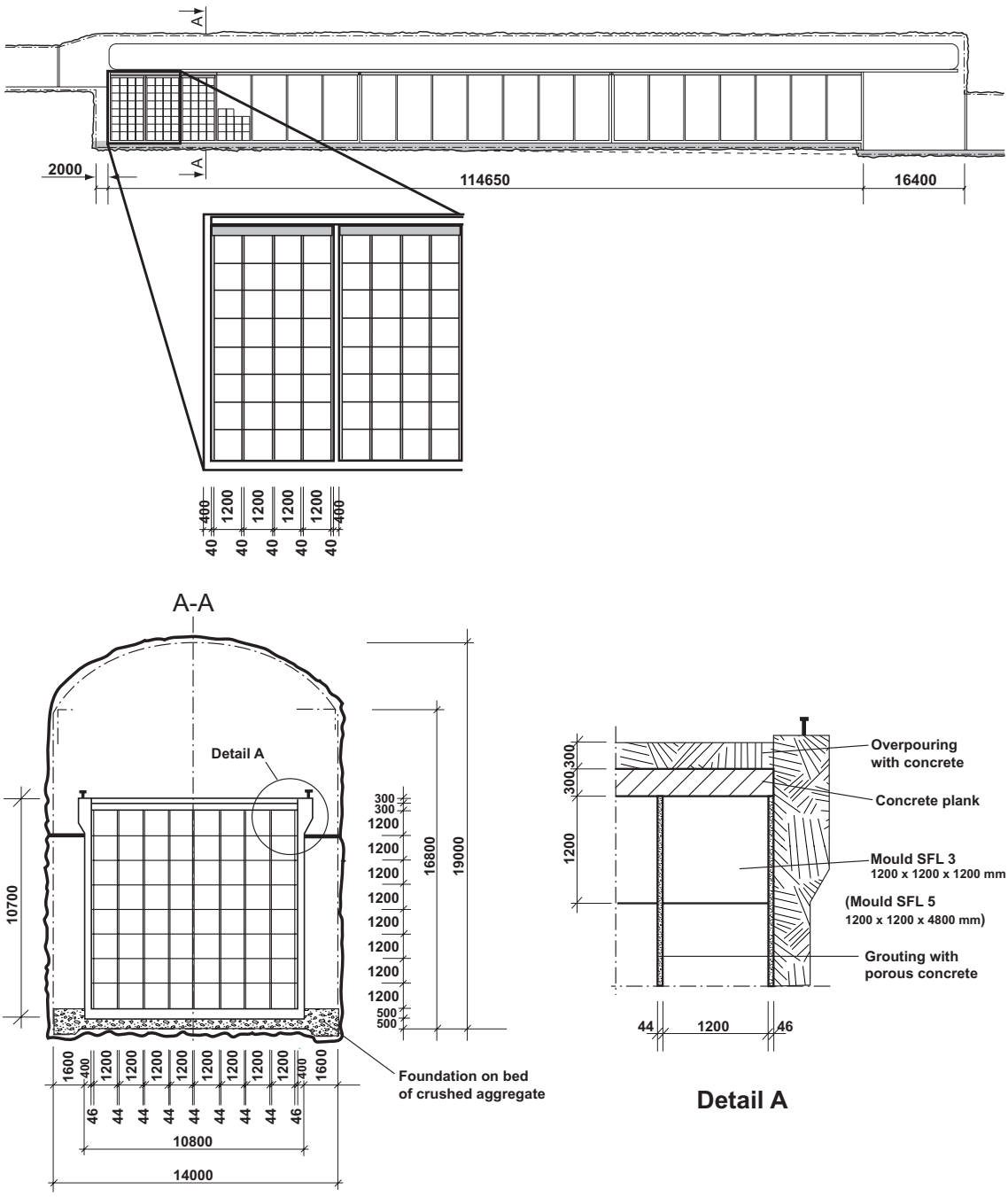

Figure 3-2 Illustration of the SFL 3 and the SFL 5 repository. Dimensions in mm.

When deposition is completed, the SFL 3 tunnel and the loading zones leading to SFL 4 will be backfilled in order to support the internal structure and the tunnel walls. The backfill will also have a function to retain released radionuclides by sorption. A concrete plug will be constructed in each loading zone in order to reduce the water flow through the tunnel. Excavated rock from the construction of the SFL 3-5 repository will

be crushed and sieved, and the size fraction 4 – 32 mm will be used as backfill material (Karlsson *et al.,* 1999). In this report, the backfill material is described as 'gravel backfill' or simply 'gravel'. The dimensions and volumes of different construction materials in SFL 3 and SFL 5 are summarised in Table 3-1.

Table 3-1 Dimensions and approximate volume of construction materials used in SFL 3 and SFL 5.

Material	Volume [m^3]	Thickness [m]
Structural concrete	3,190	
- bottom plate	620	0.5
- lid	680	0.6
- outer walls	1,020	0.4
- inner walls	870	0.4
Shotcrete	~ 500	
- roof	~ 250	0.05-0.1
- walls	~ 250	0.03-0.05
Porous concrete [a)]	~ 800	
Gravel backfill	21,000	
- foundation		0.5
- outside concrete walls		1.6
- above concrete lid		7-8

[a)] *Volume available for porous concrete inside the compartments if all waste packages are containers or moulds. The volume of porous concrete will be larger in SFL 3 since it also will contain waste drums.*

3.2 SFL 4

The SFL 4 tunnel consists of the transport tunnels surrounding SFL 3 and SFL 5. It forms a rectangle 220 × 206 m (Figure 3-1), making a total length of 852 m. The tunnel is 8 m wide and 6.5 m high. A cross section of the tunnel is shown in Figure 3-3. The ground of the tunnel is covered with 20 cm thick reinforced concrete on a layer of gravel.

The steel cases are placed directly on the concrete floor. Three cases are placed side by side (Figure 3-3), why approximately 500 m tunnel is needed for depositing the estimated 630 cases. When deposition is completed, the tunnel will be backfilled with approximately 30,000 m^3 of gravel.

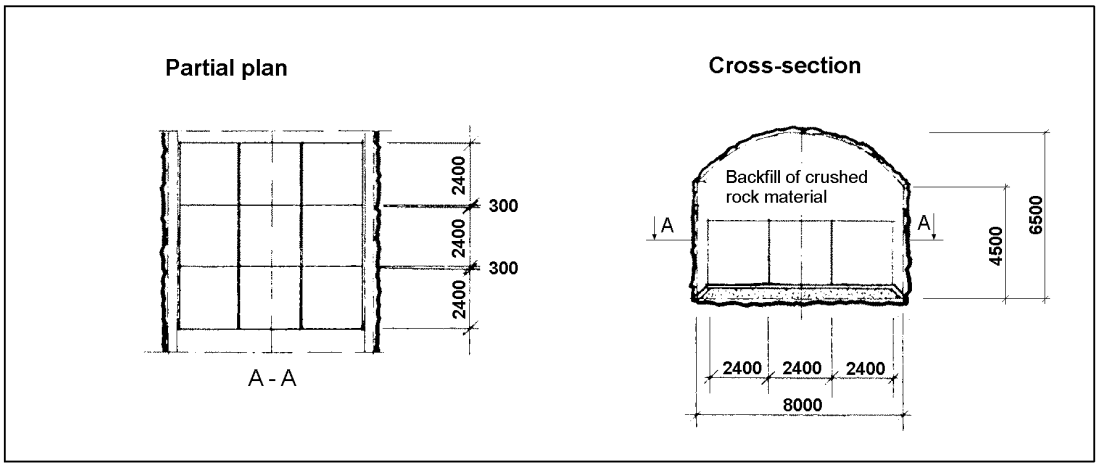

Figure 3-3 Illustration of the SFL 4 repository. Dimensions in mm.

3.3 SFL 5

The construction of the SFL 5 tunnel is identical to SFL 3. The waste packages located to SFL 5 consist of large concrete moulds only. SFL 5 can hold 1,344 of those moulds. This is somewhat less that the estimated number of moulds (1,400). Since SFL 3 and SFL 5 are more or less identical, it is possible to redistribute the waste between the rock vaults if needed. If a redistribution cannot be permitted for some reason, the lengths of the rock vaults can be adjusted to the actual need when the final requirements have been established. It is, however, assumed in this work that the waste can be concentrated so that the capacity of SFL 5 will be sufficient.

4 Description of the models used for the radionuclide transport

The models used for modelling the transport of radionuclides and toxic metals in the near field are described in this chapter. Described in brief is the model used for calculating the transport in the geosphere and the method used to evaluate the environmental impact of release of radionuclides and toxic metals to the biosphere.

4.1 Near-field model

4.1.1 Overall conceptual model for SFL 3-5

When the repository is sealed, water will intrude the tunnel, and the waste and backfill material will be saturated with water. Gas trapped in the tunnel can dissolve in the pore water or can escape through fractures in the tunnel walls. At the initial time (year 2040), most of the nuclides will be dissolved completely in the pore water in the packages containing the waste or will be sorbed on concrete and cement in the packages. The nuclides in solution will be equilibrated with the backfill material in the waste packages. Nuclides, which have a low solubility for the conditions existing in the repository, are only partially dissolved. The concentration of these nuclides will be limited to their solubility. For nuclides embedded in metallic waste, the concentration may be limited by the corrosion rate of the waste.

From the waste packages the radionuclides may be transported by diffusion and, in SFL 4, by water flow through the waste packages. The radionuclides escaping from the waste will then migrate through the barriers surrounding the waste. Sorption on barriers delays the transport. The radionuclides are then transported by the groundwater through the geosphere to the biosphere.

4.1.2 General description of the code COMP24

To calculate the transport of radionuclides and toxic metals in the near field, the code COMP24 is used. COMP24 is an extended version of the code NUCTRAN (Romero *et al.,* 1995). COMP24 calculates the non-stationary nuclide transport from a waste repository. The numerical implementation of the model is an integrated finite difference scheme and is devised to be very fast and compact by imbedding analytical solutions at some special locations where numerical schemes are cumbersome. The code takes into account diffusive and advective (water flow) transport, chain decay and sorption on the porous solid. It can simultaneously handle several sources, pathways and sinks to water flowing in fractures intersecting the deposition locations.

To represent the barrier system, through which the species are transported, the barriers are discretized into compartments of variable size and shape. The entities required to define the compartments are the geometry of the system, the dimensions of the system, and the type of materials used in the system. Each compartment is defined by its volume, the ratio between the diffusion length and the cross-sectional area used for

diffusion and by its average properties. Within a compartment, the average properties are constant in time.

4.1.3 Mathematical model

Compartments representing the waste packages are denoted ‘source terms’. A source may include for instance waste, mould walls and filling material in waste moulds. Nuclides dissolved in the pore water within the volume defined as the ‘source term’ can be transported out from the source term by diffusion, but also by advection if water is flowing through the waste packages. The material balance for a single nuclide is described by two equations. The advection-diffusion equation that describes the mass balance of the dissolved species

$$K\frac{\partial c}{\partial t} = q_d + \nabla \cdot D_e \nabla c - u_o \nabla c - K \cdot \lambda \cdot c \qquad (4.1)$$

and the mass balance of the species in the solid

$$\frac{dM}{dt} = -M \cdot \lambda - q_d \qquad (4.2)$$

where K is a distribution coefficient between the concentration of the nuclide in the water and the mass of nuclide sorbed per unit volume (-), c is the concentration of the nuclide in the pore water (mole/m^3), D_e is the effective diffusion coefficient (m^2/s), u_o is the Darcy velocity (m^3/m^2, s), λ is the decay constant (1/s) and M is the mass of nuclide as solid per unit volume (mole/m^3). The two equations are connected by a dissolution term, q_d (mole/m^3, s). The second equation is needed to describe the dissolution of the solid waste.

The distribution coefficient accounts for the nuclide dissolved in the pore water and the nuclide sorbed on the solid,

$$K = \varepsilon + (1-\varepsilon) \cdot K_d \cdot \rho_p \qquad (4.3)$$

where ε is the porosity (m^3/m^3), K_d is the sorption coefficient (m^3/kg), and ρ_p is the density of the solid material (kg/m^3).

Equation (4.1) indicates that the flux of radionuclides through the barrier system is the sum of a diffusive and an advective transport. However, for the compartments where nuclides leave the barrier system, the model takes into account only advective transport since the diffusive transport in the fractures is negligible (see Appendix F).

In general it is assumed that all radionuclides are instantaneously available for dissolution in the pore water in the source term. The initial pore water concentration is determined by its initial activity content m and source term capacity K·V:

$$c_0 = \frac{m}{K \cdot V} \qquad (4.4)$$

where V is the volume of the source (m^3). Nuclides, which have a low solubility for the conditions existing in the repository, are only partially dissolved in the pore water. The concentration of these nuclides, which will be equal to their solubility, will be kept constant during a certain time until all the nuclide in the solid phase has been dissolved. The release rate of nuclides present as induced activity in metallic waste is determined by the corrosion rate of the waste. How this is modelled is described in Appendix D.

4.1.4 Model descriptions for SFL 3-5

SFL 3

The ground water flows in the horizontal direction along the SFL 3 tunnel. The major part of the water flows through the flow barrier (gravel backfill) surrounding the concrete structure where the waste is deposited. The water flux through the concrete structure will be very low (Holmén, 1997). Therefore, most of the activity in the waste is released by diffusion through the concrete structure to the gravel backfill surrounding the concrete structure.

Radionuclides released from the concrete structure into the gravel backfill will be transported through diffusion as well as with water flowing in the backfill. The concrete plugs constructed in the loading zones are considered to be intact, why the radionuclides are transported out from the tunnel into the water flowing in fractures intersecting the end of the tunnel before they reach the plug.

In modelling the transport of radionuclides, the repository has been simplified. The important simplifications are conservative in order not to overestimate the importance of the barriers. The model include the concrete structure plus 10 m of gravel backfill at the end of the tunnel, but loading zones and concrete plugs (shown in Figure 3-1) are not included. This is a consequence of the assumption of intact plugs. Neither is the shotcrete that cover the tunnel walls included in the model.

The waste volume to be deposited in SFL 3 corresponds to approximately two thirds of the available storage volume, or a length of 76 m of the concrete structure. Conservatively it is assumed that the waste is stored in the part of the structure closest to where water leaves the tunnel. It is assumed that the remaining storage volume is filled with gravel. However, the spaces between concrete moulds and drums are filled with porous concrete.

The waste packages consist of cubic concrete moulds as well as steel drums. However, drums are together with the major part of the porous concrete filled around the drums also modelled as moulds. In the model, a large number of waste packages are grouped to a source term. Consequently, a source term includes waste, concrete in mould walls and in backfill material in packages, but also most of the porous concrete filled around the drums. It is assumed that the activity within a source term is homogeneous, and that it remains so also when part of the inventory is transported out.

The nuclides diffuse from the source terms to the surrounding porous concrete continue by diffusion through the concrete structure to the gravel backfill surrounding the structure. Along the tunnel nuclides are transported both by diffusion and by advection.

The transport paths for radionuclides are shown in Figure 4-1. Sorption is accounted for in all parts of the modelled repository. A detailed description of the discretization of the SFL 3 tunnel, and water flow through the system, is given in Appendix A.

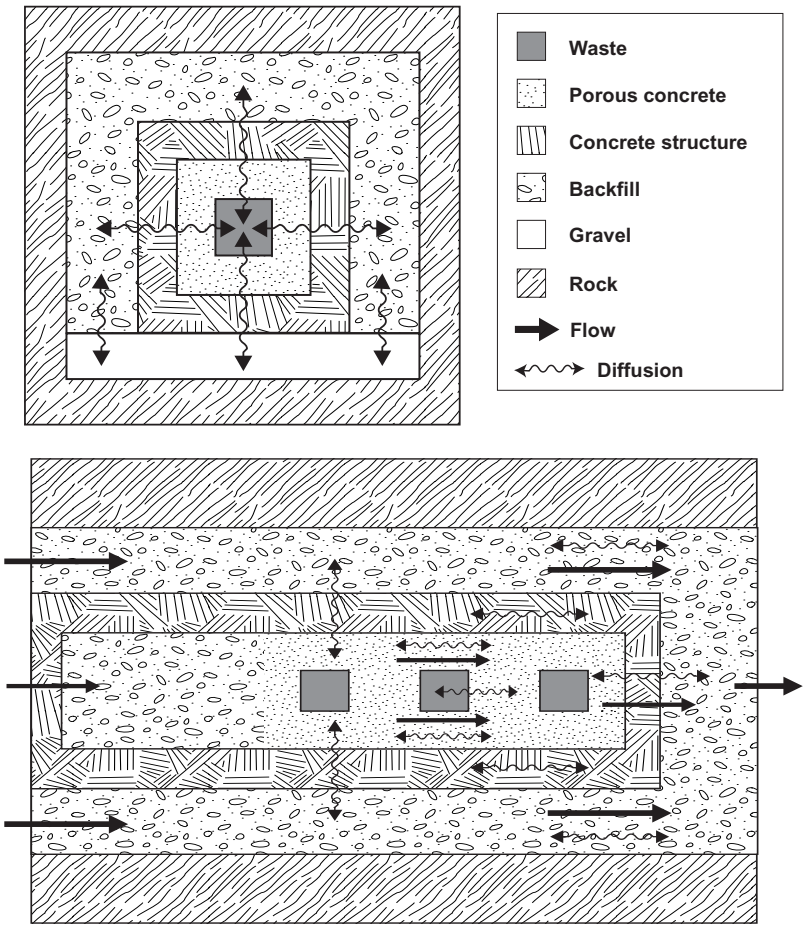

Figure 4-1 Transport paths for radionuclides in SFL 3. 'Gravel' corresponds to the bed on which the structure is built and 'Backfill' to the gravel used as backfill in the tunnel. In the model, 'Gravel' and 'Backfill has the same properties.

SFL 4

Water flows in the horizontal direction parallel to the SFL 3 and SFL 5 tunnels. This means that water enters the SFL 4 tunnel along one of its sides, flows along the tunnel, and leaves the tunnel system on the opposite side. The waste containers may be damaged by corrosion quite soon after repository closure, why the barrier effect of the steel containers is negligible. Water therefore flows through the whole cross section of the tunnel.

Fuel storage canisters and decommissioning waste from CLAB and the encapsulation plant is the only radioactive waste of importance in SFL 4. Activity in transport casks and transport containers is insignificant and can be neglected. In the model, a large number of steel casks with decommissioning waste are grouped to a source term. A source term includes waste and concrete assumed to be used as backfill material in the

casks. It is assumed that the activity within a source term is homogeneous, and that it remains so also when part of the inventory is transported out

Dissolved radionuclides will be transported along the tunnel both by diffusion and by advection in both backfill material and in waste (see Figure 4-2). In addition, there is also a diffusive transport from the waste casks into the surrounding gravel backfill. Sorption on waste and gravel backfill is accounted for, but sorption on the tunnel concrete floor and on shotcrete on tunnel walls is neglected. The radionuclides are transported out from the tunnel into the water flowing in fractures intersecting the tunnel on the opposite side to where water flows into the SFL 4 tunnel.

Only about 60% of the length of the SFL 4 tunnel contains waste with any significant activity. The remaining storage volume is assumed to be filled with gravel. Conservatively it is assumed that the waste is stored in the part of the structure closest to where water leaves the tunnel.

For symmetry reasons only half of the SFL 4 tunnel is modelled. A detailed description of the discretization of the SFL 4 tunnel, and water flow through the system, is given in Appendix B.

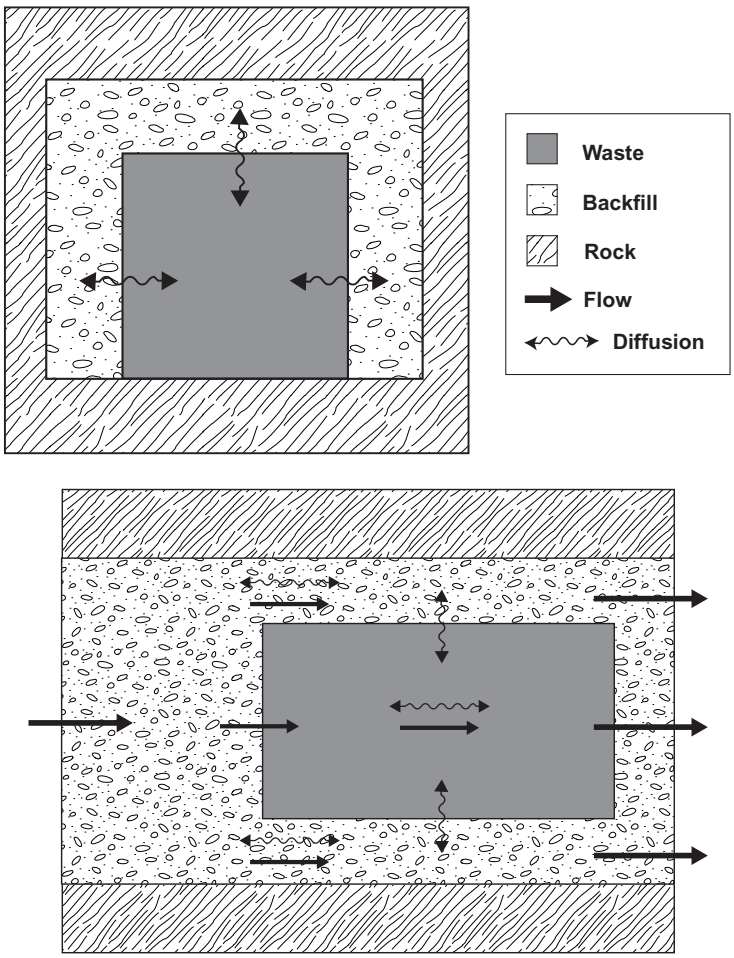

Figure 4-2 Transport paths for radionuclides in SFL 4.

SFL 5

The SFL 5 tunnel is identical to the SFL 3 tunnel, why the radionuclides are transported from waste to surrounding near-field rock in the same way as for SFL 3. The waste to be deposited in SFL 5 consists of metal parts placed in a reinforced concrete mould with an inner steel cassette. Concrete will be injected to fill the voids in the mould. Unlike SFL 3, all waste packages are the same in SFL 5. The waste volume to be deposited in SFL 5 exceeds the available volume with approximately four per cent, but in this work it is assumed that the waste volume can be concentrated so that the capacity of SFL 5 will be sufficient (see section 3.3).

The model used for studying the radionuclide transport in SFL 5 is almost identical to the model used for SFL 3. A large number of moulds with waste and injected concrete are grouped to a source term, but the mould concrete walls are modelled separately. The barrier effect of the inner steel cassette is neglected. It is assumed that the activity within a source term is homogeneous, and that it remains so also when part of the inventory is transported out. All voids inside the concrete structure are filled with porous concrete, and the structure is covered with gravel.

Dissolved radionuclides can diffuse from the waste through mould walls, the porous concrete surrounding the moulds and finally the concrete structure to the gravel backfill surrounding the structure. Along the tunnel nuclides are transported both by diffusion and by advection. The transport paths for radionuclides are shown in Figure 4-3. Sorption is accounted for in all parts of the modelled repository. A detailed description of the discretization of the SFL 5 tunnel, and water flow through the system, is given in Appendix C.

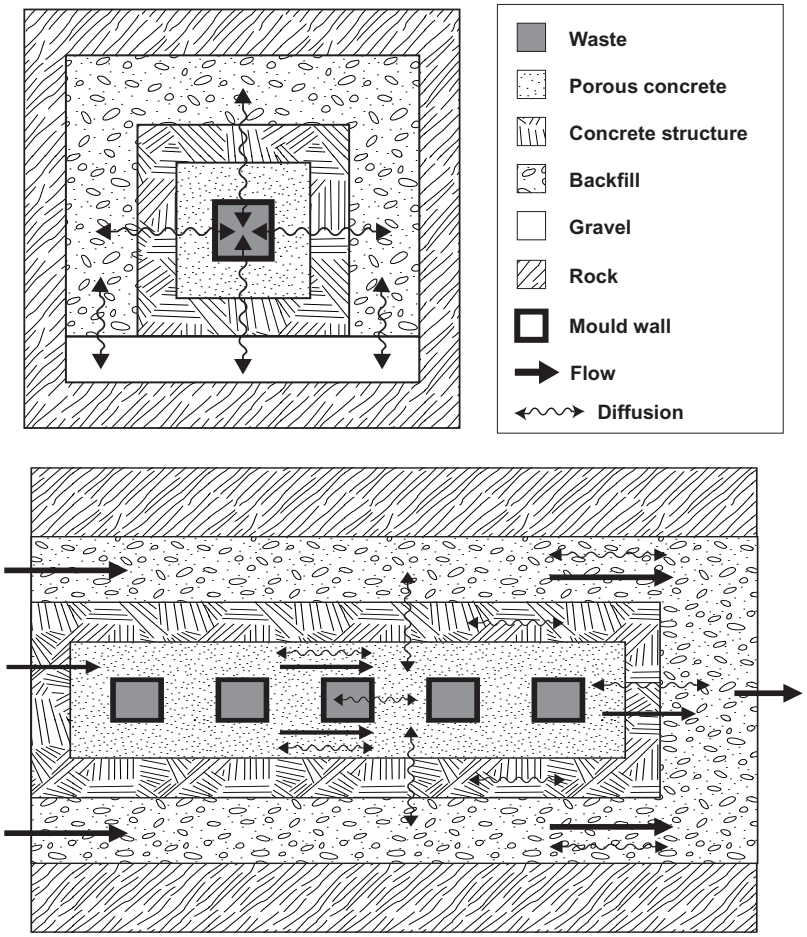

Figure 4-3 Transport paths for radionuclides in SFL 5. 'Gravel' corresponds to the bed on which the structure is built and 'Backfill' to the gravel used as backfill in the tunnel. In the model, 'Gravel' and 'Backfill has the same properties.

4.2 Far-field model

Dissolved radionuclides that are released from the near field will be transported with the groundwater through the geosphere in water bearing fractures. Sorption on the surface of these fractures delays the transport. Dissolved species can also diffuse into and sorb on micro fissures in the rock. This is known as matrix diffusion, and is an important cause of retention of radionuclides in the geosphere.

In order to calculate the transport of dissolved radionuclides and toxic metals in the geosphere, the computer code FARF31 (Norman and Kjellbert, 1990) is used. It is the same code as that used in the safety analysis of the deep repository for spent fuel (SKB, 1999a). The calculations are based on a one-dimensional model for the transport along a single path in the rock. The model takes advection and dispersion along the flow path into account as well as chain decay and matrix diffusion and sorption.

4.3 Biosphere model

The migration of radionuclides in the biosphere and resulting dose to man is estimated using the same model (Bergström *et al.,* 1999) as that used in the safety analysis of the deep repository for spent fuel (SKB, 1999a). A grid net has been used to divided each site into squares of 250 × 250 m, and each square has been classified based on the predominant ecosystem (Nordlinder *et al.,* 1999). As an example, the classification made for Ceberg is shown in Figure 4-4. For each of the ecosystems present in Aberg, Beberg and Ceberg, ecosystem-specific dose conversion factors (EDF's) have been estimated (Nordlinder *et al.,* 1999). These EDF's are used to transform the release of radionuclides to the biosphere into resulting dose to man.

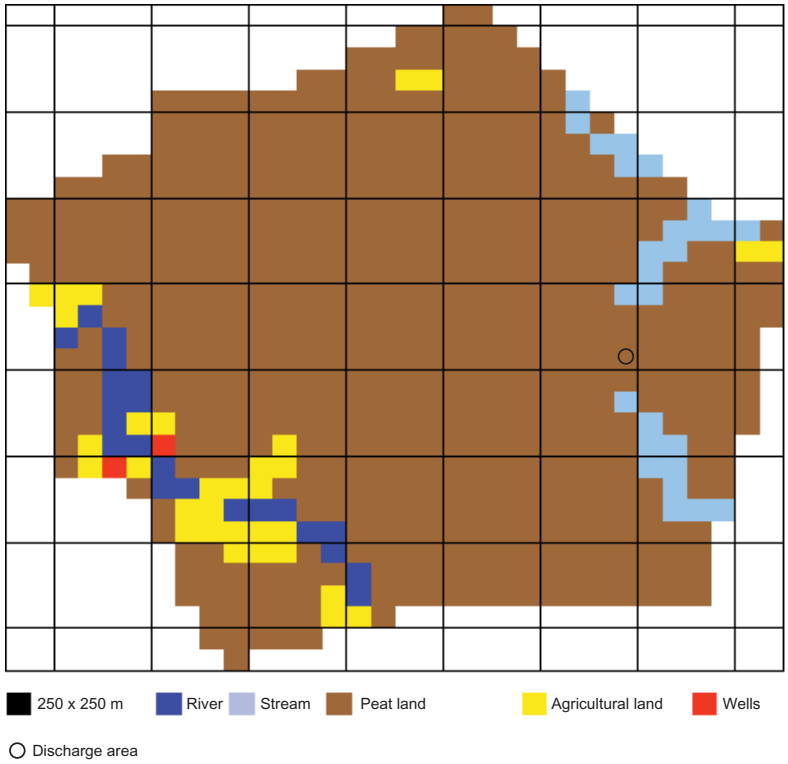

Figure 4-4 Predominant ecosystems in Ceberg.

The dissolution and transport of dissolved toxic metals are modelled in the same way as radionuclides (see sections 4.1 and 4.2). The release of toxic metals from SFL 3-5 is evaluated by comparing the resulting concentrations in different recipients with typical concentrations presently found in different types of ecosystems. For the release to a well guideline values for drinking water are used as comparison values. The ecosystems and wells in question are the same as those used for estimating the radiological dose.

For release to water (e.g. a coastal area or a well) the concentration of toxic metals is given by:

$$c_i(t) = \frac{q_i(t)}{Q} = \frac{q_i(t) \cdot t_r}{V} \qquad (4\text{-}5)$$

where $c_i(t)$ is the concentration of toxic metal in the recipient (g/m^3)

$q_i(t)$ is the release rate from the geosphere (g/year)

Q is the water discharge rate (m^3/year)

V is the recipient volume (m^3)

t_r is the mean residence time of water in recipient (year)

For release of toxic metals on land (e.g. soil or wetland), it is assumed roughly and at the same time conservatively that all material released from the geosphere enters the recipient and accumulates there. The cumulative release is obtained by integrating the far-field release rate (g/year) versus time (year). The concentration is obtained by dividing what is accumulated with the recipient volume:

$$c_i(t) = \frac{\int q_i(t)\, dt}{V} \tag{4-6}$$

The cumulative concentration, c, (g/m^3 recipient) is recalculated to a cumulative concentration based on kg dry weight (dw) of the recipient, c', using:

$$c_i'(t) = \frac{c_i(t)}{\rho \cdot (1-\varepsilon)} \tag{4-7}$$

where ρ and ε is the dry density (kg/m^3) and the porosity (m^3/m^3) of the material, respectively.

5 Input data used in the calculations

In this chapter, the input data used for modelling the radionuclide transport in the near field and the far field and for estimating the resulting dose to man are presented. A more thorough discussion of the input data and the reasons for choosing these data is given in Skagius *et al.* (1999).

5.1 Near-field data

Here, the radionuclide inventory on which the report is based upon is given. Furthermore, physical and chemical properties of the barrier materials modelled are given as well as hydrological data.

5.1.1 Radionuclide inventory

The radionuclide inventory in SFL 3-5 is discussed in Chapter 2 and is summarised in Table 2-1.

In SFL 5, ^{14}C, ^{36}Cl, ^{93}Zr and ^{93}Mo are mainly present in the form of induced activity in metal parts in the waste. The release of these nuclides in SFL 5 is therefore determined by the corrosion rate of steel and Zircalloy (see Appendix D). ^{59}Ni is also present in metal parts in SFL 5. However, modelling ^{59}Ni as corrosion rate limited gives a concentration in the water in the waste packages exceeding the solubility. The release of ^{59}Ni is therefore limited by its solubility in both SFL 3 and SFL 5.

5.1.2 Physical and chemical data

Values on density, effective diffusivity, and porosity for the materials modelled in SFL 3-5 are given in Table 5-1.

Table 5-1 Physical data for materials in SFL 3-5.

Material	Bulk density [kg/m^3]	Effective diffusivity [m^2/s]	Porosity [m^3/m^3]
Concrete in structures	2,295	$1 \cdot 10^{-11}$	0.15
Porous concrete	1,890	$1 \cdot 10^{-10}$	0.3
Gravel backfill	1,890	$6 \cdot 10^{-10}$	0.3

Sorption depends on for instance the type of material on which the nuclides can sorb and the water composition. The materials in SFL 3-5 consist mainly of concrete and gravel. The water composition is different for the different sites. In Aberg the groundwater is saline (high ionic strength), in Ceberg it is non-saline (low ionic strength), and in Beberg both types of waters can be found.

The ionic strength of water in the gravel backfill surrounding the concrete structure is determined by the groundwater composition. Sorption data for high ionic strength is

used for Aberg, but for Ceberg with non-saline groundwater sorption data for low ionic strength should be used. The groundwater in Beberg can be both saline and non-saline, and consequently both sets of data are used for Beberg.

Sorption coefficients given for sorption on granite in the far-field (Carbol and Engkvist, 1997) is used for gravel in the near field as well. Data is missing for some of the modelled nuclides. Other literature data has then been used or, when not found, analogies to other nuclides has been done (Skagius *et al.,* 1999).

Water inside the concrete structure in SFL 3 and SFL 5 will have a high ionic strength independent on the type of groundwater. For sorption on concrete, data for saline water is therefore used throughout the calculations. Sorption data for concrete is not included in the work by Carbol and Engkvist (1997). Sorption coefficients for sorption on concrete have therefore been taken from other references or using analogies to other nuclides (Skagius *et al.,* 1999).

The sorption coefficients used for gravel and concrete materials are summarised in Table 5-2.

It is known that alkaline degradation of cellulose in the waste in SFL 3 will form isosaccharinic acid (ISA). ISA has been found to decrease the sorption coefficient for some nuclides (e.g. Bradbury and Van Loon, 1998). However, it is estimated that the low concentration of ISA in SFL 3 makes the effect of ISA on sorption negligible. On the other hand, the solubility, especially of actinides, can be affected, see Table 5-3 (Skagius *et al.,* 1999).

Table 5-2 Selected sorption coefficients K_d [m^3/kg] for sorption on gravel and concrete.

Element	Concrete	Gravel	
	pH 13.5	Saline	Non-saline
H	0	0	0
Be	0.05	0.02	0.1
$C_{inorganic}$	0.2	0.001	0.001
$C_{organic}$	0	0	0
Cl	0.006	0	0
Fe	0.04	0.02	0.1
Co	0.04	0.02	0.1
Ni	0.04	0.02	0.1
Se	0.006	0.001	0.001
Sr	0.001	0.0002	0.01
Zr	0.5	1	1
Nb	0.5	1	1
Mo	0.006	0	0
Tc	0.5	1	1
Pd	0.04	0.01	0.1
Ag	0.001	0.05	0.5
Cd	0.04	0.02	0.1
Sn	0.5	0.001	0.001
Sb	5	2	2
I	0.003	0	0
Cs	0.001	0.05	0.5
Ba	0.007	0.007	0.2
Pm	5	2	2
Sm	5	2	2
Eu	5	2	2
Ho	5	2	2
Pb	0.1	0.02	0.1
Ra	0.05	0.02	0.1
Ac	1	3	3
Th	5	5	5
Pa	5	1	1
U	5	5	5
Np	5	5	5
Pu	5	5	5
Am	1	3	3
Cm	1	3	3

Table 5-3 Solubility limits in concrete pore water [mole/l].

Element	Solubility	
	no effect of ISA	effect of ISA
Ni	$1 \cdot 10^{-7}$	$2 \cdot 10^{-7}$
Am, Cm	$1 \cdot 10^{-7}$	no limit
Pm	$9 \cdot 10^{-8}$	$3 \cdot 10^{-5}$
Pa, Np, Pu	$5 \cdot 10^{-9}$	no limit
Th, U [a)]	$5 \cdot 10^{-9}$	$7 \cdot 10^{-5}$

a) Analogous to Th.

5.1.3 Hydrological data

The near-field hydrology modelling (Holmén, 1997) together with the specific groundwater flow at the three sites (Table 5-4), give the specific flow of water through the repository. The specific flow through the different parts of SFL 3-5 are given in Table 5-5 assuming a horizontal flow parallel to SFL 3 and SFL 5 (Skagius *et al.,* 1999). The specific flow and the cross sectional area of the different barriers (structure and gravel backfill) used in the migration model give the total flow (Table 5-5).

Table 5-4 Specific groundwater flows [m^3/m^2, year] at the three sites used in this work (Skagius *et al.*, 1999).

Site	Specific groundwater flow
Aberg	10^{-2}
Beberg	10^{-3}
Ceberg	10^{-4}

Table 5-5 Specific flow [m^3/m^2, year] and total flow [m^3/year] in the near-field barriers in SFL 3-5 for a horizontal regional water flow along SFL 3 and SFL 5.

Site	SFL 3		SFL 4 [a)]	SFL 5	
	concrete structure	gravel backfill	gravel backfill and waste	concrete structure	gravel backfill
			Specific flow		
Aberg	$1{\cdot}10^{-4}$	0.31	3.75	$1{\cdot}10^{-4}$	0.32
Beberg	$1{\cdot}10^{-5}$	0.031	0.375	$1{\cdot}10^{-5}$	0.032
Ceberg	$1{\cdot}10^{-6}$	0.0031	0.0375	$1{\cdot}10^{-6}$	0.0032
			Cross sectional area in migration model [m^2]		
	116	136	44	116	136
			Total flow		
Aberg	$1.2{\cdot}10^{-2}$	42.3	165.5	$1.2{\cdot}10^{-2}$	43.7
Beberg	$1.2{\cdot}10^{-3}$	4.23	16.55	$1.2{\cdot}10^{-3}$	4.37
Ceberg	$1.2{\cdot}10^{-4}$	0.423	1.655	$1.2{\cdot}10^{-4}$	0.437

a) Flow in one of the two parallel tunnel sections.

5.2 Far-field data

The input data needed for modelling the far-field transport using FARF31 are release rates of nuclides from the near field (output data from COMP24), nuclide specific effective diffusivities and sorption coefficients in the far-field rock. In addition, several parameters describing the properties of the far-field rock are needed. These parameters are water travel time, Peclet number, flow-wetted surface area (based on volume flowing water), rock matrix diffusion porosity and maximum penetration depth into the

rock matrix, see Table 5-6. Water travel time and flow-wetted surface area are based on the results from the regional hydrology models (Svensson, 1997 and Hartley and Lindgren, 1997), see Skagius *et al.* (1999). The other data given in Table 5-6 are the same as those used in the safety assessment of the deep repository for spent fuel (Andersson, 1999).

Table 5-6 Compilation of data needed for modelling the radionuclide transport in the far field.

Parameter	Aberg	Beberg	Ceberg
Water travel time [year]	10	40	900
Peclet number [–]	10	10	10
Flow-wetted surface area [m^2/m^3] [a)]	770	10 000	1 000
Matrix porosity [m^3/m^3] [b)]	0.005	0.005	0.005
Maximum penetration depth [m]	2	2	20

a) Based on volume flowing water
b) The porosity available for inorganic ^{14}C, ^{36}Cl, and ^{129}I is reduced by one order of magnitude in non-saline waters due to anion exclusion (Skagius et al., 1999)

Radionuclide specific effective diffusivities in the rock matrix, D_e, (Ohlsson and Neretnieks, 1997) and sorption coefficients, K_d, (Carbol and Engkvist, 1997) used within this work are the same as those used in the safety assessment of the deep repository for spent fuel (SKB, 1999a). Some of the elements of importance in the waste in SFL 3-5 are not included in the data presented by Ohlsson and Neretnieks (1997) and Carbol and Engkvist (1997). When data on diffusivity is missing, they are estimated using the same method as that used by Ohlsson and Neretnieks (1997). To estimate sorption data, data from other references or chemical analogies have been used. Data on D_e and K_d are summarised in Table 5-7. The selection of diffusion and sorption data is further discussed in Skagius *et al.* (1999).

For Aberg sorption data and diffusivities derived for saline conditions are used, while data derived for non-saline conditions are used for Ceberg. The groundwater in Beberg can be both saline and non-saline. Consequently, both sets of data are used for Beberg.

Table 5-7 Radionuclide specific effective diffusivities D_e [m^2/s] and sorption coefficients K_d [m^3/kg] for saline and non-saline water.

Element	D_e		K_d	
	Saline	Non-saline	Saline	Non-saline
H	$1.0 \cdot 10^{-13}$	$1.0 \cdot 10^{-13}$	0	0
Be	$2.4 \cdot 10^{-14}$	$2.4 \cdot 10^{-14}$	0.02	0.1
$C_{inorganic}$	$5.0 \cdot 10^{-14}$	$5.0 \cdot 10^{-15}$	0.001	0.001
$C_{organic}$	$4.0 \cdot 10^{-14}$	$4.0 \cdot 10^{-14}$	0	0
Cl	$8.3 \cdot 10^{-14}$	$8.3 \cdot 10^{-15}$	0	0
Co	$2.9 \cdot 10^{-14}$	$2.9 \cdot 10^{-14}$	0.02	0.1
Ni	$2.8 \cdot 10^{-14}$	$2.8 \cdot 10^{-14}$	0.02	0.1
Se	$4.0 \cdot 10^{-14}$	$4.0 \cdot 10^{-14}$	0.001	0.001
Sr	$3.3 \cdot 10^{-14}$	$3.3 \cdot 10^{-13}$	0.0002	0.01
Zr	$4.0 \cdot 10^{-14}$	$4.0 \cdot 10^{-14}$	1	1
Nb	$4.0 \cdot 10^{-14}$	$4.0 \cdot 10^{-14}$	1	1
Mo	$4.0 \cdot 10^{-14}$	$4.0 \cdot 10^{-14}$	0	0
Tc [a)]	$4.0 \cdot 10^{-14}$	$4.0 \cdot 10^{-14}$	1	1
Cd	$3.0 \cdot 10^{-14}$	$3.0 \cdot 10^{-14}$	0.02	0.1
I	$8.3 \cdot 10^{-14}$	$8.3 \cdot 10^{-15}$	0	0
Cs	$8.8 \cdot 10^{-14}$	$8.8 \cdot 10^{-13}$	0.05	0.5
Pb	$4.0 \cdot 10^{-14}$	$4.0 \cdot 10^{-14}$	0.02	0.1
Ra	$3.7 \cdot 10^{-14}$	$3.7 \cdot 10^{-14}$	0.02	0.1
Th	$6.3 \cdot 10^{-15}$	$6.3 \cdot 10^{-15}$	5	5
U [a)]	$4.0 \cdot 10^{-14}$	$4.0 \cdot 10^{-14}$	5	5
Np [a)]	$4.0 \cdot 10^{-14}$	$4.0 \cdot 10^{-14}$	5	5
Pu	$4.0 \cdot 10^{-14}$	$4.0 \cdot 10^{-14}$	5	5
Am	$4.0 \cdot 10^{-14}$	$4.0 \cdot 10^{-14}$	3	3

a) Values for Tc(IV), U(IV), and Np(IV) respectively.

5.3 Biosphere data

The results from the regional hydrology modelling give the areas on the ground surface where radionuclides and toxic metals are released. This together with a classification of each site into different ecosystems is used to define the primary recipients, see Skagius *et al.* (1999). In Aberg there are two primary recipients classified as open coast and archipelago. In Beberg the nuclides are estimated to be released in an area classified as agricultural land. An area classified as peatland is fairly close to where the nuclides are estimated to be released in Beberg. For most of the nuclides studied the ecosystem-specific dose conversion factor for a peat area in Beberg is higher, or even much higher, than for agricultural land. The consequence of release to a peat area in Beberg is therefore also illustrated. The primary recipient in Ceberg is classified as peatland. Mean values for the ecosystem-specific dose conversion factors for these recipients (Nordlinder *et al.,* 1999) are given in Table 5-8.

Table 5-8 Mean values of ecosystem-specific dose conversion factors [Sv/Bq] for primary recipients (Nordlinder *et al.*, 1999).

Radio-nuclide	Aberg		Beberg		Ceberg
	Open coast	Archipelago	Agricultural land	Peatland	Peatland
^{3}H	$1.2\cdot10^{-20}$	$3.2\cdot10^{-18}$	$1.3\cdot10^{-15}$	$3.6\cdot10^{-16}$	$2.6\cdot10^{-16}$
^{10}Be	$1.9\cdot10^{-18}$	$3.9\cdot10^{-16}$	$1.3\cdot10^{-14}$	$8.6\cdot10^{-13}$	$6.2\cdot10^{-13}$
^{14}C	$6.7\cdot10^{-18}$	$1.7\cdot10^{-15}$	$2.0\cdot10^{-17}$	$6.5\cdot10^{-15}$	$4.6\cdot10^{-15}$
^{36}Cl	$5.7\cdot10^{-19}$	$1.6\cdot10^{-16}$	$4.0\cdot10^{-13}$	$2.2\cdot10^{-11}$	$1.5\cdot10^{-11}$
^{60}Co	$3.3\cdot10^{-18}$	$5.1\cdot10^{-16}$	$5.0\cdot10^{-18}$	$2.8\cdot10^{-13}$	$2.7\cdot10^{-13}$
^{59}Ni	$9.0\cdot10^{-20}$	$2.2\cdot10^{-17}$	$1.1\cdot10^{-14}$	$2.7\cdot10^{-13}$	$1.9\cdot10^{-13}$
^{63}Ni	$2.1\cdot10^{-19}$	$5.2\cdot10^{-17}$	$7.6\cdot10^{-17}$	$1.6\cdot10^{-13}$	$1.4\cdot10^{-13}$
^{79}Se	$5.3\cdot10^{-17}$	$1.4\cdot10^{-14}$	$1.6\cdot10^{-12}$	$1.7\cdot10^{-9}$	$1.2\cdot10^{-9}$
^{90}Sr	$5.0\cdot10^{-18}$	$1.3\cdot10^{-15}$	$2.8\cdot10^{-14}$	$1.8\cdot10^{-11}$	$1.6\cdot10^{-11}$
^{93}Zr	$9.8\cdot10^{-19}$	$9.0\cdot10^{-17}$	$3.0\cdot10^{-15}$	$4.4\cdot10^{-13}$	$3.3\cdot10^{-13}$
^{94}Nb	$1.5\cdot10^{-18}$	$2.1\cdot10^{-16}$	$2.4\cdot10^{-13}$	$2.0\cdot10^{-12}$	$1.5\cdot10^{-12}$
^{93}Mo	$3.5\cdot10^{-19}$	$9.2\cdot10^{-17}$	$8.7\cdot10^{-13}$	$2.5\cdot10^{-12}$	$1.7\cdot10^{-12}$
^{99}Tc	$6.1\cdot10^{-19}$	$1.7\cdot10^{-17}$	$5.9\cdot10^{-14}$	$4.2\cdot10^{-13}$	$2.9\cdot10^{-13}$
^{107}Pd	$2.6\cdot10^{-20}$	$1.2\cdot10^{-18}$	$2.7\cdot10^{-15}$	$6.4\cdot10^{-14}$	$4.4\cdot10^{-14}$
^{108m}Ag	$4.3\cdot10^{-18}$	$1.1\cdot10^{-15}$	$1.8\cdot10^{-14}$	$1.9\cdot10^{-11}$	$1.8\cdot10^{-11}$
^{126}Sn	$3.8\cdot10^{-18}$	$9.9\cdot10^{-16}$	$1.2\cdot10^{-12}$	$8.6\cdot10^{-11}$	$6.1\cdot10^{-11}$
^{129}I	$1.1\cdot10^{-16}$	$1.8\cdot10^{-14}$	$5.0\cdot10^{-11}$	$3.0\cdot10^{-11}$	$2.1\cdot10^{-11}$
^{135}Cs	$2.9\cdot10^{-18}$	$7.8\cdot10^{-16}$	$3.1\cdot10^{-13}$	$2.7\cdot10^{-12}$	$1.8\cdot10^{-12}$
^{137}Cs	$1.8\cdot10^{-17}$	$4.8\cdot10^{-15}$	$1.7\cdot10^{-16}$	$3.5\cdot10^{-12}$	$3.1\cdot10^{-12}$
^{151}Sm	$9.1\cdot10^{-20}$	$5.9\cdot10^{-18}$	$7.0\cdot10^{-19}$	$6.0\cdot10^{-15}$	$5.7\cdot10^{-15}$
^{166m}Ho	$1.9\cdot10^{-18}$	$1.3\cdot10^{-16}$	$3.4\cdot10^{-14}$	$1.9\cdot10^{-12}$	$1.6\cdot10^{-12}$
^{210}Pb	$6.0\cdot10^{-16}$	$8.5\cdot10^{-14}$	$3.4\cdot10^{-15}$	$1.6\cdot10^{-11}$	$1.6\cdot10^{-11}$
^{226}Ra	$7.0\cdot10^{-17}$	$1.6\cdot10^{-14}$	$7.2\cdot10^{-12}$	$1.2\cdot10^{-9}$	$9.4\cdot10^{-10}$
^{227}Ac	$1.4\cdot10^{-15}$	$1.8\cdot10^{-13}$	$7.4\cdot10^{-16}$	$6.2\cdot10^{-11}$	$6.1\cdot10^{-11}$
^{229}Th	$4.0\cdot10^{-16}$	$1.3\cdot10^{-14}$	$4.6\cdot10^{-12}$	$7.0\cdot10^{-9}$	$6.5\cdot10^{-9}$
^{230}Th	$1.7\cdot10^{-16}$	$5.4\cdot10^{-15}$	$3.0\cdot10^{-12}$	$4.0\cdot10^{-9}$	$3.7\cdot10^{-9}$
^{232}Th	$1.9\cdot10^{-16}$	$5.9\cdot10^{-15}$	$3.4\cdot10^{-12}$	$4.4\cdot10^{-9}$	$4.1\cdot10^{-9}$
^{231}Pa	$4.8\cdot10^{-17}$	$1.3\cdot10^{-14}$	$6.1\cdot10^{-12}$	$3.5\cdot10^{-9}$	$2.7\cdot10^{-9}$
^{233}U	$1.1\cdot10^{-17}$	$2.6\cdot10^{-15}$	$3.7\cdot10^{-13}$	$6.1\cdot10^{-12}$	$4.3\cdot10^{-12}$
^{234}U	$1.1\cdot10^{-17}$	$2.5\cdot10^{-15}$	$3.6\cdot10^{-13}$	$5.9\cdot10^{-12}$	$4.1\cdot10^{-12}$
^{235}U	$1.0\cdot10^{-17}$	$2.4\cdot10^{-15}$	$3.4\cdot10^{-13}$	$5.4\cdot10^{-12}$	$3.7\cdot10^{-12}$
^{236}U	$1.0\cdot10^{-17}$	$2.4\cdot10^{-15}$	$3.4\cdot10^{-13}$	$5.5\cdot10^{-12}$	$3.8\cdot10^{-12}$
^{238}U	$9.7\cdot10^{-18}$	$2.3\cdot10^{-15}$	$3.1\cdot10^{-13}$	$5.1\cdot10^{-12}$	$3.5\cdot10^{-12}$
^{237}Np	$7.6\cdot10^{-18}$	$2.0\cdot10^{-15}$	$2.1\cdot10^{-12}$	$1.1\cdot10^{-10}$	$7.5\cdot10^{-11}$
^{238}Pu	$4.8\cdot10^{-17}$	$5.1\cdot10^{-15}$	$3.6\cdot10^{-16}$	$3.7\cdot10^{-11}$	$3.4\cdot10^{-11}$
^{239}Pu	$5.5\cdot10^{-17}$	$6.4\cdot10^{-15}$	$1.2\cdot10^{-12}$	$4.1\cdot10^{-10}$	$3.0\cdot10^{-10}$
^{240}Pu	$5.5\cdot10^{-17}$	$6.3\cdot10^{-15}$	$7.7\cdot10^{-13}$	$3.6\cdot10^{-10}$	$2.7\cdot10^{-10}$
^{242}Pu	$5.3\cdot10^{-17}$	$6.1\cdot10^{-15}$	$1.3\cdot10^{-12}$	$4.1\cdot10^{-10}$	$3.0\cdot10^{-10}$
^{241}Am	$2.0\cdot10^{-16}$	$1.6\cdot10^{-14}$	$6.9\cdot10^{-14}$	$2.0\cdot10^{-10}$	$2.0\cdot10^{-10}$
^{242m}Am	$1.9\cdot10^{-16}$	$1.5\cdot10^{-14}$	$6.6\cdot10^{-15}$	$6.3\cdot10^{-11}$	$6.3\cdot10^{-11}$
^{243}Am	$2.0\cdot10^{-16}$	$1.6\cdot10^{-14}$	$2.6\cdot10^{-12}$	$1.8\cdot10^{-9}$	$1.9\cdot10^{-9}$
^{244}Cm	$9.7\cdot10^{-17}$	$4.0\cdot10^{-15}$	$4.1\cdot10^{-18}$	$5.5\cdot10^{-12}$	$5.5\cdot10^{-12}$
^{245}Cm	$2.1\cdot10^{-16}$	$1.6\cdot10^{-14}$	$1.0\cdot10^{-12}$	$9.8\cdot10^{-10}$	$8.1\cdot10^{-10}$
^{246}Cm	$2.1\cdot10^{-16}$	$1.6\cdot10^{-14}$	$7.1\cdot10^{-13}$	$8.1\cdot10^{-10}$	$6.8\cdot10^{-10}$

Wells are located at all three sites today. According to the results of the regional hydrology modelling there will be no release from SFL 3-5 to them. However, new wells could be sunk on the estimated release area in the future, and it is therefore difficult to ensure that nuclides will not be released to a well in the future. Release to a well is therefore also investigated. A "mean well" has been defined for each site. This "mean well" is defined as a well having a capacity equal to the arithmetic mean value of the capacity of the wells present today at each specific site. Based on data on capacity of wells sunk today (Nordlinder *et al.,* 1999) it is suggested that the capacity of the site specific "mean wells" is set to 300 l/h (Aberg), 1,000 l/h (Beberg), and 500 l/h (Ceberg) (Skagius *et al.,* 1999). The ecosystem-specific dose conversion factors for the "mean wells" are shown in Table 5-9.

Table 5-9 Mean values of ecosystem-specific dose conversion factors [Sv/Bq] for mean wells in Aberg, Beberg and Ceberg, based on data in Nordlinder *et al.* (1999).

Radio-nuclide	Aberg [300 l/h]	Beberg [1,000 l/h]	Ceberg [500 l/h]
^{3}H	$9.4 \cdot 10^{-15}$	$2.7 \cdot 10^{-15}$	$5.2 \cdot 10^{-15}$
^{10}Be	$4.6 \cdot 10^{-13}$	$1.3 \cdot 10^{-13}$	$2.6 \cdot 10^{-13}$
^{14}C	$2.4 \cdot 10^{-13}$	$7.0 \cdot 10^{-14}$	$1.4 \cdot 10^{-13}$
^{36}Cl	$7.3 \cdot 10^{-13}$	$2.1 \cdot 10^{-13}$	$3.7 \cdot 10^{-13}$
^{60}Co	$1.1 \cdot 10^{-12}$	$3.3 \cdot 10^{-13}$	$6.6 \cdot 10^{-13}$
^{59}Ni	$5.9 \cdot 10^{-14}$	$1.8 \cdot 10^{-14}$	$3.0 \cdot 10^{-14}$
^{63}Ni	$6.2 \cdot 10^{-14}$	$1.9 \cdot 10^{-14}$	$3.7 \cdot 10^{-14}$
^{79}Se	$2.7 \cdot 10^{-12}$	$7.7 \cdot 10^{-13}$	$1.3 \cdot 10^{-12}$
^{90}Sr	$1.3 \cdot 10^{-11}$	$3.7 \cdot 10^{-12}$	$7.3 \cdot 10^{-12}$
^{93}Zr	$3.7 \cdot 10^{-13}$	$1.1 \cdot 10^{-13}$	$2.2 \cdot 10^{-13}$
^{94}Nb	$3.4 \cdot 10^{-12}$	$9.8 \cdot 10^{-13}$	$1.7 \cdot 10^{-12}$
^{93}Mo	$2.5 \cdot 10^{-12}$	$7.7 \cdot 10^{-13}$	$1.2 \cdot 10^{-12}$
^{99}Tc	$5.5 \cdot 10^{-13}$	$1.6 \cdot 10^{-13}$	$2.8 \cdot 10^{-13}$
^{107}Pd	$2.3 \cdot 10^{-14}$	$6.6 \cdot 10^{-15}$	$1.2 \cdot 10^{-14}$
^{108m}Ag	$1.3 \cdot 10^{-12}$	$4.0 \cdot 10^{-13}$	$7.4 \cdot 10^{-13}$
^{126}Sn	$3.9 \cdot 10^{-12}$	$1.1 \cdot 10^{-12}$	$1.8 \cdot 10^{-12}$
^{129}I	$9.2 \cdot 10^{-11}$	$2.7 \cdot 10^{-11}$	$4.6 \cdot 10^{-11}$
^{135}Cs	$1.9 \cdot 10^{-12}$	$5.7 \cdot 10^{-13}$	$1.0 \cdot 10^{-12}$
^{137}Cs	$5.6 \cdot 10^{-12}$	$1.7 \cdot 10^{-12}$	$3.4 \cdot 10^{-12}$
^{151}Sm	$3.2 \cdot 10^{-14}$	$9.8 \cdot 10^{-15}$	$1.9 \cdot 10^{-14}$
^{166m}Ho	$2.0 \cdot 10^{-12}$	$6.1 \cdot 10^{-13}$	$1.2 \cdot 10^{-12}$
^{210}Pb	$1.9 \cdot 10^{-10}$	$5.6 \cdot 10^{-11}$	$1.1 \cdot 10^{-10}$
^{226}Ra	$1.2 \cdot 10^{-10}$	$3.4 \cdot 10^{-11}$	$6.5 \cdot 10^{-11}$
^{227}Ac	$3.4 \cdot 10^{-10}$	$9.8 \cdot 10^{-11}$	$2.0 \cdot 10^{-10}$
^{229}Th	$4.2 \cdot 10^{-10}$	$1.3 \cdot 10^{-10}$	$2.4 \cdot 10^{-10}$
^{230}Th	$2.1 \cdot 10^{-10}$	$6.2 \cdot 10^{-11}$	$1.2 \cdot 10^{-10}$
^{232}Th	$2.3 \cdot 10^{-10}$	$6.8 \cdot 10^{-11}$	$1.3 \cdot 10^{-10}$
^{231}Pa	$6.8 \cdot 10^{-10}$	$2.0 \cdot 10^{-10}$	$4.0 \cdot 10^{-10}$
^{233}U	$1.9 \cdot 10^{-11}$	$5.5 \cdot 10^{-12}$	$1.1 \cdot 10^{-11}$
^{234}U	$1.8 \cdot 10^{-11}$	$5.3 \cdot 10^{-12}$	$1.0 \cdot 10^{-11}$
^{235}U	$1.7 \cdot 10^{-11}$	$5.0 \cdot 10^{-12}$	$9.7 \cdot 10^{-12}$
^{236}U	$1.7 \cdot 10^{-11}$	$5.0 \cdot 10^{-12}$	$9.7 \cdot 10^{-12}$
^{238}U	$1.6 \cdot 10^{-11}$	$4.8 \cdot 10^{-12}$	$9.2 \cdot 10^{-12}$
^{237}Np	$4.7 \cdot 10^{-11}$	$1.3 \cdot 10^{-11}$	$2.5 \cdot 10^{-11}$
^{238}Pu	$6.6 \cdot 10^{-11}$	$2.0 \cdot 10^{-11}$	$4.0 \cdot 10^{-11}$
^{239}Pu	$2.2 \cdot 10^{-10}$	$6.7 \cdot 10^{-11}$	$1.3 \cdot 10^{-10}$
^{240}Pu	$1.8 \cdot 10^{-10}$	$5.5 \cdot 10^{-11}$	$1.1 \cdot 10^{-10}$
^{242}Pu	$2.3 \cdot 10^{-10}$	$7.0 \cdot 10^{-11}$	$1.3 \cdot 10^{-10}$
^{241}Am	$6.8 \cdot 10^{-11}$	$2.0 \cdot 10^{-11}$	$4.1 \cdot 10^{-11}$
^{242m}Am	$5.6 \cdot 10^{-11}$	$1.7 \cdot 10^{-11}$	$3.4 \cdot 10^{-11}$
^{243}Am	$1.3 \cdot 10^{-10}$	$3.9 \cdot 10^{-11}$	$7.4 \cdot 10^{-11}$
^{244}Cm	$3.2 \cdot 10^{-11}$	$9.8 \cdot 10^{-12}$	$1.9 \cdot 10^{-11}$
^{245}Cm	$1.6 \cdot 10^{-10}$	$4.8 \cdot 10^{-11}$	$9.6 \cdot 10^{-11}$
^{246}Cm	$1.4 \cdot 10^{-10}$	$4.2 \cdot 10^{-11}$	$8.3 \cdot 10^{-11}$

The data needed for calculating the concentration of toxic metals in the different recipients are compiled in Table 5-10. To get a measure of the consequences of the release of toxic metals from the SFL 3-5 repository the concentration arising in the different recipients from the release of metals is compared with typical concentrations presently found in different types of ecosystems (Skagius *et al.,* 1999). For the release of the toxic metals to a well guideline values for drinking water are used as comparison values, The values to which the estimated concentrations are compared are given in Table 5-11.

Table 5-10 General data on recipients (Bergström *et al.*, 1999).

	Aberg		Beberg		Ceberg
	Open coast	Archipelago	Agricultural land	Peatland	Peatland
Volume [m^3] [a)]	$1.7 \cdot 10^8$	$3.2 \cdot 10^6$	$6.3 \cdot 10^{4}$ [b)]	$5 \cdot 10^4$	$5 \cdot 10^4$
Mean residence time [year] [a)]	0.023	0.12	–	–	–
Water discharge rate [m^3/year]	$7.5 \cdot 10^9$	$2.6 \cdot 10^7$	–	–	–
Density [kg/m^3)	–	–	2,400	100	100
Porosity [m^3/m^3]	–	–	0.30	0.90	0.90

a) Value defined as mean value by Bergström et al. (1999).
b) Sum of topsoil, deep soil, and saturated zone.

Table 5-11 Suggested comparison values for toxic metals released from SFL 3-5.

Recipient	Be	Cd	Pb
Open coast and archipelago [µg/l]	0.01[a)]	0.01[a)]	0.24[a)]
Agricultural land [mg/kg dw]	0.6[b)]	0.23[c)]	17.1[c)]
Peatland [mg/kg dw]	0.095[d)]	0.095-0.95[d)]	0.38-19[d)]
Well water [mg/l]	0.004[e)]	0.001[f)]	0.01[f)]

[a)] *Naturvårdsverket (1999a)*
[b)] *IPCS (1990)*
[c)] *Naturvårdsverket (1999b)*
[d)] *Naturvårdsverket (1983)*
[e)] *US EPA (1996)*
[f)] *SLV (1993)*

6 Release calculations for the reference scenario

Using the models described in Chapter 4 and the input data given in Chapter 5, the transport of radionuclides in the near field and the far field has been studied. The different cases analysed are inside the scope of the reference scenario (SKB, 1999b). To illustrate the consequences of a release from the near field, the transport through the geosphere to the biosphere has also been modelled, resulting in dose to man. In the reference scenario, the geosphere and the biosphere are assumed to be stable. They are, as far as possible, treated in the same way as in the safety assessment of the deep repository for spent fuel (SKB, 1999a).

Transport of toxic metals has also been analysed. The elements modelled are lead, cadmium and beryllium.

6.1 Investigated cases

Several different cases within the reference scenario for the near field have been studied.

The waste allocated to SFL 3 contains cellulose that by alkaline hydrolysis can generate isosaccharinic acid (ISA). ISA is a strong complexing agent that increases the solubility of some nuclides, and can therefore influence the transport rate of radionuclides. In order to show the effect of organic complexing agents, SFL 3 has been modelled both with and without influence of ISA on the solubility of radionuclides.

The waste to be deposited in SFL 4 contains a great deal of surface contaminated material. An alternative being discussed is to wash the fuel storage canisters before depositing the waste. The activity being washed off would instead be disposed of in SFL 3. Even though this would reduce the activity in SFL 4 substantially, it would have a very little influence on the total activity within SFL 3. Two options have therefore been evaluated, a radionuclide inventory in SFL 4 with and without the activity deposited on the surfaces of the waste materials. The consequence of including the CRUD inventory has been studied for the near field only.

Three different regional water flow rates have been used: 0.1, 1 and 10 l/m^2, year. These flow rates correspond approximately to the flow rates estimated for Ceberg, Beberg and Aberg, respectively.

The groundwater condition in Beberg is such that both a saline and a non-saline groundwater may exist at repository depth. A high salinity reduces the sorption for some radionuclides, and thus increases their release rate. Two cases have therefore been defined with identical conditions, corresponding to those prevailing at Beberg, except for the water composition. One case with non-saline water, and the other with saline water.

6.2 Premises

The reference scenario defined for the analysis of the SFL 3-5 repository, and the expected evaluation of the conditions in the near-field barriers are described in the main report of the preliminary safety assessment (SKB, 1999b). All the investigated cases are based on the reference scenario and the results from hydrology studies (Holmén, 1997, Hartley and Lindgren, 1997 and Svensson, 1997). The following premises have therefore been chosen for calculating radionuclide transport in the barriers:

- The time it takes to refill the repository with groundwater after closure is neglected and all repository sections are saturated with water in year 2040.

- Waste containers of steel are already fully permeable to water at repository closure. The corrosion products that eventually form will not affect water flows through the containers or diffusive transport of dissolved components in the water.

- The properties of concrete moulds and concrete enclosures in SFL 3 and SFL 5 do not change with time.

- In all repository sections, the gravel backfill has high permeability to water. Most of the water that flows through SFL 3 and SFL 5 goes through the gravel backfill in the space between the concrete structure and the tunnel wall. Any small change that may occur in the porosity and sorption properties of the fill over long periods of time can be neglected.

- Gas initially entrapped in the repository or produced, e.g. by corrosion, do not influence the water flow in the repository or the migration of radionuclides.

- The water flow through SFL 3-5 is horizontal and parallel to SFL 3 and SFL 5 for all three repository sites.

- Due to the slow leaching of portlandite from cement and concrete, it is assumed that water within the concrete structure in SFL 3 and SFL 5 as well as water within the waste containers in SFL 4 (backfilled with concrete) has a pH of at least 12.5.

- Water in gravel surrounding the concrete structure in SFL 3 and SFL 5 as well as water outside the waste packages in SFL 4 is assumed to have the same composition as the ground water representative for the three sites.

- ^{14}C, ^{36}Cl, ^{93}Zr and ^{93}Mo, which are mainly present in the form of induced activity in metal parts in the waste in SFL 5, are released as the metal parts corrode (see Appendix D). The main part of the inventory of ^{3}H and ^{10}Be in SFL 5 are present within boron carbide in control rods. Due to possible damages in the material it is assumed that 5% of the inventory of ^{3}H and ^{10}Be is immediately accessible for dissolution in the water. For the remaining part it is assumed that it will take 100 years of corrosion before it can dissolve in the water (see Appendix D). The rest of the radionuclides, as well as the toxic metals, are immediately accessible for dissolution in the water regardless of where they are located in SFL 3-5.

- The radionuclide ^{59}Ni is solubility-limited in SFL 3 and SFL 5. This also applies to ^{232}Th and ^{238}U in SFL 3, provided the conditions are not affected by ISA. The toxic metal lead is also solubility-limited in SFL 3 and SFL 5. No further reduction in solubility due to isotope dilution has been accounted for.

- Dissolved radionuclides and toxic metals are transported out from waste packages to surrounding rock both by diffusion and by water flowing through the repository. Sorption in concrete and gravel retards their transport.

- Sorption data for high pH (≥ 12.5) and reducing conditions are chosen in waste packages and enclosures. However, different sorption data are used for the gravel backfill surrounding the concrete structure in SFL 3 and SFL 5 as well as the waste packages in SFL 4 depending on the type of ground water (saline or non-saline).

- The influence of the complexing agent isosaccharinic acid (ISA) on sorption is neglected, since its concentration will remain low. However, the possibility that ISA will influence solubility cannot be ruled out, so such a case is also calculated (applies only to SFL 3).

- The groundwater transports radionuclides and toxic metals in the far field. Transport is retarded due to diffusion and sorption in the rock matrix. Sorption data are chosen according to the groundwater representative for the site in question.

6.3 Screening calculations

The radionuclides reported for the waste in SFL 3-5 are summarised in Table 2.1. However, the estimated activity of many of them is low and/or the nuclides have a half-life that is short in comparison to the time scales for their migration to the biosphere. To reduce the calculation time, and the amount of nuclide specific input data needed for modelling the geosphere migration, screening calculations have been performed. This procedure is described and the results are given in Appendix E.

It has been possible to reduce the number of nuclides modelled within the chains further by taking the nuclide half-life into account. The chain 4N is for example one of the chains that are included in the modelled inventory in SFL 3. The half-life of ^{244}Cm and ^{240}Pu is much shorter than that for the next nuclide in the chain, ^{236}U. The initial inventory (in mole) of ^{244}Cm and ^{240}Pu can therefore be transferred to the initial inventory of ^{236}U. This leads to an overestimation of the release rate of ^{236}U for short times, but the maximum release rate is not affected. The nuclides, which are treated in this way, are summarised in Table 6-1.

Table 6-1 Inventories transferred from one nuclide to another.

Chain	SFL 3	SFL 4	SFL 5
4N	^{244}Cm, ^{240}Pu $\Rightarrow$ ^{236}U	not modelled	not modelled
4N+1	^{245}Cm, ^{241}Pu, ^{241}Am $\Rightarrow$ ^{237}Np	not modelled	not modelled
4N+2	^{246}Cm, ^{242}Pu $\Rightarrow$ ^{238}U	^{246}Cm, ^{242}Pu $\Rightarrow$ ^{238}U	^{246}Cm, ^{242}Pu $\Rightarrow$ ^{238}U
	^{242m}Am, ^{238}Pu $\Rightarrow$ ^{234}U	^{242m}Am, ^{238}Pu $\Rightarrow$ ^{234}U	^{242m}Am, ^{238}Pu $\Rightarrow$ ^{234}U
4N+3	not modelled	not modelled	not modelled

The activity of the radionuclides used in the migration calculations is given in Table 6-2. The inventory of ^{234}U, ^{236}U, ^{238}U and ^{237}Np is the total inventory after transferring the inventory from other nuclides as shown in Table 6-1. The inventory of inorganic ^{14}C, ^{36}Cl and ^{93}Mo in SFL 5 does not include the inventory in the waste category "PWR reactor tank". Scooping calculations have shown that this has an insignificant effect on the far-field release rate. This is discussed in Appendix D. The case where CRUD is included in the inventory in SFL 4 has been analysed for the near field only, and the inventory used in these calculations is that given in Table 2-1.

Table 6-2 Initial inventory [Bq] of the radionuclides included in the entire calculation chain (year 2040).

Radionuclide	Half-life [year]	SFL 3	SFL 4 w/o CRUD	SFL 5
^{3}H	12	$3.2 \cdot 10^{12}$	$1.6 \cdot 10^{9}$	$2.5 \cdot 10^{15}$
^{10}Be	$1.5 \cdot 10^{6}$	– [c]	– [c]	$1.4 \cdot 10^{11}$
$^{14}C_{inorg}$	$5.7 \cdot 10^{3}$	$3.5 \cdot 10^{13}$	$3.1 \cdot 10^{7}$	$1.3 \cdot 10^{14}$ [a]
$^{14}C_{org}$	$5.7 \cdot 10^{3}$	$8.2 \cdot 10^{4}$	–	–
^{36}Cl	$3.0 \cdot 10^{5}$	$2.1 \cdot 10^{10}$	$2.6 \cdot 10^{4}$	$2.0 \cdot 10^{11}$ [a]
^{60}Co	5.3	– [c]	$4.1 \cdot 10^{10}$	– [c]
^{59}Ni	$7.6 \cdot 10^{4}$	$1.6 \cdot 10^{14}$	$1.2 \cdot 10^{8}$	$1.2 \cdot 10^{15}$
^{63}Ni	$1.0 \cdot 10^{2}$	– [c]	$1.7 \cdot 10^{10}$	– [c]
^{79}Se	$1.1 \cdot 10^{6}$	$4.6 \cdot 10^{8}$	$5.0 \cdot 10^{3}$	$4.5 \cdot 10^{7}$
^{90}Sr	29	$2.3 \cdot 10^{12}$	$1.6 \cdot 10^{8}$	$5.6 \cdot 10^{11}$
^{93}Zr	$1.5 \cdot 10^{6}$	$2.1 \cdot 10^{10}$	– [c]	$2.2 \cdot 10^{12}$
^{94}Nb	$2.0 \cdot 10^{4}$	– [c]	$6.6 \cdot 10^{6}$	– [c]
^{93}Mo	$4.0 \cdot 10^{3}$	$2.4 \cdot 10^{11}$	$2.0 \cdot 10^{5}$	$1.4 \cdot 10^{12}$ [a]
^{99}Tc	$2.1 \cdot 10^{5}$	$5.8 \cdot 10^{11}$	$6.2 \cdot 10^{6}$	$3.2 \cdot 10^{11}$
^{129}I	$1.6 \cdot 10^{7}$	$3.4 \cdot 10^{7}$	$3.7 \cdot 10^{2}$	$3.4 \cdot 10^{6}$
^{135}Cs	$2.3 \cdot 10^{6}$	$5.7 \cdot 10^{8}$	– [c]	– [c]
^{137}Cs	30	– [c]	$1.2 \cdot 10^{9}$	– [c]
^{210}Pb	22	$2.7 \cdot 10^{11}$	< 1	< 1
^{226}Ra	$1.6 \cdot 10^{3}$	$3.8 \cdot 10^{11}$	< 1	< 1
^{229}Th	$7.3 \cdot 10^{3}$	$1.4 \cdot 10^{2}$	– [c]	– [c]
^{230}Th	$7.5 \cdot 10^{4}$	$1.8 \cdot 10^{5}$	< 1	73
^{232}Th	$1.4 \cdot 10^{10}$	$1.1 \cdot 10^{10}$	– [c]	– [c]
^{233}U	$1.6 \cdot 10^{5}$	$3.1 \cdot 10^{4}$	– [c]	– [c]
^{234}U [b]	$2.5 \cdot 10^{5}$	$9.1 \cdot 10^{8}$	56	$4.6 \cdot 10^{5}$
^{236}U [b]	$2.3 \cdot 10^{7}$	$5.8 \cdot 10^{8}$	– [c]	– [c]
^{238}U [b]	$4.5 \cdot 10^{9}$	$4.6 \cdot 10^{10}$	9.6	$7.5 \cdot 10^{4}$
^{237}Np [b]	$2.1 \cdot 10^{6}$	$1.2 \cdot 10^{9}$	– [c]	– [c]

a) Inventory of inorganic ^{14}C, ^{36}Cl and ^{93}Mo given in this table excludes the activity in the PWR reactor tank.
b) The inventory of ^{234}U, ^{236}U, ^{238}U and ^{237}Np is the total inventory after transferring the inventory from other nuclides as shown in Table 6-1.
c) Screened out due to low near-field release

7 Release calculations for the near field

In this chapter, the results of the calculations of radionuclide transport in the near field are presented. The chapter is divided into three sections, each section focusing on one repository part. All sections have the same disposition. First, the near-field release rate as a function of time is shown in graphical form (Figures 7-1, 7-5 and 7-9) for the case with the water flow rate that prevails in Beberg and saline water. Next, the effect of different water flow rates is discussed, followed by the influence of water composition (saline or non-saline) on the near-field release rate. Results are presented for those nuclides for which the release rate varies between saline and non-saline waters only.

In addition, release rates from the near field of SFL 3 are given when effects of ISA on radionuclide solubility is taken into account, as well as release rates from the near field of SFL 4 when the surface contamination in included in the radionuclide inventory.

The maximum release rate and the time when the maximum release rate is obtained are also compiled in tables for all modelled nuclides and the calculation cases representing the water flow rate in Aberg, Beberg (saline and non-saline) and Ceberg, respectively.

The release rates in the figures are shown up to a time of 10^7 years from repository closure at the year 2040. The lower limit for which the release rate is specified is set to $1 \cdot 10^{-3}$ Bq/year. The maximum near-field release rate is, for some nuclides, below this limit. The maximum release rate is in that case specified as $< 1 \cdot 10^{-3}$ Bq/year and the time when it is obtained is omitted. In all figures and tables in this and the following chapters, inorganic ^{14}C and organic ^{14}C are labelled ^{14}C and $^{14}C_{org}$, respectively.

For symmetry reasons, only half of the SFL 4 tunnel is modelled. However, the results presented for SFL 4 in this and in subsequent chapters are the total release from SFL 4.

Some of the data given in tables indicate that the results for two different cases differ even though one a priori knows that they should not. For example, the migration of ^{79}Se is independent of the water composition. However, the time of maximum near-field release rate of ^{79}Se in SFL 4 from Beberg is different for saline and non-saline groundwater conditions (see Table 7-3). This is an effect of differences in the time discretization used by COMP24. The effect can also be exaggerated when the results are rounded off as presented in the tables.

7.1 SFL 3

The radionuclide release from SFL 3 in Beberg (saline waters) as a function of time is shown in Figure 7-1. In the beginning, ^3H dominates the release rate. The maximum release rate is about 10^4 Bq/year and is obtained after some 100 years. Later the release rate is dominated by ^{93}Mo and, to same extent, ^{36}Cl and inorganic ^{14}C. ^{93}Mo have a maximum release rate of approximately $1 \cdot 10^6$ Bq/year, and ^{36}Cl and inorganic ^{14}C around $3 \cdot 10^5$ Bq/year. The overall highest release rate (10^7 Bq/year) is obtained after some 10^5 years when ^{59}Ni dominates. ^{93}Zr, ^{226}Ra and ^{210}Pb are the most important nuclides for times around 10^6 years and longer. The release curves for ^{226}Ra and ^{210}Pb have two peaks. The first peak after 10^4 years stems from the initial inventory of ^{226}Ra,

and the second is obtained when ^{238}U and its daughters ^{234}U and ^{230}Th in the chain 4N+2 decay on the way towards the stable ^{206}Pb.

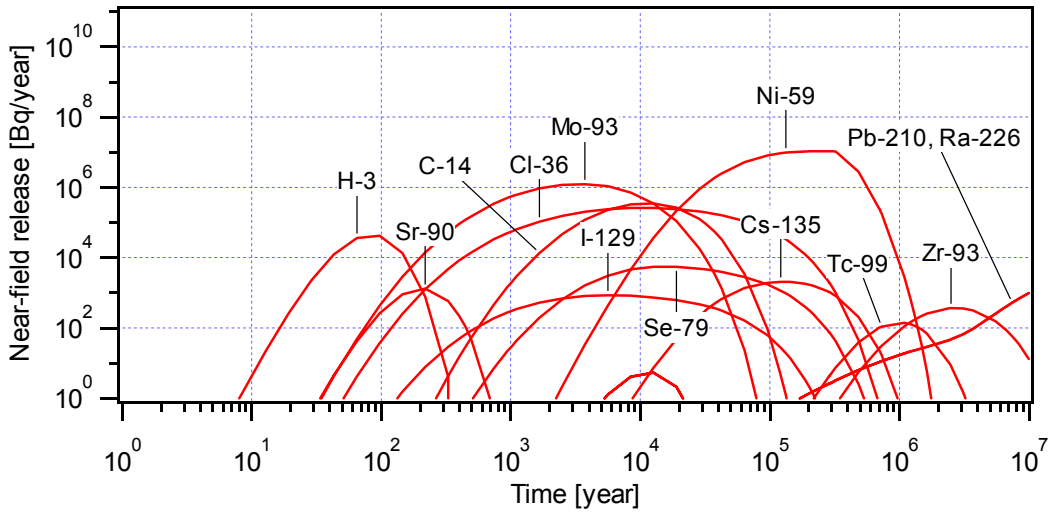

Figure 7-1 Near-field release from SFL 3 in Beberg, saline water.

7.1.1 Effect of water flow rate

Three different specific water flow rates have been examined, high (10 l/m^2, year), medium (1) and low (0.1) representative for Aberg, Beberg and Ceberg, respectively. The results for dominating nuclides are shown in Figure 7-2. For ^{59}Ni, ^{90}Sr and ^{210}Pb results are given for a high and a medium flow only. For these nuclides, the result for Ceberg (lowest flow rate) is not only affected by the difference in water flow rate, but also by the difference in water composition (non-saline in Ceberg versus saline in Aberg and Beberg).

The water flow rate has a significant influence on the near-field release rate of some nuclides. The major effect of reducing the flow rate from 10 l/m^2, year to 0.1 l/m^2, year is that the release rate of the short-lived nuclides ^{3}H and ^{90}Sr is reduced significantly. There is also a large effect on the release rate of ^{99}Tc and ^{237}Np.

At 10 l/m^2, year ^{3}H and ^{59}Ni have the highest release rates (10^7 Bq/year) followed by inorganic ^{14}C, ^{90}Sr and ^{93}Mo at 10^6 Bq/year. Reducing the flow rate by one order of magnitude, the maximum release rate of ^{3}H, and also of ^{90}Sr, is reduced approximately 10^3 times (Figure 7-2). ^{59}Ni on the other hand is almost unaffected. Even though the flow is reduced to 0.1 l/m^2, year, ^{3}H will still dominate the release at short times but its maximum release rate is reduced to less than 10^2 Bq/year.

Inorganic ^{14}C, and even more ^{36}Cl and ^{93}Mo, are less sensitive to changes in the flow rate. Reducing the flow rate from 10 to 1 l/m^2, year has a limited effect on the release rate of these nuclides. At 0.1 l/m^2, year the release rate of inorganic ^{14}C and ^{93}Mo is reduced between one and two orders of magnitude in comparison to that at the highest flow rate. For ^{36}Cl the reduction is even smaller.

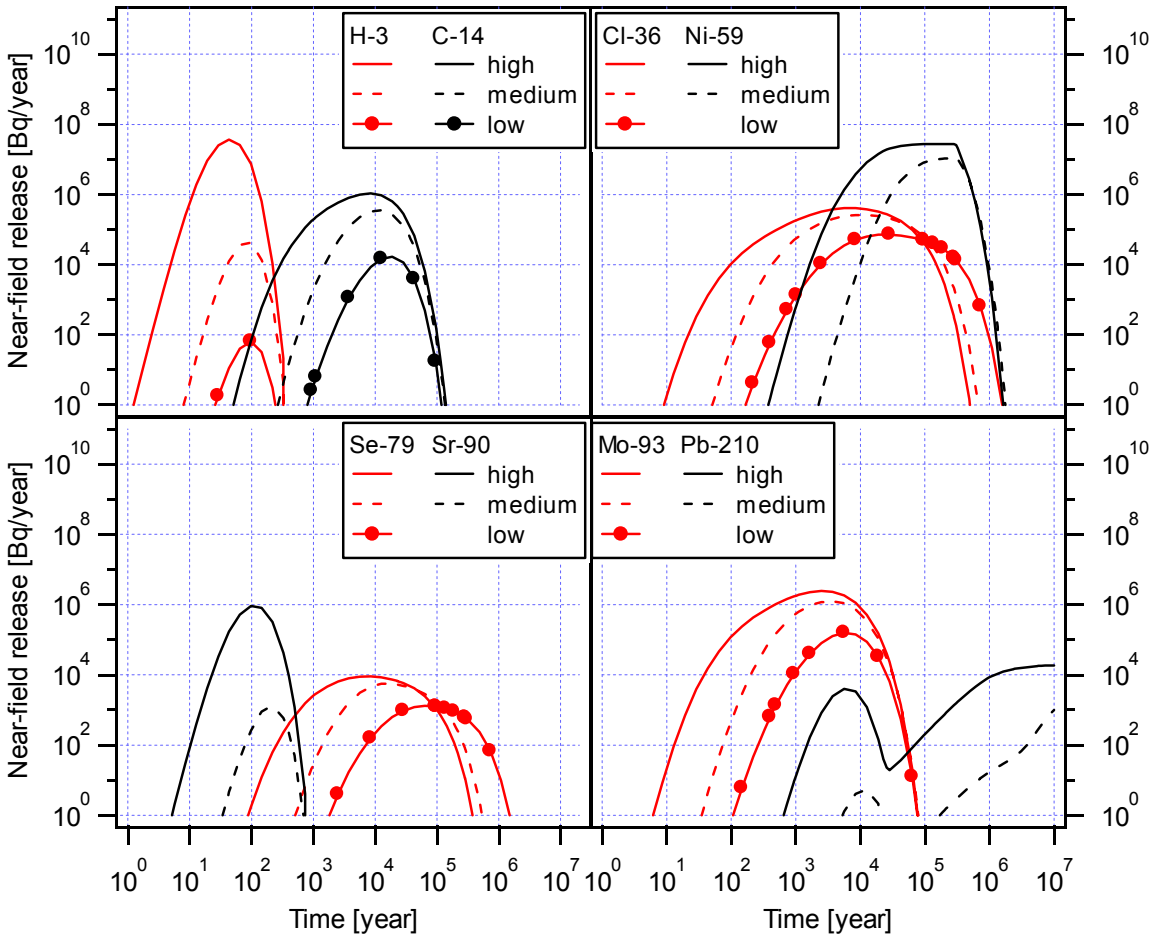

Figure 7-2 Effect of water flow rate on the near-field release from SFL 3.

7.1.2 Effect of water composition

As shown in Chapter 5, the sorption coefficient for sorption on gravel is the only physical or chemical property used as input data to the near-field model that is dependent on water composition. Most of the nuclides of importance for the resulting dose from SFL 3 (see Chapter 9) have a sorption coefficient on gravel that is independent of the type of water (saline or non-saline). However, for ^{59}Ni, ^{90}Sr, ^{135}Cs, ^{210}Pb and ^{226}Ra the sorption coefficient is higher in non-saline water. The release of these nuclides is therefore delayed and the release rate reduced in comparison to that in saline water.

Based on the conditions prevailing in Beberg, the reduction in release rate in non-saline water for ^{59}Ni, ^{210}Pb and ^{226}Ra is a factor of 5 and for ^{135}Cs a factor of 13. The release rate of ^{90}Sr on the other hand is reduced by eight orders of magnitude. The effect of having non-saline water in Beberg instead of saline on the near-field release rate is shown in Figure 7-3.

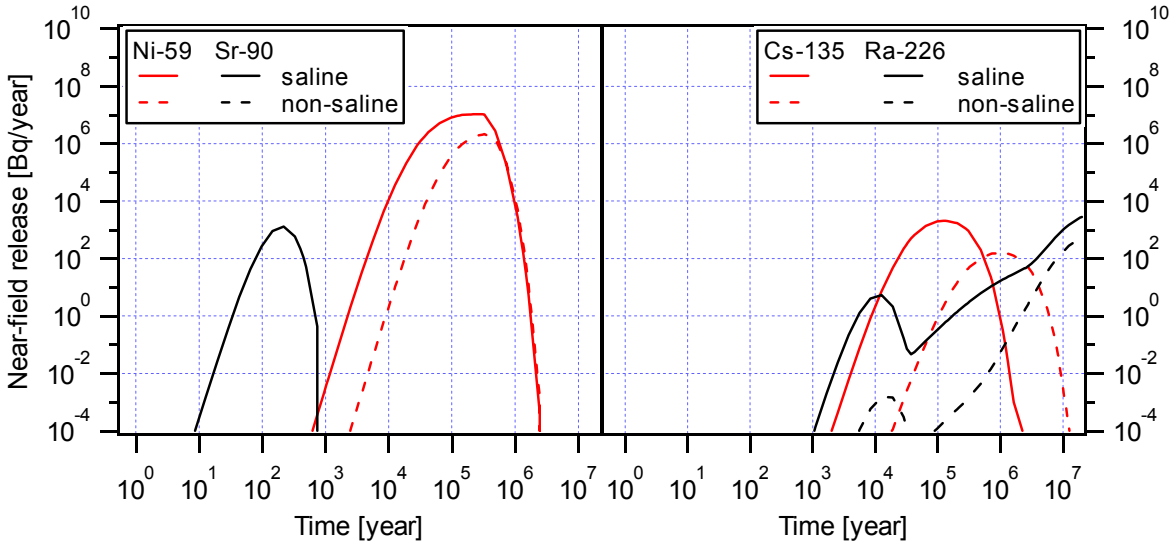

Figure 7-3 Effect of water composition on the near-field release from SFL 3. Medium flow rate.

The maximum near-field release rates from SFL 3 based on the water flow rates and water composition representative for the three sites are summarised in Table 7-1.

Table 7-1 Maximum near-field release rates from SFL 3 (no influence of ISA).

Nuclide	Half-life	Aberg (saline)		Beberg (saline)		Beberg (non-saline)		Ceberg (non-saline)	
		Time of maximum release rate	Maximum release rate	Time of maximum release rate	Maximum release rate	Time of maximum release rate	Maximum release rate	Time of maximum release rate	Maximum release rate
	[year]	[year]	[Bq/year]	[year]	[Bq/year]	[year]	[Bq/year]	[year]	[Bq/year]
^{3}H	12	$4 \cdot 10^{1}$	$4 \cdot 10^{7}$	$1 \cdot 10^{2}$	$4 \cdot 10^{4}$	$1 \cdot 10^{2}$	$4 \cdot 10^{4}$	$1 \cdot 10^{2}$	$6 \cdot 10^{1}$
^{14}C	$5.7 \cdot 10^{3}$	$8 \cdot 10^{3}$	$1 \cdot 10^{6}$	$1 \cdot 10^{4}$	$4 \cdot 10^{5}$	$1 \cdot 10^{4}$	$4 \cdot 10^{5}$	$2 \cdot 10^{4}$	$2 \cdot 10^{4}$
$^{14}C_{org}$	$5.7 \cdot 10^{3}$	$2 \cdot 10^{2}$	$6 \cdot 10^{1}$	$9 \cdot 10^{2}$	$3 \cdot 10^{1}$	$9 \cdot 10^{2}$	$3 \cdot 10^{1}$	$4 \cdot 10^{3}$	3
^{36}Cl	$3.0 \cdot 10^{5}$	$6 \cdot 10^{3}$	$4 \cdot 10^{5}$	$8 \cdot 10^{3}$	$3 \cdot 10^{5}$	$8 \cdot 10^{3}$	$3 \cdot 10^{5}$	$3 \cdot 10^{4}$	$7 \cdot 10^{4}$
^{59}Ni	$7.6 \cdot 10^{4}$	$3 \cdot 10^{5}$	$3 \cdot 10^{7}$	$3 \cdot 10^{5}$	$1 \cdot 10^{7}$	$3 \cdot 10^{5}$	$2 \cdot 10^{6}$	$5 \cdot 10^{5}$	$2 \cdot 10^{4}$
^{79}Se	$1.1 \cdot 10^{6}$	$8 \cdot 10^{3}$	$9 \cdot 10^{3}$	$2 \cdot 10^{4}$	$5 \cdot 10^{3}$	$2 \cdot 10^{4}$	$5 \cdot 10^{3}$	$6 \cdot 10^{4}$	$1 \cdot 10^{3}$
^{90}Sr	29	$1 \cdot 10^{2}$	$9 \cdot 10^{5}$	$2 \cdot 10^{2}$	$1 \cdot 10^{3}$	–	$< 1 \cdot 10^{-3}$	–	$< 1 \cdot 10^{-3}$
^{93}Zr	$1.5 \cdot 10^{6}$	$9 \cdot 10^{5}$	$3 \cdot 10^{3}$	$3 \cdot 10^{6}$	$4 \cdot 10^{2}$	$3 \cdot 10^{6}$	$4 \cdot 10^{2}$	$4 \cdot 10^{6}$	6
^{93}Mo	$4.0 \cdot 10^{3}$	$2 \cdot 10^{3}$	$2 \cdot 10^{6}$	$4 \cdot 10^{3}$	$1 \cdot 10^{6}$	$4 \cdot 10^{3}$	$1 \cdot 10^{6}$	$6 \cdot 10^{3}$	$2 \cdot 10^{5}$
^{99}Tc	$2.1 \cdot 10^{5}$	$5 \cdot 10^{5}$	$2 \cdot 10^{4}$	$1 \cdot 10^{6}$	$1 \cdot 10^{2}$	$1 \cdot 10^{6}$	$1 \cdot 10^{2}$	$1 \cdot 10^{6}$	$4 \cdot 10^{-1}$
^{129}I	$1.6 \cdot 10^{7}$	$4 \cdot 10^{3}$	$1 \cdot 10^{3}$	$6 \cdot 10^{3}$	$9 \cdot 10^{2}$	$6 \cdot 10^{3}$	$9 \cdot 10^{2}$	$2 \cdot 10^{4}$	$2 \cdot 10^{2}$
^{135}Cs	$2.3 \cdot 10^{6}$	$2 \cdot 10^{4}$	$2 \cdot 10^{4}$	$1 \cdot 10^{5}$	$2 \cdot 10^{3}$	$1 \cdot 10^{6}$	$2 \cdot 10^{2}$	$3 \cdot 10^{6}$	4
^{236}U	$2.3 \cdot 10^{7}$	$6 \cdot 10^{6}$	$1 \cdot 10^{1}$	$2 \cdot 10^{7}$	3	$2 \cdot 10^{7}$	3	$5 \cdot 10^{7}$	$1 \cdot 10^{-1}$
^{232}Th	$1.4 \cdot 10^{10}$	$4 \cdot 10^{7}$	9	$1 \cdot 10^{8}$	6	$1 \cdot 10^{8}$	6	$2 \cdot 10^{9}$	2
^{237}Np	$2.1 \cdot 10^{6}$	$4 \cdot 10^{6}$	6	$8 \cdot 10^{6}$	$2 \cdot 10^{-1}$	$8 \cdot 10^{6}$	$2 \cdot 10^{-1}$	–	$< 1 \cdot 10^{-3}$
^{233}U	$1.6 \cdot 10^{5}$	$4 \cdot 10^{6}$	6	$8 \cdot 10^{6}$	$2 \cdot 10^{-1}$	$8 \cdot 10^{6}$	$2 \cdot 10^{-1}$	$1 \cdot 10^{7}$	$1 \cdot 10^{-3}$
^{229}Th	$7.3 \cdot 10^{3}$	$4 \cdot 10^{6}$	7	$8 \cdot 10^{6}$	$2 \cdot 10^{-1}$	$8 \cdot 10^{6}$	$2 \cdot 10^{-1}$	$1 \cdot 10^{7}$	$1 \cdot 10^{-3}$
^{238}U	$4.5 \cdot 10^{9}$	$2 \cdot 10^{8}$	$3 \cdot 10^{1}$	$3 \cdot 10^{8}$	$2 \cdot 10^{1}$	$3 \cdot 10^{8}$	$2 \cdot 10^{1}$	$2 \cdot 10^{9}$	5
^{234}U	$2.5 \cdot 10^{5}$	$2 \cdot 10^{7}$	$4 \cdot 10^{1}$	$1 \cdot 10^{8}$	$2 \cdot 10^{1}$	$1 \cdot 10^{8}$	$2 \cdot 10^{1}$	$1 \cdot 10^{9}$	5
^{230}Th	$7.5 \cdot 10^{4}$	$2 \cdot 10^{7}$	$4 \cdot 10^{1}$	$1 \cdot 10^{8}$	$2 \cdot 10^{1}$	$1 \cdot 10^{8}$	$2 \cdot 10^{1}$	$1 \cdot 10^{9}$	5
^{226}Ra	$1.6 \cdot 10^{3}$	$2 \cdot 10^{7}$	$2 \cdot 10^{4}$	$9 \cdot 10^{7}$	$5 \cdot 10^{3}$	$1 \cdot 10^{8}$	$9 \cdot 10^{2}$	$1 \cdot 10^{9}$	$3 \cdot 10^{2}$
^{210}Pb	22	$2 \cdot 10^{7}$	$2 \cdot 10^{4}$	$9 \cdot 10^{7}$	$5 \cdot 10^{3}$	$1 \cdot 10^{8}$	$9 \cdot 10^{2}$	$1 \cdot 10^{9}$	$3 \cdot 10^{2}$

7.1.3 Effect of ISA

The concentration of ISA in SFL 3 is estimated to be too low to have an influence on nuclide sorption, but the solubility of some elements is increased (see Table 5-3 and Skagius *et al.,* 1999). When the effect of ISA on solubility is neglected, ^{59}Ni, ^{232}Th and ^{238}U in SFL 3 are all solubility-limited. The near-field release of ^{232}Th and of nuclides in chain 4N+2 in Aberg for the uninfluenced case is shown in the left part of Figure 7-4.

When the effect of ISA is taken into account, the solubility of ^{232}Th and ^{238}U is increased by approximately four orders of magnitude. As a consequence, none of them are solubility-limited any more. Indirectly this also affects the release rate of the daughters of ^{238}U. The maximum release rate of ^{232}Th and of ^{238}U and its daughters increases by approximately one order of magnitude (see the right part of Figure 7-4). Note that ^{226}Ra and ^{210}Pb dominate the total release rate from SFL 3 after about 10^6 years from repository closure. The solubility of ^{59}Ni is doubled under the influence of ISA, and so is the maximum release rate.

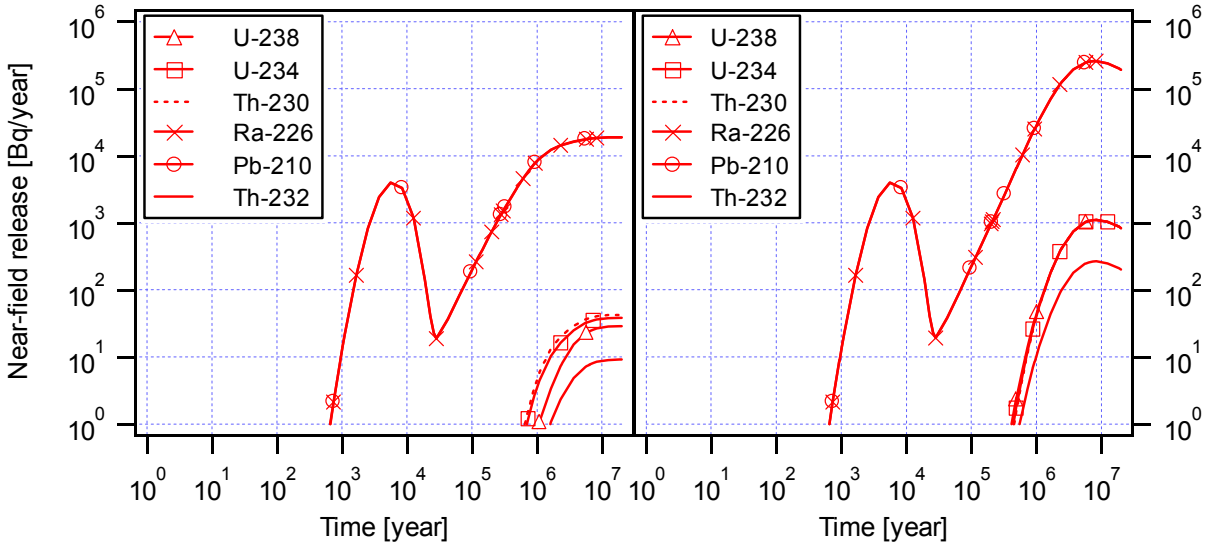

Figure 7-4 Effect of ISA on the near-field release from SFL 3 in Aberg. High flow rate. Without (left) and with influence of ISA (right).

The effect of ISA on the near-field release rate from SFL 3 in Aberg, Beberg and Ceberg is summarised in Table 7-2. With the exception of ^{226}Ra and ^{210}Pb, the release rate of nuclides being affected by ISA is not affected by water composition why the differences between Ceberg and Aberg/Beberg in this table are due to the difference in water flow.

Table 7-2 Maximum near-field release rates from SFL 3 (influence of ISA).

Nuclide	Chain	Half-life	Aberg (saline)		Beberg (saline)		Beberg (non-saline)		Ceberg (non-saline)	
			Time of maximum release rate	Maximum release rate	Time of maximum release rate	Maximum release rate	Time of maximum release rate	Maximum release rate	Time of maximum release rate	Maximum release rate
		[year]	[year]	[Bq/year]	[year]	[Bq/year]	[year]	[Bq/year]	[year]	[Bq/year]
^{59}Ni		$7.6 \cdot 10^{4}$	$2 \cdot 10^{5}$	$5 \cdot 10^{7}$	$2 \cdot 10^{5}$	$2 \cdot 10^{7}$	$3 \cdot 10^{5}$	$4 \cdot 10^{6}$	$3 \cdot 10^{5}$	$4 \cdot 10^{4}$
^{236}U	4N	$2.3 \cdot 10^{7}$	$6 \cdot 10^{6}$	$1 \cdot 10^{1}$	$2 \cdot 10^{7}$	3	$2 \cdot 10^{7}$	3	$5 \cdot 10^{7}$	$1 \cdot 10^{-1}$
^{232}Th	4N	$1.4 \cdot 10^{10}$	$8 \cdot 10^{6}$	$3 \cdot 10^{2}$	$4 \cdot 10^{7}$	$1 \cdot 10^{2}$	$3 \cdot 10^{7}$	$1 \cdot 10^{2}$	$2 \cdot 10^{8}$	$2 \cdot 10^{1}$
^{237}Np	4N+1	$2.1 \cdot 10^{6}$	$4 \cdot 10^{6}$	6	$8 \cdot 10^{6}$	$2 \cdot 10^{-1}$	$8 \cdot 10^{6}$	$2 \cdot 10^{-1}$	–	$< 1 \cdot 10^{-3}$
^{233}U	4N+1	$1.6 \cdot 10^{5}$	$4 \cdot 10^{6}$	6	$8 \cdot 10^{6}$	$2 \cdot 10^{-1}$	$8 \cdot 10^{6}$	$2 \cdot 10^{-1}$	$1 \cdot 10^{7}$	$1 \cdot 10^{-3}$
^{229}Th	4N+1	$7.3 \cdot 10^{3}$	$4 \cdot 10^{6}$	7	$8 \cdot 10^{6}$	$2 \cdot 10^{-1}$	$8 \cdot 10^{6}$	$2 \cdot 10^{-1}$	$1 \cdot 10^{7}$	$1 \cdot 10^{-3}$
^{238}U	4N+2	$4.5 \cdot 10^{9}$	$8 \cdot 10^{6}$	$1 \cdot 10^{3}$	$4 \cdot 10^{7}$	$5 \cdot 10^{2}$	$3 \cdot 10^{7}$	$5 \cdot 10^{2}$	$1 \cdot 10^{8}$	$9 \cdot 10^{1}$
^{234}U	4N+2	$2.5 \cdot 10^{5}$	$8 \cdot 10^{6}$	$1 \cdot 10^{3}$	$4 \cdot 10^{7}$	$5 \cdot 10^{2}$	$3 \cdot 10^{7}$	$5 \cdot 10^{2}$	$1 \cdot 10^{8}$	$9 \cdot 10^{1}$
^{230}Th	4N+2	$7.5 \cdot 10^{4}$	$8 \cdot 10^{6}$	$1 \cdot 10^{3}$	$4 \cdot 10^{7}$	$5 \cdot 10^{2}$	$3 \cdot 10^{7}$	$5 \cdot 10^{2}$	$1 \cdot 10^{8}$	$9 \cdot 10^{1}$
^{226}Ra	4N+2	$1.6 \cdot 10^{3}$	$8 \cdot 10^{6}$	$3 \cdot 10^{5}$	$3 \cdot 10^{7}$	$1 \cdot 10^{5}$	$3 \cdot 10^{7}$	$3 \cdot 10^{4}$	$1 \cdot 10^{8}$	$4 \cdot 10^{3}$
^{210}Pb	4N+2	22	$8 \cdot 10^{6}$	$3 \cdot 10^{5}$	$3 \cdot 10^{7}$	$1 \cdot 10^{5}$	$3 \cdot 10^{7}$	$3 \cdot 10^{4}$	$1 \cdot 10^{8}$	$4 \cdot 10^{3}$

7.2 SFL 4

The radionuclide release from SFL 4 in Beberg (saline waters) as a function of time is shown in Figure 7-5. The radionuclide inventory is based on the assumption that the waste does not contain any surface contamination. The inventory then contains only small amounts of long-lived nuclides in comparison to SFL 3 and SFL 5. As a result, the total release rate from SFL 4 decreases rapidly with time.

The nuclides are released much faster from SFL 4 than from SFL 3 and SFL 5. There are two reasons for this. The first reason is the flow rate of water, which is higher through SFL 4 than through the other two tunnels. The second reason is the repository layout, where the SFL 3 and SFL 5 repositories with their concrete structure and backfill material force the water to flow predominantly outside the structure (see Chapter 5). The transport inside the structure along the tunnel is therefore slow in comparison to that outside the structure. The nuclides must diffuse from the waste to the backfill material surrounding the structure before being transported along the tunnel. In SFL 4 there is no concrete structure, and the waste containers made of steel are assumed to be degraded why there is water flowing through the waste. During the first 10 to 100 years after repository closure, the total near-field release from SFL 3-5 is therefore dominated by the release from SFL 4.

In the beginning, ^{3}H and ^{90}Sr dominate the release from SFL 4 (Figure 7-5). ^{3}H gives the highest release rate in SFL 4, $6 \cdot 10^{6}$ Bq/year. After some 100 years from repository closure, ^{63}Ni and later ^{59}Ni dominates the release.

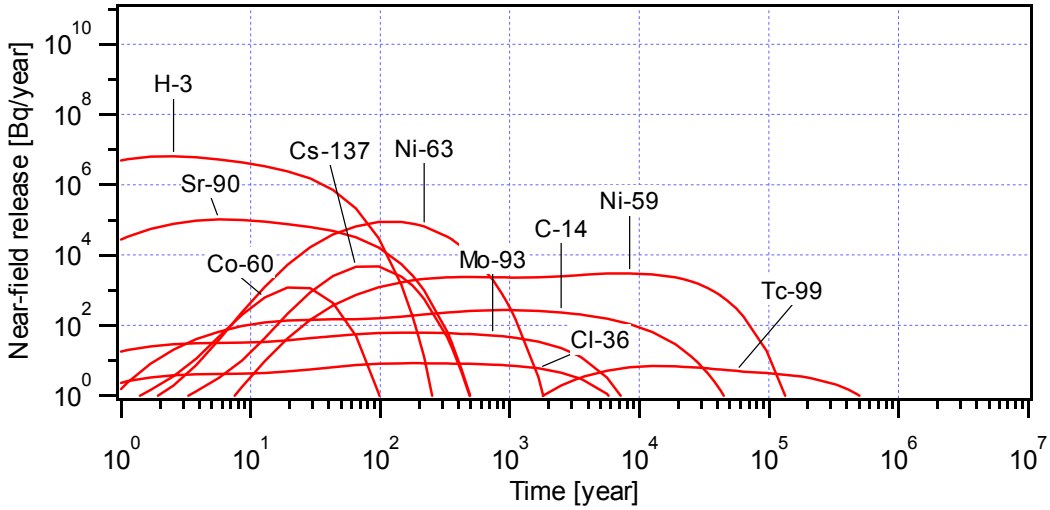

Figure 7-5 Near-field release from SFL 4 in Beberg, saline water.

7.2.1 Effect of water flow rate

Even though the specific water flow rate is reduced from 10 l/m^2, year to 0.1 l/m^2, year, it is the same nuclides that dominate the release rate. A general conclusion is that the maximum release rate roughly scales with the water flow rate. In SFL 3 and SFL 5 this is not the case. The explanation is that the release rate is determined by the advective transport solely in SFL 4, and that, in some cases, the barriers in SFL 3 and SFL 5 can control the release.

The near-field release rate for selected nuclides at different water flow rates are shown in Figure 7-6. Changing the water flow rate in SFL 3 had a significant influence on the release rate of ^{3}H and ^{90}Sr. This is to some extent also true for SFL 4. However, these nuclides are released so fast, that they still dominate the near-field release rate at all three sites for time scales up to 50 - 100 years from repository closure. Sorption in concrete and backfill material results in that ^{63}Ni decays to a large extent before being released. The importance of this effect increases at a lower water flow rate. This is also true for ^{59}Ni, but not as marked due to its longer half-life.

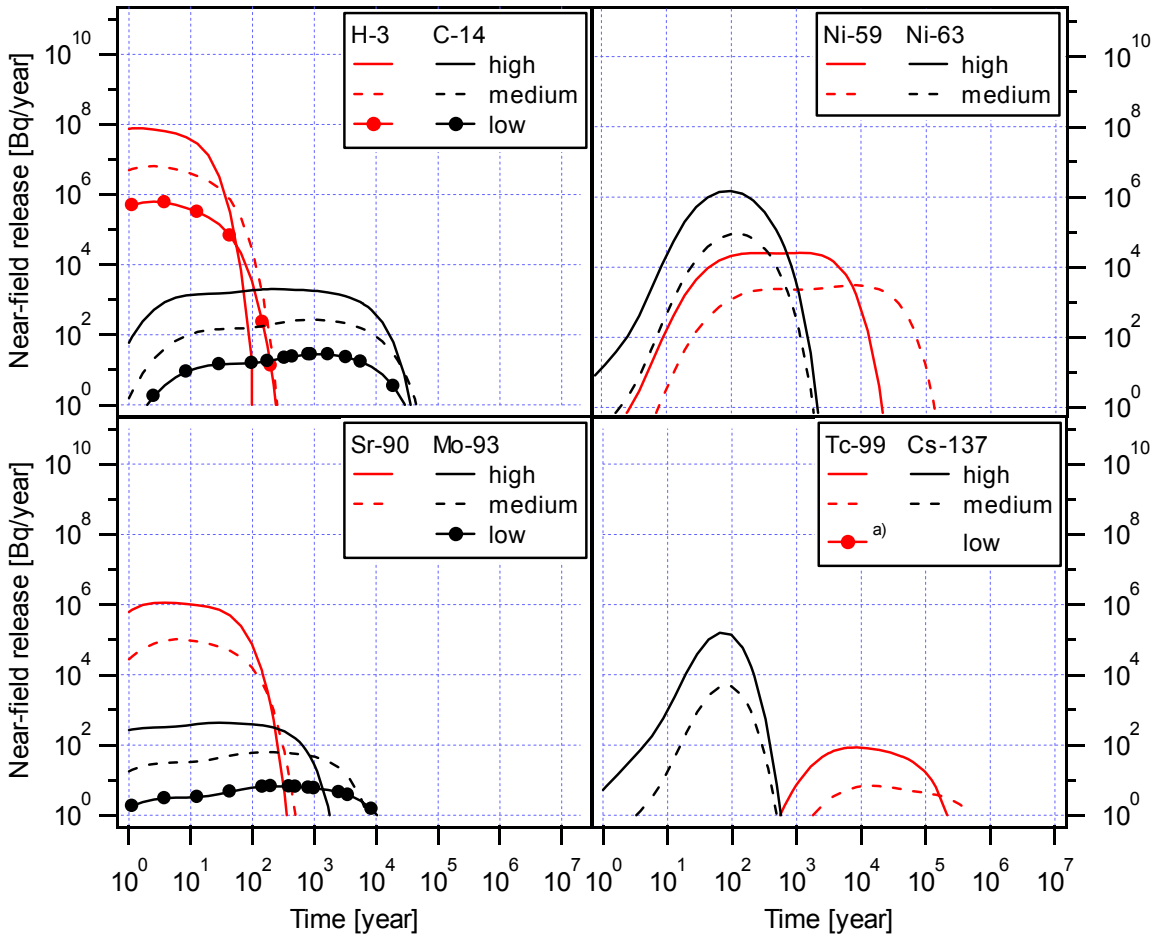

Figure 7-6 Effect of water flow rate on the near-field release from SFL 4. a) release rate is < 1 Bq/year.

7.2.2 Effect of water composition

For some nuclides the sorption coefficient is higher for non-saline waters than for saline waters. The effect of having non-saline water in Beberg instead of saline on the near-field release rate is shown in Figure 7-7 for a selection of nuclides. The increased sorption has a smaller effect on the release from SFL 4 than on that from SFL 3 and SFL 5. This is especially evident for ^{90}Sr. Changing the water from saline to non-saline reduced the maximum release rate of ^{90}Sr from SFL 3 by eight orders of magnitude. For SFL 4 the corresponding result is one order of magnitude. Of the nuclides modelled in SFL 4, it is especially the release rate of ^{60}Co and of ^{137}Cs that are affected by water composition.

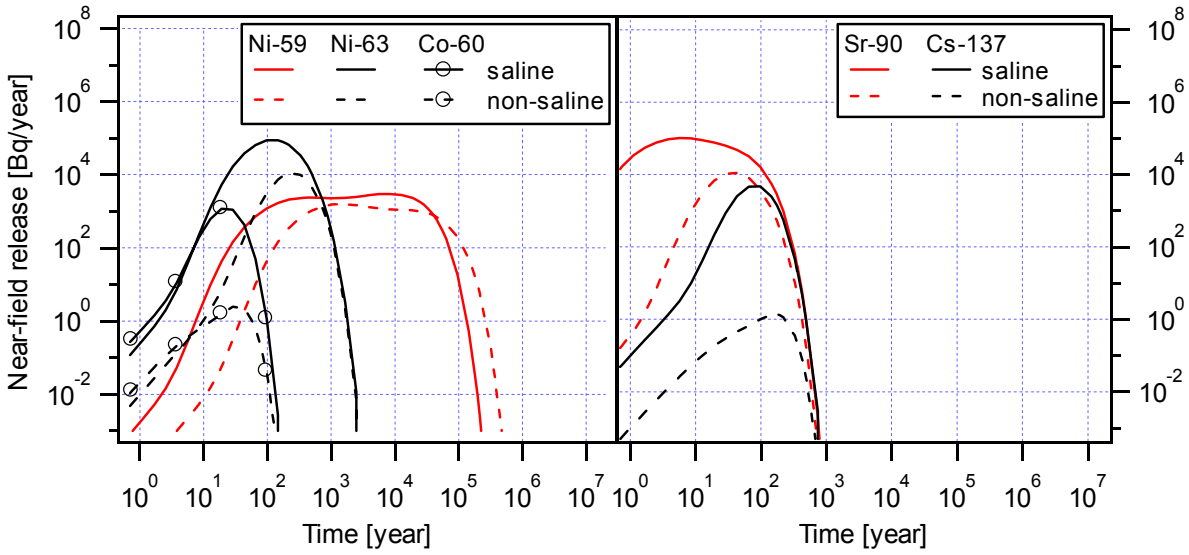

Figure 7-7 Effect of water composition on the near-field release from SFL 4. Medium flow rate.

The maximum near-field release rates from SFL 4 based on the water flow rates and water composition representative for the three sites are summarised in Table 7-3.

Table 7-3 Maximum near-field release rates from SFL 4 (without CRUD).

Nuclide	Half-life	Aberg (saline)		Beberg (saline)		Beberg (non-saline)		Ceberg (non-saline)	
		Time of maximum release rate	Maximum release rate	Time of maximum release rate	Maximum release rate	Time of maximum release rate	Maximum release rate	Time of maximum release rate	Maximum release rate
	[year]	[year]	[Bq/year]	[year]	[Bq/year]	[year]	[Bq/year]	[year]	[Bq/year]
^{3}H	12	1	$8\cdot10^{7}$	3	$6\cdot10^{6}$	3	$6\cdot10^{6}$	3	$6\cdot10^{5}$
^{14}C	$5.7\cdot10^{3}$	$2\cdot10^{2}$	$2\cdot10^{3}$	$9\cdot10^{2}$	$3\cdot10^{2}$	$9\cdot10^{2}$	$3\cdot10^{2}$	$1\cdot10^{3}$	$3\cdot10^{1}$
^{36}Cl	$3.0\cdot10^{5}$	$3\cdot10^{1}$	$6\cdot10^{1}$	$2\cdot10^{2}$	8	$2\cdot10^{2}$	8	$5\cdot10^{2}$	$9\cdot10^{-1}$
^{60}Co	5.3	$2\cdot10^{1}$	$4\cdot10^{4}$	$2\cdot10^{1}$	$1\cdot10^{3}$	$3\cdot10^{1}$	2	$3\cdot10^{1}$	$2\cdot10^{-1}$
^{59}Ni	$7.6\cdot10^{4}$	$1\cdot10^{3}$	$3\cdot10^{4}$	$8\cdot10^{3}$	$3\cdot10^{3}$	$2\cdot10^{3}$	$2\cdot10^{3}$	$2\cdot10^{3}$	$1\cdot10^{2}$
^{63}Ni	$1.0\cdot10^{2}$	$1\cdot10^{2}$	$1\cdot10^{6}$	$1\cdot10^{2}$	$9\cdot10^{4}$	$2\cdot10^{2}$	$1\cdot10^{4}$	$2\cdot10^{2}$	$1\cdot10^{3}$
^{79}Se	$1.1\cdot10^{6}$	$1\cdot10^{2}$	9	$7\cdot10^{2}$	1	$8\cdot10^{2}$	1	$2\cdot10^{3}$	$1\cdot10^{-1}$
^{90}Sr	29	4	$1\cdot10^{6}$	6	$1\cdot10^{5}$	$4\cdot10^{1}$	$1\cdot10^{4}$	$4\cdot10^{1}$	$1\cdot10^{3}$
^{94}Nb	$2.0\cdot10^{4}$	$6\cdot10^{3}$	$7\cdot10^{1}$	$8\cdot10^{3}$	5	$8\cdot10^{3}$	5	$8\cdot10^{3}$	$5\cdot10^{-1}$
^{93}Mo	$4.0\cdot10^{3}$	$3\cdot10^{1}$	$4\cdot10^{2}$	$2\cdot10^{2}$	$6\cdot10^{1}$	$2\cdot10^{2}$	$6\cdot10^{1}$	$2\cdot10^{2}$	7
^{99}Tc	$2.1\cdot10^{5}$	$8\cdot10^{3}$	$9\cdot10^{1}$	$1\cdot10^{4}$	7	$1\cdot10^{4}$	7	$1\cdot10^{4}$	$7\cdot10^{-1}$
^{129}I	$1.6\cdot10^{7}$	$3\cdot10^{1}$	1	$2\cdot10^{2}$	$2\cdot10^{-1}$	$2\cdot10^{2}$	$2\cdot10^{-1}$	$4\cdot10^{2}$	$2\cdot10^{-2}$
^{137}Cs	30	$6\cdot10^{1}$	$2\cdot10^{5}$	$1\cdot10^{2}$	$5\cdot10^{3}$	$2\cdot10^{2}$	1	$2\cdot10^{2}$	$1\cdot10^{-1}$
^{238}U	$4.5\cdot10^{9}$	–	$< 1\cdot10^{-3}$	–	$< 1\cdot10^{-3}$	–	$< 1\cdot10^{-3}$	–	$< 1\cdot10^{-3}$
^{234}U	$2.5\cdot10^{5}$	–	$< 1\cdot10^{-3}$	–	$< 1\cdot10^{-3}$	–	$< 1\cdot10^{-3}$	–	$< 1\cdot10^{-3}$
^{230}Th	$7.5\cdot10^{4}$	–	$< 1\cdot10^{-3}$	–	$< 1\cdot10^{-3}$	–	$< 1\cdot10^{-3}$	–	$< 1\cdot10^{-3}$
^{226}Ra	$1.6\cdot10^{3}$	$1\cdot10^{5}$	$5\cdot10^{-3}$	–	$< 1\cdot10^{-3}$	–	$< 1\cdot10^{-3}$	–	$< 1\cdot10^{-3}$
^{210}Pb	22	$1\cdot10^{5}$	$5\cdot10^{-3}$	–	$< 1\cdot10^{-3}$	–	$< 1\cdot10^{-3}$	–	$< 1\cdot10^{-3}$

7.2.3 Effect of including the surface contamination, CRUD

If the waste deposited in SFL 4 is not decontaminated, the inventory of some nuclides will be increased considerably in comparison to the case when surface contamination is removed, while other nuclides are only marginally increased. As shown in Table 2.1 the inventory of ^{14}C, ^{90}Sr, ^{93}Mo and ^{99}Tc is increased by three orders of magnitude, and ^{59}Ni and ^{63}Ni by two orders of magnitude. The inventory of ^{3}H on the other hand is almost the same.

The release rate from SFL 4 in Beberg (saline conditions) obtained when including the surface contamination in SFL 4 is shown in Figure 7-8. Overall, the total release rate from SFL 4 is increased between one and two orders of magnitude. When surface contamination is excluded from the inventory in SFL 4, ^{3}H dominates the release rate. Including surface contamination, the release rate of ^{3}H is increased somewhat in comparison to the results shown in Figure 7-5. However, the maximum release rate of ^{90}Sr increases by three orders of magnitude why ^{90}Sr gives the highest release rate.

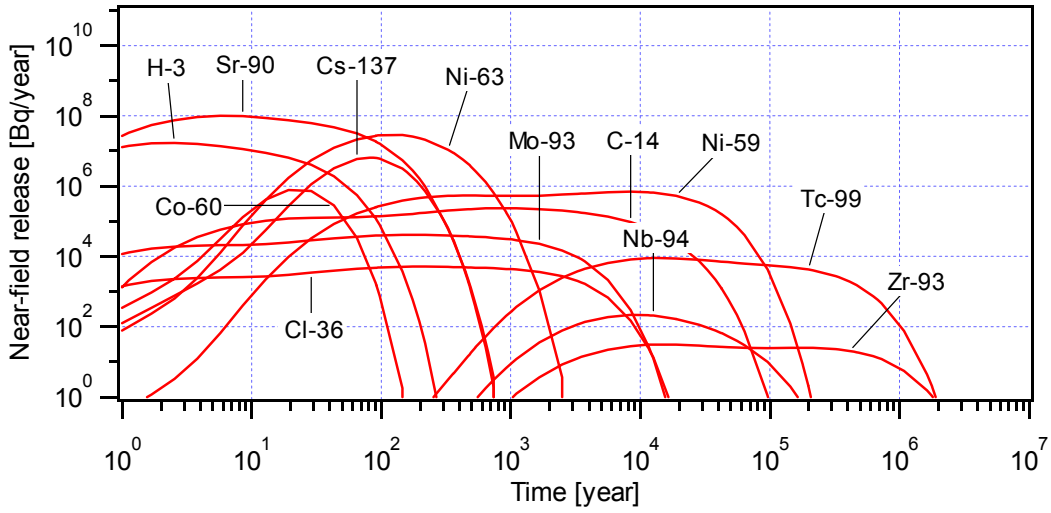

Figure 7-8 Near-field release from SFL 4 including CRUD activity. Medium flow rate.

The maximum near-field release rates when the CRUD inventory is included in SFL 4 are summarised in Table 7-4.

Table 7-4 Maximum near-field release rates from SFL 4 (with CRUD).

Nuclide	Half-life	Aberg (saline)		Beberg (saline)		Beberg (non-saline)		Ceberg (non-saline)	
		Time of maximum release rate	Maximum release rate	Time of maximum release rate	Maximum release rate	Time of maximum release rate	Maximum release rate	Time of maximum release rate	Maximum release rate
	[year]	[year]	[Bq/year]	[year]	[Bq/year]	[year]	[Bq/year]	[year]	[Bq/year]
^{3}H	12	1	$2\cdot10^{8}$	3	$2\cdot10^{7}$	3	$2\cdot10^{7}$	3	$2\cdot10^{6}$
^{10}Be	$1.5\cdot10^{6}$	$2\cdot10^{3}$	3	$1\cdot10^{4}$	$4\cdot10^{-1}$	$2\cdot10^{3}$	$2\cdot10^{-1}$	$2\cdot10^{3}$	$2\cdot10^{-2}$
^{14}C	$5.7\cdot10^{3}$	$2\cdot10^{2}$	$2\cdot10^{6}$	$9\cdot10^{2}$	$2\cdot10^{5}$	$9\cdot10^{2}$	$2\cdot10^{5}$	$1\cdot10^{3}$	$2\cdot10^{4}$
^{36}Cl	$3.0\cdot10^{5}$	$3\cdot10^{1}$	$3\cdot10^{4}$	$2\cdot10^{2}$	$5\cdot10^{3}$	$2\cdot10^{2}$	$5\cdot10^{3}$	$4\cdot10^{2}$	$6\cdot10^{2}$
^{55}Fe	2.7	$1\cdot10^{1}$	$4\cdot10^{6}$	$1\cdot10^{1}$	$8\cdot10^{4}$	9	$1\cdot10^{2}$	9	8
^{60}Co	5.3	$2\cdot10^{1}$	$3\cdot10^{7}$	$2\cdot10^{1}$	$8\cdot10^{5}$	$3\cdot10^{1}$	$2\cdot10^{3}$	$3\cdot10^{1}$	$1\cdot10^{2}$
^{59}Ni	$7.6\cdot10^{4}$	$1\cdot10^{3}$	$6\cdot10^{6}$	$8\cdot10^{3}$	$7\cdot10^{5}$	$2\cdot10^{3}$	$4\cdot10^{5}$	$2\cdot10^{3}$	$3\cdot10^{4}$
^{63}Ni	$1.0\cdot10^{2}$	$9\cdot10^{1}$	$5\cdot10^{8}$	$1\cdot10^{2}$	$3\cdot10^{7}$	$2\cdot10^{2}$	$4\cdot10^{6}$	$2\cdot10^{2}$	$3\cdot10^{5}$
^{79}Se	$1.1\cdot10^{6}$	$1\cdot10^{2}$	$1\cdot10^{4}$	$7\cdot10^{2}$	$2\cdot10^{3}$	$7\cdot10^{2}$	$2\cdot10^{3}$	$2\cdot10^{3}$	$2\cdot10^{2}$
^{90}Sr	29	4	$1\cdot10^{9}$	6	$1\cdot10^{8}$	$4\cdot10^{1}$	$1\cdot10^{7}$	$4\cdot10^{1}$	$1\cdot10^{6}$
^{93}Zr	$1.5\cdot10^{6}$	$8\cdot10^{3}$	$4\cdot10^{2}$	$1\cdot10^{4}$	$3\cdot10^{1}$	$1\cdot10^{4}$	$3\cdot10^{1}$	$2\cdot10^{4}$	3
^{93m}Nb	16	$4\cdot10^{1}$	$2\cdot10^{-1}$	$4\cdot10^{1}$	$4\cdot10^{-3}$	$4\cdot10^{1}$	$4\cdot10^{-3}$	–	$< 1\cdot10^{-3}$
^{94}Nb	$2.0\cdot10^{4}$	$6\cdot10^{3}$	$3\cdot10^{3}$	$8\cdot10^{3}$	$2\cdot10^{2}$	$8\cdot10^{3}$	$2\cdot10^{2}$	$1\cdot10^{4}$	$2\cdot10^{1}$
^{93}Mo	$4.0\cdot10^{3}$	$3\cdot10^{1}$	$3\cdot10^{5}$	$1\cdot10^{2}$	$4\cdot10^{4}$	$1\cdot10^{2}$	$4\cdot10^{4}$	$2\cdot10^{2}$	$4\cdot10^{3}$
^{99}Tc	$2.1\cdot10^{5}$	$8\cdot10^{3}$	$1\cdot10^{5}$	$1\cdot10^{4}$	$9\cdot10^{3}$	$1\cdot10^{4}$	$9\cdot10^{3}$	$1\cdot10^{4}$	$9\cdot10^{2}$
^{107}Pd	$6.5\cdot10^{6}$	$1\cdot10^{3}$	$4\cdot10^{2}$	$6\cdot10^{3}$	$6\cdot10^{1}$	$2\cdot10^{3}$	$2\cdot10^{1}$	$2\cdot10^{3}$	2
^{108m}Ag	$4.2\cdot10^{2}$	$1\cdot10^{2}$	$2\cdot10^{6}$	$2\cdot10^{2}$	$8\cdot10^{4}$	$9\cdot10^{2}$	$2\cdot10^{3}$	$9\cdot10^{2}$	$1\cdot10^{2}$
^{113m}Cd	14	$4\cdot10^{1}$	$9\cdot10^{3}$	$4\cdot10^{1}$	$4\cdot10^{2}$	$6\cdot10^{1}$	3	$6\cdot10^{1}$	$3\cdot10^{-1}$
^{126}Sn	$1.0\cdot10^{5}$	$3\cdot10^{2}$	$2\cdot10^{1}$	$2\cdot10^{3}$	3	$2\cdot10^{3}$	3	$2\cdot10^{3}$	$3\cdot10^{-1}$
^{125}Sb	2.8	9	$1\cdot10^{-2}$	–	$< 1\cdot10^{-3}$	–	$< 1\cdot10^{-3}$	–	$< 1\cdot10^{-3}$
^{129}I	$1.6\cdot10^{7}$	$3\cdot10^{1}$	$2\cdot10^{3}$	$2\cdot10^{2}$	$3\cdot10^{2}$	$2\cdot10^{2}$	$3\cdot10^{2}$	$5\cdot10^{2}$	$3\cdot10^{1}$
^{134}Cs	2.1	$1\cdot10^{1}$	$5\cdot10^{4}$	$1\cdot10^{1}$	$1\cdot10^{3}$	6	6	6	$3\cdot10^{-1}$
^{135}Cs	$2.3\cdot10^{6}$	$2\cdot10^{2}$	$1\cdot10^{4}$	$3\cdot10^{2}$	$6\cdot10^{2}$	$2\cdot10^{3}$	$6\cdot10^{1}$	$2\cdot10^{3}$	5
^{137}Cs	30	$6\cdot10^{1}$	$2\cdot10^{8}$	$8\cdot10^{1}$	$6\cdot10^{6}$	$2\cdot10^{2}$	$2\cdot10^{3}$	$2\cdot10^{2}$	$1\cdot10^{2}$
^{133}Ba	11	$2\cdot10^{1}$	$4\cdot10^{4}$	$2\cdot10^{1}$	$2\cdot10^{3}$	$7\cdot10^{1}$	$8\cdot10^{-2}$	$7\cdot10^{1}$	$6\cdot10^{-3}$
^{147}Pm	2.6	9	$7\cdot10^{-3}$	–	$< 1\cdot10^{-3}$	–	$< 1\cdot10^{-3}$	–	$< 1\cdot10^{-3}$
^{155}Sm	90	$6\cdot10^{2}$	$6\cdot10^{-2}$	$6\cdot10^{2}$	$1\cdot10^{-3}$	$6\cdot10^{2}$	$1\cdot10^{-3}$	–	$< 1\cdot10^{-3}$
^{152}Eu	14	–	$< 1\cdot10^{-3}$	–	$< 1\cdot10^{-3}$	–	$< 1\cdot10^{-3}$	–	$< 1\cdot10^{-3}$
^{154}Eu	8.6	$3\cdot10^{1}$	$8\cdot10^{-3}$	–	$< 1\cdot10^{-3}$	–	$< 1\cdot10^{-3}$	–	$< 1\cdot10^{-3}$
^{155}Eu	4.8	$1\cdot10^{1}$	$2\cdot10^{-3}$	–	$< 1\cdot10^{-3}$	–	$< 1\cdot10^{-3}$	–	$< 1\cdot10^{-3}$
^{166m}Ho	$1.2\cdot10^{3}$	$3\cdot10^{3}$	6	$4\cdot10^{3}$	$2\cdot10^{-1}$	$4\cdot10^{3}$	$2\cdot10^{-1}$	$4\cdot10^{3}$	$2\cdot10^{-2}$
^{244}Cm	18	–	$< 1\cdot10^{-3}$	–	$< 1\cdot10^{-3}$	–	$< 1\cdot10^{-3}$	–	$< 1\cdot10^{-3}$
^{240}Pu	$6.6\cdot10^{3}$	$1\cdot10^{4}$	4	$1\cdot10^{4}$	$2\cdot10^{-1}$	$1\cdot10^{4}$	$2\cdot10^{-1}$	$1\cdot10^{4}$	$1\cdot10^{-2}$
^{236}U	$2.3\cdot10^{7}$	$6\cdot10^{4}$	$2\cdot10^{-2}$	$2\cdot10^{6}$	$2\cdot10^{-3}$	$2\cdot10^{6}$	$2\cdot10^{-3}$	–	$< 1\cdot10^{-3}$
^{232}Th	$1.4\cdot10^{10}$	–	$< 1\cdot10^{-3}$	–	$< 1\cdot10^{-3}$	–	$< 1\cdot10^{-3}$	–	$< 1\cdot10^{-3}$
^{232}U	69	–	$< 1\cdot10^{-3}$	–	$< 1\cdot10^{-3}$	–	$< 1\cdot10^{-3}$	–	$< 1\cdot10^{-3}$
^{245}Cm	$8.5\cdot10^{3}$	$8\cdot10^{3}$	$2\cdot10^{-2}$	–	$< 1\cdot10^{-3}$	–	$< 1\cdot10^{-3}$	–	$< 1\cdot10^{-3}$
^{241}Pu	14	$8\cdot10^{3}$	$1\cdot10^{-2}$	–	$< 1\cdot10^{-3}$	–	$< 1\cdot10^{-3}$	–	$< 1\cdot10^{-3}$
^{241}Am	$4.3\cdot10^{2}$	$2\cdot10^{3}$	$8\cdot10^{-1}$	$2\cdot10^{3}$	$2\cdot10^{-2}$	$2\cdot10^{3}$	$2\cdot10^{-2}$	$2\cdot10^{3}$	$2\cdot10^{-3}$
^{237}Np	$2.1\cdot10^{6}$	$4\cdot10^{4}$	$5\cdot10^{-2}$	$1\cdot10^{5}$	$5\cdot10^{-3}$	$1\cdot10^{5}$	$5\cdot10^{-3}$	–	$< 1\cdot10^{-3}$
^{233}U	$1.6\cdot10^{5}$	$3\cdot10^{5}$	$3\cdot10^{-2}$	$7\cdot10^{5}$	$4\cdot10^{-3}$	$7\cdot10^{5}$	$4\cdot10^{-3}$	–	$< 1\cdot10^{-3}$
^{229}Th	$7.3\cdot10^{3}$	$3\cdot10^{5}$	$3\cdot10^{-2}$	$1\cdot10^{6}$	$4\cdot10^{-3}$	$1\cdot10^{6}$	$4\cdot10^{-3}$	–	$< 1\cdot10^{-3}$
^{244}Pu	$8.1\cdot10^{7}$	–	$< 1\cdot10^{-3}$	–	$< 1\cdot10^{-3}$	–	$< 1\cdot10^{-3}$	–	$< 1\cdot10^{-3}$
^{246}Cm	$4.7\cdot10^{3}$	$8\cdot10^{3}$	$3\cdot10^{-3}$	–	$< 1\cdot10^{-3}$	–	$< 1\cdot10^{-3}$	–	$< 1\cdot10^{-3}$
^{242}Pu	$3.7\cdot10^{5}$	$4\cdot10^{4}$	$1\cdot10^{-1}$	$6\cdot10^{4}$	$1\cdot10^{-2}$	$6\cdot10^{4}$	$1\cdot10^{-2}$	–	$< 1\cdot10^{-3}$
^{238}U	$4.5\cdot10^{9}$	$6\cdot10^{4}$	$2\cdot10^{-2}$	$2\cdot10^{6}$	$2\cdot10^{-3}$	$2\cdot10^{6}$	$2\cdot10^{-3}$	–	$< 1\cdot10^{-3}$
^{234}U	$2.5\cdot10^{5}$	$4\cdot10^{4}$	$9\cdot10^{-2}$	$6\cdot10^{4}$	$8\cdot10^{-3}$	$6\cdot10^{4}$	$8\cdot10^{-3}$	–	$< 1\cdot10^{-3}$
^{230}Th	$7.5\cdot10^{4}$	$2\cdot10^{5}$	$3\cdot10^{-2}$	$2\cdot10^{5}$	$3\cdot10^{-3}$	$2\cdot10^{5}$	$3\cdot10^{-3}$	–	$< 1\cdot10^{-3}$
^{226}Ra	$1.6\cdot10^{3}$	$2\cdot10^{5}$	3	$3\cdot10^{5}$	$4\cdot10^{-1}$	$2\cdot10^{5}$	$2\cdot10^{-1}$	$2\cdot10^{5}$	$2\cdot10^{-2}$
^{210}Pb	22	$2\cdot10^{5}$	2	$3\cdot10^{5}$	$4\cdot10^{-1}$	$2\cdot10^{5}$	$2\cdot10^{-1}$	$2\cdot10^{5}$	$2\cdot10^{-2}$
^{242m}Am	$1.4\cdot10^{2}$	–	$< 1\cdot10^{-3}$	–	$< 1\cdot10^{-3}$	–	$< 1\cdot10^{-3}$	–	$< 1\cdot10^{-3}$
^{238}Pu	88	–	$< 1\cdot10^{-3}$	–	$< 1\cdot10^{-3}$	–	$< 1\cdot10^{-3}$	–	$< 1\cdot10^{-3}$
^{243}Am	$7.4\cdot10^{3}$	$8\cdot10^{3}$	1	$1\cdot10^{4}$	$7\cdot10^{-2}$	$1\cdot10^{4}$	$7\cdot10^{-2}$	$1\cdot10^{4}$	$7\cdot10^{-3}$
^{239}Pu	$2.4\cdot10^{4}$	$2\cdot10^{4}$	6	$3\cdot10^{4}$	$4\cdot10^{-1}$	$3\cdot10^{4}$	$4\cdot10^{-1}$	$3\cdot10^{4}$	$4\cdot10^{-2}$
^{235}U	$7.0\cdot10^{8}$	$1\cdot10^{5}$	$1\cdot10^{-3}$	–	$< 1\cdot10^{-3}$	–	$< 1\cdot10^{-3}$	–	$< 1\cdot10^{-3}$
^{231}Pa	$3.3\cdot10^{4}$	$2\cdot10^{5}$	$2\cdot10^{-3}$	–	$< 1\cdot10^{-3}$	–	$< 1\cdot10^{-3}$	–	$< 1\cdot10^{-3}$
^{227}Ac	22	–	$< 1\cdot10^{-3}$	–	$< 1\cdot10^{-3}$	–	$< 1\cdot10^{-3}$	–	$< 1\cdot10^{-3}$
^{243}Cm	29	–	$< 1\cdot10^{-3}$	–	$< 1\cdot10^{-3}$	–	$< 1\cdot10^{-3}$	–	$< 1\cdot10^{-3}$

7.3 SFL 5

The radionuclide release rate from SFL 5 in Beberg (saline waters) as a function of time is shown in Figure 7-9. SFL 5 is the repository part giving the highest release rates in SFL 3-5. The model for SFL 5 is to a large extent identical to the model used for SFL 3. This explains why the time scale for the release of most nuclides is approximately the same for SFL 3 and SFL 5. The difference in release rates between SFL 3 and SFL 5 reflects the difference in initial inventory between the two repository parts. The release of ^{14}C, ^{36}Cl, ^{93}Mo and ^{93}Zr in SFL 5 takes place somewhat later than from SFL 3. This is an effect of a corrosion rate limited release of these nuclides in SFL 5. The nuclides dominating the release rate up to about 10^6 years are very much the same as for SFL 3, but at longer times ^{93}Zr is dominating in SFL 5.

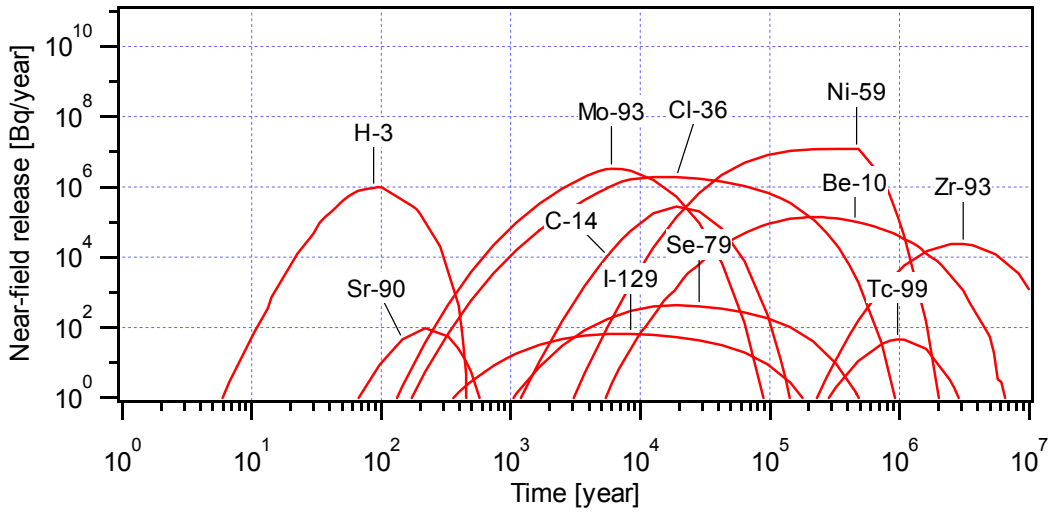

Figure 7-9 Near-field release from SFL 5 in Beberg, saline water.

7.3.1 Effect of water flow rate

The effect of different water flow rates through SFL 5 on the near-field release rates resembles that for SFL 3. In Figure 7-10, results are therefore presented for ^{10}Be and ^{93}Zr which where not discussed in Section 7.1.1, but which make a significant contribution to the total release rate from SFL 5. For ^{10}Be results are given for a high and a medium flow only. For ^{10}Be, the result for Ceberg is not only affected by the difference in water flow rate, but also by the difference in water composition (non-saline in Ceberg versus saline in Aberg and Beberg).

Reducing the flow rate from 10 to 1 l/m^2, year reduces the maximum release rate of ^{10}Be and ^{93}Zr by a factor 2 and 10, respectively. Reducing the flow rate another magnitude reduces the maximum release rate of ^{93}Zr by a factor 700 in total.

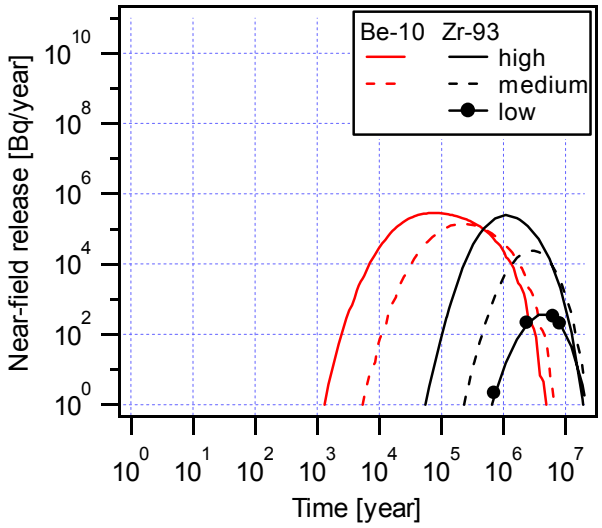

Figure 7-10 Effect of water flow rate on the near-field release of ^{10}Be and ^{93}Zr from SFL 5.

7.3.2 Effect of water composition

The effect of having non-saline water in Beberg instead of saline on the near-field release rate is shown in Figure 7-11. Most of the nuclides of importance for the resulting dose from SFL 5 (see Chapter 9) have a sorption coefficient on gravel that is independent of the type of water (saline or non-saline). However, for ^{10}Be, ^{59}Ni, ^{90}Sr, ^{210}Pb and ^{226}Ra the sorption coefficient increases in non-saline water. The release of these nuclides is therefore delayed somewhat. As for SFL 3, the maximum release rate of ^{90}Sr is reduced by eight orders of magnitude, and of ^{59}Ni, ^{210}Pb and ^{226}Ra a factor of 5. For ^{10}Be the corresponding reduction is a factor of 2.

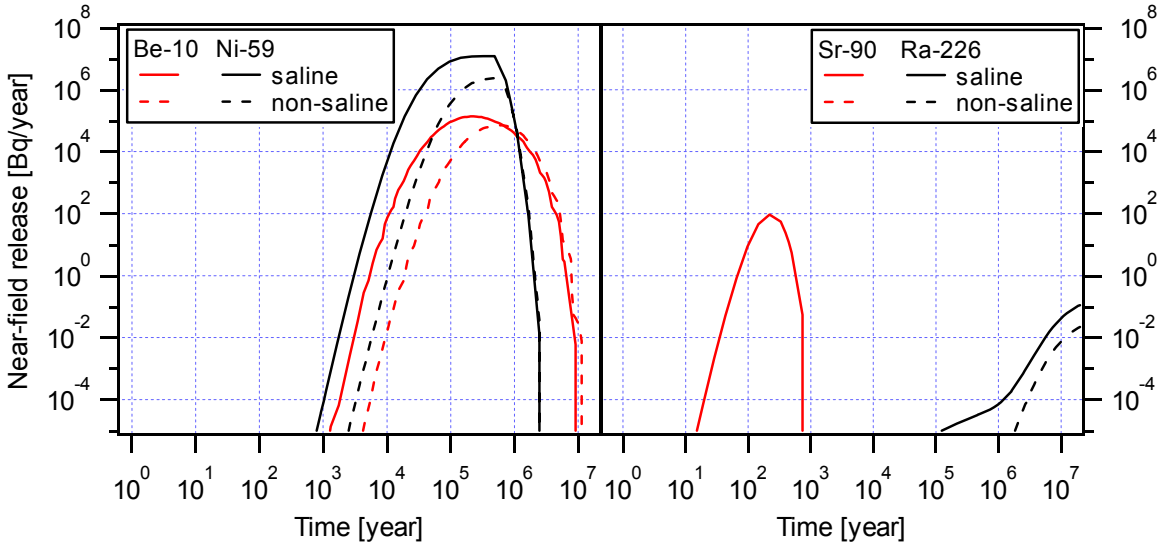

Figure 7-11 Effect of water composition on the near-field release from SFL 5. Medium flow rate.

The maximum near-field release rates from SFL 5 based on the water flow rates and type of water representative for the three sites are summarised in Table 7-5.

Table 7-5 Maximum near-field release rates from SFL 5.

Nuclide	Half-life	Aberg (saline)		Beberg (saline)		Beberg (non-saline)		Ceberg (non-saline)	
		Time of maximum release rate	Maximum release rate	Time of maximum release rate	Maximum release rate	Time of maximum release rate	Maximum release rate	Time of maximum release rate	Maximum release rate
	[year]	[year]	[Bq/year]	[year]	[Bq/year]	[year]	[Bq/year]	[year]	[Bq/year]
^{3}H	12	$4{\cdot}10^{1}$	$8{\cdot}10^{8}$	$9{\cdot}10^{1}$	$1{\cdot}10^{6}$	$9{\cdot}10^{1}$	$1{\cdot}10^{6}$	$1{\cdot}10^{2}$	$1{\cdot}10^{3}$
^{10}Be	$1.5{\cdot}10^{6}$	$7{\cdot}10^{4}$	$3{\cdot}10^{5}$	$2{\cdot}10^{5}$	$1{\cdot}10^{5}$	$5{\cdot}10^{5}$	$7{\cdot}10^{4}$	$2{\cdot}10^{6}$	$5{\cdot}10^{3}$
^{14}C	$5.7{\cdot}10^{3}$	$2{\cdot}10^{4}$	$1{\cdot}10^{6}$	$2{\cdot}10^{4}$	$3{\cdot}10^{5}$	$2{\cdot}10^{4}$	$3{\cdot}10^{5}$	$3{\cdot}10^{4}$	$1{\cdot}10^{4}$
^{36}Cl	$3.0{\cdot}10^{5}$	$1{\cdot}10^{4}$	$3{\cdot}10^{6}$	$1{\cdot}10^{4}$	$2{\cdot}10^{6}$	$1{\cdot}10^{4}$	$2{\cdot}10^{6}$	$3{\cdot}10^{4}$	$5{\cdot}10^{5}$
^{59}Ni	$7.6{\cdot}10^{4}$	$4{\cdot}10^{5}$	$4{\cdot}10^{7}$	$5{\cdot}10^{5}$	$1{\cdot}10^{7}$	$5{\cdot}10^{5}$	$2{\cdot}10^{6}$	$5{\cdot}10^{5}$	$3{\cdot}10^{4}$
^{79}Se	$1.1{\cdot}10^{6}$	$8{\cdot}10^{3}$	$8{\cdot}10^{2}$	$2{\cdot}10^{4}$	$4{\cdot}10^{2}$	$2{\cdot}10^{4}$	$4{\cdot}10^{2}$	$6{\cdot}10^{4}$	$9{\cdot}10^{1}$
^{90}Sr	29	$1{\cdot}10^{2}$	$6{\cdot}10^{4}$	$2{\cdot}10^{2}$	$1{\cdot}10^{2}$	–	$< 1{\cdot}10^{-3}$	–	$< 1{\cdot}10^{-3}$
^{93}Zr	$1.5{\cdot}10^{6}$	$1{\cdot}10^{6}$	$2{\cdot}10^{5}$	$3{\cdot}10^{6}$	$2{\cdot}10^{4}$	$3{\cdot}10^{6}$	$2{\cdot}10^{4}$	$6{\cdot}10^{6}$	$4{\cdot}10^{2}$
^{93}Mo	$4.0{\cdot}10^{3}$	$5{\cdot}10^{3}$	$7{\cdot}10^{6}$	$6{\cdot}10^{3}$	$3{\cdot}10^{6}$	$6{\cdot}10^{3}$	$3{\cdot}10^{6}$	$8{\cdot}10^{3}$	$4{\cdot}10^{5}$
^{99}Tc	$2.1{\cdot}10^{5}$	$5{\cdot}10^{5}$	$5{\cdot}10^{3}$	$1{\cdot}10^{6}$	$5{\cdot}10^{1}$	$1{\cdot}10^{6}$	$5{\cdot}10^{1}$	$1{\cdot}10^{6}$	$1{\cdot}10^{-1}$
^{129}I	$1.6{\cdot}10^{7}$	$4{\cdot}10^{3}$	$1{\cdot}10^{2}$	$8{\cdot}10^{3}$	$7{\cdot}10^{1}$	$8{\cdot}10^{3}$	$7{\cdot}10^{1}$	$2{\cdot}10^{4}$	$2{\cdot}10^{1}$
^{238}U	$4.5{\cdot}10^{9}$	$8{\cdot}10^{6}$	$2{\cdot}10^{-3}$	–	$< 1{\cdot}10^{-3}$	–	$< 1{\cdot}10^{-3}$	–	$< 1{\cdot}10^{-3}$
^{234}U	$2.5{\cdot}10^{5}$	$8{\cdot}10^{6}$	$2{\cdot}10^{-3}$	–	$< 1{\cdot}10^{-3}$	–	$< 1{\cdot}10^{-3}$	–	$< 1{\cdot}10^{-3}$
^{230}Th	$7.5{\cdot}10^{4}$	$8{\cdot}10^{6}$	$2{\cdot}10^{-3}$	–	$< 1{\cdot}10^{-3}$	–	$< 1{\cdot}10^{-3}$	–	$< 1{\cdot}10^{-3}$
^{226}Ra	$1.6{\cdot}10^{3}$	$8{\cdot}10^{6}$	$4{\cdot}10^{-1}$	$4{\cdot}10^{7}$	$2{\cdot}10^{-1}$	$4{\cdot}10^{7}$	$3{\cdot}10^{-2}$	$2{\cdot}10^{8}$	$5{\cdot}10^{-3}$
^{210}Pb	22	$8{\cdot}10^{6}$	$4{\cdot}10^{-1}$	$4{\cdot}10^{7}$	$2{\cdot}10^{-1}$	$4{\cdot}10^{7}$	$3{\cdot}10^{-2}$	$2{\cdot}10^{8}$	$5{\cdot}10^{-3}$

8 Release calculations for the far field

In this chapter, the results of the calculations of radionuclide transport in the far field are presented. This chapter is divided into three sections. Each section focuses on one site (Aberg, Beberg or Ceberg). For each repository part the release rate is shown in graphical form for the dominant nuclides only. For SFL 3 results on the far-field release rate are given both for the case when the effect of ISA on solubility in the near field is accounted for as well as when it is not taken into account. The effect of including the surface contamination in SFL 4 on the far-field release rate is not considered. The results are also compiled in tables in which the maximum release rate and the time when the maximum release rate is obtained are presented for all three sites.

The results of the calculations are given as release rates (Bq/year) from the geosphere to the biosphere. The lower limit for which FARF31 specifies the release rate is set to $1 \cdot 10^{-3}$ Bq/year. The maximum release rate from the far field is, for some nuclides, below this limit. The maximum release rate is in that case specified as $< 1 \cdot 10^{-3}$ Bq/year and the time when it is obtained is not specified.

Similarly to some results presented for the near field, the far-field results for two cases may differ even though they should be the same. For example, the migration of ^{3}H is independent of whether ISA is accounted for or not. However, the time of maximum far-field release rate of ^{3}H in SFL 3 from Aberg for the case where ISA is accounted for and that where ISA is neglected are different (see Table 8-1). It is the result of differences in the time discretization used by COMP24 that propagates to the far-field calculation. As well as for the near-field results, this effect can be exaggerated when the results are rounded off in the tables.

8.1 Aberg

The release rate of radionuclides in SFL 3 from the far field in Aberg as a function of time is shown in Figure 8-1. The results are based on the assumption that ISA has no influence on the near-field transport. Due to the short travel time for the groundwater in the far-field rock in Aberg, the far-field release differs very little from that from the near field. For SFL 3 the differences in maximum release rate for the different nuclides between the near field and the far field is in general a factor between one and two, and at the most a factor three. The nuclides dominating the release rate are ^{3}H followed by ^{93}Mo and ^{59}Ni. For times scales around 10^{6} years and longer, ^{210}Pb and ^{226}Ra, and to some extent ^{99}Tc and ^{93}Zr are the most important nuclides in terms of release rate.

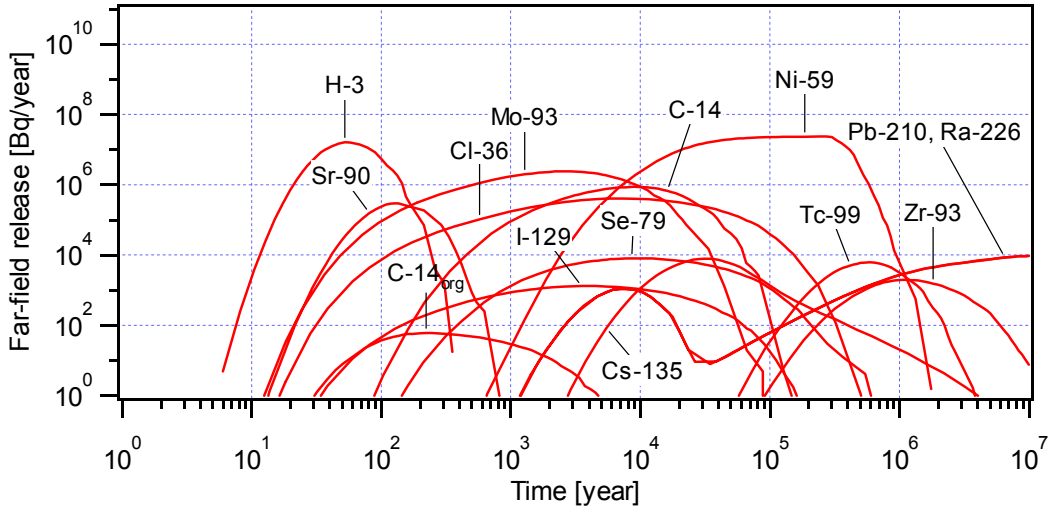

Figure 8-1 Far-field release from SFL 3 in Aberg, no influence of ISA.

As discussed in Section 7.1.3 and shown in Figure 7-4, the only nuclides modelled in SFL 3 which are affected by ISA are ^{59}Ni, ^{232}Th and ^{238}U and its daughters. In the near field the maximum release rate of ^{59}Ni is doubled and for ^{232}Th, ^{238}U and its daughters it is increased by approximately one order of magnitude when affected by ISA. This is also true for the far-field release.

In Section 7.2 it was concluded for SFL 4 that nuclides with no or very little sorption are released from the near field almost instantly after repository closing. For Aberg, this is reflected in the far-field release as well (Figure 8-2). ^{3}H, which results in the highest release rate from SFL 4 in Aberg, has a maximum release rate (10^{7} Bq/year) after some 10 years. Other nuclides with no or very little sorption in the far-field rock (^{36}Cl, ^{90}Sr, ^{93}Mo and ^{129}I) have a maximum release rate from the far field after 30 to 60 years. At longer times inorganic ^{14}C, ^{59}Ni, ^{63}Ni and ^{99}Tc dominate the release rate. However, it is much lower than that from SFL 3 and SFL 5.

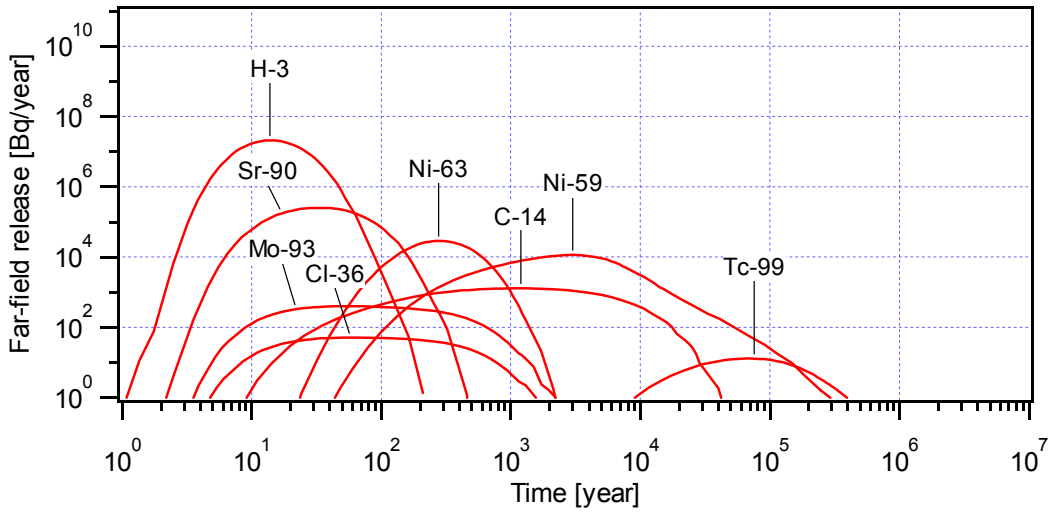

Figure 8-2 Far-field release from SFL 4 in Aberg.

The release rate of radionuclides in SFL 5 from the far field in Aberg as a function of time is shown in Figure 8-3. As for SFL 3, the near field and the far-field release are similar. The release of ^{3}H from SFL 5 results in the highest release rate from the far field in Aberg, more than 10^{8} Bq/year. At longer times ^{36}Cl, ^{93}Mo, ^{59}Ni and ^{93}Zr dominate the release rate. The total far-field release rate from SFL 5 is, with the exception of a few short periods of time, consistently slightly higher than from SFL 3 and much higher than from SFL 4.

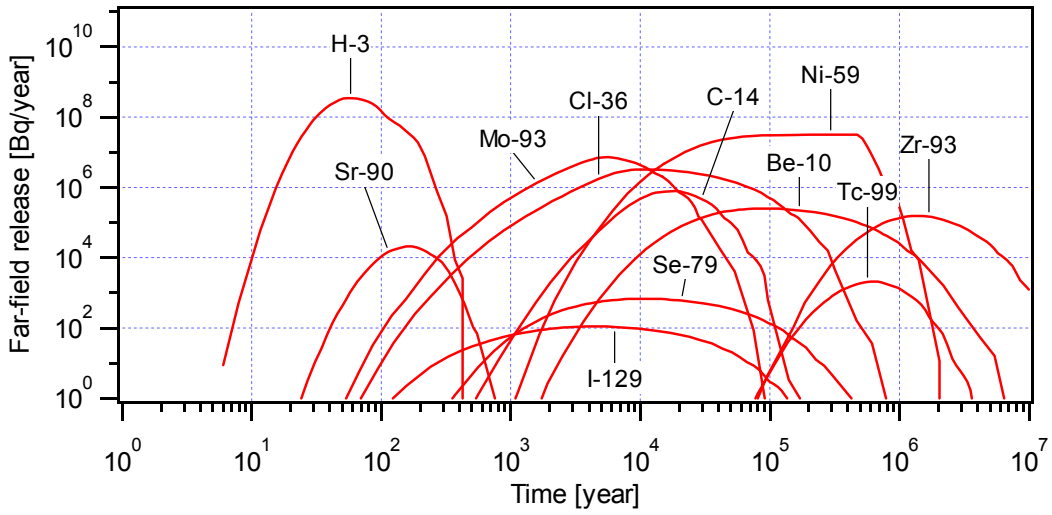

Figure 8-3 Far-field release from SFL 5 in Aberg.

The maximum far-field release rates and corresponding times in Aberg are compiled in Table 8-1.

Table 8-1 Maximum far-field release rates from SFL 3, SFL 4 and SFL 5 in Aberg.

Nuclide	Half-life	SFL 3 (without ISA)		SFL 3 (with ISA)		SFL 4		SFL 5	
		Time of maximum release rate	maximum release rate	Time of maximum release rate	maximum release rate	Time of maximum release rate	maximum release rate	Time of maximum release rate	maximum release rate
	[year]	[year]	[Bq/year]	[year]	[Bq/year]	[year]	[Bq/year]	[year]	[Bq/year]
^{3}H	12	$5 \cdot 10^{1}$	$2 \cdot 10^{7}$	$6 \cdot 10^{1}$	$2 \cdot 10^{7}$	$1 \cdot 10^{1}$	$2 \cdot 10^{7}$	$6 \cdot 10^{1}$	$3 \cdot 10^{8}$
^{10}Be	$1.5 \cdot 10^{6}$	– [a]	– [a]	– [a]	– [a]	– [a]	– [a]	$1 \cdot 10^{5}$	$3 \cdot 10^{5}$
^{14}C	$5.7 \cdot 10^{3}$	$9 \cdot 10^{3}$	$9 \cdot 10^{5}$	$8 \cdot 10^{3}$	$9 \cdot 10^{5}$	$1 \cdot 10^{3}$	$1 \cdot 10^{3}$	$2 \cdot 10^{4}$	$8 \cdot 10^{5}$
$^{14}C_{org}$	$5.7 \cdot 10^{3}$	$2 \cdot 10^{2}$	$6 \cdot 10^{1}$	$2 \cdot 10^{2}$	$6 \cdot 10^{1}$	– [a]	– [a]	– [a]	– [a]
^{36}Cl	$3.0 \cdot 10^{5}$	$7 \cdot 10^{3}$	$4 \cdot 10^{5}$	$8 \cdot 10^{3}$	$4 \cdot 10^{5}$	$6 \cdot 10^{1}$	$5 \cdot 10^{1}$	$1 \cdot 10^{4}$	$3 \cdot 10^{6}$
^{60}Co	5.3	– [a]	– [a]	– [a]	– [a]	$5 \cdot 10^{1}$	1	– [a]	– [a]
^{59}Ni	$7.6 \cdot 10^{4}$	$3 \cdot 10^{5}$	$2 \cdot 10^{7}$	$2 \cdot 10^{5}$	$5 \cdot 10^{7}$	$3 \cdot 10^{3}$	$1 \cdot 10^{4}$	$4 \cdot 10^{5}$	$3 \cdot 10^{7}$
^{63}Ni	$1.0 \cdot 10^{2}$	– [a]	– [a]	– [a]	– [a]	$3 \cdot 10^{2}$	$3 \cdot 10^{4}$	– [a]	– [a]
^{79}Se	$1.1 \cdot 10^{6}$	$9 \cdot 10^{3}$	$8 \cdot 10^{3}$	$9 \cdot 10^{3}$	$8 \cdot 10^{3}$	$3 \cdot 10^{2}$	5	$1 \cdot 10^{4}$	$7 \cdot 10^{2}$
^{90}Sr	29	$1 \cdot 10^{2}$	$3 \cdot 10^{5}$	$1 \cdot 10^{2}$	$3 \cdot 10^{5}$	$3 \cdot 10^{1}$	$3 \cdot 10^{5}$	$2 \cdot 10^{2}$	$2 \cdot 10^{4}$
^{94}Nb	$2.0 \cdot 10^{4}$	– [a]	– [a]	– [a]	– [a]	$3 \cdot 10^{4}$	4	– [a]	– [a]
^{93}Zr	$1.5 \cdot 10^{6}$	$1 \cdot 10^{6}$	$2 \cdot 10^{3}$	$1 \cdot 10^{6}$	$2 \cdot 10^{3}$	– [a]	– [a]	$1 \cdot 10^{6}$	$2 \cdot 10^{5}$
^{93}Mo	$4.0 \cdot 10^{3}$	$3 \cdot 10^{3}$	$2 \cdot 10^{6}$	$3 \cdot 10^{3}$	$2 \cdot 10^{6}$	$5 \cdot 10^{1}$	$4 \cdot 10^{2}$	$6 \cdot 10^{3}$	$7 \cdot 10^{6}$
^{99}Tc	$2.1 \cdot 10^{5}$	$6 \cdot 10^{5}$	$6 \cdot 10^{3}$	$6 \cdot 10^{5}$	$6 \cdot 10^{3}$	$7 \cdot 10^{4}$	$1 \cdot 10^{1}$	$6 \cdot 10^{5}$	$2 \cdot 10^{3}$
^{129}I	$1.6 \cdot 10^{7}$	$4 \cdot 10^{3}$	$1 \cdot 10^{3}$	$4 \cdot 10^{3}$	$1 \cdot 10^{3}$	$5 \cdot 10^{1}$	1	$4 \cdot 10^{3}$	$1 \cdot 10^{2}$
^{135}Cs	$2.3 \cdot 10^{6}$	$3 \cdot 10^{4}$	$8 \cdot 10^{3}$	$3 \cdot 10^{4}$	$8 \cdot 10^{3}$	– [a]	– [a]	– [a]	– [a]
^{137}Cs	30	– [a]	– [a]	– [a]	– [a]	$2 \cdot 10^{2}$	1	– [a]	– [a]
^{236}U	$2.3 \cdot 10^{7}$	$9 \cdot 10^{6}$	8	$9 \cdot 10^{6}$	8	– [a]	– [a]	– [a]	– [a]
^{232}Th	$1.4 \cdot 10^{10}$	$7 \cdot 10^{8}$	9	$1 \cdot 10^{7}$	$2 \cdot 10^{2}$	– [a]	– [a]	– [a]	– [a]
^{237}Np	$2.1 \cdot 10^{6}$	$4 \cdot 10^{6}$	3	$4 \cdot 10^{6}$	3	– [a]	– [a]	– [a]	– [a]
^{233}U	$1.6 \cdot 10^{5}$	$4 \cdot 10^{6}$	3	$4 \cdot 10^{6}$	3	– [a]	– [a]	– [a]	– [a]
^{229}Th	$7.3 \cdot 10^{3}$	$4 \cdot 10^{6}$	4	$4 \cdot 10^{6}$	4	– [a]	– [a]	– [a]	– [a]
^{238}U	$4.5 \cdot 10^{9}$	$1 \cdot 10^{9}$	$3 \cdot 10^{1}$	$1 \cdot 10^{7}$	$9 \cdot 10^{2}$	–	$< 1 \cdot 10^{-3}$	$1 \cdot 10^{7}$	$1 \cdot 10^{-3}$
^{234}U	$2.5 \cdot 10^{5}$	$3 \cdot 10^{8}$	$3 \cdot 10^{1}$	$1 \cdot 10^{7}$	$9 \cdot 10^{2}$	–	$< 1 \cdot 10^{-3}$	$1 \cdot 10^{7}$	$1 \cdot 10^{-3}$
^{230}Th	$7.5 \cdot 10^{4}$	$9 \cdot 10^{7}$	$3 \cdot 10^{1}$	$9 \cdot 10^{6}$	$1 \cdot 10^{3}$	–	$< 1 \cdot 10^{-3}$	$1 \cdot 10^{7}$	$1 \cdot 10^{-3}$
^{226}Ra	$1.6 \cdot 10^{3}$	$7 \cdot 10^{7}$	$1 \cdot 10^{4}$	$1 \cdot 10^{7}$	$2 \cdot 10^{5}$	$3 \cdot 10^{5}$	$3 \cdot 10^{-3}$	$1 \cdot 10^{7}$	$3 \cdot 10^{-1}$
^{210}Pb	22	$7 \cdot 10^{7}$	$1 \cdot 10^{4}$	$1 \cdot 10^{7}$	$2 \cdot 10^{5}$	$3 \cdot 10^{5}$	$3 \cdot 10^{-3}$	$1 \cdot 10^{7}$	$3 \cdot 10^{-1}$

a) Not modelled.

8.2 Beberg

The geosphere has a larger impact on the nuclide release rate in Beberg than in Aberg. Partly because of the somewhat longer water travel time in Beberg. More important is, however, the difference in flow-wetted surface area which is about one order of magnitude larger in Beberg, resulting in higher preference for the nuclides to sorb in the rock matrix. Also of importance for the release rate is the type of water present in Beberg, a factor that influences the sorption capacity and the effective diffusivity of some nuclides.

^{3}H and ^{90}Sr, which dominate the far-field release rate from SFL 3 in Aberg (Figure 8-1) up to about 100 years from repository closure, is of much less importance in Beberg (Figure 8-4). While the results for Aberg show that inorganic ^{14}C, ^{36}Cl and ^{93}Mo all result in a maximum release rate of the same order of magnitude, inorganic ^{14}C decays to a large extent before being released from the far-field rock in Beberg. The maximum release rate of ^{36}Cl and ^{93}Mo on the other hand is still about 10^{5} - 10^{6} Bq/year. The

major part of the initial inventory of ^{36}Cl is released from the far field in Beberg, but only a few per cent of the initial inventory of ^{93}Mo. The amount of ^{59}Ni released from the far field in Beberg is reduced significantly in comparison to that in Aberg, and the maximum release rate of ^{59}Ni is $4 \cdot 10^4$ Bq/year.

The effect of ISA on the far-field release rate from SFL 3 in Beberg is smaller than for Aberg discussed earlier in this chapter. The maximum release rate of ^{232}Th when ISA is accounted for is between four and five times higher than when the effect of ISA is neglected. For ^{238}U and its daughters the corresponding factor is between two and three, and for ^{59}Ni little less than two. The far-field release rate from SFL 3 in Beberg under the influence of ISA is included in Tables 8-2 and 8-4 for saline and non-saline conditions, respectively.

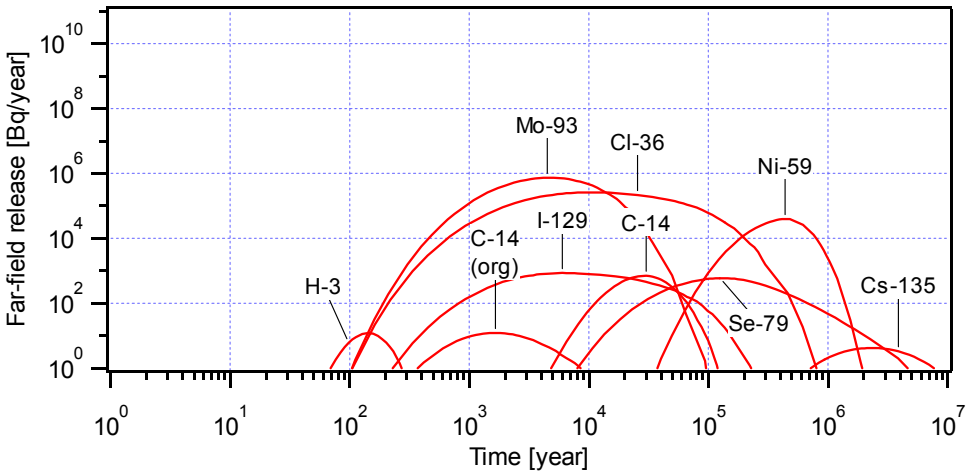

Figure 8-4 Far-field release from SFL 3 in Beberg, saline water, no influence of ISA.

Most of the nuclides in SFL 4 decay to insignificant amounts before being released from the far field in Beberg. The only nuclides having a release rate higher than 1 Bq/year from the far field in Beberg is ^{3}H, ^{36}Cl, ^{59}Ni and ^{93}Mo (Figure 8-5).

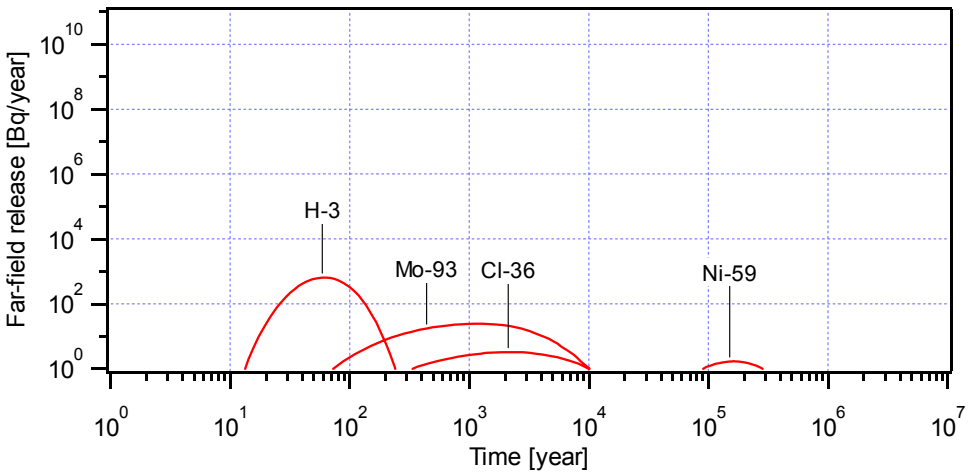

Figure 8-5 Far-field release from SFL 4 in Beberg, saline water.

For the SFL 5 repository, the release rate from the far field in Beberg is shown in Figure 8-6. The release rate of ^{3}H is reduced significantly in comparison to the release from the near field. This is also the case for inorganic ^{14}C, ^{59}Ni, ^{90}Sr and ^{93}Zr. The release rates of ^{36}Cl and ^{93}Mo on the other hand are almost the same, around 10^{6} Bq/year. After very long time, ^{10}Be dominates the release rate.

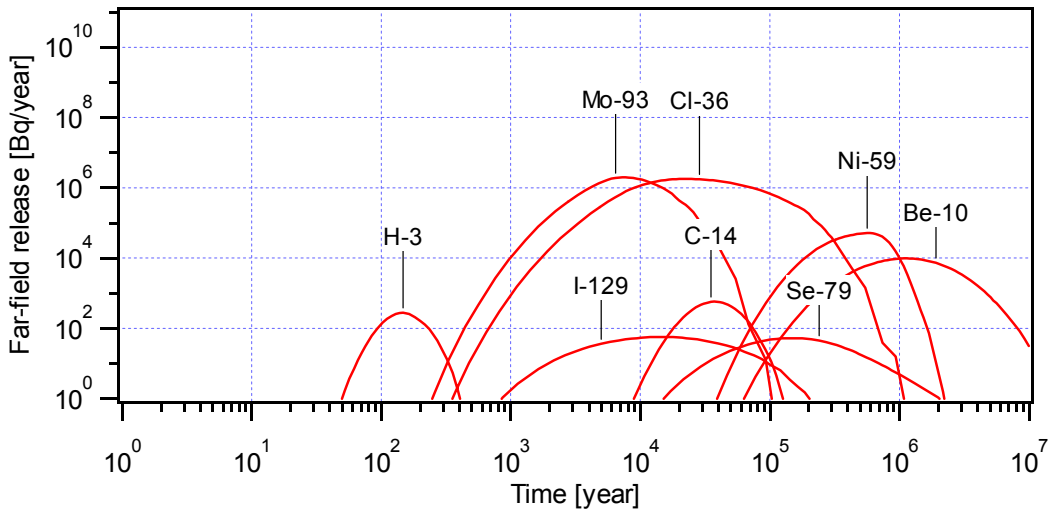

Figure 8-6 Far-field release from SFL 5 in Beberg, saline water.

The maximum far-field release rates and corresponding times in Beberg under saline conditions are compiled in Table 8-2.

Table 8-2 Maximum far-field release rates from SFL 3, SFL 4 and SFL 5 in Beberg (saline waters).

Nuclide	Half-life	SFL 3 (without ISA)		SFL 3 (with ISA)		SFL 4		SFL 5	
		Time of maximum release rate	maximum release rate	Time of maximum release rate	maximum release rate	Time of maximum release rate	maximum release rate	Time of maximum release rate	maximum release rate
	[year]	[year]	[Bq/year]	[year]	[Bq/year]	[year]	[Bq/year]	[year]	[Bq/year]
^{3}H	12	$1 \cdot 10^{2}$	$1 \cdot 10^{1}$	$1 \cdot 10^{2}$	$1 \cdot 10^{1}$	$6 \cdot 10^{1}$	$6 \cdot 10^{2}$	$1 \cdot 10^{2}$	$3 \cdot 10^{2}$
^{10}Be	$1.5 \cdot 10^{6}$	– a)	– a)	– a)	– a)	– a)	– a)	$1 \cdot 10^{6}$	$1 \cdot 10^{4}$
^{14}C	$5.7 \cdot 10^{3}$	$3 \cdot 10^{4}$	$7 \cdot 10^{2}$	$3 \cdot 10^{4}$	$7 \cdot 10^{2}$	$2 \cdot 10^{4}$	$3 \cdot 10^{-1}$	$4 \cdot 10^{4}$	$6 \cdot 10^{2}$
$^{14}C_{org}$	$5.7 \cdot 10^{3}$	$2 \cdot 10^{3}$	$1 \cdot 10^{1}$	$2 \cdot 10^{3}$	$1 \cdot 10^{1}$	– a)	– a)	– a)	– a)
^{36}Cl	$3.0 \cdot 10^{5}$	$1 \cdot 10^{4}$	$3 \cdot 10^{5}$	$1 \cdot 10^{4}$	$3 \cdot 10^{5}$	$2 \cdot 10^{3}$	3	$2 \cdot 10^{4}$	$2 \cdot 10^{6}$
^{60}Co	5.3	– a)	– a)	– a)	– a)	–	$< 1 \cdot 10^{-3}$	– a)	– a)
^{59}Ni	$7.6 \cdot 10^{4}$	$4 \cdot 10^{5}$	$4 \cdot 10^{4}$	$4 \cdot 10^{5}$	$7 \cdot 10^{4}$	$2 \cdot 10^{5}$	2	$6 \cdot 10^{5}$	$5 \cdot 10^{4}$
^{63}Ni	$1.0 \cdot 10^{2}$	– a)	– a)	– a)	– a)	–	$< 1 \cdot 10^{-3}$	– a)	– a)
^{79}Se	$1.1 \cdot 10^{6}$	$1 \cdot 10^{5}$	$6 \cdot 10^{2}$	$1 \cdot 10^{5}$	$6 \cdot 10^{2}$	$5 \cdot 10^{4}$	$1 \cdot 10^{-2}$	$2 \cdot 10^{5}$	$5 \cdot 10^{1}$
^{90}Sr	29	–	$< 1 \cdot 10^{-3}$	–	$< 1 \cdot 10^{-3}$	–	$< 1 \cdot 10^{-3}$	–	$< 1 \cdot 10^{-3}$
^{94}Nb	$2.0 \cdot 10^{4}$	– a)	– a)	– a)	– a)	–	$< 1 \cdot 10^{-3}$	– a)	– a)
^{93}Zr	$1.5 \cdot 10^{6}$	$9 \cdot 10^{6}$	$3 \cdot 10^{-2}$	$9 \cdot 10^{6}$	$3 \cdot 10^{-2}$	– a)	– a)	$9 \cdot 10^{6}$	2
^{93}Mo	$4.0 \cdot 10^{3}$	$4 \cdot 10^{3}$	$7 \cdot 10^{5}$	$4 \cdot 10^{3}$	$7 \cdot 10^{5}$	$1 \cdot 10^{3}$	$2 \cdot 10^{1}$	$8 \cdot 10^{3}$	$2 \cdot 10^{6}$
^{99}Tc	$2.1 \cdot 10^{5}$	–	$< 1 \cdot 10^{-3}$	–	$< 1 \cdot 10^{-3}$	–	$< 1 \cdot 10^{-3}$	–	$< 1 \cdot 10^{-3}$
^{129}I	$1.6 \cdot 10^{7}$	$6 \cdot 10^{3}$	$8 \cdot 10^{2}$	$6 \cdot 10^{3}$	$8 \cdot 10^{2}$	$1 \cdot 10^{3}$	$7 \cdot 10^{-2}$	$1 \cdot 10^{4}$	$6 \cdot 10^{1}$
^{135}Cs	$2.3 \cdot 10^{6}$	$2 \cdot 10^{6}$	4	$2 \cdot 10^{6}$	4	– a)	– a)	– a)	– a)
^{137}Cs	30	– a)	– a)	– a)	– a)	–	$< 1 \cdot 10^{-3}$	– a)	– a)
^{236}U	$2.3 \cdot 10^{7}$	$8 \cdot 10^{7}$	$4 \cdot 10^{-3}$	$9 \cdot 10^{7}$	$4 \cdot 10^{-3}$	– a)	– a)	– a)	– a)
^{232}Th	$1.4 \cdot 10^{10}$	$1 \cdot 10^{9}$	4	$1 \cdot 10^{8}$	$2 \cdot 10^{1}$	– a)	– a)	– a)	– a)
^{237}Np	$2.1 \cdot 10^{6}$	–	$< 1 \cdot 10^{-3}$	–	$< 1 \cdot 10^{-3}$	– a)	– a)	– a)	– a)
^{233}U	$1.6 \cdot 10^{5}$	–	$< 1 \cdot 10^{-3}$	–	$< 1 \cdot 10^{-3}$	– a)	– a)	– a)	– a)
^{229}Th	$7.3 \cdot 10^{3}$	–	$< 1 \cdot 10^{-3}$	–	$< 1 \cdot 10^{-3}$	– a)	– a)	– a)	– a)
^{238}U	$4.5 \cdot 10^{9}$	$2 \cdot 10^{9}$	7	$3 \cdot 10^{8}$	$2 \cdot 10^{1}$	–	$< 1 \cdot 10^{-3}$	–	$< 1 \cdot 10^{-3}$
^{234}U	$2.5 \cdot 10^{5}$	$2 \cdot 10^{9}$	7	$3 \cdot 10^{8}$	$2 \cdot 10^{1}$	–	$< 1 \cdot 10^{-3}$	–	$< 1 \cdot 10^{-3}$
^{230}Th	$7.5 \cdot 10^{4}$	$2 \cdot 10^{9}$	7	$3 \cdot 10^{8}$	$2 \cdot 10^{1}$	–	$< 1 \cdot 10^{-3}$	–	$< 1 \cdot 10^{-3}$
^{226}Ra	$1.6 \cdot 10^{3}$	$2 \cdot 10^{9}$	$2 \cdot 10^{3}$	$3 \cdot 10^{8}$	$4 \cdot 10^{3}$	–	$< 1 \cdot 10^{-3}$	$3 \cdot 10^{8}$	$7 \cdot 10^{-3}$
^{210}Pb	22	$2 \cdot 10^{9}$	$2 \cdot 10^{3}$	$3 \cdot 10^{8}$	$4 \cdot 10^{3}$	–	$< 1 \cdot 10^{-3}$	$3 \cdot 10^{8}$	$7 \cdot 10^{-3}$

a) Not modelled.

All of the results presented above for Beberg is for saline groundwater. However, non-saline water should also be considered for this site. The water composition affects diffusion porosity (and consequently the effective diffusivity)and/or sorption coefficient in the rock matrix for some elements (Table 8-3). Included in this table is whether the parameter under non-saline conditions increases (↑), decreases (↓) or has no influence (→) on the release rate of the element in comparison to that under saline conditions. Based on this table it can theoretically be concluded that the release rate of inorganic ^{14}C, ^{36}Cl and ^{129}I increases under non-saline conditions, for the rest of the elements in Table 8-3 it decreases.

Table 8-3 Parameter influence on the release rate under non-saline conditions in comparison to saline conditions.

Element	Influence on release rate	
	D_e	K_d
Be	→	↓
$C_{inorganic}$	↑	→
Cl	↑	→
Co	→	↓
Ni	→	↓
Sr	↓	↓
I	↑	→
Cs	↓	↓
Ra	→	↓
Pb	→	↓

As shown in Table 5.7 the effective diffusivity of inorganic carbon, chloride and iodine depends on the groundwater conditions. This is due to the fact that these ions are present as anions, and anions have more difficult than cations to penetrate into micro fissures in the rock due to a phenomenon called anion exclusion. Saline groundwater reduces this effect, and thus the effective diffusivity increases. The release rate of anions in non-saline water is higher than that in saline water.

For the conditions prevailing in Beberg, this has a limited effect on the release rate of ^{36}Cl and ^{129}I. For inorganic ^{14}C the difference in maximum release rate between saline and non-saline water is larger. The release rate increases between one and two orders of magnitude in non-saline water. This difference between ^{36}Cl and ^{129}I on one hand and inorganic ^{14}C on the other, are related to when the nuclide is released in comparison to its half-life. The additional retardation obtained under saline conditions makes the contribution from radioactive decay more important for inorganic ^{14}C than for the more long-lived ^{36}Cl and ^{129}I.

The effective diffusivity of strontium and caesium, which are present as cations, is higher in non-saline water than in saline. This phenomenon has been explained by surface diffusion (Ohlsson and Neretnieks, 1997). There is another positive effect of non-saline water on the migration of strontium and caesium. Their sorption coefficient on granite is higher at a low ionic strength than at a high ionic strength. Thus, both matrix diffusion and sorption are improved in non-saline water. The calculations show, however, that both ^{90}Sr, ^{135}Cs and ^{137}Cs decay to insignificant levels even though the groundwater is saline (Table 8-2).

Of the other elements in Table 8-3, it is mainly ^{59}Ni in SFL 3 and SFL 5 for which non-saline water has a positive effect of importance for the total release rate. As shown in Figures 8-4 and 8-6 for saline water, ^{59}Ni dominates the far-field release from SFL 3 and SFL 5 at times around 10^5 and 10^6 years from repository closure. In non-saline water, the maximum release rate is reduced by a factor 400. ^{59}Ni therefore dominates the far-field release rate under a very short period only, and its release rate at that time is close to the release rate of ^{79}Se (in SFL 3) and ^{10}Be and ^{36}Cl (in SFL 5).

The maximum far-field release rates and corresponding times in Beberg under non-saline conditions are compiled in Table 8-4.

Table 8-4 Maximum far-field release rates from SFL 3, SFL 4 and SFL 5 in Beberg (non-saline waters).

Nuclide	Half-life	SFL 3 (without ISA)		SFL 3 (with ISA)		SFL 4		SFL 5	
		Time of maximum release rate	maximum release rate	Time of maximum release rate	maximum release rate	Time of maximum release rate	maximum release rate	Time of maximum release rate	maximum release rate
	[year]	[year]	[Bq/year]	[year]	[Bq/year]	[year]	[Bq/year]	[year]	[Bq/year]
^{3}H	12	$1{\cdot}10^{2}$	$1{\cdot}10^{1}$	$1{\cdot}10^{2}$	$1{\cdot}10^{1}$	$6{\cdot}10^{1}$	$6{\cdot}10^{2}$	$1{\cdot}10^{2}$	$3{\cdot}10^{2}$
^{10}Be	$1.5{\cdot}10^{6}$	– a)	– a)	– a)	– a)	– a)	– a)	$2{\cdot}10^{6}$	$1{\cdot}10^{3}$
^{14}C	$5.7{\cdot}10^{3}$	$2{\cdot}10^{4}$	$3{\cdot}10^{4}$	$2{\cdot}10^{4}$	$3{\cdot}10^{4}$	$9{\cdot}10^{3}$	$1{\cdot}10^{1}$	$3{\cdot}10^{4}$	$2{\cdot}10^{4}$
$^{14}C_{org}$	$5.7{\cdot}10^{3}$	$2{\cdot}10^{3}$	$1{\cdot}10^{1}$	$2{\cdot}10^{3}$	$1{\cdot}10^{1}$	– a)	– a)	– a)	– a)
^{36}Cl	$3.0{\cdot}10^{5}$	$1{\cdot}10^{4}$	$3{\cdot}10^{5}$	$1{\cdot}10^{4}$	$3{\cdot}10^{5}$	$4{\cdot}10^{2}$	7	$2{\cdot}10^{4}$	$2{\cdot}10^{6}$
^{60}Co	5.3	– a)	– a)	– a)	– a)	–	$< 1{\cdot}10^{-3}$	– a)	– a)
^{59}Ni	$7.6{\cdot}10^{4}$	$7{\cdot}10^{5}$	$1{\cdot}10^{2}$	$6{\cdot}10^{5}$	$2{\cdot}10^{2}$	$3{\cdot}10^{5}$	$1{\cdot}10^{-2}$	$8{\cdot}10^{5}$	$1{\cdot}10^{2}$
^{63}Ni	$1.0{\cdot}10^{2}$	– a)	– a)	– a)	– a)	–	$< 1{\cdot}10^{-3}$	– a)	– a)
^{79}Se	$1.1{\cdot}10^{6}$	$1{\cdot}10^{5}$	$6{\cdot}10^{2}$	$1{\cdot}10^{5}$	$6{\cdot}10^{2}$	$5{\cdot}10^{4}$	$1{\cdot}10^{-2}$	$2{\cdot}10^{5}$	$5{\cdot}10^{1}$
^{90}Sr	29	–	$< 1{\cdot}10^{-3}$	–	$< 1{\cdot}10^{-3}$	–	$< 1{\cdot}10^{-3}$	–	$< 1{\cdot}10^{-3}$
^{94}Nb	$2.0{\cdot}10^{4}$	– a)	– a)	– a)	– a)	–	$< 1{\cdot}10^{-3}$	– a)	– a)
^{93}Zr	$1.5{\cdot}10^{6}$	$9{\cdot}10^{6}$	$3{\cdot}10^{-2}$	$9{\cdot}10^{6}$	$3{\cdot}10^{-2}$	– a)	– a)	$9{\cdot}10^{6}$	2
^{93}Mo	$4.0{\cdot}10^{3}$	$5{\cdot}10^{3}$	$7{\cdot}10^{5}$	$4{\cdot}10^{3}$	$7{\cdot}10^{5}$	$1{\cdot}10^{3}$	$2{\cdot}10^{1}$	$8{\cdot}10^{3}$	$2{\cdot}10^{6}$
^{99}Tc	$2.1{\cdot}10^{5}$	–	$< 1{\cdot}10^{-3}$	–	$< 1{\cdot}10^{-3}$	–	$< 1{\cdot}10^{-3}$	–	$< 1{\cdot}10^{-3}$
^{129}I	$1.6{\cdot}10^{7}$	$6{\cdot}10^{3}$	$8{\cdot}10^{2}$	$6{\cdot}10^{3}$	$8{\cdot}10^{2}$	$4{\cdot}10^{2}$	$2{\cdot}10^{-1}$	$8{\cdot}10^{3}$	$6{\cdot}10^{1}$
^{135}Cs	$2.3{\cdot}10^{6}$	–	$< 1{\cdot}10^{-3}$	–	$< 1{\cdot}10^{-3}$	– a)	– a)	– a)	– a)
^{137}Cs	30	– a)	– a)	– a)	– a)	–	$< 1{\cdot}10^{-3}$	– a)	– a)
^{236}U	$2.3{\cdot}10^{7}$	$9{\cdot}10^{7}$	$4{\cdot}10^{-3}$	$9{\cdot}10^{7}$	$4{\cdot}10^{-3}$	– a)	– a)	– a)	– a)
^{232}Th	$1.4{\cdot}10^{10}$	$1{\cdot}10^{9}$	4	$1{\cdot}10^{8}$	$2{\cdot}10^{1}$	– a)	– a)	– a)	– a)
^{237}Np	$2.1{\cdot}10^{6}$	–	$< 1{\cdot}10^{-3}$	–	$< 1{\cdot}10^{-3}$	– a)	– a)	– a)	– a)
^{233}U	$1.6{\cdot}10^{5}$	–	$< 1{\cdot}10^{-3}$	–	$< 1{\cdot}10^{-3}$	– a)	– a)	– a)	– a)
^{229}Th	$7.3{\cdot}10^{3}$	–	$< 1{\cdot}10^{-3}$	–	$< 1{\cdot}10^{-3}$	– a)	– a)	– a)	– a)
^{238}U	$4.5{\cdot}10^{9}$	$2{\cdot}10^{9}$	7	$3{\cdot}10^{8}$	$2{\cdot}10^{1}$	–	$< 1{\cdot}10^{-3}$	–	$< 1{\cdot}10^{-3}$
^{234}U	$2.5{\cdot}10^{5}$	$2{\cdot}10^{9}$	7	$3{\cdot}10^{8}$	$2{\cdot}10^{1}$	–	$< 1{\cdot}10^{-3}$	–	$< 1{\cdot}10^{-3}$
^{230}Th	$7.5{\cdot}10^{4}$	$2{\cdot}10^{9}$	7	$3{\cdot}10^{8}$	$2{\cdot}10^{1}$	–	$< 1{\cdot}10^{-3}$	–	$< 1{\cdot}10^{-3}$
^{226}Ra	$1.6{\cdot}10^{3}$	$2{\cdot}10^{9}$	$3{\cdot}10^{2}$	$3{\cdot}10^{8}$	$9{\cdot}10^{2}$	–	$< 1{\cdot}10^{-3}$	$4{\cdot}10^{8}$	$1{\cdot}10^{-3}$
^{210}Pb	22	$2{\cdot}10^{9}$	$3{\cdot}10^{2}$	$3{\cdot}10^{8}$	$9{\cdot}10^{2}$	–	$< 1{\cdot}10^{-3}$	$3{\cdot}10^{8}$	$1{\cdot}10^{-3}$

a) Not modelled.

8.3 Ceberg

The water travel time used for Ceberg is 900 years, i.e. much longer than that for Aberg and Beberg. The flow-wetted surface area on the other hand is 10^3 m^2/m^3, which is of the same order of magnitude as for Aberg. The penetration depth in the rock matrix in Ceberg is ten times that in Aberg and Beberg. This could be of importance for non-sorbing nuclides, and possibly also for low-sorbing nuclides.

The release of nuclides from the far field rock in Ceberg is retarded significantly. ^{3}H therefore decays entirely in the far field rock. More long-lived nuclides are affected as well. ^{59}Ni in SFL 3 and SFL 5 which dominates the far-field release in Aberg to a large extent and to some extent in Beberg, decays significantly why the maximum release rate

is much lower than in Beberg (<1 Bq year). The release of other long-lived nuclides (e.g. ^{36}Cl, ^{79}Se and ^{93}Mo) is delayed, but the effect on maximum release rate is limited. The whole initial inventory of ^{129}I and a significant part of the initial inventory of ^{36}Cl and ^{79}Se (2/3 and 1/4 respectively) is still released from the far field rock.

^{36}Cl and ^{93}Mo in both SFL 3 and SFL 5 dominate the release rate (Figure 8-7 and 8-8). The highest release rate is obtained from ^{36}Cl ($7 \cdot 10^4$ Bq/year for SFL 3 and $4 \cdot 10^5$ Bq/year for SFL 5). For SFL 4 ^{93}Mo is the only nuclide with a release rate exceeding 1 Bq/year.

The effect of ISA on the far-field release rate from SFL 3 in Ceberg is approximately the same as for Beberg discussed earlier in this chapter. The far-field release rate from SFL 3 in Ceberg under the influence of ISA is included in Table 8-5.

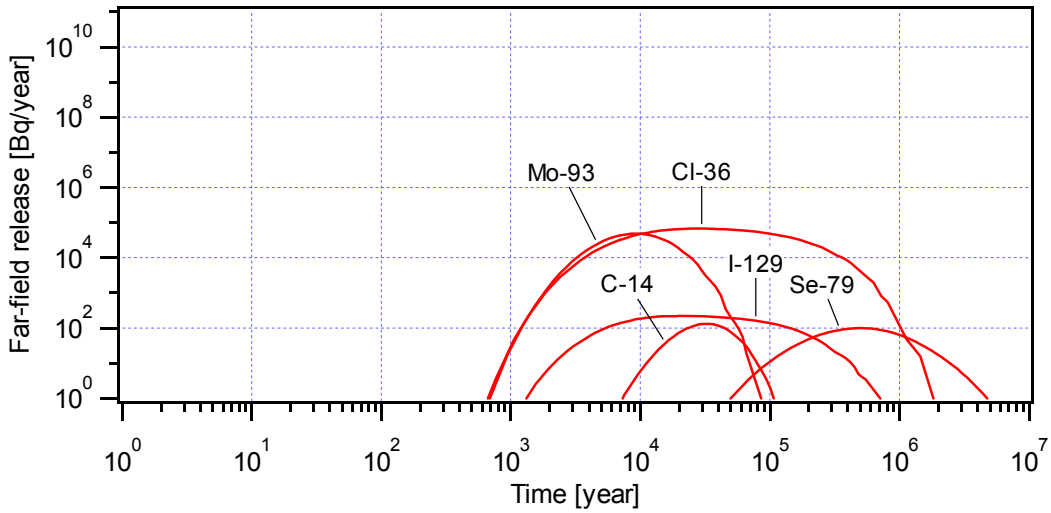

Figure 8-7 Far-field release from SFL 3 in Ceberg, no influence of ISA.

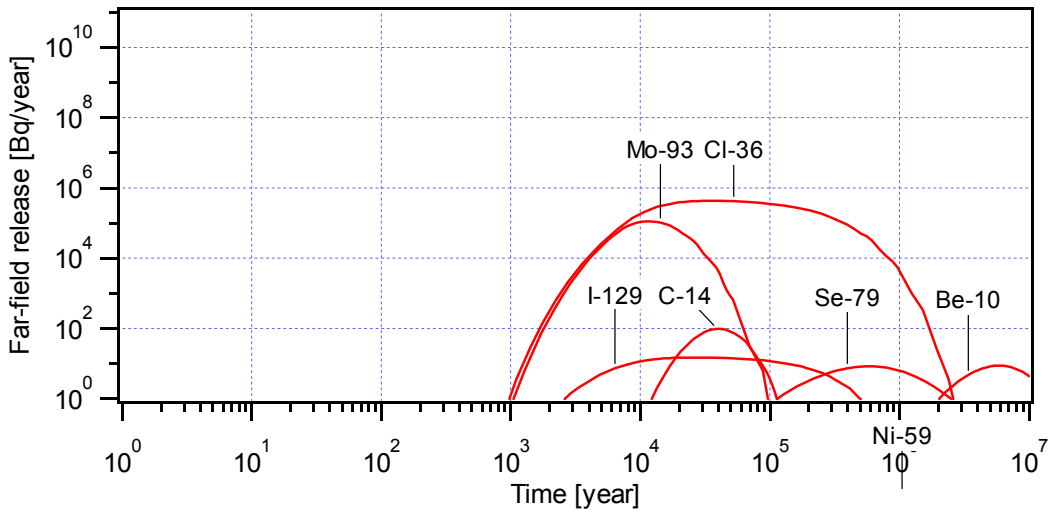

Figure 8-8 Far-field release from SFL 5 in Ceberg.

The maximum far-field release rates in Ceberg are compiled in Table 8-5.

Table 8-5 Maximum far-field release rates from SFL 3, SFL 4 and SFL 5 in Ceberg.

Nuclide	Half-life	SFL 3 (without ISA)		SFL 3 (with ISA)		SFL 4		SFL 5	
		Time of maximum release rate	maximum release rate	Time of maximum release rate	maximum release rate	Time of maximum release rate	maximum release rate	Time of maximum release rate	maximum release rate
	[year]	[year]	[Bq/year]	[year]	[Bq/year]	[year]	[Bq/year]	[year]	[Bq/year]
^{3}H	12	–	$< 1 \cdot 10^{-3}$	–	$< 1 \cdot 10^{-3}$	–	$< 1 \cdot 10^{-3}$	–	$< 1 \cdot 10^{-3}$
^{10}Be	$1.5 \cdot 10^{6}$	– [a]	– [a]	– [a]	– [a]	– [a]	– [a]	$6 \cdot 10^{6}$	9
^{14}C	$5.7 \cdot 10^{3}$	$3 \cdot 10^{4}$	$1 \cdot 10^{2}$	$3 \cdot 10^{4}$	$1 \cdot 10^{2}$	$2 \cdot 10^{4}$	$1 \cdot 10^{-1}$	$4 \cdot 10^{4}$	$1 \cdot 10^{2}$
$^{14}C_{org}$	$5.7 \cdot 10^{3}$	$7 \cdot 10^{3}$	1	$7 \cdot 10^{3}$	1	– [a]	– [a]	– [a]	– [a]
^{36}Cl	$3.0 \cdot 10^{5}$	$3 \cdot 10^{4}$	$7 \cdot 10^{4}$	$3 \cdot 10^{4}$	$7 \cdot 10^{4}$	$5 \cdot 10^{3}$	$8 \cdot 10^{-1}$	$3 \cdot 10^{4}$	$4 \cdot 10^{5}$
^{60}Co	5.3	– [a]	– [a]	– [a]	– [a]	–	$< 1 \cdot 10^{-3}$	– [a]	– [a]
^{59}Ni	$7.6 \cdot 10^{4}$	$1 \cdot 10^{6}$	$2 \cdot 10^{-3}$	$9 \cdot 10^{5}$	$3 \cdot 10^{-3}$	–	$< 1 \cdot 10^{-3}$	$1 \cdot 10^{6}$	$2 \cdot 10^{-3}$
^{63}Ni	$1.0 \cdot 10^{2}$	– [a]	– [a]	– [a]	– [a]	–	$< 1 \cdot 10^{-3}$	– [a]	– [a]
^{79}Se	$1.1 \cdot 10^{6}$	$5 \cdot 10^{5}$	$1 \cdot 10^{2}$	$5 \cdot 10^{5}$	$1 \cdot 10^{2}$	–	$< 1 \cdot 10^{-3}$	$6 \cdot 10^{5}$	8
^{90}Sr	29	–	$< 1 \cdot 10^{-3}$	–	$< 1 \cdot 10^{-3}$	–	$< 1 \cdot 10^{-3}$	–	$< 1 \cdot 10^{-3}$
^{94}Nb	$2.0 \cdot 10^{4}$	– [a]	– [a]	– [a]	– [a]	–	$< 1 \cdot 10^{-3}$	– [a]	– [a]
^{93}Zr	$1.5 \cdot 10^{6}$	–	$< 1 \cdot 10^{-3}$	–	$< 1 \cdot 10^{-3}$	– [a]	– [a]	–	$< 1 \cdot 10^{-3}$
^{93}Mo	$4.0 \cdot 10^{3}$	$9 \cdot 10^{3}$	$5 \cdot 10^{4}$	$9 \cdot 10^{3}$	$5 \cdot 10^{4}$	$4 \cdot 10^{3}$	1	$1 \cdot 10^{4}$	$1 \cdot 10^{5}$
^{99}Tc	$2.1 \cdot 10^{5}$	–	$< 1 \cdot 10^{-3}$	–	$< 1 \cdot 10^{-3}$	–	$< 1 \cdot 10^{-3}$	–	$< 1 \cdot 10^{-3}$
^{129}I	$1.6 \cdot 10^{7}$	$2 \cdot 10^{4}$	$2 \cdot 10^{2}$	$2 \cdot 10^{4}$	$2 \cdot 10^{2}$	$4 \cdot 10^{3}$	$2 \cdot 10^{-2}$	$2 \cdot 10^{4}$	$1 \cdot 10^{1}$
^{135}Cs	$2.3 \cdot 10^{6}$	–	$< 1 \cdot 10^{-3}$	–	$< 1 \cdot 10^{-3}$	– [a]	– [a]	– [a]	– [a]
^{137}Cs	30	– [a]	– [a]	– [a]	– [a]	–	$< 1 \cdot 10^{-3}$	– [a]	– [a]
^{236}U	$2.3 \cdot 10^{7}$	–	$< 1 \cdot 10^{-3}$	–	$< 1 \cdot 10^{-3}$	– [a]	– [a]	– [a]	– [a]
^{232}Th	$1.4 \cdot 10^{10}$	$4 \cdot 10^{9}$	1	$7 \cdot 10^{8}$	4	– [a]	– [a]	– [a]	– [a]
^{237}Np	$2.1 \cdot 10^{6}$	–	$< 1 \cdot 10^{-3}$	–	$< 1 \cdot 10^{-3}$	– [a]	– [a]	– [a]	– [a]
^{233}U	$1.6 \cdot 10^{5}$	–	$< 1 \cdot 10^{-3}$	–	$< 1 \cdot 10^{-3}$	– [a]	– [a]	– [a]	– [a]
^{229}Th	$7.3 \cdot 10^{3}$	–	$< 1 \cdot 10^{-3}$	–	$< 1 \cdot 10^{-3}$	– [a]	– [a]	– [a]	– [a]
^{238}U	$4.5 \cdot 10^{9}$	$5 \cdot 10^{9}$	1	$1 \cdot 10^{9}$	3	–	$< 1 \cdot 10^{-3}$	–	$< 1 \cdot 10^{-3}$
^{234}U	$2.5 \cdot 10^{5}$	$5 \cdot 10^{9}$	1	$1 \cdot 10^{9}$	3	–	$< 1 \cdot 10^{-3}$	–	$< 1 \cdot 10^{-3}$
^{230}Th	$7.5 \cdot 10^{4}$	$5 \cdot 10^{9}$	1	$1 \cdot 10^{9}$	3	–	$< 1 \cdot 10^{-3}$	–	$< 1 \cdot 10^{-3}$
^{226}Ra	$1.6 \cdot 10^{3}$	$5 \cdot 10^{9}$	$5 \cdot 10^{1}$	$1 \cdot 10^{9}$	$1 \cdot 10^{2}$	–	$< 1 \cdot 10^{-3}$	–	$< 1 \cdot 10^{-3}$
^{210}Pb	22	$5 \cdot 10^{9}$	$5 \cdot 10^{1}$	$1 \cdot 10^{9}$	$1 \cdot 10^{2}$	–	$< 1 \cdot 10^{-3}$	–	$< 1 \cdot 10^{-3}$

a) Not modelled.

9 Consequences of release to recipients

In this section, the consequences of release of radionuclides to the biosphere, expressed as dose to man, are presented for the reference scenario on the three sites. Results are given in graphical form for dominating nuclides, and also in tables including the maximum dose and time when this is obtained for all modelled nuclides. For nuclides whose maximum release rate from the far field is less than $1 \cdot 10^{-3}$ Bq/year, the dose presented is set to $< 10^{-3}$ times the ecosystem-specific dose conversion factor (EDF) and the time when the maximum dose is obtained is not specified. In addition, the results for the release of toxic metals are given in the end of this chapter.

In Aberg there are two primary recipients classified as open coast and archipelago, respectively. In Beberg the nuclides are estimated to be released in an area classified as agricultural land. An area classified as peatland is fairly close to where the nuclides are estimated to be released in Beberg. For most of the nuclides studied the ecosystem-specific dose conversion factor for a peatland in Beberg is higher, or even much higher, than for agricultural land (Table 5.8). The consequences of release to a peatland in Beberg are therefore also illustrated. The primary recipient in Ceberg is classified as peatland.

9.1 Dose calculations for release of radionuclides

In the following sub-sections, the dose from the release of dominating nuclides from each repository part is given as a function of time. Also shown in these figures is the aggregate dose (sum of dose for all modelled nuclides within a repository part) from SFL 3, SFL 4 and SFL 5, respectively. Since it is expected that the releases from all three repository parts end up in the same recipient, the total dose (sum of aggregate dose from SFL 3, SFL 4 and SFL 5) is also given.

The results are presented for times up to 10^7 years after repository closure. In such a perspective, the future evolution of the environment is uncertain. Long-term changes in the climate, for instance development of a continental ice sheet, are expected. To indicate the uncertainty due to long-term changes, the results presented in graphical form are shaded from 100,000 years onward.

In accordance with SSI's (National Radiation Protection Institute) regulations regarding protection of human health and the environment in conjunction with the final disposal of spent nuclear fuel and nuclear waste (SSI, 1998), a final repository shall be designed so that the annual risk of deleterious effects after repository closure does not exceed 10^{-6} year^{-1} for an individual exposed to the highest risk. When estimating the probability for deleterious effects, probability coefficients presented in the International Commission on Radiological Protection's (ICRP) publication No. 60 (ICRP, 1991) should be used. The effects that should be accounted for according to SSI are cancer (lethal and non-lethal) and hereditary effects. ICRP reports for this case a probability coefficient of $7.3 \cdot 10^{-2}$ Sv^{-1}. This probability and an annual risk of 10^{-6} year^{-1} correspond to an annual dose of 14 μSv for an individual, provided that the probability that this individual will be exposed to radionuclides leaking from the repository is 100 %. This dose is indicated in the figures in the following sub-sections as a comparison level.

Radiation from ground, outer space and radioactive substances naturally occurring in a human body results in an individual dose in the order of 1 mSv/year. Radiation from other sources (e.g. radon in indoor air and medical radiation) results in an average individual dose in Sweden of approximately 4 mSv/year. In the figures showing the results of the calculations, the dose 1 mSv/year is included as a background level.

9.1.1 Aberg

The release from SFL 3-5 will emerge into areas classified as open coast and archipelago. A significant dilution takes place in such recipients why the nuclides released corresponds to a dose to man that is well below the comparison level. For SFL 3 the nuclide dominating the dose is inorganic ^{14}C (Figure 9-1). The maximum aggregate dose, obtained after some 10,000 years, is $2 \cdot 10^{-9}$ Sv/year for release to archipelago. If the nuclides are released to open coast instead, the maximum aggregate dose is below 10^{-10} Sv/year. For the case where the radionuclide transport in the near field is affected by ISA, the maximum dose is obtained by ^{210}Pb. However, ^{210}Pb is released after very long time, and the maximum aggregate dose ($2 \cdot 10^{-8}$ Sv/year) is obtained after some 10 million years.

The estimated release from SFL 4 is very small. When released to archipelago the dose is dominated by ^{90}Sr which gives a maximum dose of $3 \cdot 10^{-10}$ Sv/year after 35 years (Figure 9-1). Other nuclides in SFL 4 result in a dose less than 10^{-10} Sv/year. Release to open coast instead corresponds to a maximum aggregate dose that does not exceed 10^{-10} Sv/year.

The estimated release from SFL 5 results in two peaks in the dose curve. At first the major contribution is given by ^{3}H, which after 60 years gives a dose of $1 \cdot 10^{-9}$ Sv/year if released to archipelago (Figure 9-1). When the release rate of ^{3}H decreases, the aggregate dose is reduced, but increases again when ^{93}Mo reaches the recipient. Between 5,000 and 500,000 years after repository closure, when in turn ^{93}Mo, inorganic ^{14}C and ^{59}Ni dominates the dose, the aggregate dose for release to archipelago is in the order of 10^{-9} Sv/year again. The maximum aggregate dose is $2 \cdot 10^{-9}$ Sv/year and is obtained after approximately 20,000 years. Release from SFL 5 to open coast in Aberg results in an aggregate dose not exceeding 10^{-10} Sv/year.

The effect of a corrosion rate limited release of inorganic ^{14}C and ^{93}Mo is indicated in the results shown in Figure 9-1. The maximum release rate is obtained somewhat earlier for the release from SFL 3 in comparison to that from SFL 5 where the two nuclides are contained primarily within metallic waste.

The total dose for release to archipelago is included in Figure 9-1. Except for a short period of time (up to about 100 years after repository closure) SFL 4 gives an insignificant contribution to the total dose. For longer times, SFL 3 and SFL 5 alternate in dominating the total dose. The total dose is significantly below the comparison level for release to archipelago. Release to open coast gives a total dose that is ten to hundred times lower than for release to archipelago.

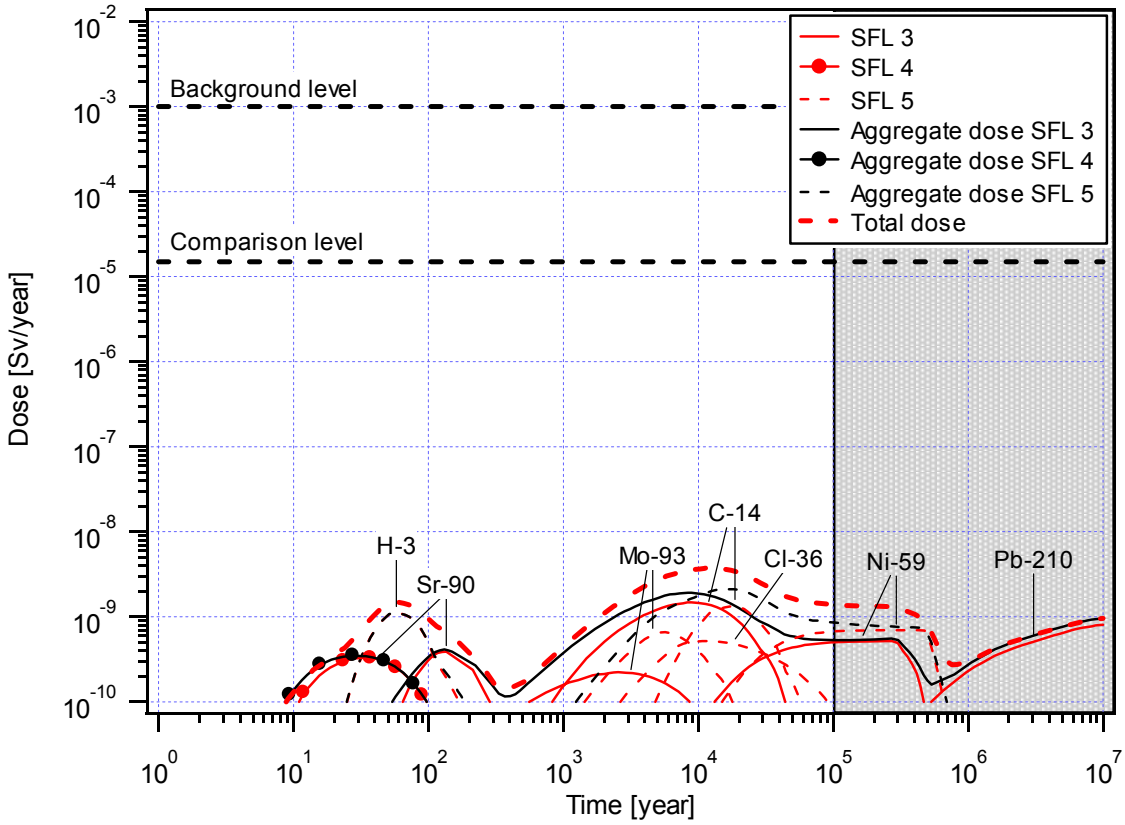

Figure 9-1 Dose from release of radionuclides from SFL 3 (no effect of ISA), SFL 4 (excluding CRUD) and SFL 5 to archipelago in Aberg.

The maximum doses for release to open coast and archipelago in Aberg are compiled in Tables 9-1 and 9-2, respectively.

Table 9-1 Maximum dose for release to open coast in Aberg.

Nuclide	Half-life	SFL 3 (without ISA)		SFL 3 (with ISA)		SFL 4		SFL 5	
		Time of maximum dose	Maximum dose	Time of maximum dose	Maximum dose	Time of maximum dose	Maximum dose	Time of maximum dose	Maximum dose
	[year]	[year]	[Sv/year]	[year]	[Sv/year]	[year]	[Sv/year]	[year]	[Sv/year]
^{3}H	12	$5\cdot10^{1}$	$2\cdot10^{-13}$	$6\cdot10^{1}$	$2\cdot10^{-13}$	$1\cdot10^{1}$	$2\cdot10^{-13}$	$6\cdot10^{1}$	$4\cdot10^{-12}$
^{10}Be	$1.5\cdot10^{6}$	– [a]	– [a]	– [a]	– [a]	– [a]	– [a]	$1\cdot10^{5}$	$5\cdot10^{-13}$
^{14}C	$5.7\cdot10^{3}$	$9\cdot10^{3}$	$6\cdot10^{-12}$	$8\cdot10^{3}$	$6\cdot10^{-12}$	$1\cdot10^{3}$	$9\cdot10^{-15}$	$2\cdot10^{4}$	$5\cdot10^{-12}$
$^{14}C_{org}$	$5.7\cdot10^{3}$	$2\cdot10^{2}$	$4\cdot10^{-16}$	$2\cdot10^{2}$	$4\cdot10^{-16}$	– [a]	– [a]	– [a]	– [a]
^{36}Cl	$3.0\cdot10^{5}$	$7\cdot10^{3}$	$2\cdot10^{-13}$	$8\cdot10^{3}$	$2\cdot10^{-13}$	$6\cdot10^{1}$	$3\cdot10^{-17}$	$1\cdot10^{4}$	$2\cdot10^{-12}$
^{60}Co	5.3	– [a]	– [a]	– [a]	– [a]	$5\cdot10^{1}$	$3\cdot10^{-18}$	– [a]	– [a]
^{59}Ni	$7.6\cdot10^{4}$	$3\cdot10^{5}$	$2\cdot10^{-12}$	$2\cdot10^{5}$	$4\cdot10^{-12}$	$3\cdot10^{3}$	$1\cdot10^{-15}$	$4\cdot10^{5}$	$3\cdot10^{-12}$
^{63}Ni	$1.0\cdot10^{2}$	– [a]	– [a]	– [a]	– [a]	$3\cdot10^{2}$	$6\cdot10^{-15}$	– [a]	– [a]
^{79}Se	$1.1\cdot10^{6}$	$9\cdot10^{3}$	$4\cdot10^{-13}$	$9\cdot10^{3}$	$4\cdot10^{-13}$	$3\cdot10^{2}$	$2\cdot10^{-16}$	$1\cdot10^{4}$	$4\cdot10^{-14}$
^{90}Sr	29	$1\cdot10^{2}$	$1\cdot10^{-12}$	$1\cdot10^{2}$	$1\cdot10^{-12}$	$3\cdot10^{1}$	$1\cdot10^{-12}$	$2\cdot10^{2}$	$1\cdot10^{-13}$
^{94}Nb	$2.0\cdot10^{4}$	– [a]	– [a]	– [a]	– [a]	$3\cdot10^{4}$	$6\cdot10^{-18}$	– [a]	– [a]
^{93}Zr	$1.5\cdot10^{6}$	$1\cdot10^{6}$	$2\cdot10^{-15}$	$1\cdot10^{6}$	$2\cdot10^{-15}$	– [a]	– [a]	$1\cdot10^{6}$	$2\cdot10^{-13}$
^{93}Mo	$4.0\cdot10^{3}$	$3\cdot10^{3}$	$8\cdot10^{-13}$	$3\cdot10^{3}$	$8\cdot10^{-13}$	$5\cdot10^{1}$	$1\cdot10^{-16}$	$6\cdot10^{3}$	$3\cdot10^{-12}$
^{99}Tc	$2.1\cdot10^{5}$	$6\cdot10^{5}$	$4\cdot10^{-15}$	$6\cdot10^{5}$	$4\cdot10^{-15}$	$7\cdot10^{4}$	$8\cdot10^{-18}$	$6\cdot10^{5}$	$1\cdot10^{-15}$
^{129}I	$1.6\cdot10^{7}$	$4\cdot10^{3}$	$1\cdot10^{-13}$	$4\cdot10^{3}$	$1\cdot10^{-13}$	$5\cdot10^{1}$	$1\cdot10^{-16}$	$4\cdot10^{3}$	$1\cdot10^{-14}$
^{135}Cs	$2.3\cdot10^{6}$	$3\cdot10^{4}$	$2\cdot10^{-14}$	$3\cdot10^{4}$	$2\cdot10^{-14}$	– [a]	– [a]	– [a]	– [a]
^{137}Cs	30	– [a]	– [a]	– [a]	– [a]	$2\cdot10^{2}$	$3\cdot10^{-17}$	– [a]	– [a]
^{236}U	$2.3\cdot10^{7}$	$9\cdot10^{6}$	$8\cdot10^{-17}$	$9\cdot10^{6}$	$8\cdot10^{-17}$	– [a]	– [a]	– [a]	– [a]
^{232}Th	$1.4\cdot10^{10}$	$7\cdot10^{8}$	$2\cdot10^{-15}$	$1\cdot10^{7}$	$5\cdot10^{-14}$	– [a]	– [a]	– [a]	– [a]
^{237}Np	$2.1\cdot10^{6}$	$4\cdot10^{6}$	$2\cdot10^{-17}$	$4\cdot10^{6}$	$2\cdot10^{-17}$	– [a]	– [a]	– [a]	– [a]
^{233}U	$1.6\cdot10^{5}$	$4\cdot10^{6}$	$4\cdot10^{-17}$	$4\cdot10^{6}$	$4\cdot10^{-17}$	– [a]	– [a]	– [a]	– [a]
^{229}Th	$7.3\cdot10^{3}$	$4\cdot10^{6}$	$2\cdot10^{-15}$	$4\cdot10^{6}$	$2\cdot10^{-15}$	– [a]	– [a]	– [a]	– [a]
^{238}U	$4.5\cdot10^{9}$	$1\cdot10^{9}$	$3\cdot10^{-16}$	$1\cdot10^{7}$	$8\cdot10^{-15}$	–	$< 1\cdot10^{-20}$	$1\cdot10^{7}$	$1\cdot10^{-20}$
^{234}U	$2.5\cdot10^{5}$	$3\cdot10^{8}$	$3\cdot10^{-16}$	$1\cdot10^{7}$	$9\cdot10^{-15}$	–	$< 1\cdot10^{-20}$	$1\cdot10^{7}$	$1\cdot10^{-20}$
^{230}Th	$7.5\cdot10^{4}$	$9\cdot10^{7}$	$6\cdot10^{-15}$	$9\cdot10^{6}$	$2\cdot10^{-13}$	–	$< 2\cdot10^{-19}$	$1\cdot10^{7}$	$2\cdot10^{-19}$
^{226}Ra	$1.6\cdot10^{3}$	$7\cdot10^{7}$	$7\cdot10^{-13}$	$1\cdot10^{7}$	$1\cdot10^{-11}$	$3\cdot10^{5}$	$2\cdot10^{-19}$	$1\cdot10^{7}$	$2\cdot10^{-17}$
^{210}Pb	22	$7\cdot10^{7}$	$6\cdot10^{-12}$	$1\cdot10^{7}$	$1\cdot10^{-10}$	$3\cdot10^{5}$	$2\cdot10^{-18}$	$1\cdot10^{7}$	$2\cdot10^{-16}$

a) Not modelled.

Table 9-2 Maximum dose for release to archipelago in Aberg.

Nuclide	Half-life	SFL 3 (without ISA)		SFL 3 (with ISA)		SFL 4		SFL 5	
		Time of maximum dose	Maximum dose	Time of maximum dose	Maximum dose	Time of maximum dose	Maximum dose	Time of maximum dose	Maximum dose
	[year]	[year]	[Sv/year]	[year]	[Sv/year]	[year]	[Sv/year]	[year]	[Sv/year]
^{3}H	12	$5{\cdot}10^{1}$	$5{\cdot}10^{-11}$	$6{\cdot}10^{1}$	$5{\cdot}10^{-11}$	$1{\cdot}10^{1}$	$7{\cdot}10^{-11}$	$6{\cdot}10^{1}$	$1{\cdot}10^{-9}$
^{10}Be	$1.5{\cdot}10^{6}$	– [a]	– [a]	– [a]	– [a]	– [a]	– [a]	$1{\cdot}10^{5}$	$1{\cdot}10^{-10}$
^{14}C	$5.7{\cdot}10^{3}$	$9{\cdot}10^{3}$	$1{\cdot}10^{-9}$	$8{\cdot}10^{3}$	$1{\cdot}10^{-9}$	$1{\cdot}10^{3}$	$2{\cdot}10^{-12}$	$2{\cdot}10^{4}$	$1{\cdot}10^{-9}$
$^{14}C_{org}$	$5.7{\cdot}10^{3}$	$2{\cdot}10^{2}$	$1{\cdot}10^{-13}$	$2{\cdot}10^{2}$	$1{\cdot}10^{-13}$	– [a]	– [a]	– [a]	– [a]
^{36}Cl	$3.0{\cdot}10^{5}$	$7{\cdot}10^{3}$	$6{\cdot}10^{-11}$	$8{\cdot}10^{3}$	$6{\cdot}10^{-11}$	$6{\cdot}10^{1}$	$8{\cdot}10^{-15}$	$1{\cdot}10^{4}$	$5{\cdot}10^{-10}$
^{60}Co	5.3	– [a]	– [a]	– [a]	– [a]	$5{\cdot}10^{1}$	$5{\cdot}10^{-16}$	– [a]	– [a]
^{59}Ni	$7.6{\cdot}10^{4}$	$3{\cdot}10^{5}$	$5{\cdot}10^{-10}$	$2{\cdot}10^{5}$	$1{\cdot}10^{-9}$	$3{\cdot}10^{3}$	$3{\cdot}10^{-13}$	$4{\cdot}10^{5}$	$7{\cdot}10^{-10}$
^{63}Ni	$1.0{\cdot}10^{2}$	– [a]	– [a]	– [a]	– [a]	$3{\cdot}10^{2}$	$1{\cdot}10^{-12}$	– [a]	– [a]
^{79}Se	$1.1{\cdot}10^{6}$	$9{\cdot}10^{3}$	$1{\cdot}10^{-10}$	$9{\cdot}10^{3}$	$1{\cdot}10^{-10}$	$3{\cdot}10^{2}$	$6{\cdot}10^{-14}$	$1{\cdot}10^{4}$	$1{\cdot}10^{-11}$
^{90}Sr	29	$1{\cdot}10^{2}$	$4{\cdot}10^{-10}$	$1{\cdot}10^{2}$	$4{\cdot}10^{-10}$	$3{\cdot}10^{1}$	$3{\cdot}10^{-10}$	$2{\cdot}10^{2}$	$3{\cdot}10^{-11}$
^{94}Nb	$2.0{\cdot}10^{4}$	– [a]	– [a]	– [a]	– [a]	$3{\cdot}10^{4}$	$8{\cdot}10^{-16}$	– [a]	– [a]
^{93}Zr	$1.5{\cdot}10^{6}$	$1{\cdot}10^{6}$	$2{\cdot}10^{-13}$	$1{\cdot}10^{6}$	$2{\cdot}10^{-13}$	– [a]	– [a]	$1{\cdot}10^{6}$	$1{\cdot}10^{-11}$
^{93}Mo	$4.0{\cdot}10^{3}$	$3{\cdot}10^{3}$	$2{\cdot}10^{-10}$	$3{\cdot}10^{3}$	$2{\cdot}10^{-10}$	$5{\cdot}10^{1}$	$4{\cdot}10^{-14}$	$6{\cdot}10^{3}$	$7{\cdot}10^{-10}$
^{99}Tc	$2.1{\cdot}10^{5}$	$6{\cdot}10^{5}$	$1{\cdot}10^{-13}$	$6{\cdot}10^{5}$	$1{\cdot}10^{-13}$	$7{\cdot}10^{4}$	$2{\cdot}10^{-16}$	$6{\cdot}10^{5}$	$4{\cdot}10^{-14}$
^{129}I	$1.6{\cdot}10^{7}$	$4{\cdot}10^{3}$	$2{\cdot}10^{-11}$	$4{\cdot}10^{3}$	$2{\cdot}10^{-11}$	$5{\cdot}10^{1}$	$2{\cdot}10^{-14}$	$4{\cdot}10^{3}$	$2{\cdot}10^{-12}$
^{135}Cs	$2.3{\cdot}10^{6}$	$3{\cdot}10^{4}$	$6{\cdot}10^{-12}$	$3{\cdot}10^{4}$	$6{\cdot}10^{-12}$	– [a]	– [a]	– [a]	– [a]
^{137}Cs	30	– [a]	– [a]	– [a]	– [a]	$2{\cdot}10^{2}$	$7{\cdot}10^{-15}$	– [a]	– [a]
^{236}U	$2.3{\cdot}10^{7}$	$9{\cdot}10^{6}$	$2{\cdot}10^{-14}$	$9{\cdot}10^{6}$	$2{\cdot}10^{-14}$	– [a]	– [a]	– [a]	– [a]
^{232}Th	$1.4{\cdot}10^{10}$	$7{\cdot}10^{8}$	$5{\cdot}10^{-14}$	$1{\cdot}10^{7}$	$1{\cdot}10^{-12}$	– [a]	– [a]	– [a]	– [a]
^{237}Np	$2.1{\cdot}10^{6}$	$4{\cdot}10^{6}$	$6{\cdot}10^{-15}$	$4{\cdot}10^{6}$	$6{\cdot}10^{-15}$	– [a]	– [a]	– [a]	– [a]
^{233}U	$1.6{\cdot}10^{5}$	$4{\cdot}10^{6}$	$9{\cdot}10^{-15}$	$4{\cdot}10^{6}$	$9{\cdot}10^{-15}$	– [a]	– [a]	– [a]	– [a]
^{229}Th	$7.3{\cdot}10^{3}$	$4{\cdot}10^{6}$	$5{\cdot}10^{-14}$	$4{\cdot}10^{6}$	$5{\cdot}10^{-14}$	– [a]	– [a]	– [a]	– [a]
^{238}U	$4.5{\cdot}10^{9}$	$1{\cdot}10^{9}$	$7{\cdot}10^{-14}$	$1{\cdot}10^{7}$	$2{\cdot}10^{-12}$	–	$< 2{\cdot}10^{-18}$	$1{\cdot}10^{7}$	$3{\cdot}10^{-18}$
^{234}U	$2.5{\cdot}10^{5}$	$3{\cdot}10^{8}$	$7{\cdot}10^{-14}$	$1{\cdot}10^{7}$	$2{\cdot}10^{-12}$	–	$< 3{\cdot}10^{-18}$	$1{\cdot}10^{7}$	$3{\cdot}10^{-18}$
^{230}Th	$7.5{\cdot}10^{4}$	$9{\cdot}10^{7}$	$2{\cdot}10^{-13}$	$9{\cdot}10^{6}$	$5{\cdot}10^{-12}$	–	$< 5{\cdot}10^{-18}$	$1{\cdot}10^{7}$	$7{\cdot}10^{-18}$
^{226}Ra	$1.6{\cdot}10^{3}$	$7{\cdot}10^{7}$	$2{\cdot}10^{-10}$	$1{\cdot}10^{7}$	$3{\cdot}10^{-9}$	$3{\cdot}10^{5}$	$5{\cdot}10^{-17}$	$1{\cdot}10^{7}$	$5{\cdot}10^{-15}$
^{210}Pb	22	$7{\cdot}10^{7}$	$9{\cdot}10^{-10}$	$1{\cdot}10^{7}$	$2{\cdot}10^{-8}$	$3{\cdot}10^{5}$	$2{\cdot}10^{-16}$	$1{\cdot}10^{7}$	$3{\cdot}10^{-14}$

a) Not modelled.

9.1.2 Beberg

In Beberg the nuclides released from SFL 3-5 will migrate to an area classified as agricultural land. The highest dose for release to agricultural land is given by ^{93}Mo in both SFL 3 and SFL 5 (Figure 9-2). The maximum aggregate dose is $8{\cdot}10^{-7}$ Sv/year and $2{\cdot}10^{-6}$ Sv/year for SFL 3 and SFL 5, respectively and is obtained after 5,000 and 8,000 years after repository closure. After some 20,000 years, ^{36}Cl becomes the dominating nuclide. However, the aggregate dose is at that time decreasing.

The estimated release from SFL 4 results in a maximum aggregate dose that is below 10^{-10} Sv/year for release to agricultural land.

The maximum total dose occurs about 8,000 years after repository closure and is about $3{\cdot}10^{-6}$ Sv/year for release to agricultural land.

If the nuclides are released to an area classified as peatland instead, ^{36}Cl will be the dominating nuclide in terms of dose. ^{36}Cl in SFL 3 results in a maximum dose of

$6 \cdot 10^{-6}$ Sv/year after 10,000 years. Release of ^{226}Ra to peatland gives a maximum dose which is of the same order of magnitude as that for ^{36}Cl. This is, however, obtained after more than 10^{9} years. The corresponding results for ^{36}Cl in SFL 5 is $4 \cdot 10^{-5}$ Sv/year after some 20,000 years. The maximum aggregate dose from release of radionuclides in SFL 4 is about 10^{-10} Sv/year. The maximum total dose will be about $5 \cdot 10^{-5}$ Sv/year.

The results given above are for a saline groundwater. In Section 8.2 it was shown that the salt content of the groundwater in Beberg has no influence on the maximum far-field release rate of ^{36}Cl and ^{93}Mo. Thus, the maximum aggregate dose is the same for saline and non-saline conditions in Beberg.

The release of ^{36}Cl and ^{93}Mo in SFL 3 is not affected by the presence of ISA. However, ISA will affect the solubility of for example ^{238}U, and thereby cause an increase in the far-field release rate and the maximum dose given by ^{226}Ra in SFL 3 released to agricultural land or peatland.

The maximum doses for release to agricultural land and peatland in Beberg are summarised in Tables 9-3 to 9-6.

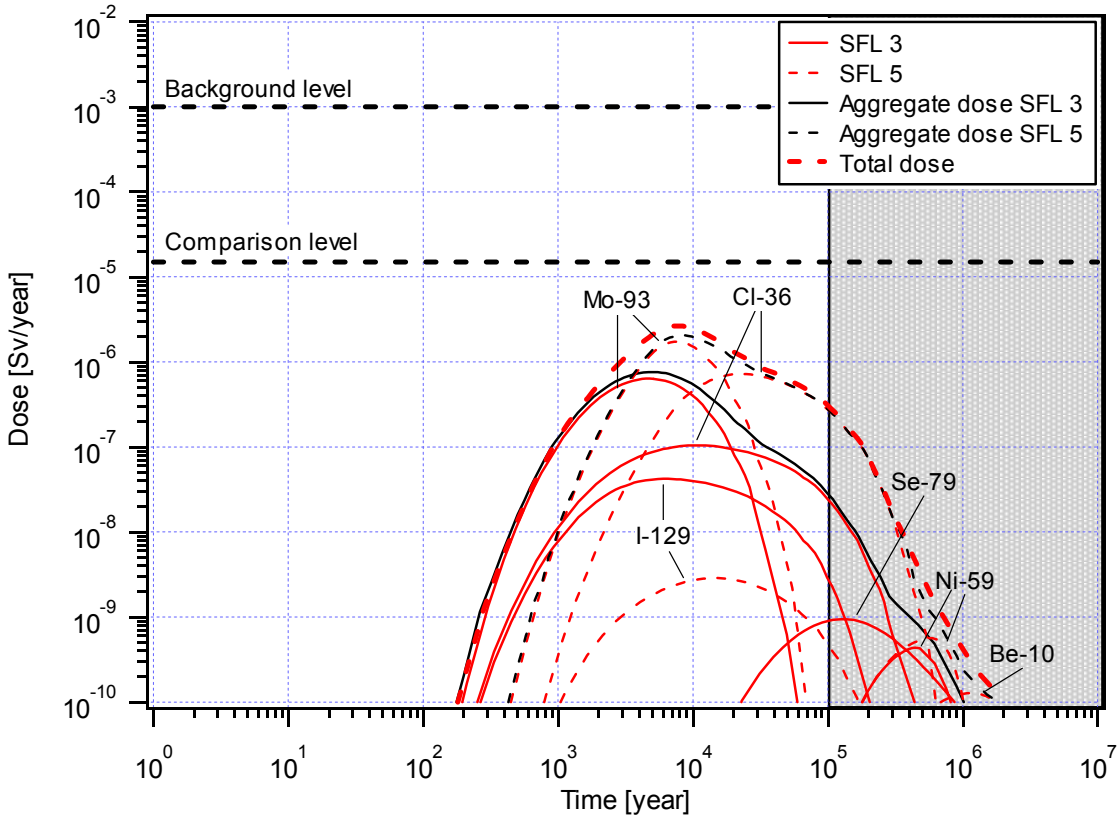

Figure 9-2 Dose from release of radionuclides from SFL 3 (no effect of ISA) and SFL 5 to agricultural land in Beberg (saline water).

Table 9-3 Maximum dose for release to agricultural land in Beberg (saline water).

Nuclide	Half-life	SFL 3 (without ISA)		SFL 3 (with ISA)		SFL 4		SFL 5	
		Time of maximum dose	Maximum dose	Time of maximum dose	Maximum dose	Time of maximum dose	Maximum dose	Time of maximum dose	Maximum dose
	[year]	[year]	[Sv/year]	[year]	[Sv/year]	[year]	[Sv/year]	[year]	[Sv/year]
^{3}H	12	$1{\cdot}10^{2}$	$2{\cdot}10^{-14}$	$1{\cdot}10^{2}$	$2{\cdot}10^{-14}$	$6{\cdot}10^{1}$	$8{\cdot}10^{-13}$	$1{\cdot}10^{2}$	$4{\cdot}10^{-13}$
^{10}Be	$1.5{\cdot}10^{6}$	– a)	– a)	– a)	– a)	– a)	– a)	$1{\cdot}10^{6}$	$1{\cdot}10^{-10}$
^{14}C	$5.7{\cdot}10^{3}$	$3{\cdot}10^{4}$	$1{\cdot}10^{-14}$	$3{\cdot}10^{4}$	$1{\cdot}10^{-14}$	$2{\cdot}10^{4}$	$5{\cdot}10^{-18}$	$4{\cdot}10^{4}$	$1{\cdot}10^{-14}$
$^{14}C_{org}$	$5.7{\cdot}10^{3}$	$2{\cdot}10^{3}$	$2{\cdot}10^{-16}$	$2{\cdot}10^{3}$	$2{\cdot}10^{-16}$	– a)	– a)	– a)	– a)
^{36}Cl	$3.0{\cdot}10^{5}$	$1{\cdot}10^{4}$	$1{\cdot}10^{-7}$	$1{\cdot}10^{4}$	$1{\cdot}10^{-7}$	$2{\cdot}10^{3}$	$1{\cdot}10^{-12}$	$2{\cdot}10^{4}$	$7{\cdot}10^{-7}$
^{60}Co	5.3	– a)	– a)	– a)	– a)	–	$< 5{\cdot}10^{-21}$	– a)	– a)
^{59}Ni	$7.6{\cdot}10^{4}$	$4{\cdot}10^{5}$	$4{\cdot}10^{-10}$	$4{\cdot}10^{5}$	$7{\cdot}10^{-10}$	$2{\cdot}10^{5}$	$2{\cdot}10^{-14}$	$6{\cdot}10^{5}$	$6{\cdot}10^{-10}$
^{63}Ni	$1.0{\cdot}10^{2}$	– a)	– a)	– a)	– a)	–	$< 8{\cdot}10^{-20}$	– a)	– a)
^{79}Se	$1.1{\cdot}10^{6}$	$1{\cdot}10^{5}$	$9{\cdot}10^{-10}$	$1{\cdot}10^{5}$	$9{\cdot}10^{-10}$	$5{\cdot}10^{4}$	$2{\cdot}10^{-14}$	$2{\cdot}10^{5}$	$8{\cdot}10^{-11}$
^{90}Sr	29	–	$< 3{\cdot}10^{-17}$	–	$< 3{\cdot}10^{-17}$	–	$< 3{\cdot}10^{-17}$	–	$< 3{\cdot}10^{-17}$
^{94}Nb	$2.0{\cdot}10^{4}$	– a)	– a)	– a)	– a)	–	$< 2{\cdot}10^{-16}$	– a)	– a)
^{93}Zr	$1.5{\cdot}10^{6}$	$9{\cdot}10^{6}$	$1{\cdot}10^{-16}$	$9{\cdot}10^{6}$	$1{\cdot}10^{-16}$	– a)	– a)	$9{\cdot}10^{6}$	$7{\cdot}10^{-15}$
^{93}Mo	$4.0{\cdot}10^{3}$	$4{\cdot}10^{3}$	$6{\cdot}10^{-7}$	$4{\cdot}10^{3}$	$6{\cdot}10^{-7}$	$1{\cdot}10^{3}$	$2{\cdot}10^{-11}$	$8{\cdot}10^{3}$	$2{\cdot}10^{-6}$
^{99}Tc	$2.1{\cdot}10^{5}$	–	$< 6{\cdot}10^{-17}$	–	$< 6{\cdot}10^{-17}$	–	$< 6{\cdot}10^{-17}$	–	$< 6{\cdot}10^{-17}$
^{129}I	$1.6{\cdot}10^{7}$	$6{\cdot}10^{3}$	$4{\cdot}10^{-8}$	$6{\cdot}10^{3}$	$4{\cdot}10^{-8}$	$1{\cdot}10^{3}$	$3{\cdot}10^{-12}$	$1{\cdot}10^{4}$	$3{\cdot}10^{-9}$
^{135}Cs	$2.3{\cdot}10^{6}$	$2{\cdot}10^{6}$	$1{\cdot}10^{-12}$	$2{\cdot}10^{6}$	$1{\cdot}10^{-12}$	– a)	– a)	– a)	– a)
^{137}Cs	30	– a)	– a)	– a)	– a)	–	$< 2{\cdot}10^{-19}$	– a)	– a)
^{236}U	$2.3{\cdot}10^{7}$	$8{\cdot}10^{7}$	$1{\cdot}10^{-15}$	$9{\cdot}10^{7}$	$1{\cdot}10^{-15}$	– a)	– a)	– a)	– a)
^{232}Th	$1.4{\cdot}10^{10}$	$1{\cdot}10^{9}$	$1{\cdot}10^{-11}$	$1{\cdot}10^{8}$	$7{\cdot}10^{-11}$	– a)	– a)	– a)	– a)
^{237}Np	$2.1{\cdot}10^{6}$	–	$< 2{\cdot}10^{-15}$	–	$< 2{\cdot}10^{-15}$	– a)	– a)	– a)	– a)
^{233}U	$1.6{\cdot}10^{5}$	–	$< 4{\cdot}10^{-16}$	–	$< 4{\cdot}10^{-16}$	– a)	– a)	– a)	– a)
^{229}Th	$7.3{\cdot}10^{3}$	–	$< 5{\cdot}10^{-15}$	–	$< 5{\cdot}10^{-15}$	– a)	– a)	– a)	– a)
^{238}U	$4.5{\cdot}10^{9}$	$2{\cdot}10^{9}$	$2{\cdot}10^{-12}$	$3{\cdot}10^{8}$	$5{\cdot}10^{-12}$	–	$< 3{\cdot}10^{-16}$	–	$< 3{\cdot}10^{-16}$
^{234}U	$2.5{\cdot}10^{5}$	$2{\cdot}10^{9}$	$2{\cdot}10^{-12}$	$3{\cdot}10^{8}$	$6{\cdot}10^{-12}$	–	$< 4{\cdot}10^{-16}$	–	$< 4{\cdot}10^{-16}$
^{230}Th	$7.5{\cdot}10^{4}$	$2{\cdot}10^{9}$	$2{\cdot}10^{-11}$	$3{\cdot}10^{8}$	$5{\cdot}10^{-11}$	–	$< 3{\cdot}10^{-15}$	–	$< 3{\cdot}10^{-15}$
^{226}Ra	$1.6{\cdot}10^{3}$	$2{\cdot}10^{9}$	$1{\cdot}10^{-8}$	$3{\cdot}10^{8}$	$3{\cdot}10^{-8}$	–	$< 7{\cdot}10^{-15}$	$3{\cdot}10^{8}$	$5{\cdot}10^{-14}$
^{210}Pb	22	$2{\cdot}10^{9}$	$6{\cdot}10^{-12}$	$3{\cdot}10^{8}$	$1{\cdot}10^{-11}$	–	$< 3{\cdot}10^{-18}$	$3{\cdot}10^{8}$	$2{\cdot}10^{-17}$

a) Not modelled.

Table 9-4 Maximum dose for release to agricultural land in Beberg (non-saline water).

Nuclide	Half-life	SFL 3 (without ISA)		SFL 3 (with ISA)		SFL 4		SFL 5	
		Time of maximum dose	Maximum dose	Time of maximum dose	Maximum dose	Time of maximum dose	Maximum dose	Time of maximum dose	Maximum dose
	[year]	[year]	[Sv/year]	[year]	[Sv/year]	[year]	[Sv/year]	[year]	[Sv/year]
^{3}H	12	$1{\cdot}10^{2}$	$2{\cdot}10^{-14}$	$1{\cdot}10^{2}$	$2{\cdot}10^{-14}$	$6{\cdot}10^{1}$	$8{\cdot}10^{-13}$	$1{\cdot}10^{2}$	$4{\cdot}10^{-13}$
^{10}Be	$1.5{\cdot}10^{6}$	– a)	– a)	– a)	– a)	– a)	– a)	$2{\cdot}10^{6}$	$2{\cdot}10^{-11}$
^{14}C	$5.7{\cdot}10^{3}$	$2{\cdot}10^{4}$	$5{\cdot}10^{-13}$	$2{\cdot}10^{4}$	$5{\cdot}10^{-13}$	$9{\cdot}10^{3}$	$2{\cdot}10^{-16}$	$3{\cdot}10^{4}$	$4{\cdot}10^{-13}$
$^{14}C_{org}$	$5.7{\cdot}10^{3}$	$2{\cdot}10^{3}$	$2{\cdot}10^{-16}$	$2{\cdot}10^{3}$	$2{\cdot}10^{-16}$	– a)	– a)	– a)	– a)
^{36}Cl	$3.0{\cdot}10^{5}$	$1{\cdot}10^{4}$	$1{\cdot}10^{-7}$	$1{\cdot}10^{4}$	$1{\cdot}10^{-7}$	$4{\cdot}10^{2}$	$3{\cdot}10^{-12}$	$2{\cdot}10^{4}$	$8{\cdot}10^{-7}$
^{60}Co	5.3	– a)	– a)	– a)	– a)	–	$< 5{\cdot}10^{-21}$	– a)	– a)
^{59}Ni	$7.6{\cdot}10^{4}$	$7{\cdot}10^{5}$	$1{\cdot}10^{-12}$	$6{\cdot}10^{5}$	$2{\cdot}10^{-12}$	$3{\cdot}10^{5}$	$2{\cdot}10^{-16}$	$8{\cdot}10^{5}$	$2{\cdot}10^{-12}$
^{63}Ni	$1.0{\cdot}10^{2}$	– a)	– a)	– a)	– a)	–	$< 8{\cdot}10^{-20}$	– a)	– a)
^{79}Se	$1.1{\cdot}10^{6}$	$1{\cdot}10^{5}$	$9{\cdot}10^{-10}$	$1{\cdot}10^{5}$	$9{\cdot}10^{-10}$	$5{\cdot}10^{4}$	$2{\cdot}10^{-14}$	$2{\cdot}10^{5}$	$8{\cdot}10^{-11}$
^{90}Sr	29	–	$< 3{\cdot}10^{-17}$	–	$< 3{\cdot}10^{-17}$	–	$< 3{\cdot}10^{-17}$	–	$< 3{\cdot}10^{-17}$
^{94}Nb	$2.0{\cdot}10^{4}$	– a)	– a)	– a)	– a)	–	$< 2{\cdot}10^{-16}$	– a)	– a)
^{93}Zr	$1.5{\cdot}10^{6}$	$9{\cdot}10^{6}$	$1{\cdot}10^{-16}$	$9{\cdot}10^{6}$	$1{\cdot}10^{-16}$	– a)	– a)	$9{\cdot}10^{6}$	$7{\cdot}10^{-15}$
^{93}Mo	$4.0{\cdot}10^{3}$	$5{\cdot}10^{3}$	$6{\cdot}10^{-7}$	$4{\cdot}10^{3}$	$6{\cdot}10^{-7}$	$1{\cdot}10^{3}$	$2{\cdot}10^{-11}$	$8{\cdot}10^{3}$	$2{\cdot}10^{-6}$
^{99}Tc	$2.1{\cdot}10^{5}$	–	$< 6{\cdot}10^{-17}$	–	$< 6{\cdot}10^{-17}$	–	$< 6{\cdot}10^{-17}$	–	$< 6{\cdot}10^{-17}$
^{129}I	$1.6{\cdot}10^{7}$	$6{\cdot}10^{3}$	$4{\cdot}10^{-8}$	$6{\cdot}10^{3}$	$4{\cdot}10^{-8}$	$4{\cdot}10^{2}$	$9{\cdot}10^{-12}$	$8{\cdot}10^{3}$	$3{\cdot}10^{-9}$
^{135}Cs	$2.3{\cdot}10^{6}$	–	$< 3{\cdot}10^{-16}$	–	$< 3{\cdot}10^{-16}$	– a)	– a)	– a)	– a)
^{137}Cs	30	– a)	– a)	– a)	– a)	–	$< 2{\cdot}10^{-19}$	– a)	– a)
^{236}U	$2.3{\cdot}10^{7}$	$9{\cdot}10^{7}$	$1{\cdot}10^{-15}$	$9{\cdot}10^{7}$	$1{\cdot}10^{-15}$	– a)	– a)	– a)	– a)
^{232}Th	$1.4{\cdot}10^{10}$	$1{\cdot}10^{9}$	$1{\cdot}10^{-11}$	$1{\cdot}10^{8}$	$7{\cdot}10^{-11}$	– a)	– a)	– a)	– a)
^{237}Np	$2.1{\cdot}10^{6}$	–	$< 2{\cdot}10^{-15}$	–	$< 2{\cdot}10^{-15}$	– a)	– a)	– a)	– a)
^{233}U	$1.6{\cdot}10^{5}$	–	$< 4{\cdot}10^{-16}$	–	$< 4{\cdot}10^{-16}$	– a)	– a)	– a)	– a)
^{229}Th	$7.3{\cdot}10^{3}$	–	$< 5{\cdot}10^{-15}$	–	$< 5{\cdot}10^{-15}$	– a)	– a)	– a)	– a)
^{238}U	$4.5{\cdot}10^{9}$	$2{\cdot}10^{9}$	$2{\cdot}10^{-12}$	$3{\cdot}10^{8}$	$5{\cdot}10^{-12}$	–	$< 3{\cdot}10^{-16}$	–	$< 3{\cdot}10^{-16}$
^{234}U	$2.5{\cdot}10^{5}$	$2{\cdot}10^{9}$	$2{\cdot}10^{-12}$	$3{\cdot}10^{8}$	$6{\cdot}10^{-12}$	–	$< 4{\cdot}10^{-16}$	–	$< 4{\cdot}10^{-16}$
^{230}Th	$7.5{\cdot}10^{4}$	$2{\cdot}10^{9}$	$2{\cdot}10^{-11}$	$3{\cdot}10^{8}$	$5{\cdot}10^{-11}$	–	$< 3{\cdot}10^{-15}$	–	$< 3{\cdot}10^{-15}$
^{226}Ra	$1.6{\cdot}10^{3}$	$2{\cdot}10^{9}$	$3{\cdot}10^{-9}$	$3{\cdot}10^{8}$	$6{\cdot}10^{-9}$	–	$< 7{\cdot}10^{-15}$	$4{\cdot}10^{8}$	$1{\cdot}10^{-14}$
^{210}Pb	22	$2{\cdot}10^{9}$	$1{\cdot}10^{-12}$	$3{\cdot}10^{8}$	$3{\cdot}10^{-12}$	–	$< 3{\cdot}10^{-18}$	$3{\cdot}10^{8}$	$5{\cdot}10^{-18}$

a) Not modelled.

Table 9-5 Maximum dose for release to peatland in Beberg (saline water).

Nuclide	Half-life	SFL 3 (without ISA)		SFL 3 (with ISA)		SFL 4		SFL 5	
		Time of maximum dose	Maximum dose	Time of maximum dose	Maximum dose	Time of maximum dose	Maximum dose	Time of maximum dose	Maximum dose
	[year]	[year]	[Sv/year]	[year]	[Sv/year]	[year]	[Sv/year]	[year]	[Sv/year]
^{3}H	12	$1\cdot10^{2}$	$4\cdot10^{-15}$	$1\cdot10^{2}$	$4\cdot10^{-15}$	$6\cdot10^{1}$	$2\cdot10^{-13}$	$1\cdot10^{2}$	$1\cdot10^{-13}$
^{10}Be	$1.5\cdot10^{6}$	– [a]	– [a]	– [a]	– [a]	– [a]	– [a]	$1\cdot10^{6}$	$8\cdot10^{-9}$
^{14}C	$5.7\cdot10^{3}$	$3\cdot10^{4}$	$5\cdot10^{-12}$	$3\cdot10^{4}$	$5\cdot10^{-12}$	$2\cdot10^{4}$	$2\cdot10^{-15}$	$4\cdot10^{4}$	$4\cdot10^{-12}$
$^{14}C_{org}$	$5.7\cdot10^{3}$	$2\cdot10^{3}$	$8\cdot10^{-14}$	$2\cdot10^{3}$	$8\cdot10^{-14}$	– [a]	– [a]	– [a]	– [a]
^{36}Cl	$3.0\cdot10^{5}$	$1\cdot10^{4}$	$6\cdot10^{-6}$	$1\cdot10^{4}$	$6\cdot10^{-6}$	$2\cdot10^{3}$	$7\cdot10^{-11}$	$2\cdot10^{4}$	$4\cdot10^{-5}$
^{60}Co	5.3	– [a]	– [a]	– [a]	– [a]	–	$< 3\cdot10^{-16}$	– [a]	– [a]
^{59}Ni	$7.6\cdot10^{4}$	$4\cdot10^{5}$	$1\cdot10^{-8}$	$4\cdot10^{5}$	$2\cdot10^{-8}$	$2\cdot10^{5}$	$5\cdot10^{-13}$	$6\cdot10^{5}$	$1\cdot10^{-8}$
^{63}Ni	$1.0\cdot10^{2}$	– [a]	– [a]	– [a]	– [a]	–	$< 2\cdot10^{-16}$	– [a]	– [a]
^{79}Se	$1.1\cdot10^{6}$	$1\cdot10^{5}$	$1\cdot10^{-6}$	$1\cdot10^{5}$	$1\cdot10^{-6}$	$5\cdot10^{4}$	$2\cdot10^{-11}$	$2\cdot10^{5}$	$9\cdot10^{-8}$
^{90}Sr	29	–	$< 2\cdot10^{-14}$	–	$< 2\cdot10^{-14}$	–	$< 2\cdot10^{-14}$	–	$< 2\cdot10^{-14}$
^{94}Nb	$2.0\cdot10^{4}$	– [a]	– [a]	– [a]	– [a]	–	$< 2\cdot10^{-15}$	– [a]	– [a]
^{93}Zr	$1.5\cdot10^{6}$	$9\cdot10^{6}$	$1\cdot10^{-14}$	$9\cdot10^{6}$	$1\cdot10^{-14}$	– [a]	– [a]	$9\cdot10^{6}$	$1\cdot10^{-12}$
^{93}Mo	$4.0\cdot10^{3}$	$4\cdot10^{3}$	$2\cdot10^{-6}$	$4\cdot10^{3}$	$2\cdot10^{-6}$	$1\cdot10^{3}$	$6\cdot10^{-11}$	$8\cdot10^{3}$	$5\cdot10^{-6}$
^{99}Tc	$2.1\cdot10^{5}$	–	$< 4\cdot10^{-16}$	–	$< 4\cdot10^{-16}$	–	$< 4\cdot10^{-16}$	–	$< 4\cdot10^{-16}$
^{129}I	$1.6\cdot10^{7}$	$6\cdot10^{3}$	$3\cdot10^{-8}$	$6\cdot10^{3}$	$3\cdot10^{-8}$	$1\cdot10^{3}$	$2\cdot10^{-12}$	$1\cdot10^{4}$	$2\cdot10^{-9}$
^{135}Cs	$2.3\cdot10^{6}$	$2\cdot10^{6}$	$1\cdot10^{-11}$	$2\cdot10^{6}$	$1\cdot10^{-11}$	– [a]	– [a]	– [a]	– [a]
^{137}Cs	30	– [a]	– [a]	– [a]	– [a]	–	$< 4\cdot10^{-15}$	– [a]	– [a]
^{236}U	$2.3\cdot10^{7}$	$8\cdot10^{7}$	$2\cdot10^{-14}$	$9\cdot10^{7}$	$2\cdot10^{-14}$	– [a]	– [a]	– [a]	– [a]
^{232}Th	$1.4\cdot10^{10}$	$1\cdot10^{9}$	$2\cdot10^{-8}$	$1\cdot10^{8}$	$8\cdot10^{-8}$	– [a]	– [a]	– [a]	– [a]
^{237}Np	$2.1\cdot10^{6}$	–	$< 1\cdot10^{-13}$	–	$< 1\cdot10^{-13}$	– [a]	– [a]	– [a]	– [a]
^{233}U	$1.6\cdot10^{5}$	–	$< 6\cdot10^{-15}$	–	$< 6\cdot10^{-15}$	– [a]	– [a]	– [a]	– [a]
^{229}Th	$7.3\cdot10^{3}$	–	$< 7\cdot10^{-12}$	–	$< 7\cdot10^{-12}$	– [a]	– [a]	– [a]	– [a]
^{238}U	$4.5\cdot10^{9}$	$2\cdot10^{9}$	$3\cdot10^{-11}$	$3\cdot10^{8}$	$9\cdot10^{-11}$	–	$< 5\cdot10^{-15}$	–	$< 5\cdot10^{-15}$
^{234}U	$2.5\cdot10^{5}$	$2\cdot10^{9}$	$4\cdot10^{-11}$	$3\cdot10^{8}$	$1\cdot10^{-10}$	–	$< 6\cdot10^{-15}$	–	$< 6\cdot10^{-15}$
^{230}Th	$7.5\cdot10^{4}$	$2\cdot10^{9}$	$3\cdot10^{-8}$	$3\cdot10^{8}$	$7\cdot10^{-8}$	–	$< 4\cdot10^{-12}$	–	$< 4\cdot10^{-12}$
^{226}Ra	$1.6\cdot10^{3}$	$2\cdot10^{9}$	$2\cdot10^{-6}$	$3\cdot10^{8}$	$5\cdot10^{-6}$	–	$< 1\cdot10^{-12}$	$3\cdot10^{8}$	$8\cdot10^{-12}$
^{210}Pb	22	$2\cdot10^{9}$	$3\cdot10^{-8}$	$3\cdot10^{8}$	$7\cdot10^{-8}$	–	$< 2\cdot10^{-14}$	$3\cdot10^{8}$	$1\cdot10^{-13}$

a) Not modelled.

Table 9-6 Maximum dose for release to peatland in Beberg (non-saline water).

Nuclide	Half-life	SFL 3 (without ISA)		SFL 3 (with ISA)		SFL 4		SFL 5	
		Time of maximum dose	Maximum dose	Time of maximum dose	Maximum dose	Time of maximum dose	Maximum dose	Time of maximum dose	Maximum dose
	[year]	[year]	[Sv/year]	[year]	[Sv/year]	[year]	[Sv/year]	[year]	[Sv/year]
^{3}H	12	$1{\cdot}10^{2}$	$4{\cdot}10^{-15}$	$1{\cdot}10^{2}$	$4{\cdot}10^{-15}$	$6{\cdot}10^{1}$	$2{\cdot}10^{-13}$	$1{\cdot}10^{2}$	$1{\cdot}10^{-13}$
^{10}Be	$1.5{\cdot}10^{6}$	– [a]	– [a]	– [a]	– [a]	– [a]	– [a]	$2{\cdot}10^{6}$	$1{\cdot}10^{-9}$
^{14}C	$5.7{\cdot}10^{3}$	$2{\cdot}10^{4}$	$2{\cdot}10^{-10}$	$2{\cdot}10^{4}$	$2{\cdot}10^{-10}$	$9{\cdot}10^{3}$	$8{\cdot}10^{-14}$	$3{\cdot}10^{4}$	$1{\cdot}10^{-10}$
$^{14}C_{org}$	$5.7{\cdot}10^{3}$	$2{\cdot}10^{3}$	$8{\cdot}10^{-14}$	$2{\cdot}10^{3}$	$8{\cdot}10^{-14}$	– [a]	– [a]	– [a]	– [a]
^{36}Cl	$3.0{\cdot}10^{5}$	$1{\cdot}10^{4}$	$6{\cdot}10^{-6}$	$1{\cdot}10^{4}$	$6{\cdot}10^{-6}$	$4{\cdot}10^{2}$	$2{\cdot}10^{-10}$	$2{\cdot}10^{4}$	$4{\cdot}10^{-5}$
^{60}Co	5.3	– [a]	– [a]	– [a]	– [a]	–	$< 3{\cdot}10^{-16}$	– [a]	– [a]
^{59}Ni	$7.6{\cdot}10^{4}$	$7{\cdot}10^{5}$	$3{\cdot}10^{-11}$	$6{\cdot}10^{5}$	$5{\cdot}10^{-11}$	$3{\cdot}10^{5}$	$4{\cdot}10^{-15}$	$8{\cdot}10^{5}$	$4{\cdot}10^{-11}$
^{63}Ni	$1.0{\cdot}10^{2}$	– [a]	– [a]	– [a]	– [a]	–	$< 2{\cdot}10^{-16}$	– [a]	– [a]
^{79}Se	$1.1{\cdot}10^{6}$	$1{\cdot}10^{5}$	$1{\cdot}10^{-6}$	$1{\cdot}10^{5}$	$1{\cdot}10^{-6}$	$5{\cdot}10^{4}$	$2{\cdot}10^{-11}$	$2{\cdot}10^{5}$	$9{\cdot}10^{-8}$
^{90}Sr	29	–	$< 2{\cdot}10^{-14}$	–	$< 2{\cdot}10^{-14}$	–	$< 2{\cdot}10^{-14}$	–	$< 2{\cdot}10^{-14}$
^{94}Nb	$2.0{\cdot}10^{4}$	– [a]	– [a]	– [a]	– [a]	–	$< 2{\cdot}10^{-15}$	– [a]	– [a]
^{93}Zr	$1.5{\cdot}10^{6}$	$9{\cdot}10^{6}$	$1{\cdot}10^{-14}$	$9{\cdot}10^{6}$	$1{\cdot}10^{-14}$	– [a]	– [a]	$9{\cdot}10^{6}$	$1{\cdot}10^{-12}$
^{93}Mo	$4.0{\cdot}10^{3}$	$5{\cdot}10^{3}$	$2{\cdot}10^{-6}$	$4{\cdot}10^{3}$	$2{\cdot}10^{-6}$	$1{\cdot}10^{3}$	$6{\cdot}10^{-11}$	$8{\cdot}10^{3}$	$5{\cdot}10^{-6}$
^{99}Tc	$2.1{\cdot}10^{5}$	–	$< 4{\cdot}10^{-16}$	–	$< 4{\cdot}10^{-16}$	–	$< 4{\cdot}10^{-16}$	–	$< 4{\cdot}10^{-16}$
^{129}I	$1.6{\cdot}10^{7}$	$6{\cdot}10^{3}$	$2{\cdot}10^{-8}$	$6{\cdot}10^{3}$	$2{\cdot}10^{-8}$	$4{\cdot}10^{2}$	$5{\cdot}10^{-12}$	$8{\cdot}10^{3}$	$2{\cdot}10^{-9}$
^{135}Cs	$2.3{\cdot}10^{6}$	–	$< 3{\cdot}10^{-15}$	–	$< 3{\cdot}10^{-15}$	– [a]	– [a]	– [a]	– [a]
^{137}Cs	30	– [a]	– [a]	– [a]	– [a]	–	$< 4{\cdot}10^{-15}$	– [a]	– [a]
^{236}U	$2.3{\cdot}10^{7}$	$9{\cdot}10^{7}$	$2{\cdot}10^{-14}$	$9{\cdot}10^{7}$	$2{\cdot}10^{-14}$	– [a]	– [a]	– [a]	– [a]
^{232}Th	$1.4{\cdot}10^{10}$	$1{\cdot}10^{9}$	$2{\cdot}10^{-8}$	$1{\cdot}10^{8}$	$8{\cdot}10^{-8}$	– [a]	– [a]	– [a]	– [a]
^{237}Np	$2.1{\cdot}10^{6}$	–	$< 1{\cdot}10^{-13}$	–	$< 1{\cdot}10^{-13}$	– [a]	– [a]	– [a]	– [a]
^{233}U	$1.6{\cdot}10^{5}$	–	$< 6{\cdot}10^{-15}$	–	$< 6{\cdot}10^{-15}$	– [a]	– [a]	– [a]	– [a]
^{229}Th	$7.3{\cdot}10^{3}$	–	$< 7{\cdot}10^{-12}$	–	$< 7{\cdot}10^{-12}$	– [a]	– [a]	– [a]	– [a]
^{238}U	$4.5{\cdot}10^{9}$	$2{\cdot}10^{9}$	$4{\cdot}10^{-11}$	$3{\cdot}10^{8}$	$9{\cdot}10^{-11}$	–	$< 5{\cdot}10^{-15}$	–	$< 5{\cdot}10^{-15}$
^{234}U	$2.5{\cdot}10^{5}$	$2{\cdot}10^{9}$	$4{\cdot}10^{-11}$	$3{\cdot}10^{8}$	$1{\cdot}10^{-10}$	–	$< 6{\cdot}10^{-15}$	–	$< 6{\cdot}10^{-15}$
^{230}Th	$7.5{\cdot}10^{4}$	$2{\cdot}10^{9}$	$3{\cdot}10^{-8}$	$3{\cdot}10^{8}$	$7{\cdot}10^{-8}$	–	$< 4{\cdot}10^{-12}$	–	$< 4{\cdot}10^{-12}$
^{226}Ra	$1.6{\cdot}10^{3}$	$2{\cdot}10^{9}$	$4{\cdot}10^{-7}$	$3{\cdot}10^{8}$	$1{\cdot}10^{-6}$	–	$< 1{\cdot}10^{-12}$	$4{\cdot}10^{8}$	$2{\cdot}10^{-12}$
^{210}Pb	22	$2{\cdot}10^{9}$	$6{\cdot}10^{-9}$	$3{\cdot}10^{8}$	$1{\cdot}10^{-8}$	–	$< 2{\cdot}10^{-14}$	$3{\cdot}10^{8}$	$2{\cdot}10^{-14}$

a) Not modelled.

9.1.3 Ceberg

The primary recipient in Ceberg is an area classified as peatland. As shown in Figure 9-3, the dominating nuclide is ^{36}Cl in both SFL 3 and SFL 5. The maximum dose rates are $1{\cdot}10^{-6}$ Sv/year after 25,000 years (SFL 3) and $6{\cdot}10^{-6}$ Sv/year after 30,000 years (SFL 5). ^{79}Se also gives a significant contribution to the aggregate dose. However, this occurs after very long time after repository closure.

The estimated release from SFL 4 results in a maximum aggregate dose that is below 10^{-10} Sv/year.

The effect of ISA in SFL 3 is the same as discussed for release to peatland in Beberg, and is of no importance.

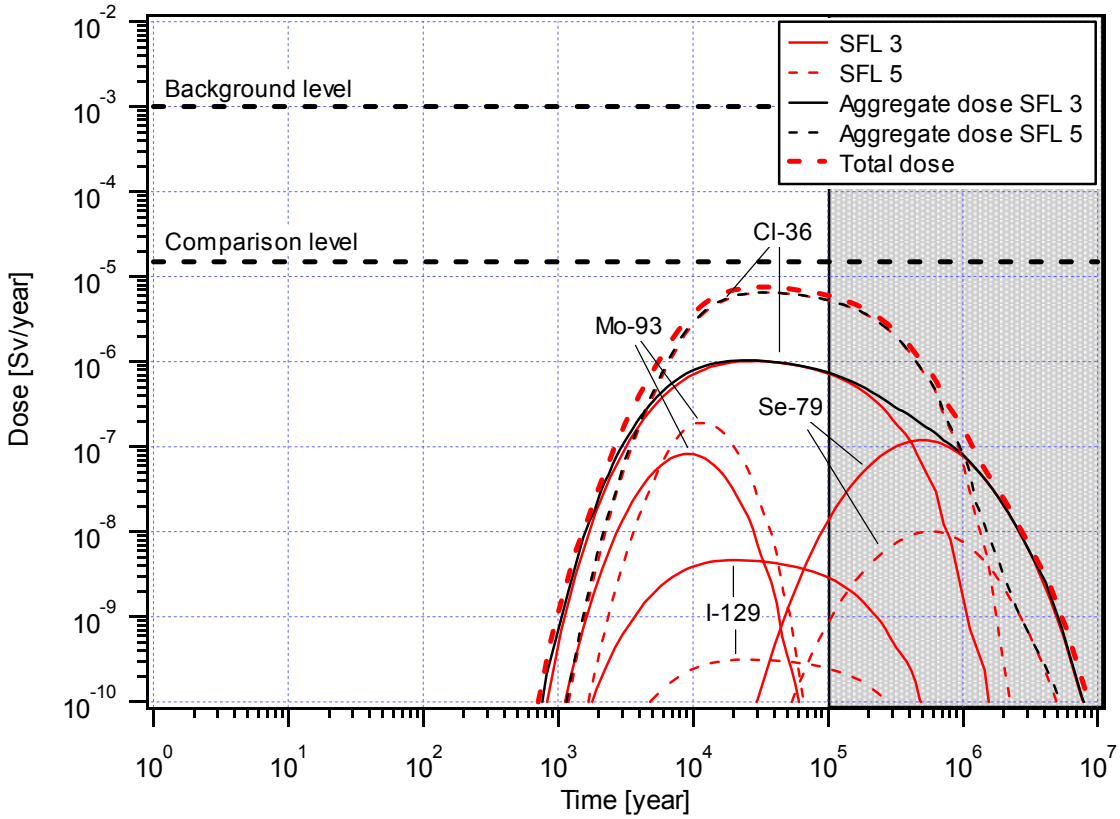

Figure 9-3 Dose from release of radionuclides from SFL 3 (no effect of ISA) and SFL 5 to peatland in Ceberg.

The maximum doses for release to peatland in Ceberg are compiled in Table 9-7.

Table 9-7 Maximum dose for release to peatland in Ceberg.

Nuclide	Half-life	SFL 3 (without ISA)		SFL 3 (with ISA)		SFL 4		SFL 5	
		Time of maximum dose	Maximum dose	Time of maximum dose	Maximum dose	Time of maximum dose	Maximum dose	Time of maximum dose	Maximum dose
	[year]	[year]	[Sv/year]	[year]	[Sv/year]	[year]	[Sv/year]	[year]	[Sv/year]
^{3}H	12	–	$< 3 \cdot 10^{-19}$	–	$< 3 \cdot 10^{-19}$	–	$< 3 \cdot 10^{-19}$	–	$< 3 \cdot 10^{-19}$
^{10}Be	$1.5 \cdot 10^{6}$	– [a]	– [a]	– [a]	– [a]	– [a]	– [a]	$6 \cdot 10^{6}$	$5 \cdot 10^{-12}$
^{14}C	$5.7 \cdot 10^{3}$	$3 \cdot 10^{4}$	$6 \cdot 10^{-13}$	$3 \cdot 10^{4}$	$6 \cdot 10^{-13}$	$2 \cdot 10^{4}$	$5 \cdot 10^{-16}$	$4 \cdot 10^{4}$	$5 \cdot 10^{-13}$
$^{14}C_{org}$	$5.7 \cdot 10^{3}$	$7 \cdot 10^{3}$	$5 \cdot 10^{-15}$	$7 \cdot 10^{3}$	$5 \cdot 10^{-15}$	– [a]	– [a]	– [a]	– [a]
^{36}Cl	$3.0 \cdot 10^{5}$	$3 \cdot 10^{4}$	$1 \cdot 10^{-6}$	$3 \cdot 10^{4}$	$1 \cdot 10^{-6}$	$5 \cdot 10^{3}$	$1 \cdot 10^{-11}$	$3 \cdot 10^{4}$	$6 \cdot 10^{-6}$
^{60}Co	5.3	– [a]	– [a]	– [a]	– [a]	–	$< 3 \cdot 10^{-16}$	– [a]	– [a]
^{59}Ni	$7.6 \cdot 10^{4}$	$1 \cdot 10^{6}$	$3 \cdot 10^{-16}$	$9 \cdot 10^{5}$	$5 \cdot 10^{-16}$	–	$< 2 \cdot 10^{-16}$	$1 \cdot 10^{6}$	$4 \cdot 10^{-16}$
^{63}Ni	$1.0 \cdot 10^{2}$	– [a]	– [a]	– [a]	– [a]	–	$< 1 \cdot 10^{-16}$	– [a]	– [a]
^{79}Se	$1.1 \cdot 10^{6}$	$5 \cdot 10^{5}$	$1 \cdot 10^{-7}$	$5 \cdot 10^{5}$	$1 \cdot 10^{-7}$	–	$< 1 \cdot 10^{-12}$	$6 \cdot 10^{5}$	$1 \cdot 10^{-8}$
^{90}Sr	29	–	$< 2 \cdot 10^{-14}$	–	$< 2 \cdot 10^{-14}$	–	$< 2 \cdot 10^{-14}$	–	$< 2 \cdot 10^{-14}$
^{94}Nb	$2.0 \cdot 10^{4}$	– [a]	– [a]	– [a]	– [a]	–	$< 2 \cdot 10^{-15}$	– [a]	– [a]
^{93}Zr	$1.5 \cdot 10^{6}$	–	$< 3 \cdot 10^{-16}$	–	$< 3 \cdot 10^{-16}$	– [a]	– [a]	–	$< 3 \cdot 10^{-16}$
^{93}Mo	$4.0 \cdot 10^{3}$	$9 \cdot 10^{3}$	$8 \cdot 10^{-8}$	$9 \cdot 10^{3}$	$8 \cdot 10^{-8}$	$4 \cdot 10^{3}$	$2 \cdot 10^{-12}$	$1 \cdot 10^{4}$	$2 \cdot 10^{-7}$
^{99}Tc	$2.1 \cdot 10^{5}$	–	$< 3 \cdot 10^{-16}$	–	$< 3 \cdot 10^{-16}$	–	$< 3 \cdot 10^{-16}$	–	$< 3 \cdot 10^{-16}$
^{129}I	$1.6 \cdot 10^{7}$	$2 \cdot 10^{4}$	$5 \cdot 10^{-9}$	$2 \cdot 10^{4}$	$5 \cdot 10^{-9}$	$4 \cdot 10^{3}$	$4 \cdot 10^{-13}$	$2 \cdot 10^{4}$	$3 \cdot 10^{-10}$
^{135}Cs	$2.3 \cdot 10^{6}$	–	$< 2 \cdot 10^{-15}$	–	$< 2 \cdot 10^{-15}$	– [a]	– [a]	– [a]	– [a]
^{137}Cs	30	– [a]	– [a]	– [a]	– [a]	–	$< 3 \cdot 10^{-15}$	– [a]	– [a]
^{236}U	$2.3 \cdot 10^{7}$	–	$< 4 \cdot 10^{-15}$	–	$< 4 \cdot 10^{-15}$	– [a]	– [a]	– [a]	– [a]
^{232}Th	$1.4 \cdot 10^{10}$	$4 \cdot 10^{9}$	$4 \cdot 10^{-9}$	$7 \cdot 10^{8}$	$1 \cdot 10^{-8}$	– [a]	– [a]	– [a]	– [a]
^{237}Np	$2.1 \cdot 10^{6}$	–	$< 8 \cdot 10^{-14}$	–	$< 8 \cdot 10^{-14}$	– [a]	– [a]	– [a]	– [a]
^{233}U	$1.6 \cdot 10^{5}$	–	$< 4 \cdot 10^{-15}$	–	$< 4 \cdot 10^{-15}$	– [a]	– [a]	– [a]	– [a]
^{229}Th	$7.3 \cdot 10^{3}$	–	$< 7 \cdot 10^{-12}$	–	$< 7 \cdot 10^{-12}$	– [a]	– [a]	– [a]	–
^{238}U	$4.5 \cdot 10^{9}$	$5 \cdot 10^{9}$	$4 \cdot 10^{-12}$	$1 \cdot 10^{9}$	$1 \cdot 10^{-11}$	–	$< 4 \cdot 10^{-15}$	–	$< 4 \cdot 10^{-15}$
^{234}U	$2.5 \cdot 10^{5}$	$5 \cdot 10^{9}$	$4 \cdot 10^{-12}$	$1 \cdot 10^{9}$	$1 \cdot 10^{-11}$	–	$< 4 \cdot 10^{-15}$	–	$< 4 \cdot 10^{-15}$
^{230}Th	$7.5 \cdot 10^{4}$	$5 \cdot 10^{9}$	$4 \cdot 10^{-9}$	$1 \cdot 10^{9}$	$1 \cdot 10^{-8}$	–	$< 4 \cdot 10^{-12}$	–	$< 4 \cdot 10^{-12}$
^{226}Ra	$1.6 \cdot 10^{3}$	$5 \cdot 10^{9}$	$5 \cdot 10^{-8}$	$1 \cdot 10^{9}$	$1 \cdot 10^{-7}$	–	$< 9 \cdot 10^{-13}$	–	$< 9 \cdot 10^{-13}$
^{210}Pb	22	$5 \cdot 10^{9}$	$8 \cdot 10^{-10}$	$1 \cdot 10^{9}$	$2 \cdot 10^{-9}$	–	$< 2 \cdot 10^{-14}$	–	$< 2 \cdot 10^{-14}$

a) Not modelled.

9.2 Release of toxic metals

The transport of the toxic metals lead, cadmium and beryllium has also been modelled in this work. The result of the near-field and the far-field modelling is the release rate (mole/year) from the geosphere to the biosphere. In these calculations the lower limit for which FARF31 specifies the release rate is set to a limit corresponding to about 10^{-19} mole/year. The release rate is recalculated to a concentration in recipient using the equations given in Chapter 4. The estimated concentration is based on the same assumptions as for release of radionuclides to recipient, i.e. it is assumed that the metals reach the recipient at the same rate as the release from the geosphere and without any delay. The estimated concentrations are compared with typical concentrations found in different types of ecosystems (Skagius *et al.,* 1999).

The amount of toxic metals in SFL 3-5 is given in Table 2-2. The results of the calculations are summarised in Tables 9-8 to 9-12. It can be concluded that the concentration of metals in agricultural land and peatland is significantly below the comparison values for times up to 10,000 years after repository closure. The

concentrations are at that time increasing, and exceed, in general, the comparison values after times between 100,000 and 10 million years. At that time several glacial periods have past. It seems very unlikely that all metals released to the recipient is still there (the estimated concentration is based one the accumulated release, see Section 4-3). The metal concentration in archipelago and open coast in Aberg is also very low. The calculations show that the concentration never exceeds the comparison values.

Table 9-8 Concentration in recipient water for release to open coast in Aberg [µg/l].

Time	SFL 3		SFL 5	
[year]	Pb	Cd	Pb	Be
100	$< 10^{-16}$	$< 10^{-15}$	$< 10^{-17}$	$< 10^{-16}$
1,000	10^{-14}	10^{-12}	10^{-16}	10^{-15}
10,000	$1 \cdot 10^{-9}$	$5 \cdot 10^{-8}$	$5 \cdot 10^{-10}$	$4 \cdot 10^{-9}$
Comparison value	0.24	0.01	0.24	0.01

Table 9-9 Concentration in recipient water for release to archipelago in Aberg [µg/l].

Time	SFL 3		SFL 5	
[year]	Pb	Cd	Pb	Be
100	$< 10^{-13}$	$< 10^{-12}$	$< 10^{-15}$	$< 10^{-14}$
1,000	10^{-12}	10^{-10}	10^{-15}	10^{-12}
10,000	$5 \cdot 10^{-7}$	$1 \cdot 10^{-5}$	$1 \cdot 10^{-7}$	$1 \cdot 10^{-6}$
Comparison value	0.24	0.01	0.24	0.01

Table 9-10 Accumulated concentration in soil for release to agricultural land in Beberg [mg/kg dw].

Time	SFL 3		SFL 5	
[year]	Pb	Cd	Pb	Be
100	$< 6 \cdot 10^{-10}$	$< 2 \cdot 10^{-10}$	$< 5 \cdot 10^{-10}$	$< 1 \cdot 10^{-11}$
1,000	$< 6 \cdot 10^{-10}$	$< 2 \cdot 10^{-10}$	$< 5 \cdot 10^{-10}$	$< 1 \cdot 10^{-11}$
10,000	$< 6 \cdot 10^{-10}$	$< 2 \cdot 10^{-10}$	$< 5 \cdot 10^{-10}$	$< 1 \cdot 10^{-11}$
Comparison value	17.1	0.23	17.1	6

Table 9-11 Accumulated concentration in peat for release to peatland in Beberg [mg/kg dw].

Time [year]	SFL 3		SFL 5	
	Pb	Cd	Pb	Be
100	$< 1 \cdot 10^{-7}$	$< 4 \cdot 10^{-8}$	$< 1 \cdot 10^{-7}$	$< 3 \cdot 10^{-9}$
1,000	$< 1 \cdot 10^{-7}$	$< 4 \cdot 10^{-8}$	$< 1 \cdot 10^{-7}$	$< 3 \cdot 10^{-9}$
10,000	$< 1 \cdot 10^{-7}$	$< 4 \cdot 10^{-8}$	$< 1 \cdot 10^{-7}$	$< 3 \cdot 10^{-9}$
Comparison value	0.38 – 19	0.095 – 0.95	0.38 – 19	0.095

Table 9-12 Accumulated concentration in peat for release to peatland in Ceberg [mg/kg dw].

Time [year]	SFL 3		SFL 5	
	Pb	Cd	Pb	Be
100	$< 1 \cdot 10^{-7}$	$< 2 \cdot 10^{-9}$	$< 1 \cdot 10^{-7}$	$< 7 \cdot 10^{-10}$
1,000	$< 1 \cdot 10^{-7}$	$< 2 \cdot 10^{-9}$	$< 1 \cdot 10^{-7}$	$< 7 \cdot 10^{-10}$
10,000	$< 1 \cdot 10^{-7}$	$< 2 \cdot 10^{-9}$	$< 1 \cdot 10^{-7}$	$< 7 \cdot 10^{-10}$
Comparison value	0.38 – 19	0.095 – 0.95	0.38 – 19	0.095

10 Release calculations for other scenarios

10.1 Introduction

The results presented in the previous chapters are based on assumptions describing the reference scenario. However, deviations from this scenario are possible. Examples of such deviations are changes in the climate, tectonic activity and future impact by humans. This is further discussed in the main report (SKB, 1999b). In addition, the construction and the operating phase of SFL 3-5 can affect the long-term performance of the repository. Stray materials will be brought down to the repository and some of these will be left after the repository closure. However, it is estimated that this will have a negligible effect on the performance of SFL 3-5 (SKB, 1999b).

For SFL 3-5 the effect of human activities has been investigated by analysing the consequences of a release of radionuclides and toxic metals to future wells in Aberg, Beberg and Ceberg. The same assumptions, models and data as for the reference scenario (see Chapters 4 – 6) are used to calculate the near-field and the far-field migration. The only difference in comparison to the reference scenario is that the radionuclides and toxic metals are released to a well.

10.2 Release of radionuclides to well

The model used for estimating the resulting dose for radionuclides released to a well is outlined briefly in Chapter 4. Site-specific mean wells have been defined (see Skagius *et al.,* 1999). The dose conversion factors for these wells are summarised in Chapter 5. The results are presented in two different ways. Firstly, the results for nuclides dominating the dose and the aggregate dose for each repository part are shown in graphs. Secondly, the maximum dose and the time when this dose is obtained are summarised for all modelled nuclides in tables. For nuclides whose maximum release rate from the far field is less than $1 \cdot 10^{-3}$ Bq/year, the dose given in this chapter is set to $< 10^{-3}$ times the ecosystem-specific dose conversion factor (EDF) and the time when the maximum dose is obtained is not specified. The results are based on the assumption that nuclides and toxic metals reaches the well at the same rate (Bq/year) as the far-field release rate, and that there is no delay in time between far-field release and release to well. It is also assumed that the waste in SFL 4 contains no surface contamination. If not otherwise stated, the effect of ISA on the near-field transport in SFL 3 is neglected.

It is reasonable to assume that it takes at least three generations, or about 100 years, before knowledge of a repository can be said to be lost (Morén *et al.,* 1998). The location of the repository can therefore be assumed to be known for at least 100 years after repository closure. It is also possible that the repository is under institutional control during this period. Consequently, it is unlikely that a well will be sunk in the area where a repository is located during this time. The results shown in graphs are therefore shaded for the first 100 years, and also for times larger than 100,000 years (see Section 9.1). The comparison level 14 μSv/year and the background level 1 mSv/year (see Section 9.1) are both included in the graphs.

10.2.1 Aberg

The results for release to a mean well in Aberg are shown in Figures 10-1 to 10-3.

The release of ^{3}H and ^{90}Sr in SFL 3 to a mean well in Aberg gives a maximum dose of 0.2 µSv/year and 4 µSv/year, respectively (Figure 10-1). These nuclides are mainly released during the first 100 – 300 years after repository closure. At longer times, the dose is dominated by ^{93}Mo and ^{59}Ni. The maximum dose is 6 µSv/year and is obtained by ^{93}Mo after approximately 2,000 to 3,000 years.

Taking the effect of ISA on solubility in the near field into account, the maximum dose corresponding to the release of ^{210}Pb and ^{226}Ra is increased one order of magnitude and of ^{59}Ni by a factor two. The results for ^{59}Ni, ^{210}Pb and ^{226}Ra are included in Figure 10-1. The maximum aggregate dose is increased to 66 µSv/year, but is obtained after very long time (10^{7} years).

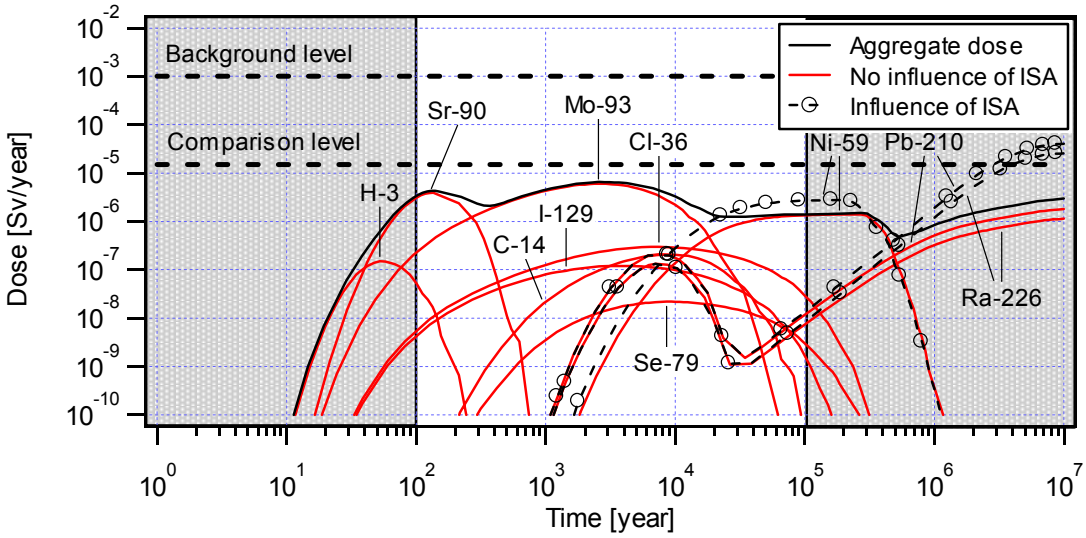

Figure 10-1 Dose from release of radionuclides from SFL 3 to mean well in Aberg.

The calculations for SFL 4 are based on the assumption that all surface contamination has been removed before deposition. The radionuclide content in SFL 4 is therefore small, and the release rate from the far field decreases with time (see Figure 8.2). This is reflected in the corresponding dose as well (Figure 10-2). The maximum dose is 3 µSv/year and is obtained by ^{90}Sr. This is, however, obtained during the first 100 years after closure. After this period, the aggregate dose has decreased and is significantly below the comparison level.

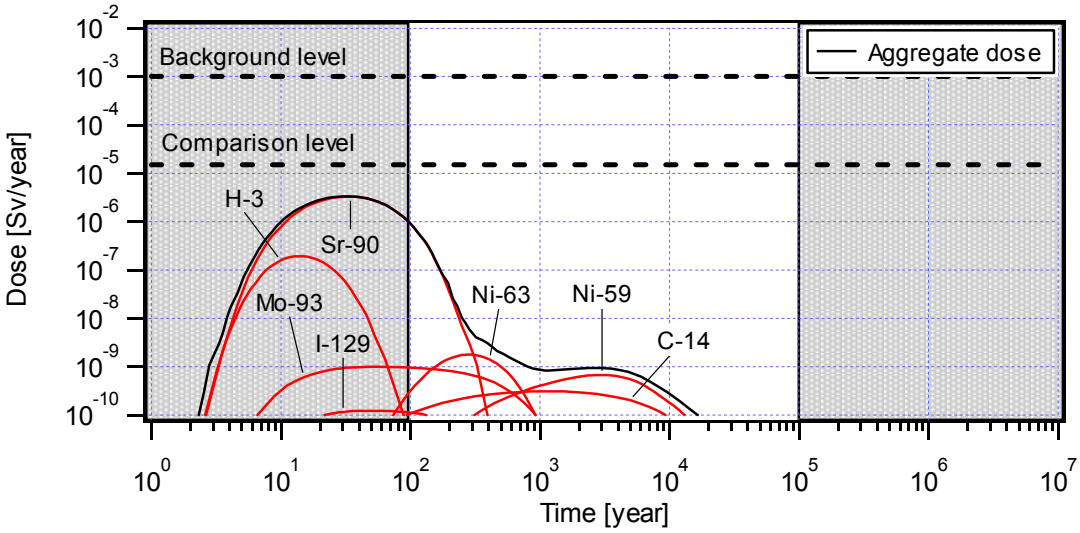

Figure 10-2 Dose from release of radionuclides from SFL 4 (without CRUD) to mean well in Aberg.

During the first 100 years after repository closure, the dose corresponding to release from SFL 5 to a mean well in Aberg is dominated by the release of ^{3}H (Figure 10-3). Later the dose is dominated primarily by ^{93}Mo, but ^{90}Sr, ^{36}Cl, ^{59}Ni and ^{93}Zr also make substantial contributions to the aggregate dose at different times. Release of ^{93}Mo from SFL 5 to the mean well in Aberg results in a maximum dose of 18 µSv/year.

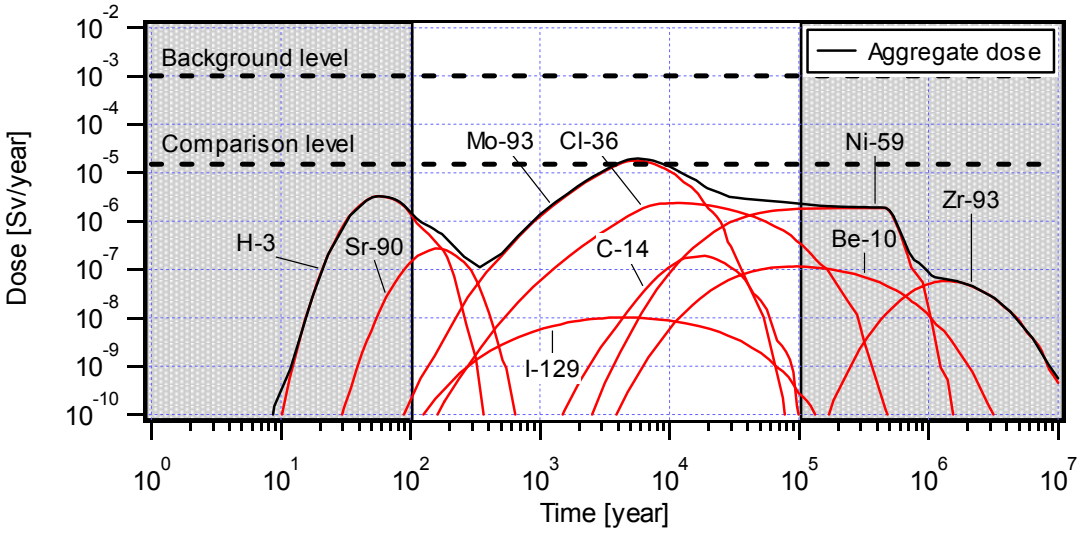

Figure 10-3 Dose from release of radionuclides from SFL 5 to mean well in Aberg.

The maximum doses for release to a mean well in Aberg are compiled in Table 10-1.

Table 10-1 Maximum dose for release to mean well in Aberg.

Nuclide	Half-life	SFL 3 (without ISA)		SFL 3 (with ISA)		SFL 4		SFL 5	
		Time for maximum dose	Maximum dose	Time for maximum dose	Maximum dose	Time for maximum dose	Maximum dose	Time for maximum dose	Maximum dose
	[year]	[year]	[Sv/year]	[year]	[Sv/year]	[year]	[Sv/year]	[year]	[Sv/year]
^{3}H	12	$5\cdot10^{1}$	$2\cdot10^{-7}$	$6\cdot10^{1}$	$2\cdot10^{-7}$	$1\cdot10^{1}$	$2\cdot10^{-7}$	$6\cdot10^{1}$	$3\cdot10^{-6}$
^{10}Be	$1.5\cdot10^{6}$	– a)	– a)	– a)	– a)	– a)	– a)	$1\cdot10^{5}$	$1\cdot10^{-7}$
^{14}C	$5.7\cdot10^{3}$	$9\cdot10^{3}$	$2\cdot10^{-7}$	$8\cdot10^{3}$	$2\cdot10^{-7}$	$1\cdot10^{3}$	$3\cdot10^{-10}$	$2\cdot10^{4}$	$2\cdot10^{-7}$
$^{14}C_{org}$	$5.7\cdot10^{3}$	$2\cdot10^{2}$	$1\cdot10^{-11}$	$2\cdot10^{2}$	$1\cdot10^{-11}$	– a)	– a)	– a)	– a)
^{36}Cl	$3.0\cdot10^{5}$	$7\cdot10^{3}$	$3\cdot10^{-7}$	$8\cdot10^{3}$	$3\cdot10^{-7}$	$6\cdot10^{1}$	$4\cdot10^{-11}$	$1\cdot10^{4}$	$2\cdot10^{-6}$
^{60}Co	5.3	– a)	– a)	– a)	– a)	$5\cdot10^{1}$	$1\cdot10^{-12}$	– a)	– a)
^{59}Ni	$7.6\cdot10^{4}$	$3\cdot10^{5}$	$1\cdot10^{-6}$	$2\cdot10^{5}$	$3\cdot10^{-6}$	$3\cdot10^{3}$	$7\cdot10^{-10}$	$4\cdot10^{5}$	$2\cdot10^{-6}$
^{63}Ni	$1.0\cdot10^{2}$	– a)	– a)	– a)	– a)	$3\cdot10^{2}$	$2\cdot10^{-9}$	– a)	– a)
^{79}Se	$1.1\cdot10^{6}$	$9\cdot10^{3}$	$2\cdot10^{-8}$	$9\cdot10^{3}$	$2\cdot10^{-8}$	$3\cdot10^{2}$	$1\cdot10^{-11}$	$1\cdot10^{4}$	$2\cdot10^{-9}$
^{90}Sr	29	$1\cdot10^{2}$	$4\cdot10^{-6}$	$1\cdot10^{2}$	$4\cdot10^{-6}$	$3\cdot10^{1}$	$3\cdot10^{-6}$	$2\cdot10^{2}$	$3\cdot10^{-7}$
^{94}Nb	$2.0\cdot10^{4}$	– a)	– a)	– a)	– a)	$3\cdot10^{4}$	$1\cdot10^{-11}$	– a)	– a)
^{93}Zr	$1.5\cdot10^{6}$	$1\cdot10^{6}$	$7\cdot10^{-10}$	$1\cdot10^{6}$	$7\cdot10^{-10}$	– a)	– a)	$1\cdot10^{6}$	$6\cdot10^{-8}$
^{93}Mo	$4.0\cdot10^{3}$	$3\cdot10^{3}$	$6\cdot10^{-6}$	$3\cdot10^{3}$	$6\cdot10^{-6}$	$5\cdot10^{1}$	$1\cdot10^{-9}$	$6\cdot10^{3}$	$2\cdot10^{-5}$
^{99}Tc	$2.1\cdot10^{5}$	$6\cdot10^{5}$	$3\cdot10^{-9}$	$6\cdot10^{5}$	$3\cdot10^{-9}$	$7\cdot10^{4}$	$7\cdot10^{-12}$	$6\cdot10^{5}$	$1\cdot10^{-9}$
^{129}I	$1.6\cdot10^{7}$	$4\cdot10^{3}$	$1\cdot10^{-7}$	$4\cdot10^{3}$	$1\cdot10^{-7}$	$5\cdot10^{1}$	$1\cdot10^{-10}$	$4\cdot10^{3}$	$1\cdot10^{-8}$
^{135}Cs	$2.3\cdot10^{6}$	$3\cdot10^{4}$	$1\cdot10^{-8}$	$3\cdot10^{4}$	$1\cdot10^{-8}$	– a)	– a)	– a)	– a)
^{137}Cs	30	– a)	– a)	– a)	– a)	$2\cdot10^{2}$	$8\cdot10^{-12}$	– a)	– a)
^{236}U	$2.3\cdot10^{7}$	$9\cdot10^{6}$	$1\cdot10^{-10}$	$9\cdot10^{6}$	$1\cdot10^{-10}$	– a)	– a)	– a)	– a)
^{232}Th	$1.4\cdot10^{10}$	$7\cdot10^{8}$	$2\cdot10^{-9}$	$1\cdot10^{7}$	$5\cdot10^{-8}$	– a)	– a)	– a)	– a)
^{237}Np	$2.1\cdot10^{6}$	$4\cdot10^{6}$	$1\cdot10^{-10}$	$4\cdot10^{6}$	$1\cdot10^{-10}$	– a)	– a)	– a)	– a)
^{233}U	$1.6\cdot10^{5}$	$4\cdot10^{6}$	$6\cdot10^{-11}$	$4\cdot10^{6}$	$6\cdot10^{-11}$	– a)	– a)	– a)	– a)
^{229}Th	$7.3\cdot10^{3}$	$4\cdot10^{6}$	$2\cdot10^{-9}$	$4\cdot10^{6}$	$2\cdot10^{-9}$	– a)	– a)	– a)	– a)
^{238}U	$4.5\cdot10^{9}$	$1\cdot10^{9}$	$5\cdot10^{-10}$	$1\cdot10^{7}$	$1\cdot10^{-8}$	–	$< 2\cdot10^{-14}$	$1\cdot10^{7}$	$2\cdot10^{-14}$
^{234}U	$2.5\cdot10^{5}$	$3\cdot10^{8}$	$5\cdot10^{-10}$	$1\cdot10^{7}$	$2\cdot10^{-8}$	–	$< 2\cdot10^{-14}$	$1\cdot10^{7}$	$2\cdot10^{-14}$
^{230}Th	$7.5\cdot10^{4}$	$9\cdot10^{7}$	$7\cdot10^{-9}$	$9\cdot10^{6}$	$2\cdot10^{-7}$	–	$< 2\cdot10^{-13}$	$1\cdot10^{7}$	$3\cdot10^{-13}$
^{226}Ra	$1.6\cdot10^{3}$	$7\cdot10^{7}$	$1\cdot10^{-6}$	$1\cdot10^{7}$	$3\cdot10^{-5}$	$3\cdot10^{5}$	$3\cdot10^{-13}$	$1\cdot10^{7}$	$4\cdot10^{-11}$
^{210}Pb	22	$7\cdot10^{7}$	$2\cdot10^{-6}$	$1\cdot10^{7}$	$4\cdot10^{-5}$	$3\cdot10^{5}$	$5\cdot10^{-13}$	$1\cdot10^{7}$	$6\cdot10^{-11}$

a) Not modelled.

10.2.2 Beberg

The results for release of dose dominating radionuclides in SFL 3 and SFL 5 to a mean well in Beberg are shown in Figures 10-4 and 10-5. The results are for the case with a saline groundwater, but the influence of groundwater composition in Beberg on the aggregate dose is limited. The release rate of short-lived nuclides, e.g. ^{3}H and ^{90}Sr, from the far field in Beberg is low, and consequently the corresponding dose for release to a mean well is very low during the first 100 years after repository closure.

The aggregate dose from nuclides released from SFL 3 is increasing for times up to 4,000 years after which it decreases again. Dominating nuclides are ^{93}Mo and ^{36}Cl. ^{93}Mo gives the highest maximum dose, 0.6 μSv/year. ^{210}Pb and ^{226}Ra are released to a well at times that are beyond the scope of this work. ISA has no effect on the maximum aggregate dose.

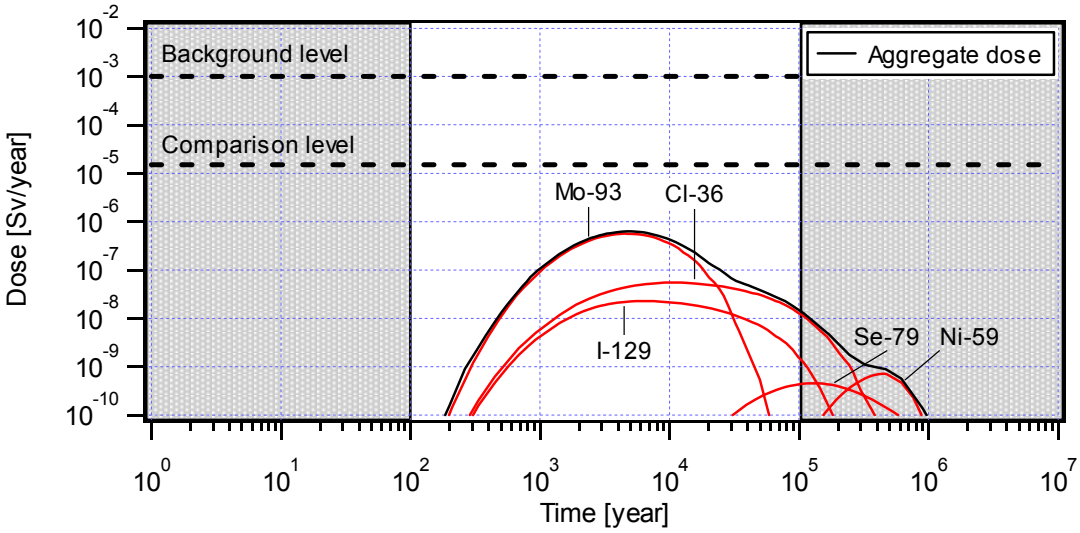

Figure 10-4 Dose from release of radionuclides from SFL 3 (no effect of ISA on the near-field transport) to mean well in Beberg (saline water).

The release rate from SFL 4 is very low, and the maximum dose for release to a mean well in Beberg does not exceed 10^{-10} Sv/year.

The nuclides (^{93}Mo and ^{36}Cl) that dominate the dose from nuclides in SFL 3 are also dominating the dose from nuclides in SFL 5. The maximum dose is 2 µSv/year, which is obtained after approximately 7,000 years (see Figure 10-5).

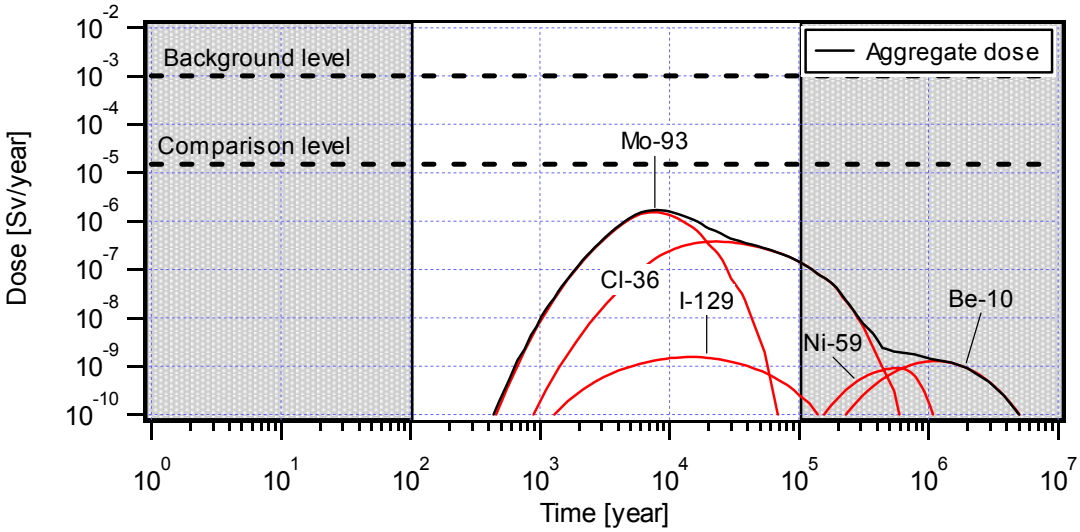

Figure 10-5 Dose from release of radionuclides from SFL 5 to mean well in Beberg (saline water).

^{59}Ni and ^{10}Be are the only nuclides of importance for the aggregate dose in SFL 3 and in SFL 5 that are affected by the groundwater conditions. However, the dose from ^{59}Ni and ^{10}Be is lower when the groundwater is non-saline in comparison to that for saline water.

The maximum doses for release to a mean well in Beberg are compiled in Tables 10-2 and 10-3.

Table 10-2 Maximum dose for release to mean well in Beberg (saline water).

Nuclide	Half-life	SFL 3 (without ISA)		SFL 3 (with ISA)		SFL 4		SFL 5	
		Time for maximum dose	Maximum dose	Time for maximum dose	Maximum dose	Time for maximum dose	Maximum dose	Time for maximum dose	Maximum dose
	[year]	[year]	[Sv/year]	[year]	[Sv/year]	[year]	[Sv/year]	[year]	[Sv/year]
^{3}H	12	$1{\cdot}10^{2}$	$3{\cdot}10^{-14}$	$1{\cdot}10^{2}$	$3{\cdot}10^{-14}$	$6{\cdot}10^{1}$	$2{\cdot}10^{-12}$	$1{\cdot}10^{2}$	$8{\cdot}10^{-13}$
^{10}Be	$1.5{\cdot}10^{6}$	– [a]	– [a]	– [a]	– [a]	– [a]	– [a]	$1{\cdot}10^{6}$	$1{\cdot}10^{-9}$
^{14}C	$5.7{\cdot}10^{3}$	$3{\cdot}10^{4}$	$5{\cdot}10^{-11}$	$3{\cdot}10^{4}$	$5{\cdot}10^{-11}$	$2{\cdot}10^{4}$	$2{\cdot}10^{-14}$	$4{\cdot}10^{4}$	$4{\cdot}10^{-11}$
$^{14}C_{org}$	$5.7{\cdot}10^{3}$	$2{\cdot}10^{3}$	$8{\cdot}10^{-13}$	$2{\cdot}10^{3}$	$8{\cdot}10^{-13}$	– [a]	– [a]	– [a]	– [a]
^{36}Cl	$3.0{\cdot}10^{5}$	$1{\cdot}10^{4}$	$5{\cdot}10^{-8}$	$1{\cdot}10^{4}$	$5{\cdot}10^{-8}$	$2{\cdot}10^{3}$	$7{\cdot}10^{-13}$	$2{\cdot}10^{4}$	$4{\cdot}10^{-7}$
^{60}Co	5.3	– [a]	– [a]	– [a]	– [a]	–	$< 3{\cdot}10^{-16}$	– [a]	– [a]
^{59}Ni	$7.6{\cdot}10^{4}$	$4{\cdot}10^{5}$	$7{\cdot}10^{-10}$	$4{\cdot}10^{5}$	$1{\cdot}10^{-9}$	$2{\cdot}10^{5}$	$3{\cdot}10^{-14}$	$6{\cdot}10^{5}$	$9{\cdot}10^{-10}$
^{63}Ni	$1.0{\cdot}10^{2}$	– [a]	– [a]	– [a]	– [a]	–	$< 2{\cdot}10^{-17}$	– [a]	– [a]
^{79}Se	$1.1{\cdot}10^{6}$	$1{\cdot}10^{5}$	$5{\cdot}10^{-10}$	$1{\cdot}10^{5}$	$5{\cdot}10^{-10}$	$5{\cdot}10^{4}$	$8{\cdot}10^{-15}$	$2{\cdot}10^{5}$	$4{\cdot}10^{-11}$
^{90}Sr	29	–	$< 4{\cdot}10^{-15}$	–	$< 4{\cdot}10^{-15}$	–	$< 4{\cdot}10^{-15}$	–	$< 4{\cdot}10^{-15}$
^{94}Nb	$2.0{\cdot}10^{4}$	– [a]	– [a]	– [a]	– [a]	–	$< 1{\cdot}10^{-15}$	– [a]	– [a]
^{93}Zr	$1.5{\cdot}10^{6}$	$9{\cdot}10^{6}$	$4{\cdot}10^{-15}$	$9{\cdot}10^{6}$	$4{\cdot}10^{-15}$	– [a]	– [a]	$9{\cdot}10^{6}$	$2{\cdot}10^{-13}$
^{93}Mo	$4.0{\cdot}10^{3}$	$4{\cdot}10^{3}$	$6{\cdot}10^{-7}$	$4{\cdot}10^{3}$	$6{\cdot}10^{-7}$	$1{\cdot}10^{3}$	$2{\cdot}10^{-11}$	$8{\cdot}10^{3}$	$2{\cdot}10^{-6}$
^{99}Tc	$2.1{\cdot}10^{5}$	–	$< 2{\cdot}10^{-16}$	–	$< 2{\cdot}10^{-16}$	–	$< 2{\cdot}10^{-16}$	–	$< 2{\cdot}10^{-16}$
^{129}I	$1.6{\cdot}10^{7}$	$6{\cdot}10^{3}$	$2{\cdot}10^{-8}$	$6{\cdot}10^{3}$	$2{\cdot}10^{-8}$	$1{\cdot}10^{3}$	$2{\cdot}10^{-12}$	$1{\cdot}10^{4}$	$2{\cdot}10^{-9}$
^{135}Cs	$2.3{\cdot}10^{6}$	$2{\cdot}10^{6}$	$2{\cdot}10^{-12}$	$2{\cdot}10^{6}$	$2{\cdot}10^{-12}$	– [a]	– [a]	– [a]	– [a]
^{137}Cs	30	– [a]	– [a]	– [a]	– [a]	–	$< 2{\cdot}10^{-15}$	– [a]	– [a]
^{236}U	$2.3{\cdot}10^{7}$	$8{\cdot}10^{7}$	$2{\cdot}10^{-14}$	$9{\cdot}10^{7}$	$2{\cdot}10^{-14}$	– [a]	– [a]	– [a]	– [a]
^{232}Th	$1.4{\cdot}10^{10}$	$1{\cdot}10^{9}$	$3{\cdot}10^{-10}$	$1{\cdot}10^{8}$	$1{\cdot}10^{-9}$	– [a]	– [a]	– [a]	– [a]
^{237}Np	$2.1{\cdot}10^{6}$	–	$< 1{\cdot}10^{-14}$	–	$< 1{\cdot}10^{-14}$	– [a]	– [a]	– [a]	– [a]
^{233}U	$1.6{\cdot}10^{5}$	–	$< 5{\cdot}10^{-15}$	–	$< 5{\cdot}10^{-15}$	– [a]	– [a]	– [a]	– [a]
^{229}Th	$7.3{\cdot}10^{3}$	–	$< 1{\cdot}10^{-13}$	–	$< 1{\cdot}10^{-13}$	– [a]	– [a]	– [a]	– [a]
^{238}U	$4.5{\cdot}10^{9}$	$2{\cdot}10^{9}$	$3{\cdot}10^{-11}$	$3{\cdot}10^{8}$	$8{\cdot}10^{-11}$	–	$< 5{\cdot}10^{-15}$	–	$< 5{\cdot}10^{-15}$
^{234}U	$2.5{\cdot}10^{5}$	$2{\cdot}10^{9}$	$4{\cdot}10^{-11}$	$3{\cdot}10^{8}$	$9{\cdot}10^{-11}$	–	$< 5{\cdot}10^{-15}$	–	$< 5{\cdot}10^{-15}$
^{230}Th	$7.5{\cdot}10^{4}$	$2{\cdot}10^{9}$	$4{\cdot}10^{-10}$	$3{\cdot}10^{8}$	$1{\cdot}10^{-9}$	–	$< 6{\cdot}10^{-14}$	–	$< 6{\cdot}10^{-14}$
^{226}Ra	$1.6{\cdot}10^{3}$	$2{\cdot}10^{9}$	$6{\cdot}10^{-8}$	$3{\cdot}10^{8}$	$1{\cdot}10^{-7}$	–	$< 3{\cdot}10^{-14}$	–	$2{\cdot}10^{-13}$
^{210}Pb	22	$2{\cdot}10^{9}$	$9{\cdot}10^{-8}$	$3{\cdot}10^{8}$	$2{\cdot}10^{-7}$	–	$< 6{\cdot}10^{-14}$	–	$4{\cdot}10^{-13}$

a) *Not modelled.*

Table 10-3 Maximum dose for release to mean well in Beberg (non-saline water).

Nuclide	Half-life	SFL 3 (without ISA)		SFL 3 (with ISA)		SFL 4		SFL 5	
		Time for maximum dose	Maximum dose	Time for maximum dose	Maximum dose	Time for maximum dose	Maximum dose	Time for maximum dose	Maximum dose
	[year]	[year]	[Sv/year]	[year]	[Sv/year]	[year]	[Sv/year]	[year]	[Sv/year]
^{3}H	12	$1 \cdot 10^{2}$	$3 \cdot 10^{-14}$	$1 \cdot 10^{2}$	$3 \cdot 10^{-14}$	$6 \cdot 10^{1}$	$2 \cdot 10^{-12}$	$1 \cdot 10^{2}$	$8 \cdot 10^{-13}$
^{10}Be	$1.5 \cdot 10^{6}$	– a)	– a)	– a)	– a)	– a)	– a)	$2 \cdot 10^{6}$	$2 \cdot 10^{-10}$
^{14}C	$5.7 \cdot 10^{3}$	$2 \cdot 10^{4}$	$2 \cdot 10^{-9}$	$2 \cdot 10^{4}$	$2 \cdot 10^{-9}$	$9 \cdot 10^{3}$	$8 \cdot 10^{-13}$	$3 \cdot 10^{4}$	$1 \cdot 10^{-9}$
$^{14}C_{org}$	$5.7 \cdot 10^{3}$	$2 \cdot 10^{3}$	$8 \cdot 10^{-13}$	$2 \cdot 10^{3}$	$8 \cdot 10^{-13}$	– a)	– a)	– a)	– a)
^{36}Cl	$3.0 \cdot 10^{5}$	$1 \cdot 10^{4}$	$5 \cdot 10^{-8}$	$1 \cdot 10^{4}$	$5 \cdot 10^{-8}$	$4 \cdot 10^{2}$	$1 \cdot 10^{-12}$	$2 \cdot 10^{4}$	$4 \cdot 10^{-7}$
^{60}Co	5.3	– a)	– a)	– a)	– a)	–	$< 3 \cdot 10^{-16}$	– a)	– a)
^{59}Ni	$7.6 \cdot 10^{4}$	$7 \cdot 10^{5}$	$2 \cdot 10^{-12}$	$6 \cdot 10^{5}$	$3 \cdot 10^{-12}$	$3 \cdot 10^{5}$	$3 \cdot 10^{-16}$	$8 \cdot 10^{5}$	$2 \cdot 10^{-12}$
^{63}Ni	$1.0 \cdot 10^{2}$	– a)	– a)	– a)	– a)	–	$< 2 \cdot 10^{-17}$	– a)	– a)
^{79}Se	$1.1 \cdot 10^{6}$	$1 \cdot 10^{5}$	$5 \cdot 10^{-10}$	$1 \cdot 10^{5}$	$5 \cdot 10^{-10}$	$5 \cdot 10^{4}$	$8 \cdot 10^{-15}$	$2 \cdot 10^{5}$	$4 \cdot 10^{-11}$
^{90}Sr	29	–	$< 4 \cdot 10^{-15}$	–	$< 4 \cdot 10^{-15}$	–	$< 4 \cdot 10^{-15}$	–	$< 4 \cdot 10^{-15}$
^{94}Nb	$2.0 \cdot 10^{4}$	– a)	– a)	– a)	– a)	–	$< 1 \cdot 10^{-15}$	– a)	– a)
^{93}Zr	$1.5 \cdot 10^{6}$	$9 \cdot 10^{6}$	$4 \cdot 10^{-15}$	$9 \cdot 10^{6}$	$4 \cdot 10^{-15}$	– a)	– a)	$9 \cdot 10^{6}$	$2 \cdot 10^{-13}$
^{93}Mo	$4.0 \cdot 10^{3}$	$5 \cdot 10^{3}$	$6 \cdot 10^{-7}$	$4 \cdot 10^{3}$	$6 \cdot 10^{-7}$	$1 \cdot 10^{3}$	$2 \cdot 10^{-11}$	$8 \cdot 10^{3}$	$2 \cdot 10^{-6}$
^{99}Tc	$2.1 \cdot 10^{5}$	–	$< 2 \cdot 10^{-16}$	–	$< 2 \cdot 10^{-16}$	–	$< 2 \cdot 10^{-16}$	–	$< 2 \cdot 10^{-16}$
^{129}I	$1.6 \cdot 10^{7}$	$6 \cdot 10^{3}$	$2 \cdot 10^{-8}$	$6 \cdot 10^{3}$	$2 \cdot 10^{-8}$	$4 \cdot 10^{2}$	$5 \cdot 10^{-12}$	$8 \cdot 10^{3}$	$2 \cdot 10^{-9}$
^{135}Cs	$2.3 \cdot 10^{6}$	–	$< 6 \cdot 10^{-16}$	–	$< 6 \cdot 10^{-16}$	– a)	– a)	– a)	– a)
^{137}Cs	30	– a)	– a)	– a)	– a)	–	$< 2 \cdot 10^{-15}$	– a)	– a)
^{236}U	$2.3 \cdot 10^{7}$	$9 \cdot 10^{7}$	$2 \cdot 10^{-14}$	$9 \cdot 10^{7}$	$2 \cdot 10^{-14}$	– a)	– a)	– a)	– a)
^{232}Th	$1.4 \cdot 10^{10}$	$1 \cdot 10^{9}$	$3 \cdot 10^{-10}$	$1 \cdot 10^{8}$	$1 \cdot 10^{-9}$	– a)	– a)	– a)	– a)
^{237}Np	$2.1 \cdot 10^{6}$	–	$< 1 \cdot 10^{-14}$	–	$< 1 \cdot 10^{-14}$	– a)	– a)	– a)	– a)
^{233}U	$1.6 \cdot 10^{5}$	–	$< 5 \cdot 10^{-15}$	–	$< 5 \cdot 10^{-15}$	– a)	– a)	– a)	– a)
^{229}Th	$7.3 \cdot 10^{3}$	–	$< 1 \cdot 10^{-13}$	–	$< 1 \cdot 10^{-13}$	– a)	– a)	– a)	– a)
^{238}U	$4.5 \cdot 10^{9}$	$2 \cdot 10^{9}$	$3 \cdot 10^{-11}$	$3 \cdot 10^{8}$	$8 \cdot 10^{-11}$	–	$< 5 \cdot 10^{-15}$	–	$< 5 \cdot 10^{-15}$
^{234}U	$2.5 \cdot 10^{5}$	$2 \cdot 10^{9}$	$4 \cdot 10^{-11}$	$3 \cdot 10^{8}$	$9 \cdot 10^{-11}$	–	$< 5 \cdot 10^{-15}$	–	$< 5 \cdot 10^{-15}$
^{230}Th	$7.5 \cdot 10^{4}$	$2 \cdot 10^{9}$	$4 \cdot 10^{-10}$	$3 \cdot 10^{8}$	$1 \cdot 10^{-9}$	–	$< 6 \cdot 10^{-14}$	–	$< 6 \cdot 10^{-14}$
^{226}Ra	$1.6 \cdot 10^{3}$	$2 \cdot 10^{9}$	$1 \cdot 10^{-8}$	$3 \cdot 10^{8}$	$3 \cdot 10^{-8}$	–	$< 3 \cdot 10^{-14}$	–	$5 \cdot 10^{-14}$
^{210}Pb	22	$2 \cdot 10^{9}$	$2 \cdot 10^{-8}$	$3 \cdot 10^{8}$	$5 \cdot 10^{-8}$	–	$< 6 \cdot 10^{-14}$	–	$8 \cdot 10^{-14}$

a) Not modelled.

10.2.3 Ceberg

The results for release of dose dominating radionuclides in SFL 3 and SFL 5 to a mean well in Ceberg are shown in Figures 10-6 and 10-7. In accordance with the results for Beberg, release to a mean well in Ceberg results in a very low aggregate dose during the first 100 years after repository closure. The maximum aggregate dose is obtained about 10,000 years after repository closure. The nuclides dominating the dose are ^{93}Mo and ^{36}Cl for both SFL 3 and SFL 5. For release from SFL 3 the maximum dose (0.06 μSv/year) is obtained by ^{93}Mo after some 9,000 years. The release of ^{36}Cl from SFL 5 results in the maximum dose (0.2 μSv/year) approximately 30,000 years after repository closure. In accordance with the results for Beberg, the maximum aggregate dose from SFL 3 is uninfluenced by ISA.

The release of radionuclides in SFL 4 results in a maximum aggregate dose in mean well that is less than 10^{-10} Sv/year.

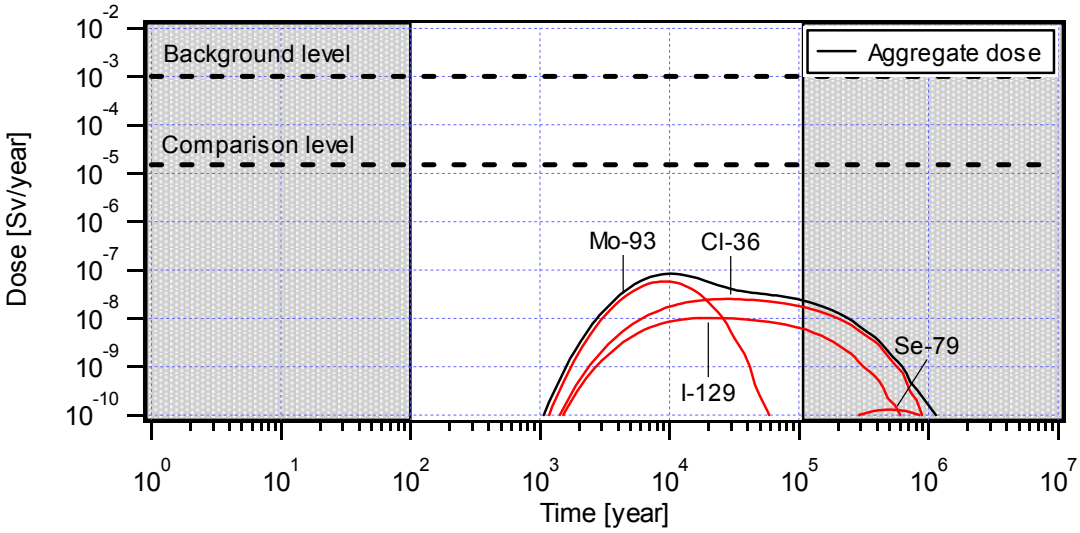

Figure 10-6 Dose from release of radionuclides from SFL 3 (no effect of ISA on the near-field transport) to mean well in Ceberg.

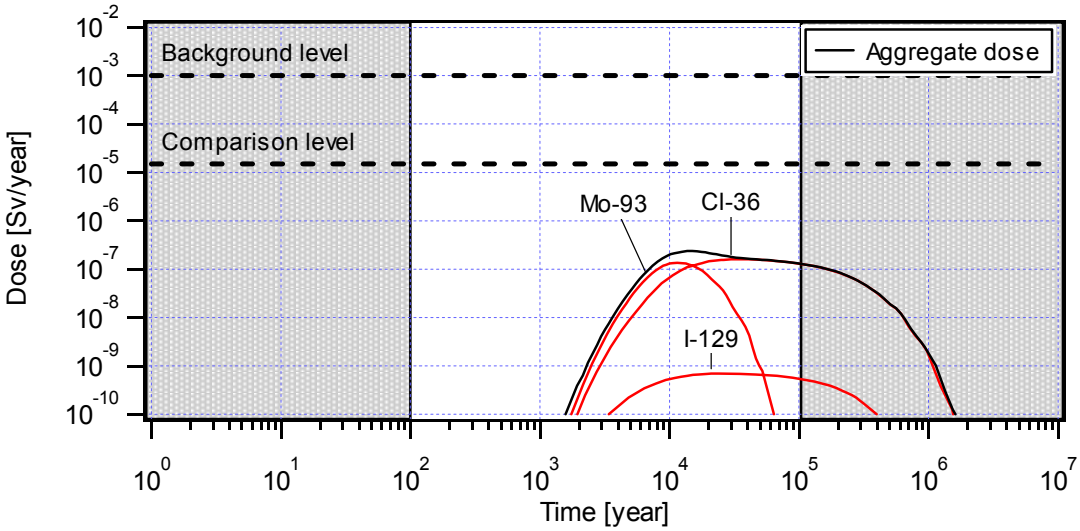

Figure 10-7 Dose from release of radionuclides from SFL 5 to mean well in Ceberg.

The maximum doses for release to a mean well in Ceberg are compiled in Table 10-4.

Table 10-4 Maximum dose for release to mean well in Ceberg.

Nuclide	Half-life	SFL 3 (without ISA)		SFL 3 (with ISA)		SFL 4		SFL 5	
		Time for maximum dose	Maximum dose	Time for maximum dose	Maximum dose	Time for maximum dose	Maximum dose	Time for maximum dose	Maximum dose
	[year]	[year]	[Sv/year]	[year]	[Sv/year]	[year]	[Sv/year]	[year]	[Sv/year]
^{3}H	12	–	$< 5 \cdot 10^{-18}$	–	$< 5 \cdot 10^{-18}$	–	$< 5 \cdot 10^{-18}$	–	$< 5 \cdot 10^{-18}$
^{10}Be	$1.5 \cdot 10^{6}$	– a)	– a)	– a)	– a)	– a)	– a)	$6 \cdot 10^{6}$	$2 \cdot 10^{-12}$
^{14}C	$5.7 \cdot 10^{3}$	$3 \cdot 10^{4}$	$2 \cdot 10^{-11}$	$3 \cdot 10^{4}$	$2 \cdot 10^{-11}$	$2 \cdot 10^{4}$	$2 \cdot 10^{-14}$	$4 \cdot 10^{4}$	$1 \cdot 10^{-11}$
$^{14}C_{org}$	$5.7 \cdot 10^{3}$	$7 \cdot 10^{3}$	$1 \cdot 10^{-13}$	$7 \cdot 10^{3}$	$1 \cdot 10^{-13}$	– a)	– a)	– a)	– a)
^{36}Cl	$3.0 \cdot 10^{5}$	$3 \cdot 10^{4}$	$3 \cdot 10^{-8}$	$3 \cdot 10^{4}$	$3 \cdot 10^{-8}$	$5 \cdot 10^{3}$	$3 \cdot 10^{-13}$	$3 \cdot 10^{4}$	$2 \cdot 10^{-7}$
^{60}Co	5.3	– a)	– a)	– a)	– a)	–	$< 7 \cdot 10^{-16}$	– a)	– a)
^{59}Ni	$7.6 \cdot 10^{4}$	$1 \cdot 10^{6}$	$5 \cdot 10^{-17}$	$9 \cdot 10^{5}$	$8 \cdot 10^{-17}$	–	$< 3 \cdot 10^{-17}$	$1 \cdot 10^{6}$	$6 \cdot 10^{-17}$
^{63}Ni	$1.0 \cdot 10^{2}$	– a)	– a)	– a)	– a)	–	$< 4 \cdot 10^{-17}$	– a)	– a)
^{79}Se	$1.1 \cdot 10^{6}$	$5 \cdot 10^{5}$	$1 \cdot 10^{-10}$	$5 \cdot 10^{5}$	$1 \cdot 10^{-10}$	–	$< 1 \cdot 10^{-15}$	$6 \cdot 10^{5}$	$1 \cdot 10^{-11}$
^{90}Sr	29	–	$< 7 \cdot 10^{-15}$	–	$< 7 \cdot 10^{-15}$	–	$< 7 \cdot 10^{-15}$	–	$< 7 \cdot 10^{-15}$
^{94}Nb	$2.0 \cdot 10^{4}$	– a)	– a)	– a)	– a)	–	$< 2 \cdot 10^{-15}$	– a)	– a)
^{93}Zr	$1.5 \cdot 10^{6}$	–	$< 2 \cdot 10^{-16}$	–	$< 2 \cdot 10^{-16}$	– a)	– a)	–	$< 2 \cdot 10^{-16}$
^{93}Mo	$4.0 \cdot 10^{3}$	$9 \cdot 10^{3}$	$6 \cdot 10^{-8}$	$9 \cdot 10^{3}$	$6 \cdot 10^{-8}$	$4 \cdot 10^{3}$	$2 \cdot 10^{-12}$	$1 \cdot 10^{4}$	$1 \cdot 10^{-7}$
^{99}Tc	$2.1 \cdot 10^{5}$	–	$< 3 \cdot 10^{-16}$	–	$< 3 \cdot 10^{-16}$	–	$< 3 \cdot 10^{-16}$	–	$< 3 \cdot 10^{-16}$
^{129}I	$1.6 \cdot 10^{7}$	$2 \cdot 10^{4}$	$1 \cdot 10^{-8}$	$2 \cdot 10^{4}$	$1 \cdot 10^{-8}$	$4 \cdot 10^{3}$	$9 \cdot 10^{-13}$	$2 \cdot 10^{4}$	$7 \cdot 10^{-10}$
^{135}Cs	$2.3 \cdot 10^{6}$	–	$< 1 \cdot 10^{-15}$	–	$< 1 \cdot 10^{-15}$	– a)	– a)	– a)	– a)
^{137}Cs	30	– a)	– a)	– a)	– a)	–	$< 3 \cdot 10^{-15}$	– a)	– a)
^{236}U	$2.3 \cdot 10^{7}$	–	$< 1 \cdot 10^{-14}$	–	$< 1 \cdot 10^{-14}$	– a)	– a)	– a)	– a)
^{232}Th	$1.4 \cdot 10^{10}$	$4 \cdot 10^{9}$	$1 \cdot 10^{-10}$	$7 \cdot 10^{8}$	$5 \cdot 10^{-10}$	– a)	– a)	– a)	– a)
^{237}Np	$2.1 \cdot 10^{6}$	–	$< 3 \cdot 10^{-14}$	–	$< 3 \cdot 10^{-14}$	– a)	– a)	– a)	– a)
^{233}U	$1.6 \cdot 10^{5}$	–	$< 1 \cdot 10^{-14}$	–	$< 1 \cdot 10^{-14}$	– a)	– a)	– a)	– a)
^{229}Th	$7.3 \cdot 10^{3}$	–	$< 2 \cdot 10^{-13}$	–	$< 2 \cdot 10^{-13}$	– a)	– a)	– a)	– a)
^{238}U	$4.5 \cdot 10^{9}$	$5 \cdot 10^{9}$	$1 \cdot 10^{-11}$	$1 \cdot 10^{9}$	$3 \cdot 10^{-11}$	–	$< 9 \cdot 10^{-15}$	–	$< 9 \cdot 10^{-15}$
^{234}U	$2.5 \cdot 10^{5}$	$5 \cdot 10^{9}$	$1 \cdot 10^{-11}$	$1 \cdot 10^{9}$	$3 \cdot 10^{-11}$	–	$< 1 \cdot 10^{-14}$	–	$< 1 \cdot 10^{-14}$
^{230}Th	$7.5 \cdot 10^{4}$	$5 \cdot 10^{9}$	$1 \cdot 10^{-10}$	$1 \cdot 10^{9}$	$3 \cdot 10^{-10}$	–	$< 1 \cdot 10^{-13}$	–	$< 1 \cdot 10^{-13}$
^{226}Ra	$1.6 \cdot 10^{3}$	$5 \cdot 10^{9}$	$3 \cdot 10^{-9}$	$1 \cdot 10^{9}$	$9 \cdot 10^{-9}$	–	$< 6 \cdot 10^{-14}$	–	$< 6 \cdot 10^{-14}$
^{210}Pb	22	$5 \cdot 10^{9}$	$6 \cdot 10^{-9}$	$1 \cdot 10^{9}$	$2 \cdot 10^{-8}$	–	$< 1 \cdot 10^{-13}$	–	$< 1 \cdot 10^{-13}$

a) Not modelled.

10.2.4 Total dose

It is expected that nuclides from SFL 3, SFL 4 and SFL 5 will be released to the same recipient. The sum of the aggregate dose from all three repository parts is therefore of importance. The total dose obtained for release to the mean wells is shown in Figures 10-8 to 10-10. These results are for the cases with no effect of ISA on the radionuclide solubility in SFL 3 and decontamination of the waste in SFL 4. The results for Beberg are for saline groundwater conditions.

It is mainly SFL 3 and SFL 5 that contributes to the total dose. SFL 4 gives a significant contribution only during the first 100 years after repository closure in Aberg (see Figure 10-8). The maximum value of the total dose is 25 μSv/year (Aberg), 2 μSv/year (Beberg) and 0.3 μSv/year (Ceberg).

The effect of ISA on the aggregate dose from SFL 3 in Aberg influences the total dose as well. The effect is, however, evident only after very long time, when ^{210}Pb and ^{226}Ra dominate the dose. In Aberg, the total dose is increased for times around 10^{6} years and

longer. This is indirectly indicated in Figure 10-1 with the results for ^{210}Pb and ^{226}Ra. The maximum total dose is 66 µSv/year obtained after 10^7 years. In Beberg and Ceberg the effect is smaller and is also obtained later.

For non-saline groundwater conditions in Beberg, the total dose will be the same as shown in Figure 10-9 except for that the total dose for times around 10^6 years and longer will be lower.

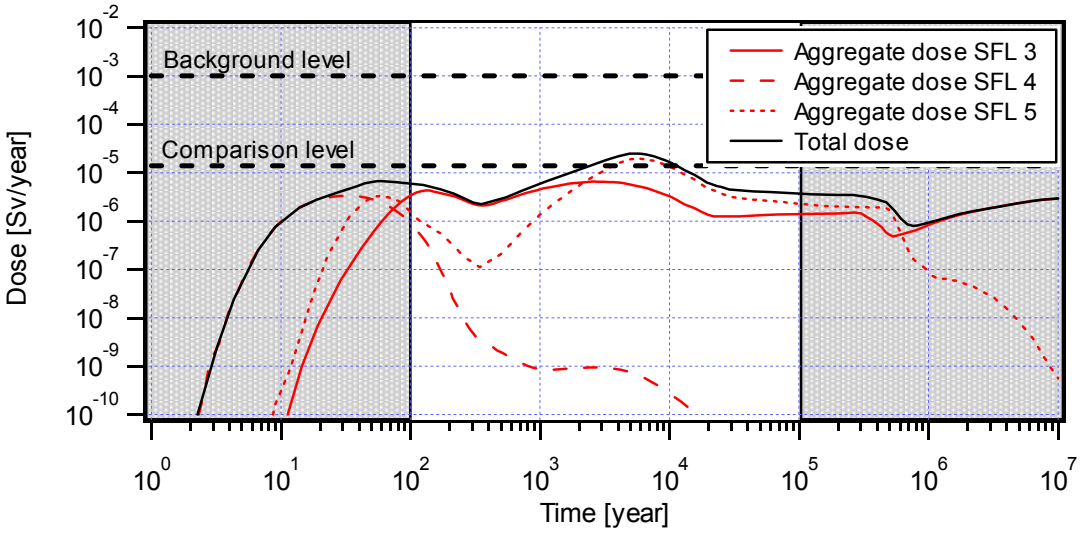

Figure 10-8 Total dose from release of radionuclides to mean well in Aberg.

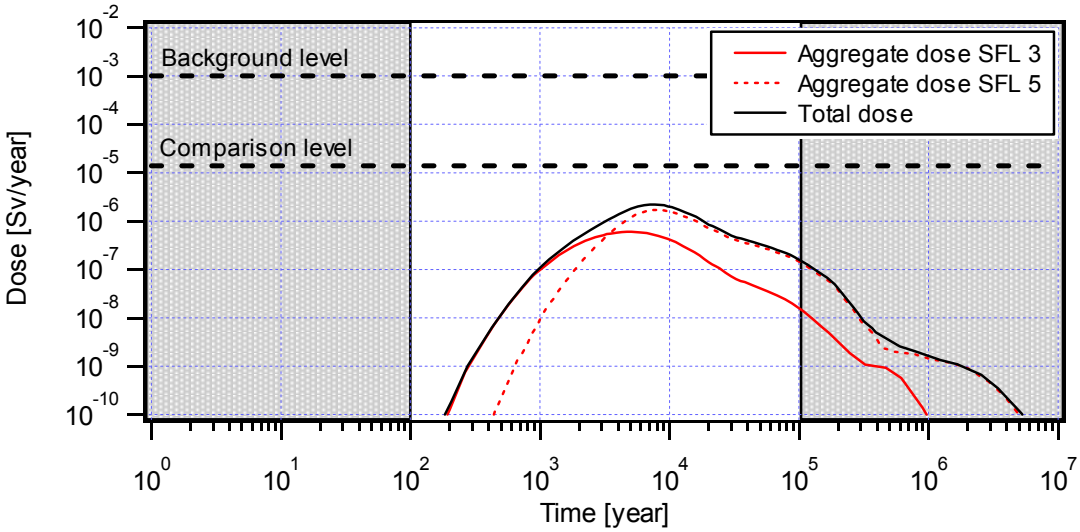

Figure 10-9 Total dose from release of radionuclides to mean well in Beberg (saline water).

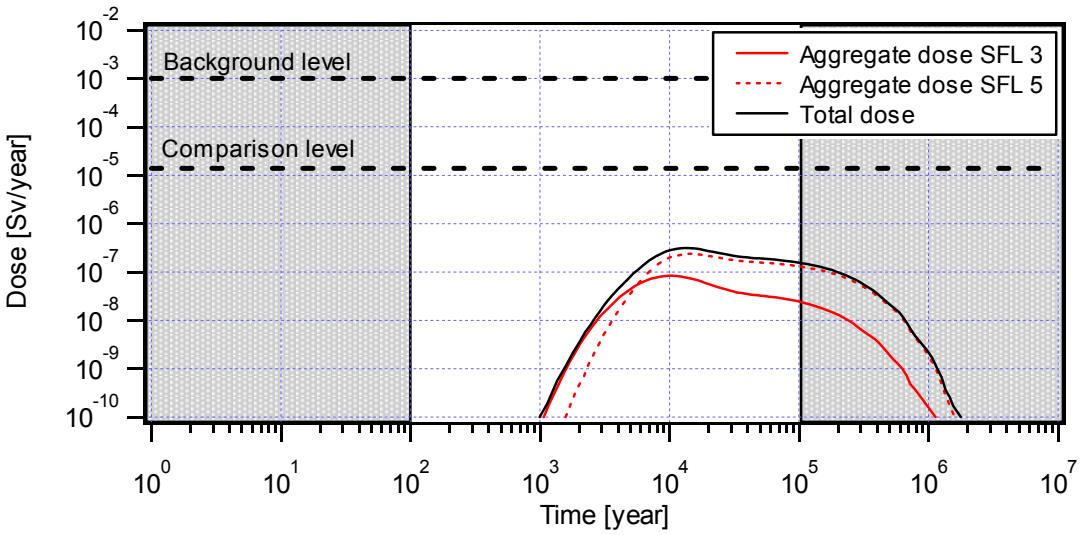

Figure 10-10 Total dose from release of radionuclides to mean well in Ceberg.

10.3 Release of toxic metals to well

The consequence of release of the toxic metals beryllium, cadmium and lead to a well has also been investigated. The model used for calculating the concentration of metals in a well is described in Chapter 4. The site-specific mean wells used as recipients are the same as those used in the calculations of the radionuclide release, see previous section. The estimated concentrations are compared with guideline values for drinking water (Skagius *et al.,* 1999).

The estimated amounts of toxic metals in SFL 3-5 are compiled in Table 2-2. The results for release of toxic metals to well are summarised in Table 10-5. The results given are the concentration after 100 years, 1,000 years and 10,000 years. It is concluded that the concentration of beryllium, cadmium and lead is well below the guideline values. The release of cadmium from SFL 3 in Aberg results in a maximum concentration in the mean well equal to the guideline value for drinking water after about 60,000 years from repository closure. The maximum concentration of the other metals as well as that resulting from the release of cadmium in Beberg and Ceberg is at least one order of magnitude below the guideline value.

The results given for Beberg are based on saline groundwater conditions. However, all modelled metals have a higher sorption coefficient in gravel in the near field as well as in the geosphere. Thus, the concentration will be even lower for non-saline conditions.

Table 10-5 Concentration of toxic metals for release to mean well in Aberg, Beberg and Ceberg [mg/l].

Time [years]	SFL 3		SFL 5	
	Pb	Cd	Pb	Be
Aberg				
100	$< 10^{-12}$	$< 10^{-11}$	$< 10^{-13}$	$< 10^{-12}$
1 000	10^{-11}	10^{-9}	10^{-13}	10^{-11}
10 000	$5 \cdot 10^{-6}$	$1 \cdot 10^{-4}$	$1 \cdot 10^{-6}$	$1 \cdot 10^{-5}$
Beberg [a)]				
100 – 10 000	$< \cdot 10^{-13}$	$< \cdot 10^{-13}$	$< 10^{-13}$	$< \cdot 10^{-14}$
Ceberg				
100 – 10 000	$< 10^{-14}$	$< 10^{-15}$	$< 10^{-14}$	$< 10^{-16}$
Guideline value	0,01	0,001	0,01	0,004

a) Assuming saline groundwater.

11 Influence of the near-field barrier on the release of radionuclides in SFL3 and SFL 5

11.1 Introduction

In a previous chapter, it was shown that the doses are dominated by long-lived radionuclides with only minor sorption in the near-field barriers. This chapter is focused on the function of the different near-field barriers on the maximum release rate of these nuclides. The chapter includes the following parts:

- Factors that control the radionuclide release
- Impact of the water flow rate in the backfill around the concrete structure.
- Impact of the diffusion resistance in the structure walls.

11.2 Factors that control the radionuclide release

As shown in Chapter 7, the release rate of radionuclides from SFL 4 is in general, for the investigated flow rate interval, roughly proportional to the water flow rate through the repository. This is explained by the fact that for SFL 4 it is assumed that the specific flow rate through the waste equals that through the backfill material. The diffusion of radionuclides is therefore of minor importance and the release rate is governed by the water flow rate through the repository.

For a repository like SFL 3 and SFL 5 the situation is much more complex. The concrete moulds containing the waste and the concrete structure with the waste packages are both assumed to act as a barrier for radionuclide transport. The radionuclides diffuse through the concrete structure to the backfill material surrounding it. There, they are transported along the tunnel by water flowing in the backfill material. Radionuclides can also be transported by advection along the tunnel with water flowing through the concrete structure. To be able to control the rate of radionuclide release in systems where the radionuclides migrate through different paths, it is important to determine which paths are controlling the release rate of radionuclides.

For a backfill material with a high permeability in comparison to that of the concrete structure, the water flow through the structure is several orders of magnitude smaller than that in the backfill material. Therefore the release rate of radionuclides transported by the water flowing in the structure is very small. Conversely, if the permeability of the backfill material and the structure are of the same order of magnitude, both paths contribute to the radionuclide transport. The conductivity of the concrete structure and of the backfill material in SFL 3 and SFL 5 is assumed to be 10^{-8} and 10^{-4} m/s, respectively (Skagius *et al.,* 1999). Consequently, the water flow rate in the concrete structure is negligible in comparison to that in the backfill material.

Since the major part of the water flowing through SFL 3 and SFL 5 flows in the backfill material, radionuclides have to diffuse through the concrete barriers before being transported by water flowing along the tunnel. They diffuse through the walls of the waste moulds, through the porous concrete surrounding them, and finally through the

walls of the concrete structure to the backfill material. The release rate of radionuclides can therefore be governed either by diffusion through the concrete structure or by the water flow rate in the backfill material.

In order to study the factors controlling the release rate of ^{36}Cl and ^{93}Mo in SFL 3 and SFL 5 in more detail, a simple model is set up. It is assumed that the radionuclides contained in the waste have migrated into the porous concrete and the concrete walls of the structure. After a while a steady state situation is reached, where the radionuclides diffuse through the concrete wall and are transported out by the water flowing around the structure. Since the release rate is small compared with the total inventory, it is also assumed that the concentration in the structure is constant with time.

The whole interior of the concrete structure with its waste and porous concrete is modelled as a single well-stirred tank where radionuclides diffuse through the outer concrete walls into the water flowing in the backfill material. The water flow inside the structure is neglected. The effective diffusivity in the concrete walls equals $3 \cdot 10^{-11}$ m^2/s. A schematic picture is shown in Figure 11-1. The calculations are done for a tank concentration of one unit of mass per cubic metre. The maximum release rate at the end of the tunnel is shown in Figure 11-2 as a function of water flow rates in the backfill material

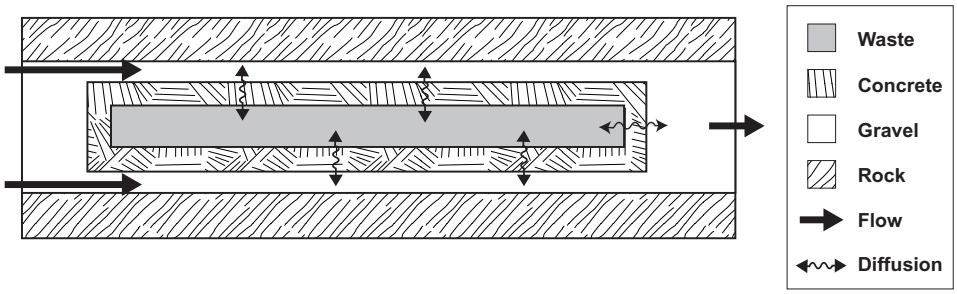

Figure 11-1 Schematic picture of the model used for studying the factors controlling the release of ^{36}Cl and ^{93}Mo.

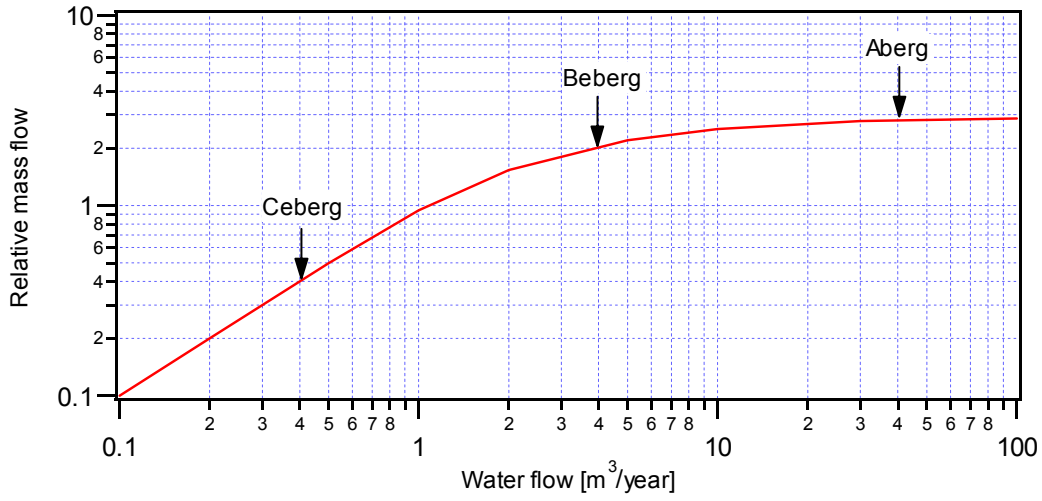

Figure 11-2 Radionuclide transported out by the water flowing in the backfill material as a function of water flow in the backfill material.

The water flow in the SFL 3 and SFL 5 tunnels is around 40, 4 and 0.4 m^3/year for Aberg, Beberg, and Ceberg, respectively (see Table 5-5). As shown in Figure 11-2, varying the flow rate in the interval 10 to 100 m^3/year has only a minor influence on the release rate for low-sorbing long-lived radionuclides. This means that for Aberg the release rate is controlled by the diffusion through the concrete walls of the structure. In this case, an increase of the diffusion resistance within the structure will reduce the release rate significantly. For a flow rate of 1 m^3/year or less the release rate for low-sorbing long-lived radionuclides is directly proportional to the water flow rate. Thus, the water flow rate in the backfill material controls the radionuclide release rate in Ceberg. The flow rate at Beberg corresponds to the region where the slope of the curve in Figure 11-2 gradually diminishes, and consequently the release rate is controlled by both mechanisms.

11.3 Impact of the backfill material on the release rate

In the previous section, it was shown that reducing the water flow rate around the structure could decrease the release rate of long-lived radionuclides. For Ceberg and to some extent also Beberg, even a small change in the water flow will affect the release rate. However, for Aberg the water flow in the tunnel must decrease at least a factor of 100 to diminish the radionuclide release rate significantly. A reduced water flow rate around the structure can be obtained by choosing a backfill material with a lower permeability than the backfill material used in the present design.

The water flow through the backfill and the concrete structure is calculated by Holmén (1997). He gives the specific flow through the concrete structure and the backfill material in SFL 3 and SFL 5 as multiples of the specific flow rate in the rock where the repository is located. It is assumed that the hydraulic conductivity of the structure is 10 times higher than that of the rock (see Table 11-1). The multiple for, and thus the flow rate of water through, the backfill material is almost the same whether the conductivity of the backfill material is 1,000 or 100,000 times larger than the conductivity of the rock. The water flow through the concrete structure, on the other hand, is 35 times higher for a backfill material with a conductivity 1,000 times that of the rock than for a backfill material with a conductivity 10 times that of the rock. However, changing the backfill material to a less permeable material reduces the flow rate through the backfill significantly, but at the same time the flow rate of water through the structure, increases.

Table 11-1 Multiples of the specific flow rate used in the calculations of the flow rate through the backfill and concrete structure. Taken from Holmén (1997).

Case	Conductivity		Multiple	
	backfill material	concrete structure	backfill material	concrete structure
1	100,000 K_{rock}	10 K_{rock}	31	0.01
2	1,000 K_{rock}	10 K_{rock}	30	0.4
3	10 K_{rock}	10 K_{rock}	4	4
4	K_{rock}	10 K_{rock}	0.6	4
5	0.1 K_{rock}	10 K_{rock}	0.1	3

In order to study the impact of the permeability of the backfill material on the release rate of chloride, some calculations are performed using the computer code COMP24. The repository model used in these calculations (see Figure 11-3) is similar to the model described in Chapter 4 in this report. The release rate through the backfill and the concrete structure is calculated at the cross-section located at the end of the concrete structure. These release rates were calculated at the time when the maximum release rate from the repository takes place.

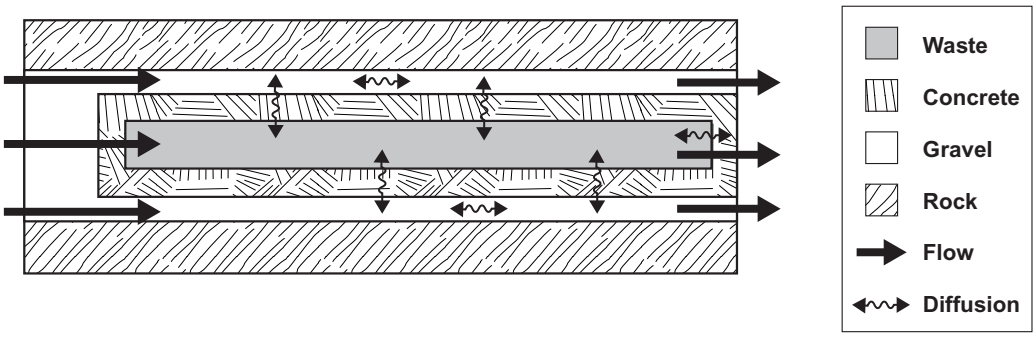

Figure 11-3 Schematic picture of the model used for studying the effect of backfill permeability on release rate of ^{36}Cl.

In these calculations, the hydraulic conductivity of the backfill material is varied from 0.1 times the hydraulic conductivity of the rock to a very large value (see Table 11-1). For the concrete structure a constant hydraulic conductivity of ten times that of the rock is used. The calculations are based on a specific groundwater flow of 10 l/m^2, year, which is equal to that of Aberg.

Figure 11-4 shows the relative maximum release rate of chloride from SFL 3 as a function of the hydraulic conductivity of the backfill material. When the backfill material has a large hydraulic conductivity, the water flowing in the backfill material transports most of the radionuclides released. When the hydraulic conductivity of the backfill material decreases, the fraction transported by water flowing through the concrete structure is increased. For a backfill material with a hydraulic conductivity of ten times that of the rock, the fraction transported by the flow through the structure is dominant.

It is interesting to note that when the hydraulic conductivity of the backfill material is decreased from a very large value to about ten times the hydraulic conductivity of the rock, the maximum release rate from the repository is increased by a factor of about two. Additional decrease of the hydraulic conductivity of the backfill material results in a slight decrease of the maximum release rate.

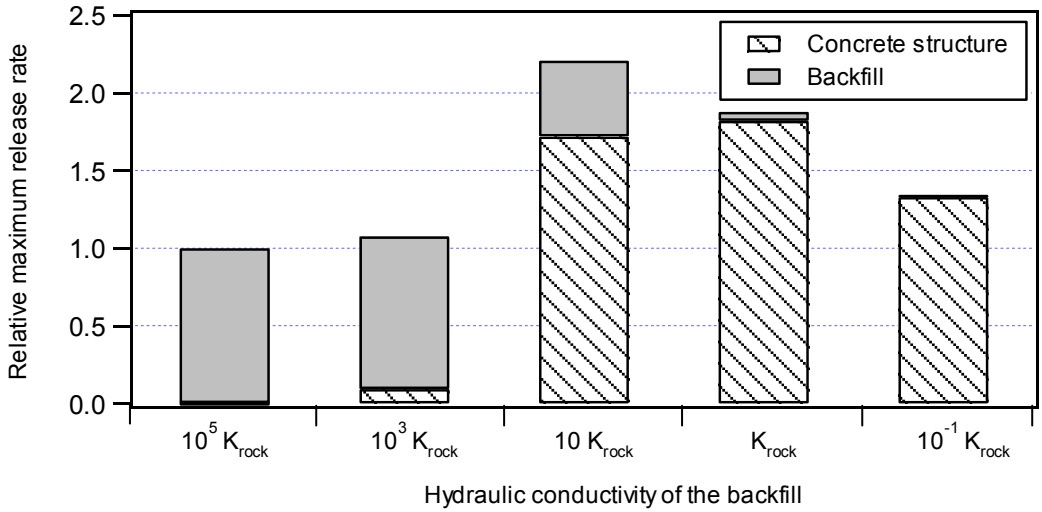

Figure 11-4 Relative maximum radionuclide release rate from the tunnel for different hydraulic conductivities of the backfill material. Hydraulic conductivity of the concrete structure is $10 \cdot K_{rock}$.

The relationship between the hydraulic conductivity of the concrete structure and the rock in SFL 3 and SFL 5 used in Holmén (1997) does not agree with the values found in Aberg, Beberg and Ceberg. The hydraulic conductivity of the concrete structure is expected to be in the order of 10^{-8} m/s. The hydraulic conductivities of the rock are estimated to be 10^{-7}, 10^{-8}, and 10^{-10} m/s for Aberg, Beberg and Ceberg, respectively. Therefore the values shown in Table 11-1 correspond to a situation between that found in Beberg and Ceberg.

As long as the hydraulic conductivity of the backfill material is much larger than that of the concrete structure, variations of the hydraulic conductivity of the structure relative that of the rock has a minor influence on the maximum release rate since the major part of the water flows in the backfill material. On the other hand, when an impervious backfill material such as bentonite is used an increase in the hydraulic conductivity of the concrete structure relative that of the rock leads to an increase in the maximum release rate. This is due to that the water flow rate through the concrete structure increases with a decreasing hydraulic conductivity of the backfill material (see Table 11-2), and the main part of the radionuclides are released through water flowing through the structure when the backfill material has a very low hydraulic conductivity.

Table 11-2 Multiples of the specific flow rate used in the calculations of the flow rate through the concrete structure. Data are given for three different conductivities of the concrete structure. Calculated from Holmén (1997).

Case	Backfill conductivity	Concrete-structure specific flow multiple		
		100 K_{rock}	10 K_{rock}	K_{rock}
1	100,000 K_{rock}	0.1	0.01	0.001
2	1,000 K_{rock}	8.1	0.35	0.09
3	10 K_{rock}	45	4	1
4	K_{rock}	38	4	1
5	0.1 K_{rock}	10	3	1

Calculations have been performed for a concrete structure with a hydraulic conductivity equal to that of the rock and a specific groundwater flow of 1 l/m^2, year. The results are shown in Figure 11-5. There is a marked difference between the results for a hydraulic conductivity of the structure of K_{rock} and those for $10 \cdot K_{rock}$ shown in Figure 11-4. With a conductivity contrast of 1, the release rate may be reduced by a factor 10 or more by changing from a permeable backfill such as gravel to a backfill material with a conductivity less than that of the rock.

If the specific groundwater flow rate is higher than that used for the results shown in Figure 11-5, the reduction in maximum release rate between a large and a small hydraulic conductivity of the backfill will be less pronounced. For a lower flow rate it will be larger.

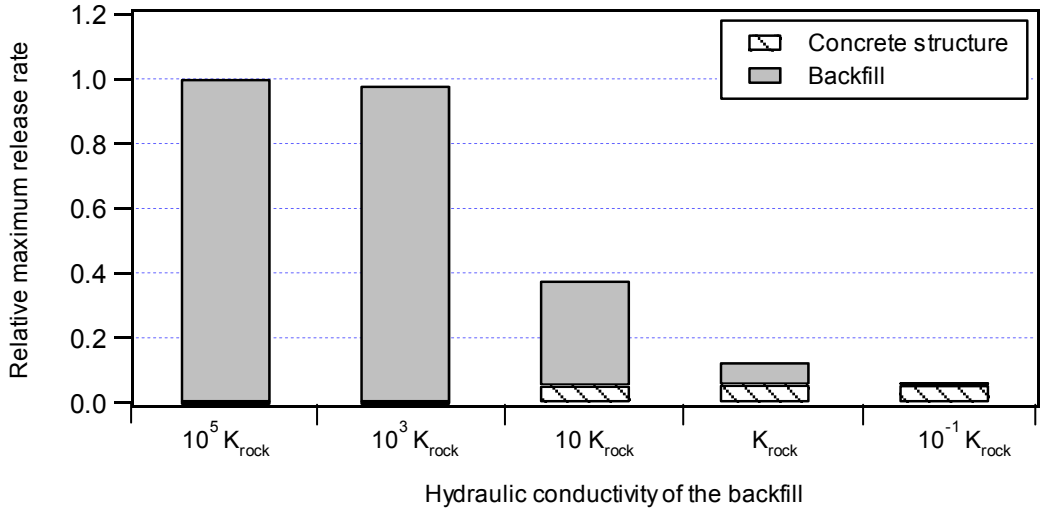

Figure 11-5 Relative maximum radionuclide release rate from the tunnel for different hydraulic conductivities of the backfill material. Hydraulic conductivity of the concrete structure is K_{rock}.

11.4 Impact of the diffusion resistance in the structure walls

Earlier in this chapter it was stated that the release rate in Aberg is controlled by the diffusion from the concrete structure into the water flowing in the backfill. Increasing the diffusion resistance through the structure wall will reduce the release rate of long-lived radionuclides with no or very little sorption in the concrete barriers.

The influence of increasing the wall thickness is investigated using the same model as that outlined in Section 11.2. The results are shown in Figure 11-6 for three different water flow rates in the backfill material; 1, 10 and 100 m^3/year. At high water flow rates (100 m^3/year) the release is totally controlled by diffusion and the release rate is inversely proportional to the wall thickness. At a flow rate of 10 m^3/year the release rate is approximately inversely proportional to the wall thickness providing the wall thickness is 0.4 m or larger. For a wall thickness below 0.4 m, the release rate is governed by both diffusion and the water flow rate. For a water flow of 1 m^3/year the influence of the wall thickness is less significant. Increasing the wall thickness from 0.1 m to 4 m reduces the release rate by a factor of about four.

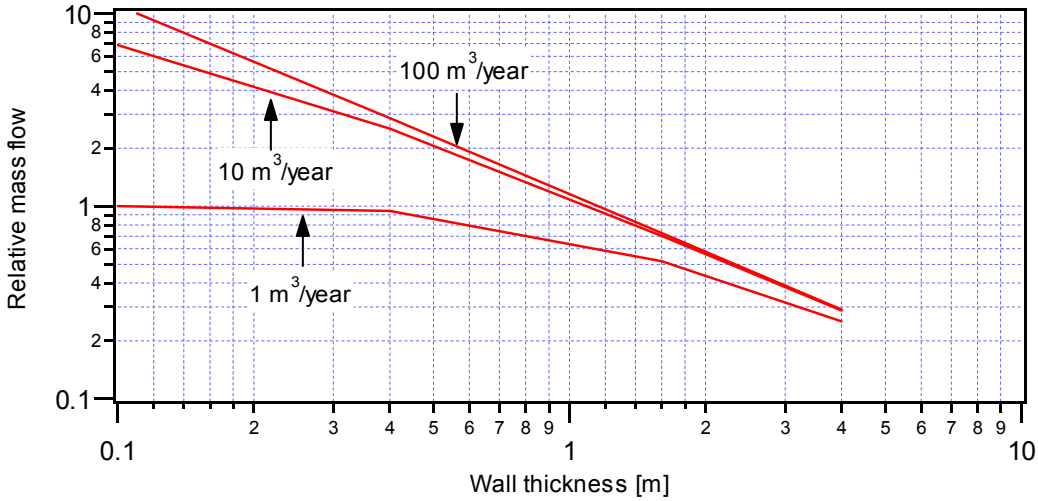

Figure 11-6 The radionuclide release rate as a function of the thickness of the wall for water flow rates in the backfill material of 1, 10 and 100 m^3/year.

12 Discussion and conclusions

12.1 Introduction

The potential migration and environmental impact of virtually all radionuclides in the waste, as well as of some toxic metals, have been analysed for a reference scenario. The reference scenario describes the expected evolution of the repository's near field when the surrounding far field is stable, i.e. no decisive changes occur in the thermal, hydrological, mechanical and chemical conditions in the rock surrounding the repository. Further, it is assumed that no changes occur in the biosphere, but that today's conditions prevail on the three sites in the future as well.

Besides the reference scenario, a well scenario is analysed for all three sites. In this scenario it is assumed that a well is sunk in the discharge area for water from the repository and that all radionuclides and toxic metals released from the repository are captured in the well.

In this last chapter, a conclusive summary of the migration calculations within the preliminary safety assessment of the SFL 3-5 repository is made. The chapter summarises the assumptions on which the calculations are based upon, the results are discussed, and possible modifications are briefly summarised.

12.2 Assumptions

12.2.1 Groundwater flow direction

In the calculations of radionuclide transport in SFL 3-5 it is assumed that the flow is horizontal and parallel to the SFL 3 and SFL 5 tunnels. That flow direction gives the highest flow through SFL 3 and SFL 5, but for SFL 4 the maximum flow is obtained for a flow at right angle to SFL 3 and SFL 5 (Skagius *et al.,* 1999).

A horizontal flow at right angle to SFL 3 and SFL 5 will increase the water flow rate through SFL 4 by 20 % in comparison to that obtained for a horizontal flow parallel to SFL 3 and SFL 5 (Skagius *et al.,* 1999). In SFL 4 the release rate is determined by the water flow rate, and thus the near-field release rate is also increased by 20 %.

The situation in SFL 3 and SFL 5 is more complex. As shown in Chapter 11, the near-field release rate of radionuclides from SFL 3 and SFL 5 is controlled by diffusion in Aberg, by the water flow rate in Ceberg, and by both mechanisms in Beberg. It can be concluded for Aberg that even though the water flow rate is reduced by a factor two (flow perpendicular to instead of parallel to SFL 3 and SFL 5) this has a negligible effect on the release rate. For Ceberg a flow at right angle to SFL 3 and SFL 5 would reduce the release rate by a factor two, and for Beberg the result is somewhere in between that for Aberg and that for Ceberg.

The results presented in Chapter 7 show that the near-field release rate from SFL 4 is negligible in comparison to that from SFL 3 and SFL 5 for time periods exceeding a few hundred years after repository closure. For the first few hundred years on the other

hand the release rate is dominated by that from SFL 4. Accordingly, assuming a water flow along the SFL 3 and SFL 5 tunnels is conservative for all times except the first few hundred years, and during that time the release rate would be at the maximum 20 % higher.

The results on far-field release rate and corresponding dose when released to recipient show that the contribution from SFL 4 to the total release rate and total dose (sum of that from SFL 3, SFL 4 and SFL 5) is negligible in Beberg and Ceberg. This is also the case for the conditions prevailing in Aberg except for the first hundred years. In general, the assumed groundwater flow direction can therefore be concluded to be conservative.

12.2.2 Water flow in tunnels

The water flow rates through the SFL 3-5 tunnels are based on results from the regional hydrology models (Svensson, 1997 and Hartley and Lindgren, 1997) and the near-field hydrology modelling (Holmén, 1997). The results presented by Holmén on the flow in the near field are based on contrasts in hydraulic conductivity between backfill material in SFL 3-5 and rock and between rock and concrete structure in SFL 3 and SFL 5 that are not in agreement with the contrasts expected to prevail at the three sites. This is discussed in Skagius *et al.* (1999). The water flow through the SFL 3 and SFL 5 tunnel in Aberg may be underestimated by up to 40 %, and that through SFL 4 overestimated by the same order of magnitude. For Ceberg the water flow through SFL 3 and SFL 5 is overestimated, while the flow in SFL 4 is unaffected. As shown in Chapter 11 this is of limited importance for the release rate from SFL 3 and SFL 5 in Aberg. For Ceberg the flow used in this work is conservative.

The total flow through the barriers used in the radionuclide migration model in this work (Table 5-5) deviate from those obtained in the near-field hydrology modelling (Holmén, 1997). This is due to differences in the cross-sectional areas assigned to the flow barriers in SFL 3-5 between the two models. The cross-sectional area used here and in Holmén (1997) is about 140 m^2 and 200 m^2, respectively. The total flow used in this work is obtained by using the specific flow rate from the near-field hydrology modelling and the cross-sectional area assigned to the flow barriers in the migration model.

It is foreseen that there are plugs in the loading zones of SFL 3 and SFL 5. In this analysis it is assumed that the plugs are intact. The effect of not including these plugs on the water flow through SFL 3-5 has been evaluated in Holmén (1997). It was found that the total flow in SFL 3 and SFL 5 will increase at most about six times in the encapsulation and about four times in the gravel backfill compared with the case where the plugs are intact. The total flow in SFL 4 will increase at most by a factor two. Consequently, the advective transport of radionuclides and toxic metals will increase if the plugs are not constructed. On the other hand, nuclides released from SFL 3 and SFL 5 will be transported a longer distance, through the loading zones into the SFL 4 tunnel before being released from the near field. Thus, the nuclides have to penetrate more sorbing material that at least for sorbing nuclides can counteract the increase in advective transport.

12.2.3 Near-field model

In the three models, it is conservatively assumed that the waste is deposited as close as possible to the area where the water leaves the tunnel. Consequently, the amount of material available for sorption is reduced. It is furthermore assumed that the radionuclides and toxic metals are homogeneously distributed within the waste volume in SFL 3, SFL 4 and SFL 5, respectively. This may not necessarily be conservative. A higher concentration close to the area where the water leaves the tunnel would give a higher release rate. Making a finer discretization of the waste is, however, believed not to be relevant considering the uncertainties prevailing regarding the waste to be deposited in SFL 3-5.

In general it is assumed that the nuclides are instantaneously dissolved in the pore water inside the waste packages. However, the activity of nuclides that almost exclusively are present in the form of induced activity in metal parts in the waste, are released as the metal parts corrode. Inorganic ^{14}C, ^{36}Cl, and ^{93}Mo in SFL 5 is predominantly present in steel parts and ^{93}Zr in Zircalloy. A corrosion rate of 1 μm/year and 0.01 μm/year is assumed for steel and Zircalloy, respectively.

The corrosion rate of steel will have a limited effect on the maximum far-field release rate (see Appendix D). If the whole inventory of the three nuclides in steel is assumed to be instantaneously dissolved in the pore water instead, the maximum release rate is increased by a factor less than two. The main effect of an instantaneous dissolution is a somewhat earlier release from the far field. Decreasing the corrosion rate to 0.1 μm/year has no important effect on the maximum release rate of ^{36}Cl, but would reduce the maximum release rate of ^{93}Mo and inorganic ^{14}C by a factor of about four.

Since the waste in SFL 5 contains a lot of metals, it will contain both radioactive and stable isotopes of the same element. The solubility of radioactive isotopes can therefore be further reduced. For radioactive nickel and zirconium an isotopic dilution factor of 100 and 1,000 respectively, is reasonable (Skagius *et al.,* 1999). If isotopic dilution had been taken into account, the maximum release rate of ^{59}Ni in SFL 5 would have decreased by two orders of magnitude. Modelling the release of ^{93}Zr as solubility-limited results in a higher maximum release rate than obtained in this work when ^{93}Zr is modelled as corrosion rate limited. This would have been the case even if isotopic dilution had been accounted for. ^{3}H in SFL 3 is contained in waste made of titanium hydride. The availability of ^{3}H for dissolution in water within the waste will therefore be limited in a similar way as induced activity in metals. Conservatively, this has not been accounted for and all ^{3}H in SFL 3 is assumed to be instantaneously dissolved in wastewater.

Isosaccharinic acid (ISA) is an acid forming complexes with cations. The effect of ISA on sorption is neglected, but its effect on the solubility of some elements is not (Skagius *et al.,* 1999). Both effects depend on the concentration of ISA. The ISA concentration depends on the yield of ISA from degradation of cellulose and on the extent of sorption of ISA on cement. Especially the yield seems to be an uncertain parameter. In this analysis it is assumed that the yield is 0.1 mole ISA/kg cellulose. Degradation of sawdust results in a yield of 0.3 mole ISA/kg cellulose (Pavasars, 1999). Pavasars' result is supported by experimental results from degradation of paper (Bradbury and van

Loon, 1998). The yield of ISA from degradation of cellulose powder is 1 mole ISA/kg cellulose after three years (Pavasars, 1999).

The nuclides that dominate the dose in recipients are mainly ^{36}Cl and ^{93}Mo, but for some recipients some of the nuclides ^{3}H, inorganic ^{14}C, ^{59}Ni, ^{90}Sr, ^{210}Pb and ^{226}Ra also make substantial contributions to the dose at different times. ^{14}C in the form of carbonate, ^{36}Cl and probably also ^{93}Mo exist as anions, why they are unaffected by ISA. ^{3}H is a non-sorbing nuclide even without the presence of ISA. ^{59}Ni, ^{90}Sr, ^{210}Pb and ^{226}Ra are all present as divalent cations. The sorption of divalent elements on cement is unaffected by ISA for ISA concentrations up to 10^{-2} M (Skagius *et al.,* 1999). In order to obtain an ISA concentration of 10^{-2} M within the waste in SFL 3, the yield of ISA from degradation of cellulose have to exceed 1 mole/kg cellulose. Note that this is based on the assumption that all organic material in SFL 3 is cellulose.

The water flow through the repository may change in the long-term perspective. Cracking and clogging of pores in the barriers may alter the permeability of the barriers, and thereby altering the magnitude of the water flow in the different parts of the repository. Settlements in the gravel backfill in the tunnels may also occur. This is not expected to influence the magnitude of the water flow through the tunnels, but may have some influence on the distribution of the water flow in the tunnels.

In the models for SFL 3 and SFL 5 it is assumed that there is no flow of water through the waste. Instead all water flowing inside the encapsulation flows in the porous concrete surrounding the waste. The hydraulic conductivity used for structural concrete in this work (10^{-8} m/s, Skagius *et al.,* 1999) is expected to be about one to two orders of magnitude lower than for porous concrete. However, the total water flow through the encapsulation is very small (see Chapter 5) why the assumption made is insignificant for the nuclides release rate.

The specific flow of water (m^3/m^2, year) through the waste in SFL 4 is assumed to be the same as that through the gravel used as tunnel backfill. The waste packages in SFL 4 are made of steel. A reasonable assumption is thus that the packages have corroded and is not a barrier to the water flow. However, the packages are assumed to be backfilled with concrete, which should be less permeable than the gravel backfill. A less conservative, but probably more realistic, assumption would be to let the major part of the water flow in the gravel backfill.

12.2.4 Far-field model

The far-field migration is modelled using FARF31 (Norman and Kjellbert, 1990). This is a one-dimensional model for the transport along a single path in the rock, taking advection and dispersion along the flow path into account as well as chain decay, matrix diffusion and sorption. Conceptual model uncertainties involve the abstracting of three-dimensional flow information into one-dimensional flow tubes. This is discussed in Andersson (1999).

12.2.5 Biosphere model

A model has been developed (Bergström *et al.,* 1999) for estimating the migration of radionuclides in the biosphere and the resulting dose to man within the safety analysis of the deep repository for spent fuel, SR 97. Using this model, ecosystem-specific dose conversion factors have been estimated (Nordlinder *et al.,* 1999). The analysis of the SFL 3-5 repository and SR 97 are made for the same locations. It is therefore reasonable to use the data given by Nordlinder and co-workers in this work as well.

The capacity of the mean well defined for Beberg is 1,000 l/h, which is twice as much as for the mean well in Ceberg, and more than three times as much as for the mean well in Aberg. The capacity of the mean well in Beberg is to a large extent affected by a well with a capacity of 3,000 l/h that has been sunk today. This well is situated on the outer edge of the area analysed in estimating ecosystem-specific dose conversion factors, EDF's (Nordlinder *et al.,* 1999). It is also the well that is located furthest away from the estimated discharge area. If it is assumed that this well is not representative for the area and therefore disregard it, the capacity of the mean well is reduced to about 600 l/h. The estimated doses obtained for release to the mean well in Beberg would then be increased by about 70 % in comparison to the results given in this report.

12.2.6 Input data

In the present safety assessment of the deep repository for spent fuel, the uncertainty in the information underlying the analysis is handled by suggesting "best estimate" input values and "pessimistic estimate" input values. Since the present analysis of SFL 3-5 is a preliminary assessment, no attempts have been made to make a systematic analysis of the effect of uncertainties in the input data on the calculated release rates and dose to man. However, the uncertainty in input data is briefly discussed in Skagius *et al.* (1999).

12.3 Results

12.3.1 Near field

In general, the radionuclides that dominate the activity in the waste are not important in terms of dose to man. The reason for this is that many of these nuclides are relatively short-lived and/or are sorbed in the engineered barriers and surrounding rock. They will therefore decay in the near field and the far field.

The cumulative release as a function of the initial inventory can be used as a measure of how effective the near-field barriers are in retaining the nuclides. This is illustrated in Figure 12-1 for dose dominating radionuclides in SFL 3. ^{3}H and ^{90}Sr are both short-lived nuclides, but the sorption of ^{90}Sr is somewhat stronger (Table 12-1). Inorganic ^{14}C, ^{36}Cl, ^{59}Ni and ^{93}Mo are all long-lived but ^{59}Ni and to some extent also inorganic ^{14}C has a stronger sorption in the barriers.

The engineered barriers in SFL 3 and SFL 5 may play an important role to prevent the nuclides to reach the biosphere. This is especially evident for short-lived nuclides, e.g. ^{3}H and ^{90}Sr, which decay to a large extent in the near field. Approximately 0.1 % of the initial inventory of ^{3}H is released from the near field in Aberg. In Beberg and Ceberg the

water flow rate is one and two orders of magnitude lower, respectively. This leads to a release rate from the near field in Beberg and Ceberg that is almost three and six orders of magnitude lower, respectively than from the near field in Aberg (Figure 12-1). For ^{90}Sr the difference between Aberg and Ceberg is even more pronounced. However, this is also an effect of different compositions of the groundwater (saline and non-saline).

The near field is an important barrier also for some more long-lived radionuclides, e.g. inorganic ^{14}C, ^{59}Ni, and ^{93}Mo. For ^{59}Ni, which is a long-lived nuclide with a relatively good capability to sorb in the near field, about 90 % of the initial inventory decays in the near field in Aberg, but almost 99.99 % in the near field in Ceberg. Inorganic ^{14}C has a lower K_d value than ^{59}Ni in the backfill. This is counteracted by a shorter half-life and a stronger sorption in the concrete barriers. Consequently, a smaller fraction of the initial inventory of inorganic ^{14}C is released from the near field. In Aberg and Beberg there is a marked difference in how large a fraction of ^{14}C and ^{59}Ni that is released from the near field. This is reasonable, since outward transport in Aberg and Beberg is controlled by diffusion out of the concrete structure, and ^{14}C has a higher K_d than ^{59}Ni in concrete. In Ceberg, where transport is controlled by the water flow through the backfill, the difference between ^{14}C and ^{59}Ni is not as great.

The effect of a stronger sorption of inorganic ^{14}C and ^{59}Ni than that of ^{93}Mo and ^{36}Cl is clearly seen in the cumulative release of these nuclides. The fraction released of ^{93}Mo is between two and three orders of magnitude larger than for inorganic ^{14}C. The difference between ^{59}Ni and ^{36}Cl varies from one order of magnitude in Aberg to four orders of magnitude in Ceberg.

Long-lived nuclides with no or little sorption in the near field (e.g. organic ^{14}C, ^{36}Cl and ^{79}Se) as well as very long-lived, sorbing nuclides (e.g. ^{232}Th and ^{238}U), are only affected insignificantly by the near-field barriers. The difference between Aberg and Ceberg is only about a factor of two or less. For ^{93}Mo, which has an identical K_d value as ^{36}Cl but a significantly shorter half-life, the cumulative release from Ceberg is 1/10 of that from Aberg.

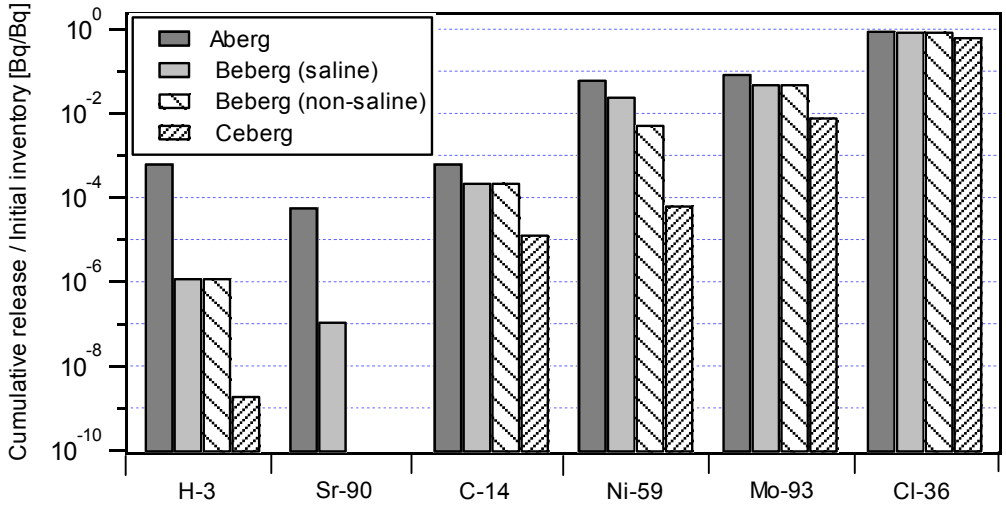

Figure 12-1 Influence of near-field barriers on cumulative release of dose-dominant radionuclides for SFL 3.

Table 12-1 Half-life and sorption coefficients for dose-dominating radionuclides.

Nuclide	Half-life [years]	Sorption coefficient, K_d [m^3/kg]		
		concrete	backfill and geosphere	
			saline	non-saline
^{3}H	12	0	0	0
^{90}Sr	29	0.001	0.0002	0.01
^{14}C	$5.7 \cdot 10^{3}$	0.2	0.001	0.001
^{59}Ni	$7.6 \cdot 10^{4}$	0.04	0.02	0.1
^{93}Mo	$4.0 \cdot 10^{3}$	0.006	0	0
^{36}Cl	$3.0 \cdot 10^{5}$	0.006	0	0

The groundwater composition (saline or non-saline) also affects the near field as a barrier to radionuclide migration. The results obtained for Beberg in this study demonstrate the importance of groundwater composition for the release of radionuclides. In this study, it is assumed that the K_d for the backfill material is the only parameter affecting the near-field radionuclide transport that depends on the groundwater composition. The groundwater composition has a significant influence on the release of ^{90}Sr from the near field of SFL 3 and SFL 5 in Beberg. The maximum release rate is almost eight orders of magnitude lower in non-saline than in saline water. For ^{59}Ni, ^{210}Pb and ^{226}Ra the maximum release rate is a factor five lower in non-saline water, and for ^{10}Be and ^{137}Cs the difference is less than a factor two.

The results show that release of radionuclides from SFL 4 will lead to a very low dose to man. These results are based on the assumption that the waste allocated to SFL 4 is decontaminated before deposition. If this is not accomplished, the inventory is two to three orders of magnitude higher for some nuclides (inorganic ^{14}C, ^{59}Ni, ^{63}Ni, ^{90}Sr, ^{93}Mo and ^{99}Tc). The transport of radionuclides in SFL 4 is governed by water flowing through the repository. The release rate is therefore roughly proportional to the inventory. Consequently, it can be concluded that even though the waste is not decontaminated, the dose obtained from the release of nuclides to the recipients in question will, with one exception, be well below the comparison level. When the surface contamination is neglected, the release to a mean well in Aberg results in a maximum aggregate dose of 3 μSv/year given by ^{90}Sr after about 30 years after repository closure (see Section 10.2). An increase in the initial inventory of three orders of magnitude (not decontaminating the waste) will lead to an aggregate dose exceeding the comparison level of 14 μSv/year.

12.3.2 Far field

The capacity of the far field to act as a barrier for the release of radionuclides to the biosphere is controlled by the water's travel time in the geosphere and by the sorbing potential of the nuclides. The latter is determined primarily by the nuclide's sorption capacity (K_d) and the rock's flow-wetted surface area. The effectiveness of the far-field barrier is demonstrated in the same way as for the near-field barrier (see Figure 12-2).

The far field in Aberg is a very limited barrier to almost all nuclides, since the water travel time is very short (10 years). The release from the far field is therefore more or less identical to the release from the near field. The cumulative release of radionuclides

from SFL 3 and SFL 5 from the far field is at most a factor of 3 lower than that from the near field. An exception from this generalisation is ^{60}Co in SFL 4. In spite of the near field in SFL 4 is a limited barrier, only a small fraction of the initial inventory of ^{60}Co is released from the near field since the half-life of ^{60}Co is five years. The far field in Aberg is, however, sufficient for the activity of ^{60}Co to decrease to an insignificant level before reaching the biosphere.

The far field in Beberg is of importance for the release of short-lived nuclides. ^{90}Sr decays almost completely, and the cumulative release of ^{3}H is reduced by three orders of magnitude in comparison to that from the near field. For inorganic ^{14}C and ^{59}Ni (long-lived sorbing nuclides) the reduction is about two orders of magnitude when the groundwater is saline. The effect on ^{93}Mo and ^{36}Cl (long-lived, non-sorbing nuclides) is limited.

The far field release of inorganic ^{14}C, ^{36}Cl and ^{129}I is delayed in saline water in comparison to that in non-saline water. This is because the diffusion into the rock matrix and hence the retention in the far field is smaller in non-saline water than in saline water due to anion exclusion. For inorganic ^{14}C this means that a larger fraction of the initial inventory in SFL 3-5 decays before being released to the biosphere and that the maximum release rate is reduced under saline conditions. The far-field release of ^{36}Cl and ^{129}I in SFL 3 and SFL 5 is also delayed, but the nuclides are so long-lived that the fraction released and the maximum release rate are independent of groundwater composition in Beberg.

For ^{59}Ni on the other hand, non-saline water has a positive effect on the far-field transport since the sorption of nickel on the rock is higher in non-saline water.

The effect of the far field in Ceberg on the transport of ^{36}Cl is insignificant as well. The effect on ^{93}Mo is also limited. The maximum far-field release rate of ^{36}Cl and ^{93}Mo is six times and 40 times lower than in Aberg, respectively. Inorganic ^{14}C decays to a large extent and ^{59}Ni almost completely.

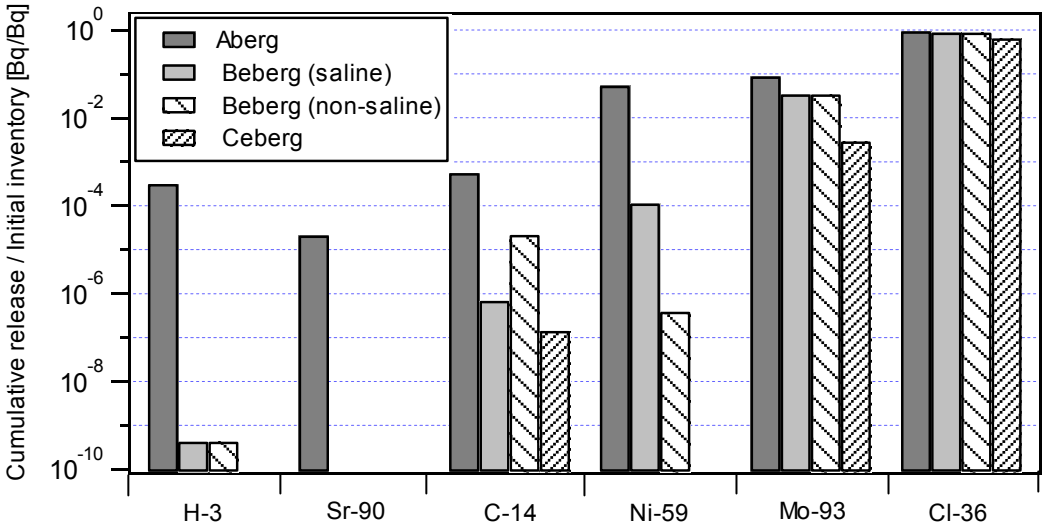

Figure 12-2 Influence of far-field barriers on cumulative release of dose-dominant radionuclides for SFL 3.

12.3.3 Biosphere

Even though the far-field rock has been shown to be an important barrier, the ecosystem to which the nuclides are released may be the most important factor. The highest release rates are obtained in Aberg. The nuclides are, however, released to a bay or the open coast. These are areas where the dilution is extensive, and the dose obtained is therefore very low. The results of the regional hydrology model (Svensson, 1997) indicate that the nuclides released are distributed to both a bay and the open coast in Aberg, but in this work it is conservatively assumed that all nuclides are released either to the bay or to the open coast. If the nuclides were released to an area classified as agricultural land or peatland in Aberg instead, considerably higher doses would be obtained.

There are also differences between agricultural land and peatland. This is most clearly seen in Beberg, where agricultural land is the primary recipient and peatland is situated immediately adjacent to the discharge area. For the same releases to the recipients, peatland gives higher maximum dose rates from the radionuclides that dominate the dose (Figure 12-3). Note that for release to agricultural land in Beberg ^{93}Mo results in the highest dose, but ^{36}Cl is the dose-dominant nuclide for release to peatland in Beberg.

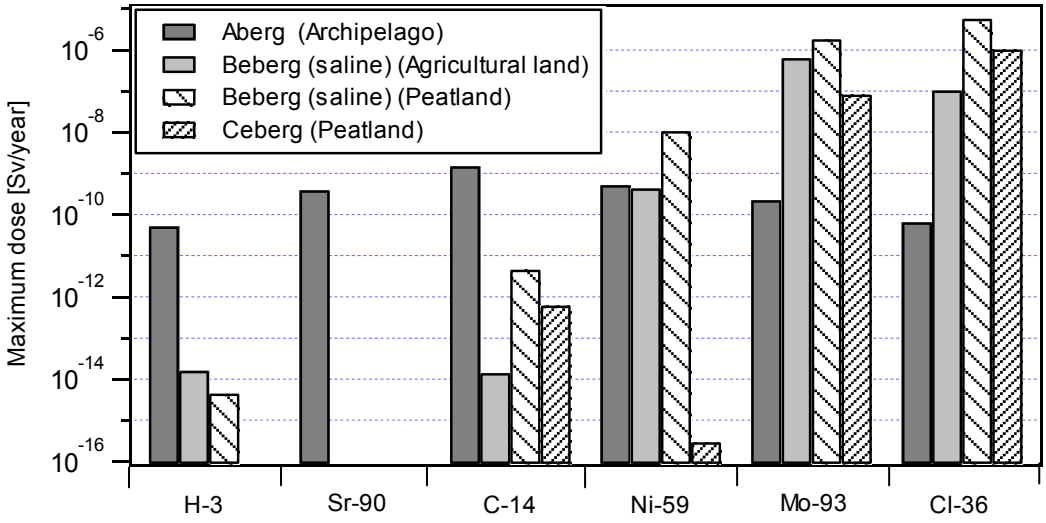

Figure 12-3 Comparison of maximum dose obtained for dose-dominant radionuclides for SFL 3.

^{93}Mo and ^{93}Zr both decay to ^{93m}Nb but this has not been accounted for in this study. Since ^{93}Mo is one of the most important nuclides in terms of dose in recipient, this should be commented. ^{93}Zr and ^{93m}Nb have identical sorption coefficients, and the far field release rate is thus the same for both nuclides. ^{93m}Nb has higher sorption coefficients in both near field and far field than ^{93}Mo. Radioactive decay of ^{93}Mo therefore gives a far-field release rate of ^{93m}Nb that is between 200 and 300 times lower than that from ^{93}Mo in Aberg and Ceberg, and almost 3000 times lower in Beberg.

The ecosystem-specific dose conversion factors (EDF) for release of ^{93m}Nb to peat in Beberg is $1.3 \cdot 10^{-15}$ Sv/Bq (Bergström, 1999). This together with the far-field release rate of ^{93m}Nb in Beberg due to decay of ^{93}Mo and ^{93}Zr, respectively, gives a dose of

^{93m}Nb that is six orders of magnitude lower than the dose from ^{93}Mo and two orders of magnitude lower than that from ^{93}Zr.

The EDF for release of ^{93m}Nb to a well with a dilution volume of 2,000 m^3/year is $5.0 \cdot 10^{-14}$ Sv/Bq (Bergström, 1999). Comparing with data presented in Bergström *et al.* (1999), this is 56 times and 4 times lower than the EDF for ^{93}Mo and ^{93}Zr, respectively. It can thus be concluded that the decay of ^{93}Mo will result in a dose from ^{93m}Nb release to a well that is significantly lower than that from ^{93}Mo. The corresponding dose from ^{93m}Nb arising from decay of ^{93}Zr will be of the same order of magnitude as the dose from ^{93}Zr.

The EDF for release of ^{93m}Nb to agricultural land is unknown. However, an indication of the dose from ^{93m}Nb in comparison to ^{93}Mo can be obtained from the following discussion. The EDF for release of ^{94}Nb to agricultural land in Beberg is lower than that for ^{93}Mo, $2.4 \cdot 10^{-13}$ Sv/Bq versus $8.7 \cdot 10^{-13}$ Sv/Bq (Nordlinder *et al.,* 1999). The dose conversion factors for intake via ingestion as well as via inhalation of radionuclides by an adult person are higher for ^{94}Nb than for ^{93m}Nb (IAEA, 1996). In addition, the half-life of ^{94}Nb is much longer than for ^{93m}Nb. This indicates that the EDF for ^{93m}Nb should be lower than for ^{94}Nb, and thus also lower than that for ^{93}Mo. Since the far-field release rate of ^{93m}Nb is orders of magnitude lower than the far-field release rate of ^{93}Mo this implies that the dose from ^{93m}Nb released to agricultural land also is orders of magnitude lower than the dose from ^{93}Mo.

In this work, the mean values of the estimated EDF's are used to convert the far-field release to a dose in biosphere. This should correspond to a "reasonable approach". If instead a "pessimistic approach" is made using the EDF's estimated as maximum values the dose would be at most a factor of about four higher for the release of dose dominating nuclides to archipelago, open coast and well. For release to soil and peat the increase in dose would in general be about a factor of ten for dose dominating nuclides.

12.4 Change in design

At high water flows, such as in Aberg, the barriers in SFL 3 and SFL 5 may need to be improved. The calculations show that the present design may give rise to excessively high releases of long-lived, low-sorbing radionuclides from the near field. Various possible improvements have been discussed. One possibility is to increase the thickness of the concrete structure and thereby increase the diffusion resistance. A significant increase is required if the release is to be appreciably reduced. Another way to limit diffusion is to reduce the area through which it takes place. The difficulty lies in finding diffusion-tight materials that are durable over the very long time spans in question. A third option is to backfill the void outside the structure in SFL 3 and SFL 5 with a backfill that is more impervious than a gravel fill, such as clay. The backfill must not be too impervious, however. Gas generated in the repository should preferably be able to escape without building up a pressure that expels water from the enclosure. If a backfill exists that meets these requirements and is durable over very long time spans, it could reduce the release of long-lived radionuclides in Aberg.

12.5 Conclusions

The principal conclusions of the completed study are:

- The radionuclides in the waste that are of importance for safety are those that are highly mobile and long-lived.

- The properties of the site are of importance for safety. Two factors stand out as being particularly important: the water flow at the depth in the rock where the repository is built, and the ecosystem in the areas on the ground surface where releases may take place in the future.

- An unfavourably high water flow in the rock around the repository can be compensated for by better barriers in the near field. However, they must perform satisfactorily over a very long period of time. This requires materials that are durable in the chemical and mechanical environment of the repository.

To reduce the uncertainties in the assessment of environmental impact, an attempt should first be made to reduce the uncertainties inherent in assumptions and calculations for the most important radionuclides, ^{36}Cl and ^{93}Mo. Better estimations of the activity in waste produced today are needed. A better understanding of the accessibility of the nuclides in the waste and an increased knowledge regarding migration in the barriers is also of interest. In addition, uncertainties in the ecosystem-specific dose conversion factors should be analysed.

References

Andersson J, 1999. SR 97 – Data and data uncertainties. Compilation of data and evaluation of data uncertainties for radionuclide transport calculations. SKB Technical Report TR-99-09, Swedish Nuclear Fuel and Waste Management Co., Stockholm.

Bergström U, 1999. Personal communication, Studsvik Eco & Safety AB, Nyköping.

Bergström U, Nordlinder S, Aggeryd I, 1999. Models for dose assessments. Modules for various biosphere types. SKB Technical Report TR-99-14, Swedish Nuclear Fuel and Waste Management Co., Stockholm.

Bradbury M H, Van Loon L R, 1998. Cementitious Near-Field Sorption Data Bases for Preformance Assessment of a L/ILW Repository in a Palris Marl Host Rock., PSI Bericht Nr. 98-01, Paul Scherrer Institute, Würenlingen and Villingen.

Carbol P, Engkvist I, 1997. Compilation of radionuclide sorption coefficients for performance assessment. SKB Report R 97-13, Swedish Nuclear Fuel and Waste Management Co., Stockholm.

Firestone R B, 1998. Table of Isotopes, 8th ed., 1998 Update, Ed. C M Baglin, John Wiley & Sons, Inc., New York.

Hartley L, Lindgren M, 1997. Flow and transport parameters for SFL 3-5 – Estimates from regional numerical models for Beberg and Ceberg. Appendix in Skagius *et al.* (1999).

Holmén J, 1997. On the flow of groundwater in closed tunnels. Generic hydrogeological modelling of nuclear waste repository SFL 3-5. SKB Technical Report TR 97-10, Swedish Nuclear Fuel and Waste Management Co., Stockholm.

IAEA, 1996. International Basic Safety Standards for Protection against Ionizing Radiation and for the Safety of Radiation Sources. Safety Series No. 115, International Atominc Energy Agency, Vienna.

ICRP, 1991. 1990, Recommendations of the International Commission on Radiological Protection. Annals of the ICRP, ICRP Publication 60, Pergamon Press, Oxford.

IPCS, 1990. Environmental Health Criteria 106; Beryllium. International Programme on Chemical Safety, World Health Organisation, Geneva.Lindgren M, Pers K, Skagius K, Wiborgh M, Brodén K, Carlsson J, Riggare P, Skogsberg M, 1998. Low and intermediate level waste in SFL 3-5: Reference inventory.
Reg. No: 19.41/DL31. Swedish Nuclear Fuel and Waste Management Co., Stockholm

Karlsson F, Lindgren M, Skagius K, Wiborgh M, Engkvist I, 1999. Evolution of the geochemical conditions in SFL 3-5. SKB Report R-99-15, Swedish Nuclear Fuel and Waste Management Co, Stockholm.

Lindgren M, Pers K, Skagius K, Wiborgh M, Brodén K, Carlsson J, Riggare P, Skogsberg M, 1998. Low and intermediate level waste in SFL 3-5: Reference inventory. Reg. No: 19.41/DL31. Swedish Nuclear Fuel and Waste Management Co., Stockholm

Morén L, Ritchey T, Stenström M, 1998. Scenarier baserade på mänskliga handlingar: Tre arbetsmöten om metod- och säkerhetsanalysfrågor. SKB Report R-98-54, Swedish Nuclear Fuel and Waste Management Co., Stockholm (in Swedish).

Naturvårdsverket, 1983. Miljöeffekter av ved- och torvförbränning. SNV PM 1708, Statens Naturvårdsverk, Solna. (in Swedish)

Naturvårdsverket, 1999a. Bedömningsgrunder för miljökvalitet - Sjöar och vattendrag, Rapport 4913, Naturvårdsverkets förlag, Stockholm. (in Swedish)

Naturvårdsverket, 1999b. Bedömningsgrunder för miljökvalitet- Odlingslandskapet, Rapport 4916, Naturvårdsverkets förlag, Stockholm. (in Swedish)

Nordlinder S, Bergström U, Mathiasson L., 1999. Ecosystem specific dose conversion factors for Aberg, Beberg and Ceberg. SKB Technical Report TR-99-15, Swedish Nuclear Fuel and Waste Management Co., Stockholm.

Norman S, Kjellbert N, 1990. FARF31 – A far-field radionuclide migration code for use with the PROPER package. SKB Technical Report TR 90-01, Swedish Nuclear Fuel and Waste Management Co., Stockholm.

Ohlsson Y, Neretnieks I, 1997. Diffusion data in granite. Recommended values. SKB Technical Report TR 97-20, Swedish Nuclear Fuel and Waste Management Co., Stockholm.

Pavasars I, 1999. Characterisation of organic substances in waste materials under alkaline conditions. Ph.D. Thesis, Linköping Studies in Arts and Science 196, Linköping University, Linköping.

Romero L, Moreno L, Neretnieks I, 1995. Fast multiple-path model to calculate radio-nuclide release from the near filed of a repository. Nucl. Technol., **112**(1), 89-98.

Skagius K, Pettersson M, Wiborgh M, Albinsson Y, Holgersson S, 1999. Compilation of data for the analysis of radionuclide migration from SFL 3-5. SKB Report R-99-13, Swedish Nuclear Fuel and Waste Management Co., Stockholm.

SKB, 1999a. SR 97 – Main Report, SKB Technical Report TR-99-06, Swedish Nuclear Fuel and Waste Management Co., Stockholm.

SKB, 1999b. Deep repository for long-lived low- and intermediate-level waste Preliminary safety assessment. SKB Technical Report TR-99-28, Swedish Nuclear Fuel and Waste Management Co., Stockholm.

SLV, 1993. Livsmedelsverkets kungörelse om dricksvatten. SLV FS 1993:35, Livsmedelsverket, Sweden (in Swedish)

SSI, 1998. Statens strålskyddsinsituts föreskrifter om skydd av människors hälsa och miljön vid slutligt omhändertagande av använt kärnbränsle och kärnavfall.
SSI FS 1998:1, Statens strålskyddsinstitut (in Swedish).

Svensson U, 1997. Flow and transport from SFL 3-5 – Estimates from regional numerical model. Appendix in Skagius *et al.* (1999).

US EPA, 1996. Drinking water regulations and health advisories.
EPA 822-B-96-002, US EPA Office of water, Washington DC

WHO, 1993. Guidelined for drinking water quality. Volume 1. Recommendations. Second edition, World Health Organisation, Geneva.

Wiborgh M (Ed.), 1995. Prestudy of final disposal of long-lived low and intermediate level waste. SKB Technical Report TR 95-03, Swedish Nuclear Fuel and Waste Management Co., Stockholm.

Appendix A: Near-field model for the radionuclide transport in SFL 3

Luis Moreno [a]

Michael Pettersson [b]

[a] Dept. Chem. Eng. and Technol., Royal Inst. of Technology

[b] Kemakta Konsult AB

1 Introduction

This appendix describes the model used for modelling the transport of radionuclides in the near field of SFL 3. Figure 1 shows an illustration of the concrete structure built inside the SFL 3 tunnel and of the deposited waste.

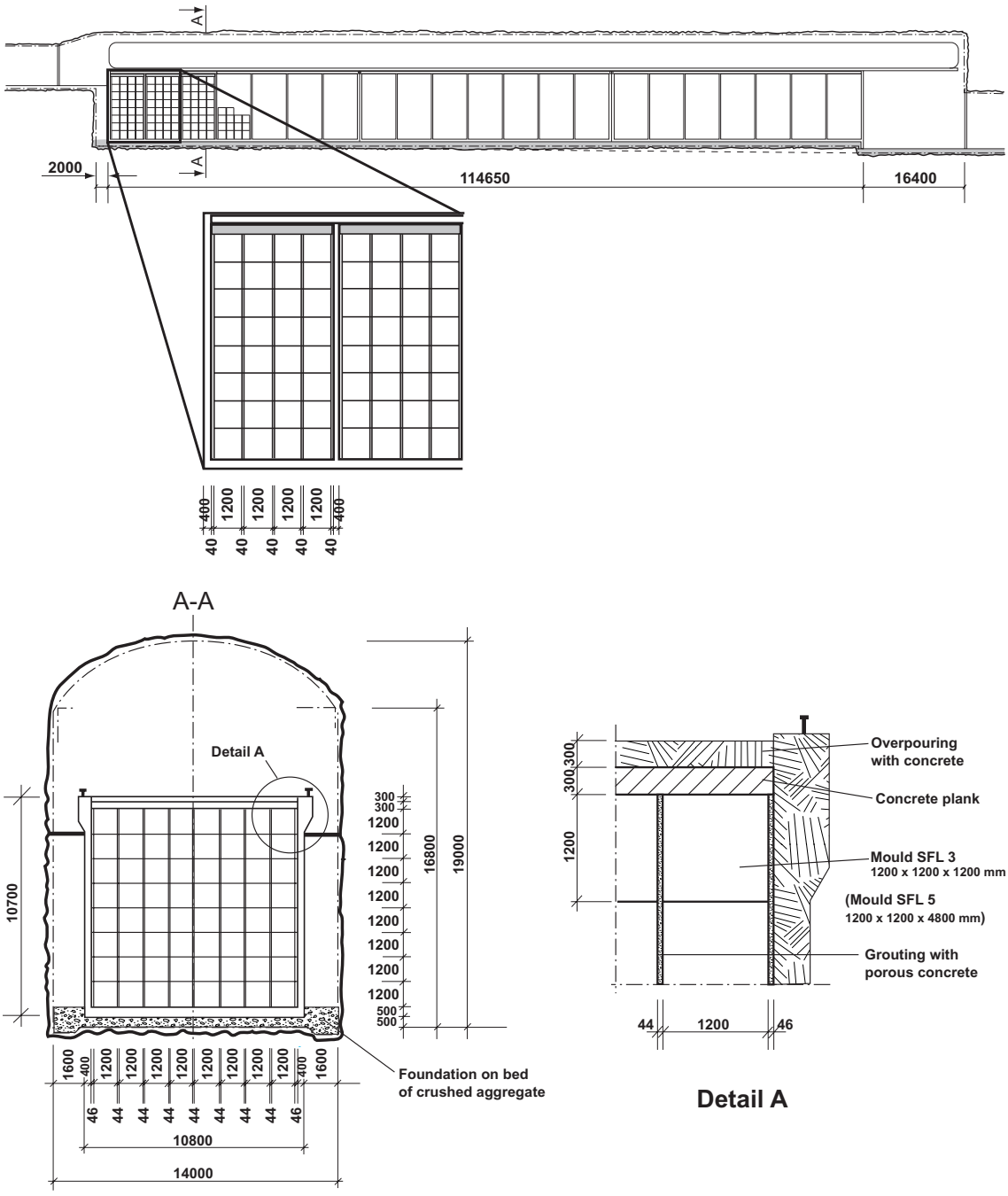

Figure 1 Illustration of the SFL 3 repository. Dimensions in mm.

2 Conceptual model for SFL 3

When the repository is sealed, water will intrude the tunnel, and the waste and backfill material will be saturated with water. Gas initially entrapped in the repository or produced, e.g. by corrosion, do not influence the water flow in the repository or the migration of radionuclides. At the initial time (year 2040), most of the nuclides will be dissolved completely in the pore water in the packages containing the waste or will be sorbed on concrete and cement in the packages. The nuclides in solution will be equilibrated with the backfill material in the waste moulds. Nuclides, which have a small solubility for the conditions existing in the repository, are only partially dissolved. The concentration of these nuclides will be limited to its solubility. For nuclides embedded in metallic waste, the concentration may be limited by the corrosion rate of the waste.

The groundwater flows in the horizontal direction along the SFL 3 tunnel. The major part of the water flows through the flow barrier (gravel backfill) surrounding the concrete structure where the waste is deposited. Water flux through the structure will be very low (Holmén, 1997). For this reason, most of the activity in the waste is released by diffusion through the concrete structure to the backfill material surrounding the concrete structure.

Nuclides can also be transported in the main direction of the tunnel within the structure. This transport is, however, of limited importance.

Radionuclides released from the concrete structure into the gravel backfill will be transported through diffusion as well as with water flowing in the backfill. Radionuclides may be sorbed on the backfill material, thus retarding the transport. The concrete plug constructed in the loading zone is considered to be intact, why the radionuclides are transported out from the tunnel into the water flowing in fractures intersecting the tunnel before they reach the plug.

3 Mathematical model for SFL 3

In modelling the transport of radionuclides, the repository has been simplified. The important simplifications are conservative in order not to overestimate importance of the barriers. The length of the modelled tunnel is 124.6 m, which corresponds to the length of the concrete structure plus 10 m of backfill material at the end of the tunnel. The loading zones with concrete plugs, shown in Figure 3-1 in main report, are not included in the model. Neither is the shotcrete that cover the tunnel walls.

The waste volume to be deposited in SFL 3 corresponds to approximately two thirds of the available storage volume, or a length of 76 m of the concrete structure. Conservatively it is assumed that the waste is stored in the part of the structure closest to where water leaves the tunnel. It is assumed that the remaining storage volume is filled with gravel, but that the spaces between concrete moulds and drums are filled with porous concrete.

The waste packages consist of cubic concrete moulds as well as steel drums. However, drums on plates are together with the major part of the porous concrete filled around the

drums also modelled as moulds with side lengths of 1.2 m and with concrete walls of 0.1 m in thickness. In the model, a large number of waste packages are grouped to a source term. Consequently, a source term includes waste, concrete in mould walls and in backfill material, but also most of the porous concrete filled around the drums. A source term is modelled as a stirred tank, i.e. it is assumed that the activity within a source term is homogeneous, and that it remains so also when part of the inventory is transported out.

The waste packages are surrounded by porous concrete, why there is no direct transfer of nuclides between different packages. Instead, the nuclides diffuse from a waste package to the surrounding porous concrete, continues by diffusion through the concrete structure to the backfill material surrounding the structure and to the gravel below the structure.

Along the tunnel there is an advective and a diffusive transport (see Figure 2). Sorption is accounted for in all parts of the modelled repository.

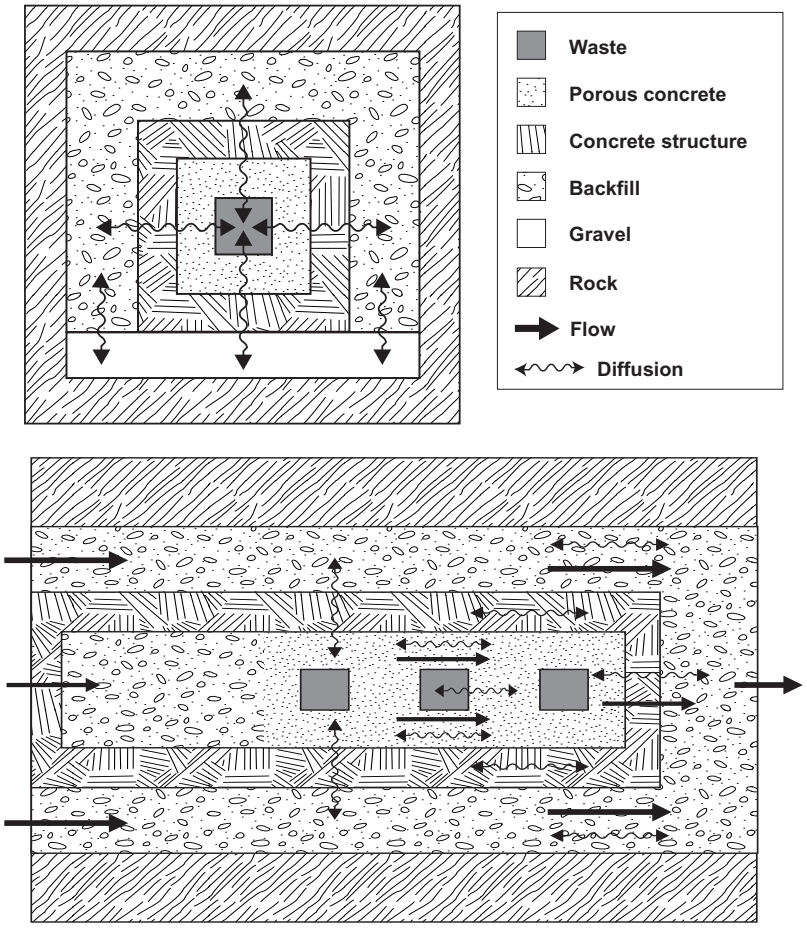

Figure 2 *Transport paths for radionuclides in SFL 3. 'Gravel' corresponds to the bed on which the structure in built and 'Backfill' to the gravel used as backfill in the tunnel. In the model, 'Gravel' and 'Backfill' has the same properties.*

The distance between the end of the concrete structure and the opening to SFL 4 is approximately 40 m, but only 10 m are included in the model. The reason is that a concrete plug is located somewhere in the 20 - 30 m long loading zone. This plug is considered to be intact why the radionuclides are transported out from the tunnel into the water flowing in fractures intersecting the end of the tunnel before the nuclides reach the plug.

Backward diffusion to the third of the tunnel and the concrete structure that initially is free of activity, is strongly reduced by assigning a very large resistance to diffusion to corresponding model blocks.

4 Discretization of the system

The volume of the waste is less than the available volume for disposal of waste in SFL 3. It is assumed that 14 rooms within the concrete structure are filled with waste, which corresponds to 76.4 m of tunnel. In order to fix the repository to the real volume of waste and keep the model flexible, the length of the concrete structure is divided into five sections:

- one large section of 38.2 m in length,
- one small section of 7.7 m in length,
- three medium sections, each of 22.9 m in length.

The modelled tunnel is also divided into twelve different groups representing different parts of the repository:

i) Waste (blocks 1-5)
ii) Concrete ceiling of the structure (blocks 6-10)
iii) Concrete walls of the structure (blocks 11-15)
iv) Concrete bottom of the structure (blocks 16-20)
v) Concrete walls between the rooms (blocks 21-25)
vi) Porous concrete around the waste moulds/drums (blocks 26-30)
vii) Volume above the structure filled with backfill material (blocks 31-35)
viii) Lateral volume on the two sides of the structure filled with backfill material (blocks 36-40)
ix) Gravel beneath the structure (blocks 41-45)
x) Last transverse concrete wall of the structure (block 46)
xi) Backfill material at the end of the tunnel (block 47)
xii) Fictitious block (block 48)

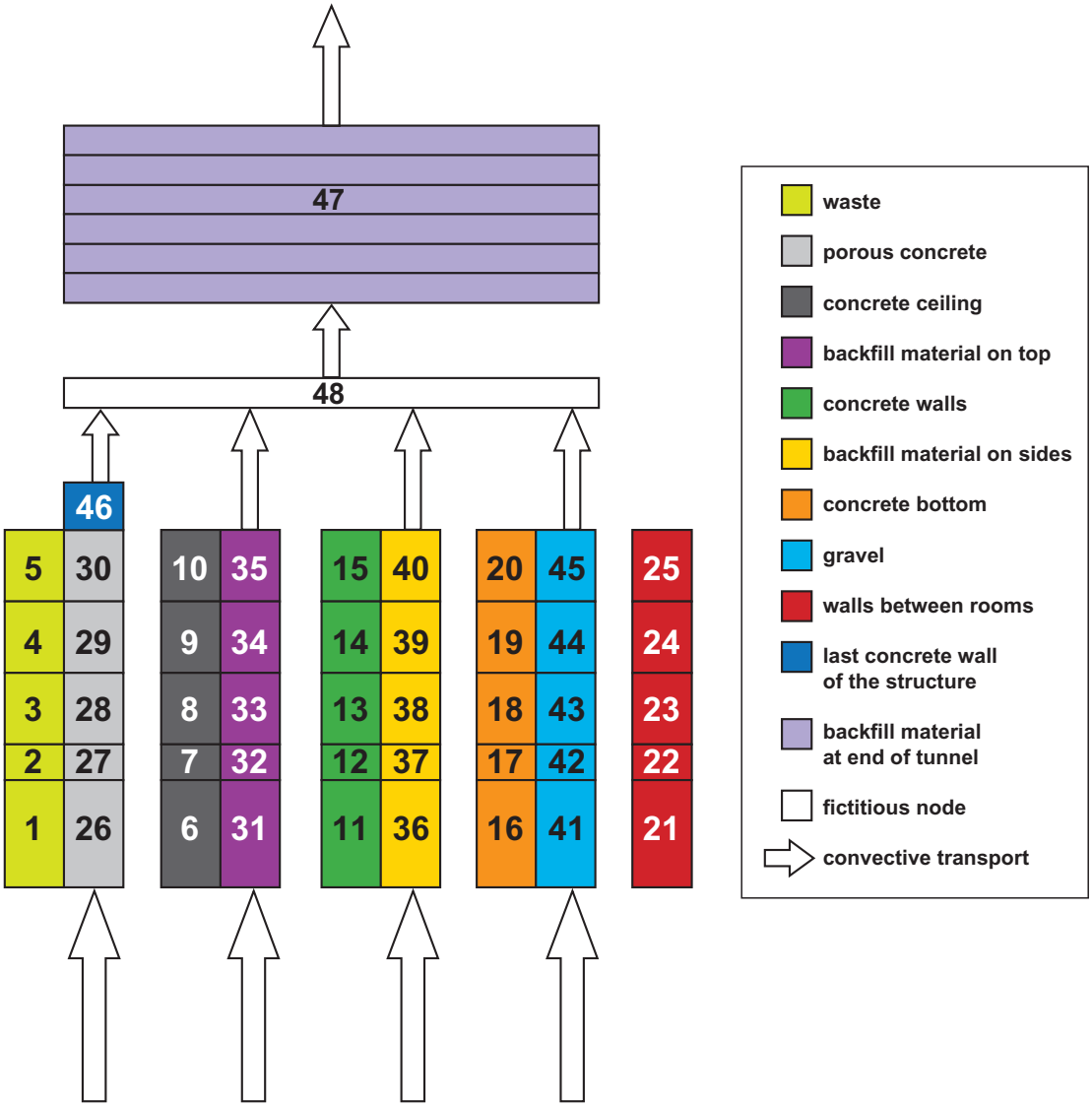

Figure 3 Detailed discretization of the SFL 3 tunnel.

The detailed discretization of the tunnel is shown in Figure 3. The arrows show where water is flowing through the system. Water flow takes place in the porous concrete surrounding the waste moulds, the backfill material around the concrete structure, gravel in bottom, the last transverse concrete wall of the structure, and the backfill material at end of the tunnel.

The block representing the backfill material at the end of the tunnel is subdivided into six compartments. COMP24 can not handle a subdivided block that simultaneously is a point where several water streams are mixed into one. A fictitious block is therefore included in the model. This block only serves to mix the fluid streams leaving the structure, the backfill material surrounding the structure and the gravel in bottom into one stream.

Block 46 corresponds to the last transverse wall in the concrete structure, and not a concrete plug in the tunnel leading to SFL 4.

The paths for mass transfer between different groups taken into account are between:

- Waste and porous concrete (diffusion)
- Porous concrete and concrete bottom of the structure (diffusion)
- Porous concrete and lateral concrete walls of the structure (diffusion)
- Porous concrete and concrete ceiling of the structure (diffusion)
- Concrete bottom of the structure and gravel beneath structure (diffusion)
- Concrete walls of the structure and backfill material on the sides of the structure (diffusion)
- Concrete ceiling of the structure and backfill material on top of the structure (diffusion)
- Backfill material on the sides of the structure and gravel beneath structure (diffusion)
- Backfill material on the sides of the structure and backfill material on top of the structure (diffusion)
- Porous concrete and the transverse concrete walls of the structure (diffusion)
- Porous concrete and last transverse concrete wall of the structure (diffusion and advection)
- Last transverse concrete wall of the structure and backfill material at the end of the tunnel (diffusion and advection)
- Backfill material on top of the structure and backfill material at the end of the tunnel (diffusion and advection)
- Backfill material on the sides of the structure and backfill material at the end of the tunnel (diffusion and advection)
- Gravel beneath structure and backfill material at the end of the tunnel (diffusion and advection)

The groups where mass transfer between blocks within the group is taken into account are:

- Porous concrete (diffusion and advection)
- Gravel beneath the structure (diffusion and advection)
- Backfill material above the structure (diffusion and advection)
- Backfill material on the two sides of the structure (diffusion and advection)
- Backfill material at the end of the tunnel (diffusion and advection)
- Concrete ceiling of the structure (diffusion)
- Concrete walls of the structure (diffusion)
- Concrete bottom of the structure (diffusion)

In the model, the initial activity is homogeneously distributed (Bq/m^3) in the three blocks of medium size (blocks 3-5) and the small block (block 2). The activity in the remaining large waste block (block 1) is set to zero, and it is given the same material properties as the backfill material (gravel).

It is assumed that a layer of porous concrete surrounds each waste mould, and that mass transfer between moulds always goes through the porous concrete. For this reason, a very large resistance to diffusion between adjacent waste blocks is added. In COMP24 this is obtained by setting the ratio of diffusion length and mass transfer area times effective diffusivity, $L/(A \cdot D_e)$, to a very large value (in this work 99999). For diffusion between waste and surrounding porous concrete, the diffusive resistance within the waste is neglected.

In order to estimate L/A for the block representing the porous concrete, the total volume of porous concrete within a room divided with the total surface area of the moulds in that room gives a mean thickness, L, of the porous concrete around the moulds. The surface area used in estimating L/A for the diffusive transport between waste and porous concrete is the total surface area of all moulds included in the waste block. This value of L/A is used for all connections in which the porous concrete takes part, except for the connection between two blocks both representing the porous concrete. This is discussed in the next paragraph.

The blocks representing the concrete walls dividing the concrete structure in separate rooms work only as sinks. There is no direct connection between two different concrete walls between the rooms, and therefore the diffusive transport between these is neglected by setting L/A equal to a high value. However, the additional resistance to diffusive transport from the porous concrete in one room to that in another room due to a concrete wall separating the rooms, is included in the diffusive resistance for the porous concrete.

To prevent that backward diffusion takes place to the part of the repository that initially is free of activity, a very large resistance to diffusion along the tunnel is added to appropriate model blocks in the concrete structure, the porous concrete between the waste, the backfill material in the top and on the sides of the waste, and in the gravel. Again, L/A, is set to 99999.

The ratio of diffusion length and surface area available for diffusion, L/A, for all blocks except the waste are given in Table 1. For the waste blocks the ratio $L/(A \cdot D_e)$ assigned to the coupling between two waste blocks is given. Included in this table are block volumes and material used to represent the modelled repository parts, as well as the waste fraction within each waste block. Note that the volume of the waste blocks with activity (blocks 2-5) corresponds to the actual bulk volume available for sorption, and not to the volume occupied by the waste in the repository. Accordingly, the density and porosity for these waste blocks is estimated from the amount of materials acting as sorbents. The total volume of different materials taken into account in the model for SFL 3 is compiled in Table 2.

Table 1 Compilation of input data to COMP24 describing the model blocks.

Block	**Material**	**Volume** [a] [m^3]	**Density** [a] [kg/m^3]	**Porosity** [a] [–]	**Activity** [% of total]	**L/(A·D_e)** [$year/m^3$]
1	backfill	3520.5	2700	0.3	0	99999
2	concrete	550.9	2700	0.34	10	99999
3	concrete	1638.4	2700	0.34	30	99999
4	concrete	1638.4	2700	0.34	30	99999
5	concrete	1638.4	2700	0.34	30	

Block	**Material**	**Volume** [m^3]	**L/A** [m^{-1}] x	**L/A** [m^{-1}] y	**L/A** [m^{-1}] z
6	concrete	247.5	–	0.0015	99999
7	concrete	49.9	–	0.0072	1.19
8	concrete	148.4	–	0.0024	3.53
9	concrete	148.4	–	0.0024	3.53
10	concrete	148.4	–	0.0024	3.53
11	concrete	293.4	–	0.00054	99999
12	concrete	59.1	–	0.0027	1.00
13	concrete	175.9	–	0.00091	2.98
14	concrete	175.9	–	0.00091	2.98
15	concrete	175.9	–	0.00091	2.98
16	concrete	206.3	–	0.0012	99999
17	concrete	41.6	–	0.0060	1.43
18	concrete	123.7	–	0.0020	4.24
19	concrete	123.7	–	0.0020	4.24
20	concrete	123.7	–	0.0020	4.24
21	concrete	294.4	–	0.00015	99999
22	concrete	59.3	–	0.00076	99999
23	concrete	176.5	–	0.00025	99999
24	concrete	176.5	–	0.00025	99999
25	concrete	176.5	–	0.00025	99999
26	porous concrete	263.2	–	$1.1 \cdot 10^{-6}$	99999
27	porous concrete	53.0	–	$5.4 \cdot 10^{-6}$	1.09
28	porous concrete	157.8	–	$1.8 \cdot 10^{-6}$	3.25
29	porous concrete	157.8	–	$1.8 \cdot 10^{-6}$	3.25
30	porous concrete	157.8	–	$1.8 \cdot 10^{-6}$	3.25
31	backfill	3636.6	0.056	0.013	99999
32	backfill	733.0	0.28	0.063	0.081
33	backfill	2180.1	0.093	0.021	0.24
34	backfill	2180.1	0.093	0.021	0.24
35	backfill	2180.1	0.093	0.021	0.24
36	backfill	1308.0	0.088	0.0020	99999
37	backfill	263.6	0.43	0.0097	0.22
38	backfill	784.1	0.15	0.0033	0.67
39	backfill	784.1	0.15	0.0033	0.67
40	backfill	784.1	0.15	0.0033	0.67
41	backfill	267.4	0.0041	0.00093	99999
42	backfill	53.9	0.0020	0.0046	1.1
43	backfill	160.3	0.0068	0.0016	3.27
44	backfill	160.3	0.0068	0.0016	3.27
45	backfill	160.3	0.0068	0.0016	3.27
46	concrete	38.4	–	2.60	0.0042
47	backfill	2520.0	–	–	0.040
48	backfill	0.01	–	–	0.0001

a) Estimated from data on waste packages given in Lindgren *et al.* (1998).

Table 2 Compilation of modelled volume [m^3] of different materials in SFL 3.

Material	Modelled volume
Waste	5,466
Structural concrete	3,163
Porous concrete	790
Gravel	21,677

5 Water flow through the system

The specific ground water flow in the near-field rock is obtained from the regional hydrology modelling (Svensson, 1997 and Hartley and Lindgren, 1997). Combining this with the results from the near-field hydrology modelling (Holmén, 1997) gives the specific flow of water in the SFL 3 tunnel.

The specific flow and the cross sectional area of the different barriers (structure and gravel outside the structure) used in this model give the total flow. The total flow through the tunnel is divided between the concrete structure including its interior and the flow barrier surrounding it. However, since the concrete structure is assumed to have a hydraulic conductivity which is 10^4 times lower than that in the flow barrier (Holmén, 1997), less than 0.03 % of the water flows through the structure.

In the model, there is no water flow through the waste. Instead all water flowing inside the concrete structure flows in the porous concrete surrounding the waste. The hydraulic conductivity used for structural concrete in this work (10^{-8} m/s, Skagius *et al.,* 1999) is expected to be about one to two orders of magnitude lower than for porous concrete. However, the total water flow through the encapsulation is very small why the assumption made is insignificant for the nuclides release rate.

The total flow through the barrier is divided between gravel beneath the structure, backfill material above the structure, and backfill material on the two sides of the structure. The magnitude of water flow through them is determined by their relationship in cross sectional area perpendicular to main flow direction through the tunnel. The cross sectional areas are approximately 7 m^2 for the gravel, 34 m^2 for the backfill material on sides and 95 m^2 for the backfill material above of the structure. Accordingly, 70 % of the water flowing in the barrier flows through the backfill material above the waste, 25 % on the sides of the waste, and the remaining 5 % through the gravel. It is assumed that there is no exchange of water in the vertical direction, but the flow is purely horizontal through the tunnel.

The flow rate of water through each block is presented in Table 3 based on a specific groundwater flow of 0.01 m^3/m^2, year.

Table 3 Flow rate of water [m^3/year] through each block based on a specific ground-water flow of 0.01 m^3/m^2, year

From block	To block	Flow rate
26	27	0.012
27	28	0.012
28	29	0.012
29	30	0.012
30	46	0.012
31	32	29.5
32	33	29.5
33	34	29.5
34	35	29.5
35	48	29.5
36	37	10.6
37	38	10.6
38	39	10.6
39	40	10.6
40	48	10.6
41	42	2.2
42	43	2.2
43	44	2.2
44	45	2.2
45	48	2.2
46	48	0.012
48	47	42.312
Inflow	26	0.012
Inflow	31	29.5
Inflow	36	10.6
Inflow	41	2.2
47	Outflow	42.312

References

Hartley L and Lindgren M, 1997. Flow and transport parameters for SFL 3-5 – Estimates from regional numerical models for Beberg and Ceberg. Appendix in Skagius *et al.* (1999).

Holmén J, 1997. On the flow of groundwater in closed tunnels. Generic hydrogeological modelling of nuclear waste repository SFL 3-5. SKB Technical Report TR 97-10, Swedish Nuclear Fuel and Waste Management Co., Stockholm.

Lindgren M, Pers K, Skagius K, Wiborgh M, Brodén K, Carlsson J, Riggare P, Skogsberg M, 1998. Low and intermediate level waste in SFL 3-5: Reference inventory. Reg. No: 19.41/DL31. Swedish Nuclear Fuel and Waste Management Co., Stockholm

Skagius K, Pettersson M, Wiborgh M, Albinsson Y, Holgersson S, 1999. Compilation of data for the analysis of radionuclide migration from SFL 3-5. SKB Report R-99-13, Swedish Nuclear Fuel and Waste Management Co., Stockholm.

Svensson U, 1997. Flow and transport from SFL 3-5 – Estimates from regional numerical model. Appendix in Skagius *et al.* (1999).

Appendix B: Near-field model for the radionuclide transport in SFL 4

Luis Moreno [a]

Michael Pettersson [b]

[a] **Dept. Chem. Eng. and Technol., Royal Inst. of Technology**

[b] **Kemakta Konsult AB**

1 Description of the model for the radionuclide transport in SFL 4

This appendix describes the model used for modelling the transport of radionuclides in the near field of SFL 4. Figure 1 shows an illustration of the SFL 4 repository.

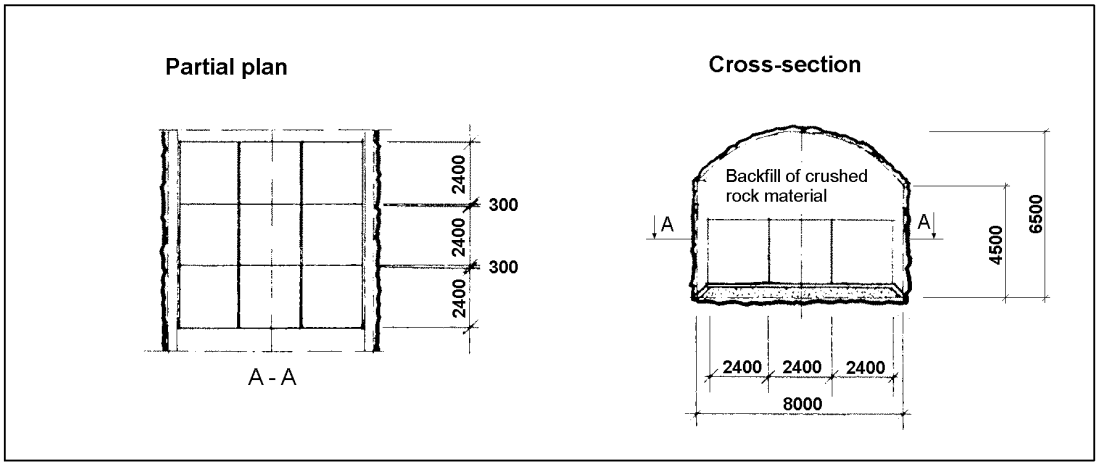

Figure 1 Illustration of the SFL 4 repository. Dimensions in mm.

2 Conceptual model for SFL 4

When the repository is sealed, water will intrude the tunnel, and the waste and backfill material will be saturated with water. Gas initially entrapped in the repository or produced, e.g. by corrosion, do not influence the water flow in the repository or the migration of radionuclides. At the initial time (year 2040), most of the nuclides will be dissolved completely in the pore water in the casks containing the waste or sorbed on concrete in the casks. The nuclides in solution will be equilibrated with the backfill material in the casks. Nuclides, which have a small solubility for the conditions existing in the repository, are only partially dissolved. The concentration of these nuclides will be limited to its solubility.

The groundwater flows in the horizontal direction parallel to the SFL 3 and SFL 5 tunnels. This means that water enters the SFL 4 tunnel along one of its sides, flows along the tunnel, and leaves the tunnel system on the opposite side. The waste casks may be damaged by corrosion quite soon after repository closure, why the barrier effect of the steel casks is negligible. Water therefore flows through the whole cross section of the tunnel.

Dissolved radionuclides will be transported along the tunnel by advection and by diffusion in both backfill material and in waste. In addition, there is also a diffusive transport from the waste casks into surrounding gravel backfill (see Figure 2). Sorption on waste and gravel backfill is accounted for, but sorption on the tunnels concrete floor and on shotcrete on tunnel walls is neglected. The radionuclides are transported out from the tunnel into the water flowing in fractures intersecting the tunnel.

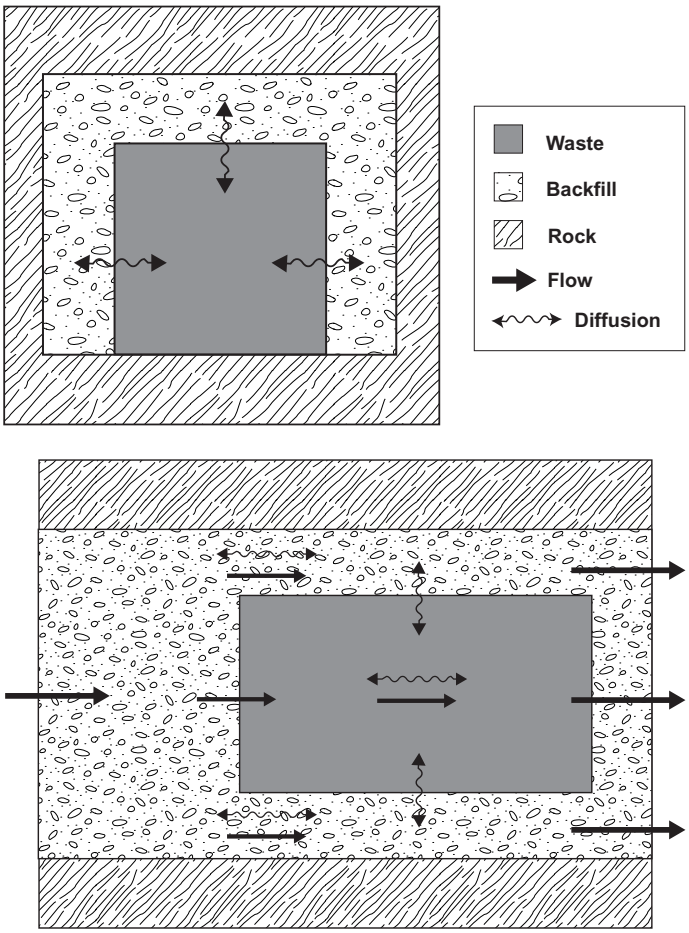

Figure 2 Transport paths for radionuclides in SFL 4.

3 Mathematical model for SFL 4

It is assumed that the tunnel is a square with 213 m long sides, i.e. the total length of the tunnel is 852 m. For symmetry reasons, only half of the tunnel (426 m), and thereby half of the waste, is modelled. The part of the tunnel modelled is straightened out and forms a straight tunnel, Figure 3.

It is assumed that the direction of the water flow is along the tunnel. Water intrudes the system from the sides along the first 106 metres, flows along the tunnel, and leaves the tunnel through the sides at the last 106 metres at the other end of the tunnel. The arrows indicate where water enters and leaves the tunnel, respectively. It is also assumed that nuclides are released to the near field rock only where water leaves the tunnel.

Fuel storage canisters and decommissioning waste from CLAB and the encapsulation plant is the only radioactive waste of importance in SFL 4. Activity in transport casks and transport containers is insignificant and can be neglected. The backfill material between each row of containers is also neglected in the model, i.e. the model considers that the containers with the waste are placed in the tunnel without backfill material between them. Consequently, 252 m of the modelled tunnel is needed for depositing half of the waste. The remaining storage volume is assumed to be filled with backfill material (gravel). A conservative assumption is made that the waste is stored in the part

of the tunnel closest to where water leaves the tunnel. Backward diffusion to the part of the tunnel that initially is free of activity, is strongly reduced by assigning a very large resistance to diffusion to corresponding model blocks.

In the model, a large number of steel casks with waste are grouped to a source term. A source term includes waste and concrete that is assumed to be used as backfill material in order to improve the mechanical stability of the casks. A source term is modelled as a stirred tank, i.e. it is assumed that the activity within a source term is homogeneous, and that it remains so also when part of the inventory is transported out.

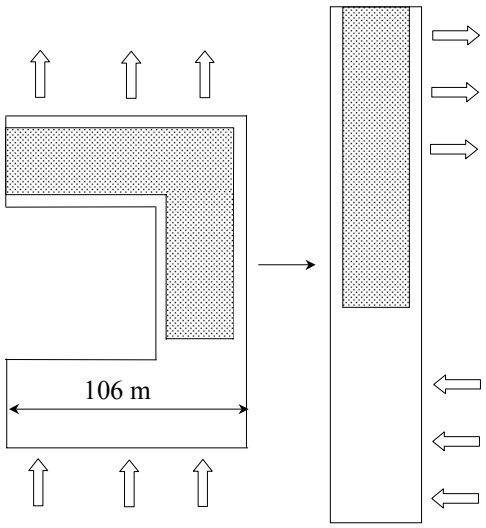

Figure 3 Schematic picture of the modelled tunnel.

4 Discretization of the system

252 m of the modelled tunnel is needed for depositing half of the waste. In order to fix the repository to the real volume of waste, and to keep the model flexible, the length of the tunnel is divided into nine sections:

- three large sections
- six small sections

The length of the larger sections is twice the length of the smaller sections, 71.0 m and 35.5 m respectively. The modelled tunnel is also divided into three different groups representing different parts of the repository (Figure 4):

i) Waste (blocks 1-9)

ii) Lateral volume on the two sides of the waste filled with backfill material (blocks 10-33)

iii) Volume above the waste filled with backfill material (blocks 34-57)

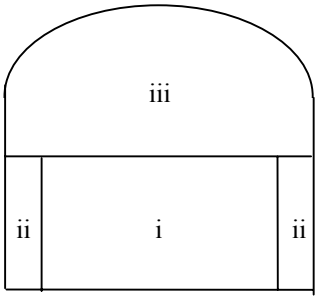

Figure 4 Cross section of the tunnel with the three groups modelled.

A detailed discretization of the tunnel is shown in Figure 5. The arrows show where water enters and leaves the system. The end of the tunnel where water leaves the system and thus the radionuclides are released, is discretized into a finer mesh. In this region, both the backfill material on the sides and on top of the waste are divided into 18 blocks. Even though it seems in Figure 5 as if the discretization for the backfill material on the sides of the waste and the backfill material above the waste are identical, they are not. Figure 6 shows the discretization at the cuts A-A and B-B.

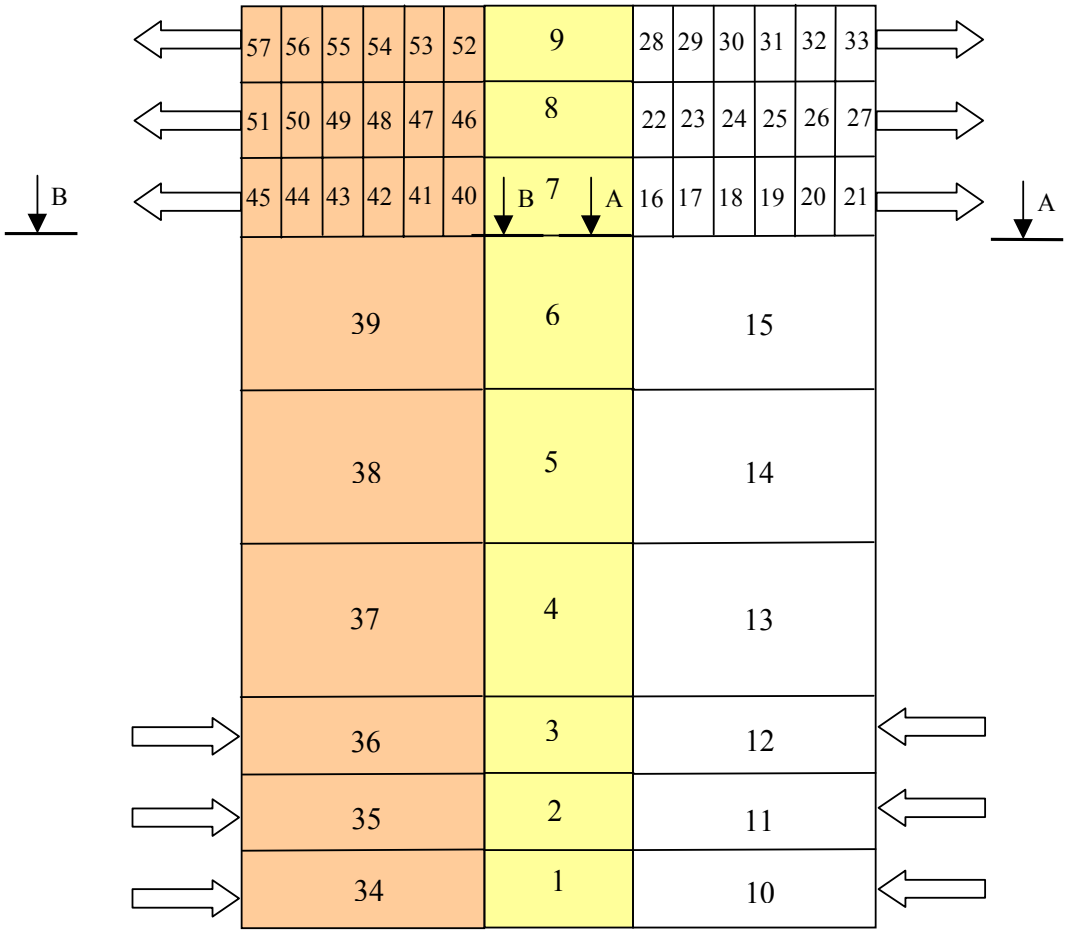

Figure 5 Discretization of the SFL 4 tunnel.

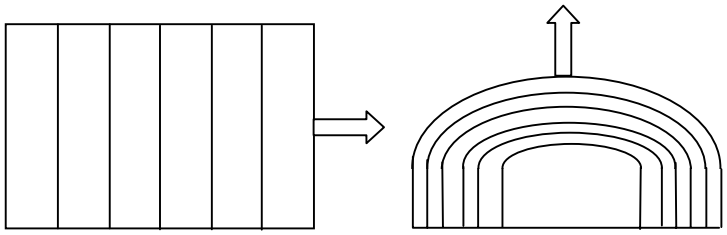

Figure 6 Schematic pictures of the discretization at A-A (blocks 16-21) and B-B (blocks 40-45).

The paths for mass transfer between different groups taken into account are between:

- Waste and backfill material on the sides of the waste (diffusion, and for some blocks also advection)
- Waste and backfill material on top of the waste (diffusion)
- Backfill material on the sides of the waste and backfill material on top of the waste (diffusion)

The groups where mass transfer between blocks within the group is taken into account are:

- Waste (diffusion and advection)
- Backfill material above the waste (diffusion and advection)
- Backfill material on the two sides of the waste (diffusion and advection)

The volume of the waste to be deposited is less than the available volume for disposal in SFL 4. It is assumed that that the waste is homogeneously distributed (in Bq/m^3) in blocks 5-9, while blocks 1-4 are free of activity. Waste blocks free of activity are given the same material properties as the backfill material (gravel).

In contrast to the models for SFL 3 and SFL 5, there is a diffusive transport between different waste blocks. The values of $L/(A \cdot D_e)$ are given in Table 1. For diffusion between waste and surrounding backfill material, the diffusive resistance within the waste is neglected.

To prevent that backward diffusion takes place to the part of the tunnel that initially is free of activity, a very large resistance to diffusion along the tunnel is added to appropriate model blocks. In COMP24 this is obtained by setting the ratio of diffusion length and mass transfer area, L/A, to a very large value (in this work 99999).

The ratio of diffusion length and surface area available for diffusion, L/A, for all blocks except the waste are given in Table 1. For the waste blocks the ratio $L/(A \cdot D_e)$ assigned to the coupling between two waste blocks is given. Included in this table are block volumes and material used to represent the modelled repository parts, as well as the waste fraction within each waste block. Note that the volume of the waste blocks with activity (blocks 5-9) corresponds to the actual bulk volume available for sorption, and not to the volume occupied by the waste in the repository. Accordingly, the density and porosity for these waste blocks is estimated from the amount of materials acting as sorbents. The total volume of different materials taken into account in the model for SFL 4 is compiled in Table 2.

Table 1 Compilation of input data to COMP24 describing the model blocks.

Block	Material	Volume [a] [m^3]	Density [a] [kg/m^3]	Porosity [a] [–]	Activity [% of total]	$L/(A \cdot D_e)$ [$year/m^3$]
1	Backfill	613	2700	0.3	0	6420
2	Backfill	613	2700	0.3	0	6420
3	Backfill	613	2700	0.3	0	9630
4	Backfill	1227	2700	0.3	0	99999
5	Concrete	1112	2700	0.29	28.6	12840
6	Concrete	1112	2700	0.29	28.6	9630
7	Concrete	556	2700	0.29	14.3	6420
8	Concrete	556	2700	0.29	14.3	6420
9	Concrete	556	2700	0.29	14.3	

Block	Material	Volume [m^3]	L/A [m^{-1}] x	L/A [m^{-1}] y	L/A [m^{-1}] z
10	Backfill	68.2	0.084	0.0023	18.5
11	Backfill	68.2	0.084	0.0023	18.5
12	Backfill	68.2	0.084	0.0023	18.5
13	Backfill	136.3	0.042	0.0012	99999
14	backfill	136.3	0.042	0.0012	37.0
15	Backfill	136.3	0.042	0.0012	37.0
16	Backfill	11.4	0.50	0.00039	110.9
17	Backfill	11.4	0.50	0.00039	110.9
18	Backfill	11.4	0.50	0.00039	110.9
19	Backfill	11.4	0.50	0.00039	110.9
20	Backfill	11.4	0.50	0.00039	110.9
21	Backfill	11.4	0.50	0.00039	110.9
22	Backfill	11.4	0.50	0.00039	110.9
23	Backfill	11.4	0.50	0.00039	110.9
24	Backfill	11.4	0.50	0.00039	110.9
25	Backfill	11.4	0.50	0.00039	110.9
26	Backfill	11.4	0.50	0.00039	110.9
27	Backfill	11.4	0.50	0.00039	110.9
28	Backfill	11.4	0.50	0.00039	110.9
29	Backfill	11.4	0.50	0.00039	110.9
30	Backfill	11.4	0.50	0.00039	110.9
31	Backfill	11.4	0.50	0.00039	110.9
32	Backfill	11.4	0.50	0.00039	110.9
33	Backfill	11.4	0.50	0.00039	110.9
34	Backfill	887.5	0.11	0.011	1.42
35	Backfill	887.5	0.11	0.011	1.42
36	Backfill	887.5	0.11	0.011	1.42
37	Backfill	1775	0.055	0.0055	99999
38	Backfill	1775	0.055	0.0055	2.84
39	Backfill	1775	0.055	0.0055	2.84
40	Backfill	146.7	0.018	0.0018	8.59
41	Backfill	146.7	0.018	0.0018	8.59
42	Backfill	146.7	0.018	0.0018	8.59
43	Backfill	146.7	0.018	0.0018	8.59
44	Backfill	146.7	0.018	0.0018	8.59
45	Backfill	146.7	0.018	0.0018	8.59
46	Backfill	146.7	0.018	0.0018	8.59
47	Backfill	146.7	0.018	0.0018	8.59
48	Backfill	146.7	0.018	0.0018	8.59
49	Backfill	146.7	0.018	0.0018	8.59
50	Backfill	146.7	0.018	0.0018	8.59
51	Backfill	146.7	0.018	0.0018	8.59
52	Backfill	146.7	0.018	0.0018	8.59
53	Backfill	146.7	0.018	0.0018	8.59
54	Backfill	146.7	0.018	0.0018	8.59
55	Backfill	146.7	0.018	0.0018	8.59
56	Backfill	146.7	0.018	0.0018	8.59
57	Backfill	146.7	0.018	0.0018	8.59

a) Estimated from data on waste packages given in Lindgren *et al.* (1998).

Table 2 Compilation of modelled volume [m^3] of different materials in SFL 4.

Material	Modelled volume
Waste	3,892
Gravel	14,503

5 Water flow through the system

The specific ground water flow in the near-field rock is obtained from the regional hydrology modelling (Svensson, 1997 and Hartley and Lindgren, 1997). Combining this with the results from the near-field hydrology modelling (Holmén, 1997) gives the specific flow of water in the SFL 4 tunnel.

In the conceptual model, water enters the SFL 4 tunnel along one of its sides corresponding to some 200 m tunnel, but since half of the tunnel is modelled, half this distance is modelled. In the mathematical model this length corresponds to the length of the first three sections.

The specific flow and the cross sectional area of the waste and the backfill around the waste used in this model give the total flow. The total flow through the tunnel is divided between the three groups modelled; waste and backfill material on sides and on top of the waste. Since the waste is modelled as having the same properties as the backfill material, the magnitude of water flow through them is determined by their relationship in cross sectional area perpendicular to main flow direction through the tunnel. The cross sectional areas are approximately 17 m^2 for the waste, 2 m^2 for the backfill material on sides and 25 m^2 for the backfill material on top of the waste. Accordingly, 57 % of the water entering the tunnel flows through the backfill material above the waste, 4 % on the sides of the waste, and the remaining 39 % through the waste. It is assumed that there is no exchange of water between the backfill material on top and the waste/the backfill material on the two sides.

In the model, each of the water streams flowing into the backfill material on the sides of the waste is divided into two streams, one flowing through the waste and one through the backfill material on the sides of the waste. Again, the magnitude of water flow through them is determined by their relationship in cross sectional area perpendicular to main flow direction. Consequently, approximately 90 % of the water flowing into the backfill material flows through the waste. This is shown in Figure 7 for a unit inflow.

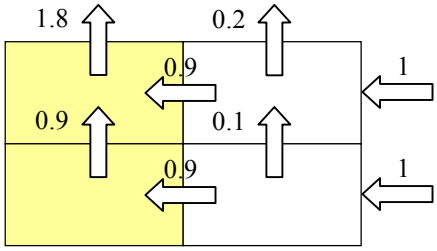

Figure 7 Distribution of incoming water between waste and backfill material on sides of waste.

The flow rate of water in the last three blocks representing the waste gradually decreases, because part of the flow is directed to the backfill on the sides of the waste. This also applies to the blocks representing the backfill material on the sides of the waste. This is indicated in Figure 8. The same approach is used regarding the distribution of water flow in the last part of the backfill material on top of waste. Figure 9 shows the flow of water in detail, and the flow rate of water through each block is presented in Table 3 based on a specific groundwater flow of 0.01 m^3/m^2, year.

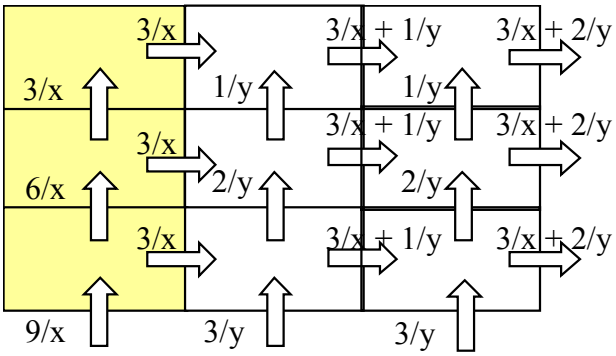

Figure 8 *Distribution of water between waste and backfill material on sides of waste.*

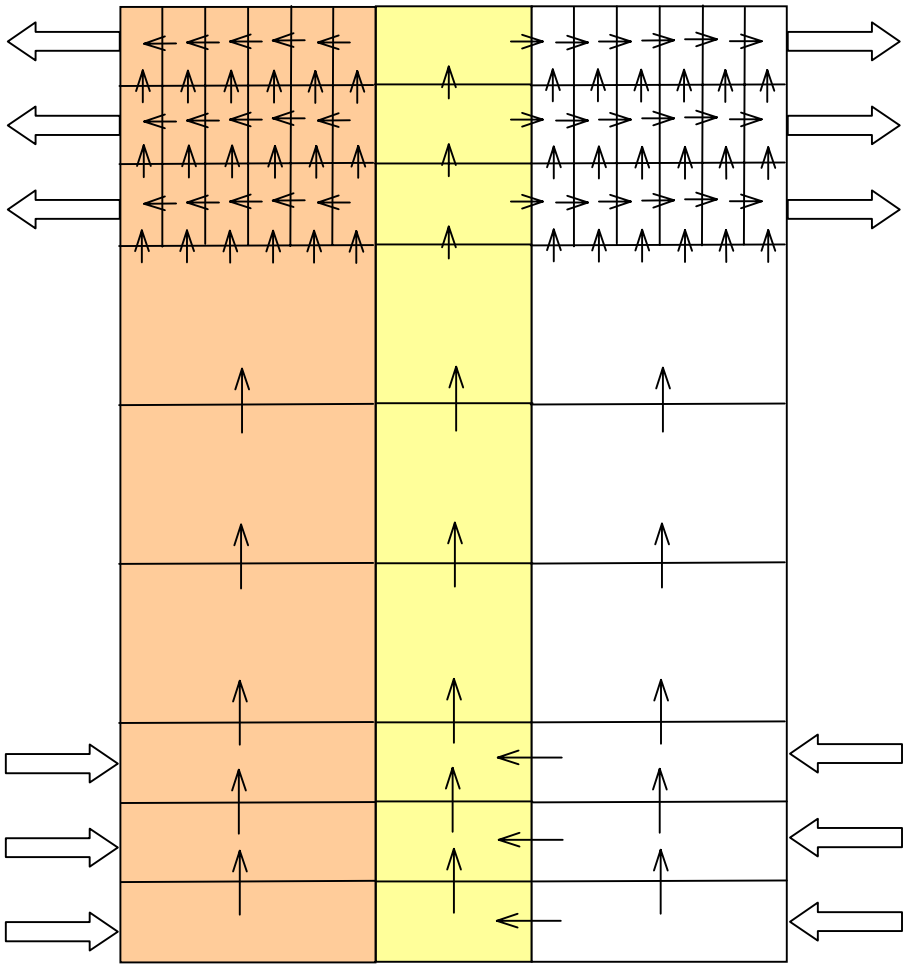

Figure 9 *Flow of water inside SFL 4.*

Table 3 Flow rate of water [m^3/year] through each block based on a specific ground-water flow of 0.01 m/m^2, year.

From block	To block	Flow	From block	To block	Flow
1	2	21.6	32	33	23.6
2	3	43.2	34	35	31.2
3	4	64.8	35	36	62.4
4	5	64.8	36	37	93.6
5	6	64.8	37	38	93.6
6	7	64.8	38	39	93.6
7	8	43.2	39	40	15.6
7	16	21.6	39	41	15.6
8	9	21.6	39	42	15.6
8	22	21.6	39	43	15.6
9	28	21.6	39	44	15.6
10	1	21.6	39	45	15.6
10	11	2.4	40	41	5.2
11	2	21.6	40	46	10.4
11	12	4.8	41	42	10.4
12	3	21.6	41	47	10.4
12	13	7.2	42	43	15.6
13	14	7.2	42	48	10.4
14	15	7.2	43	44	20.8
15	16	1.2	43	49	10.4
15	17	1.2	44	45	26
15	18	1.2	44	50	10.4
15	19	1.2	45	51	10.4
15	20	1.2	46	47	5.2
15	21	1.2	46	52	5.2
16	17	22	47	48	10.4
16	22	0.8	47	53	5.2
17	18	22.4	48	49	15.6
17	23	0.8	48	54	5.2
18	19	22.8	49	50	20.8
18	24	0.8	49	55	5.2
19	20	23.2	50	51	26
19	25	0.8	50	56	5.2
20	21	23.6	51	57	5.2
20	26	0.8	52	53	5.2
21	27	0.8	53	54	10.4
22	23	22	54	55	15.6
22	28	0.4	55	56	20.8
23	24	22.4	56	57	26
23	29	0.4	Inflow	10	24
24	25	22.8	Inflow	11	24
24	30	0.4	Inflow	12	24
25	26	23.2	Inflow	34	31.2
25	31	0.4	Inflow	35	31.2
26	27	23.6	Inflow	36	31.2
26	32	0.4	21	Outflow	24
27	33	0.4	27	Outflow	24
28	29	22	33	Outflow	24
29	30	22.4	45	Outflow	31.2
30	31	22.8	51	Outflow	31.2
31	32	23.2	57	Outflow	31.2

References

Hartley L and Lindgren M, 1997. Flow and transport parameters for SFL 3-5 – Estimates from regional numerical models for Beberg and Ceberg. Appendix in Skagius *et al.* (1999).

Holmén J, 1997. On the flow of groundwater in closed tunnels. Generic hydrogeological modelling of nuclear waste repository SFL 3-5. SKB Technical Report TR 97-10, Swedish Nuclear Fuel and Waste Management Co., Stockholm.

Lindgren M, Pers K, Skagius K, Wiborgh M, Brodén K, Carlsson J, Riggare P, Skogsberg M, 1998. Low and intermediate level waste in SFL 3-5: Reference inventory. Reg. No: 19.41/DL31. Swedish Nuclear Fuel and Waste Management Co., Stockholm

Skagius K, Pettersson M, Wiborgh M, Albinsson Y, Holgersson S, 1999. Compilation of data for the analysis of radionuclide migration from SFL 3-5. SKB Report R-99-13, Swedish Nuclear Fuel and Waste Management Co., Stockholm.

Svensson U, 1997. Flow and transport from SFL 3-5 – Estimates from regional numerical model. Appendix in Skagius *et al.* (1999).

Appendix C: Near-field model for the radionuclide transport in SFL 5

Luis Moreno [a]

Michael Pettersson [b]

[a] Dept. Chem. Eng. and Technol., Royal Inst. of Technology

[b] Kemakta Konsult AB

1 Introduction

This appendix describes the model used for modelling the transport of radionuclides in the near field of SFL 5. Figure 1 shows an illustration of the concrete structure built inside the SFL 5 tunnel and of the deposited waste.

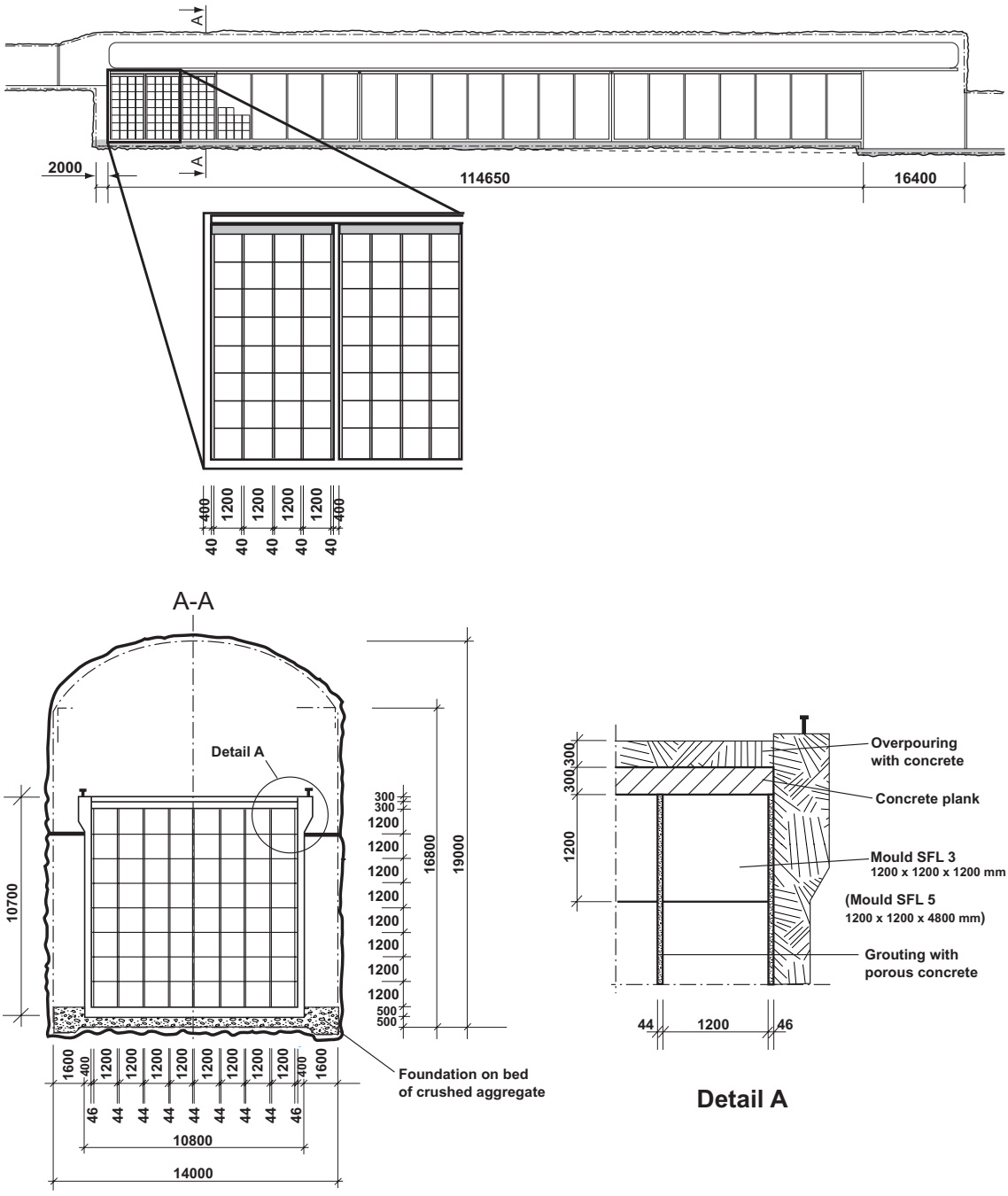

Figure 1 Illustration of the SFL 5 repository. Dimensions in mm.

2 Conceptual model for SFL 5

When the repository is sealed, water will intrude the tunnel, and the waste and backfill material will be saturated with water. Gas initially entrapped in the repository or produced, e.g. by corrosion, do not influence the water flow in the repository or the migration of radionuclides. At the initial time (year 2040), most of the nuclides will be dissolved completely in the pore water in the packages containing the waste or will be sorbed on concrete and cement in the packages. The nuclides in solution will be equilibrated with the backfill material in the waste moulds. Nuclides, which have a small solubility for the conditions existing in the repository, are only partially dissolved. The concentration of these nuclides will be limited to its solubility. For nuclides embedded in metallic waste, the concentration may be limited by the corrosion rate of the waste.

The groundwater flows in the horizontal direction along the SFL 5 tunnel. The major part of the water flows through the flow barrier (gravel backfill) surrounding the concrete structure where the waste is deposited. Water flux through the structure will be very low (Holmén, 1997). For this reason, most of the activity in the waste is released by diffusion through the concrete structure to the backfill material surrounding the concrete structure.

Nuclides can also be transported in the main direction of the tunnel within the structure. This transport is, however, of limited importance.

Radionuclides released from the concrete structure into the gravel backfill will be transported through diffusion as well as with water flowing in the backfill. Radionuclides may be sorbed on the backfill material, thus retarding the transport. The concrete plug constructed in the loading zone is considered to be intact, why the radionuclides are transported out from the tunnel into the water flowing in fractures intersecting the tunnel before they reach the plug.

3 Mathematical model for SFL 5

In modelling the transport of radionuclides, the repository has been simplified. The important simplifications are conservative in order not to overestimate importance of the barriers. The length of the modelled tunnel is 124.6 m, which corresponds to the length of the concrete structure plus 10 m of backfill material at the end of the tunnel. The loading zones with concrete plugs, shown in Figure 3-1 in main report, are not included in the model. Neither is the shotcrete that may cover the tunnel walls.

The waste to be deposited in SFL 5 consists of metal parts placed in a reinforced concrete mould with an inner steel cassette. Concrete will be injected to fill the voids in the mould, and porous concrete will be filled around the moulds. The outer dimension of the mould is $1.2 \times 1.2 \times 4.8$ m with 0.1mm thick walls. Unlike SFL 3, all waste packages are the same in SFL 5. The waste volume to be deposited in SFL 5 exceeds the available volume with approximately four per cent, but it is assumed that the waste volume can be reduced so that it will fit into SFL 5.

In the model, a large number of moulds with waste and injected concrete are grouped to a source term, but the mould concrete walls are modelled separately. The barrier effect of the inner steel cassette is neglected. A source term is modelled as a stirred tank, i.e. it is assumed that the activity within a source term is homogeneous, and that it remains so also when part of the inventory is transported out. All voids inside the concrete structure are filled with porous concrete, and the structure is covered with gravel.

The waste packages are surrounded by porous concrete, why there is no direct transfer of nuclides between different packages. Instead, the nuclides diffuse from a waste through the mould walls, the porous concrete surrounding the moulds and finally the concrete structure to the backfill material surrounding the structure and to the gravel below the structure (Figure 2).

Along the tunnel there is an advective and a diffusive transport (see Figure 2). Sorption is accounted for in all parts of the modelled repository.

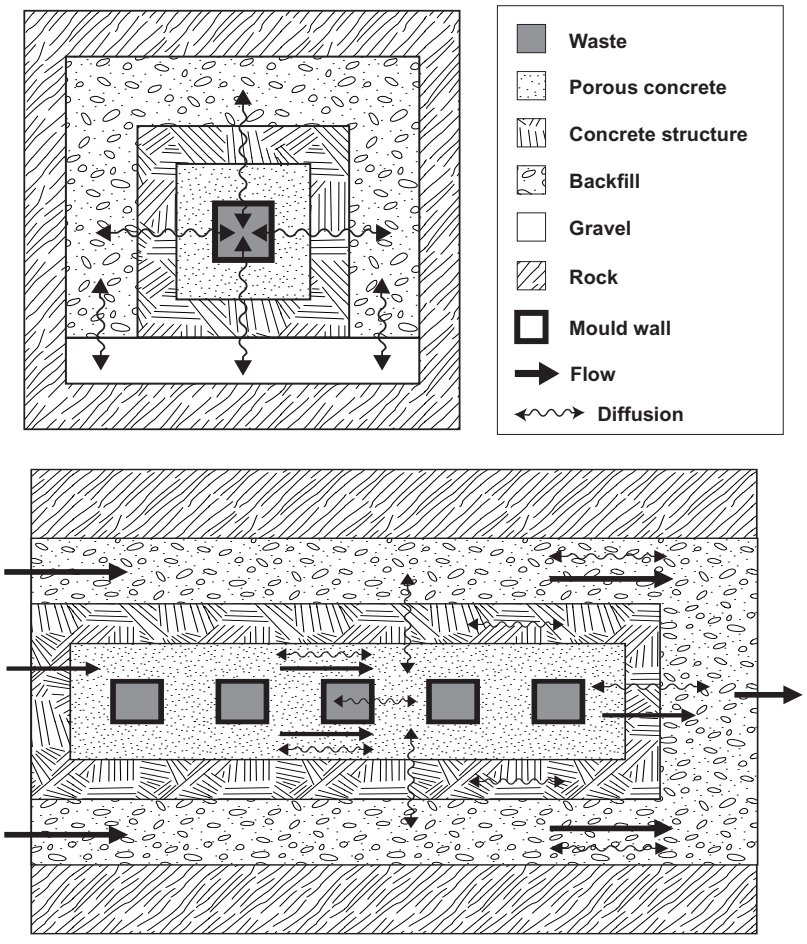

Figure 2 *Transport paths for radionuclides in SFL 5. 'Gravel' corresponds to the bed on which the structure in built and 'Backfill' to the gravel used as backfill in the tunnel. In the model, 'Gravel' and 'Backfill' has the same properties.*

The distance between the end of the concrete structure and the opening to SFL 4 is approximately 40 m, but only 10 m are included in the model. The reason is that a concrete plug is located somewhere in the 20 - 30 m long loading zone. This plug is

considered to be intact why the radionuclides are transported out from the tunnel into the water flowing in fractures intersecting the end of the tunnel before the nuclides reach the plug.

4 Discretization of the system

It is assumed that the whole volume available for waste is filled. In order to fix the repository to the real volume of waste and keep the model flexible, the length of the concrete structure is divided into five sections of 22.9 m length. The modelled tunnel is also divided into thirteen different groups representing different parts of the repository:

i) Waste (blocks 1-5)
ii) Concrete ceiling of the structure (blocks 6-10)
iii) Concrete walls of the structure (blocks 11-15)
iv) Concrete bottom of the structure (blocks 16-20)
v) Concrete walls between the rooms (blocks 21-25)
vi) Porous concrete around the waste moulds/drums (blocks 26-30)
vii) Volume above the structure filled with backfill material (blocks 31-35)
viii) Lateral volume on the two sides of the structure filled with backfill material (blocks 36-40)
ix) Gravel beneath the structure (blocks 41-45)
x) Last transverse concrete wall of the structure (block 46)
xi) Backfill material at the end of the tunnel (block 47)
xii) Fictitious block (block 48)
xiii) Concrete walls of waste moulds (blocks 49-53)

The detailed discretization of the tunnel is shown in Figure 3. The arrows show where water is flowing through the system. Water flow takes place in the porous concrete surrounding the waste moulds, the backfill material around the concrete structure, gravel in bottom, the last transverse concrete wall of the structure, and the backfill material at end of the tunnel.

The block representing the backfill material at the end of the tunnel is subdivided into six compartments. COMP24 can not handle a subdivided block that simultaneously is a point where several water streams are mixed into one. A fictitious block is therefore included in the model. This block only serves to mix the fluid streams leaving the structure, the backfill material surrounding the structure and the gravel in bottom into one stream.

Block 46 corresponds to the last transverse wall in the concrete structure, and not a concrete plug in the tunnel leading to SFL 4.

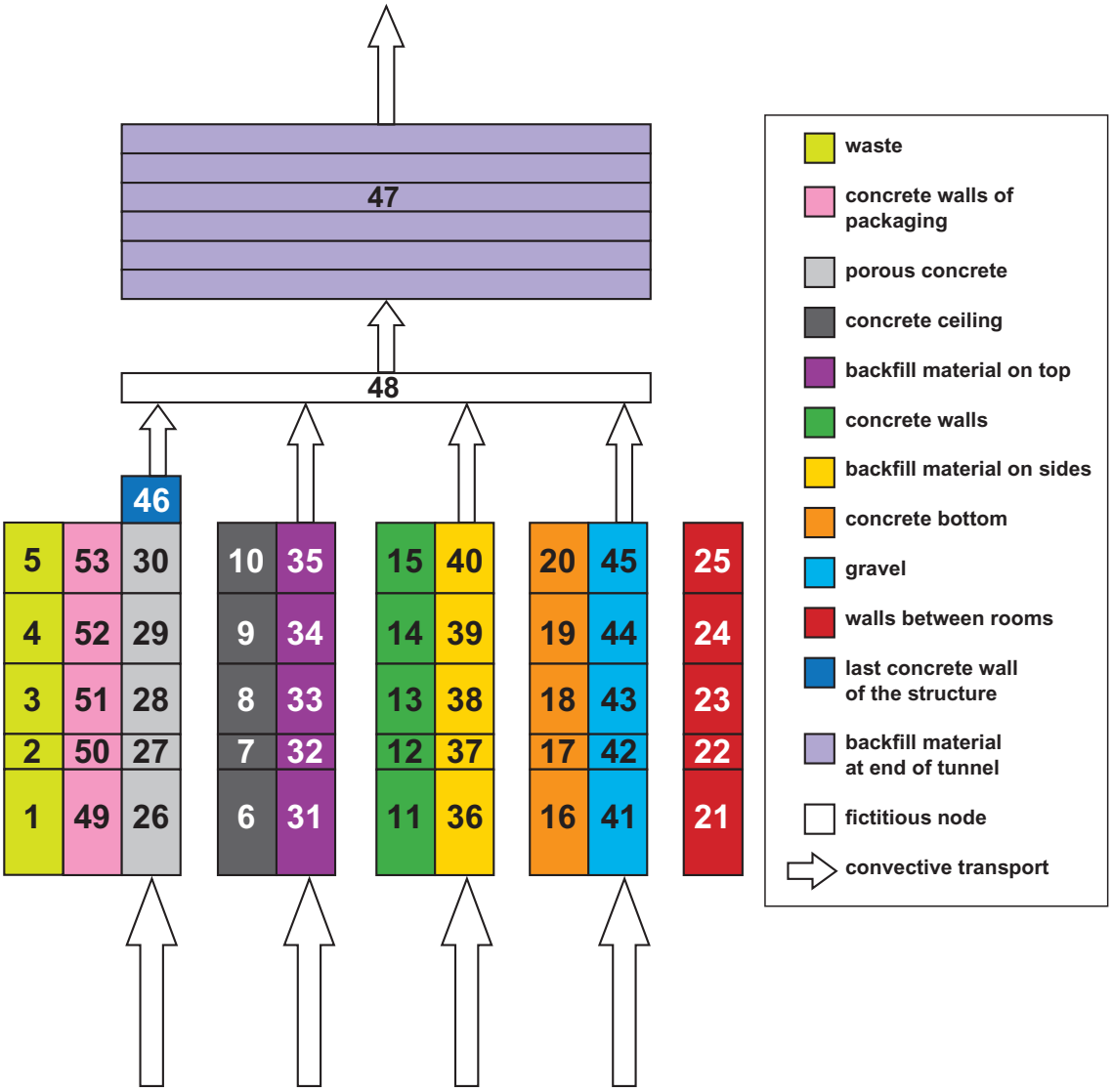

Figure 3 Detailed discretization of the SFL 5 tunnel.

The paths for mass transfer between different groups taken into account are between:

- Waste and concrete walls of waste mould (diffusion)
- Concrete walls of waste moulds and porous concrete (diffusion)
- Porous concrete and concrete bottom of the structure (diffusion)
- Porous concrete and lateral concrete walls of the structure (diffusion)
- Porous concrete and concrete ceiling of the structure (diffusion)
- Concrete bottom of the structure and gravel beneath structure (diffusion)
- Concrete walls of the structure and backfill material on the sides of the structure (diffusion)
- Concrete ceiling of the structure and backfill material on top of the structure (diffusion)

- Backfill material on the sides of the structure and gravel beneath structure (diffusion)
- Backfill material on the sides of the structure and backfill material on top of the structure (diffusion)
- Porous concrete and the transverse concrete walls of the structure (diffusion)
- Porous concrete and last transverse concrete wall of the structure (diffusion and advection)
- Last transverse concrete wall of the structure and backfill material at the end of the tunnel (diffusion and advection)
- Backfill material on top of the structure and backfill material at the end of the tunnel (diffusion and advection)
- Backfill material on the sides of the structure and backfill material at the end of the tunnel (diffusion and advection)
- Gravel beneath structure and backfill material at the end of the tunnel (diffusion and advection)

The groups where mass transfer between blocks within the group is taken into account are:

- Porous concrete (diffusion and advection)
- Gravel beneath the structure (diffusion and advection)
- Backfill material above the structure (diffusion and advection)
- Backfill material on the two sides of the structure (diffusion and advection)
- Backfill material at the end of the tunnel (diffusion and advection)
- Concrete ceiling of the structure (diffusion)
- Concrete walls of the structure (diffusion)
- Concrete bottom of the structure (diffusion)

In the model, the initial activity is homogeneously distributed (Bq/m^3) in the five blocks representing the waste.

It is assumed that a layer of porous concrete surrounds each waste mould, and that mass transfer between moulds always goes through the porous concrete. For this reason, a very large resistance to diffusion between adjacent waste blocks is added. In COMP24 this is obtained by setting the ratio of diffusion length and mass transfer area times effective diffusivity, $L/(A \cdot D_e)$, to a very large value (in this work 99999). For diffusion between waste and surrounding porous concrete, the diffusive resistance within the waste is neglected.

In order to estimate L/A for the block representing the porous concrete, the total volume of porous concrete within a room divided with the total surface area of the moulds in that room gives a mean thickness, L, of the porous concrete around the moulds. The surface area used in estimating L/A for the diffusive transport between waste and porous concrete is the total surface area of all moulds included in the waste block. This

is value of L/A is used for all connections in which the porous concrete takes part, except for the connection between two blocks both representing the porous concrete. This is discussed in the next paragraph.

The blocks representing the concrete walls dividing the concrete structure in separate rooms work only as sinks. There is no direct connection between two different concrete walls between the rooms, and therefore the diffusive transport between these is neglected by setting L/A equal to a high value. However, the additional resistance to diffusive transport from the porous concrete in one room to that in another room due to a concrete wall separating the rooms, is included in the diffusive resistance for the porous concrete.

The ratio of diffusion length and surface area available for diffusion, L/A, for all blocks except the waste are given in Table 1. For the waste blocks the ratio $L/(A \cdot D_e)$ assigned to the coupling between two waste blocks is given. Included in this table are block volumes and material used to represent the modelled repository parts, as well as the waste fraction within each waste block. Note that the volume of the waste blocks corresponds to the actual bulk volume available for sorption, and not to the volume occupied by the waste in the repository. Accordingly, the density and porosity for these waste blocks is estimated from the amount of materials acting as sorbents. The total volume of different materials taken into account in the model for SFL 3 is compiled in Table 2.

Table 1 Compilation of input data to COMP24 describing the model blocks.

Block	Material	Volume [a] [m^3]	Density [a] [kg/m^3]	Porosity [a] [–]	Activity [% of total]	$L/(A \cdot D_e)$ [$year/m^3$]
1	concrete	1217.4	2700	0.37	20	99999
2	concrete	1217.4	2700	0.37	20	99999
3	concrete	1217.4	2700	0.37	20	99999
4	concrete	1217.4	2700	0.37	20	99999
5	concrete	1217.4	2700	0.37	20	

Block	Material	Volume [m^3]	L/A [m^{-1}] x	L/A [m^{-1}] y	L/A [m^{-1}] z
6	concrete	148.4	–	0.0024	3.53
7	concrete	148.4	–	0.0024	3.53
8	concrete	148.4	–	0.0024	3.53
9	concrete	148.4	–	0.0024	3.53
10	concrete	148.4	–	0.0024	3.53
11	concrete	175.9	–	0.00091	2.98
12	concrete	175.9	–	0.00091	2.98
13	concrete	175.9	–	0.00091	2.98
14	concrete	175.9	–	0.00091	2.98
15	concrete	175.9	–	0.00091	2.98
16	concrete	123.7	–	0.0020	4.24
17	concrete	123.7	–	0.0020	4.24
18	concrete	123.7	–	0.0020	4.24
19	concrete	123.7	–	0.0020	4.24
20	concrete	123.7	–	0.0020	4.24
21	concrete	176.5	–	0.00025	99999
22	concrete	176.5	–	0.00025	99999
23	concrete	176.5	–	0.00025	99999
24	concrete	176.5	–	0.00025	99999
25	concrete	176.5	–	0.00025	99999
26	porous concrete	157.8	–	$3.2 \cdot 10^{-6}$	3.25
27	porous concrete	157.8	–	$3.2 \cdot 10^{-6}$	3.25
28	porous concrete	157.8	–	$3.2 \cdot 10^{-6}$	3.25
29	porous concrete	157.8	–	$3.2 \cdot 10^{-6}$	3.25
30	porous concrete	157.8	–	$3.2 \cdot 10^{-6}$	3.25
31	backfill	2180.1	0.093	0.021	0.24
32	backfill	2180.1	0.093	0.021	0.24
33	backfill	2180.1	0.093	0.021	0.24
34	backfill	2180.1	0.093	0.021	0.24
35	backfill	2180.1	0.093	0.021	0.24
36	backfill	784.1	0.15	0.0033	0.67
37	backfill	784.1	0.15	0.0033	0.67
38	backfill	784.1	0.15	0.0033	0.67
39	backfill	784.1	0.15	0.0033	0.67
40	backfill	784.1	0.15	0.0033	0.67
41	backfill	160.3	0.0068	0.0016	3.27
42	backfill	160.3	0.0068	0.0016	3.27
43	backfill	160.3	0.0068	0.0016	3.27
44	backfill	160.3	0.0068	0.0016	3.27
45	backfill	160.3	0.0068	0.0016	3.27
46	concrete	38.4	–	2.60	0.0042
47	Backfill	2520	–	–	0.04
48	backfill	0.01	–	–	0.0001
49	Concrete	620.6	–	$1.6 \cdot 10^{-5}$	–
50	Concrete	620.6	–	$1.6 \cdot 10^{-5}$	–
51	Concrete	620.6	–	$1.6 \cdot 10^{-5}$	–
52	Concrete	620.6	–	$1.6 \cdot 10^{-5}$	–
53	Concrete	620.6	–	$1.6 \cdot 10^{-5}$	–

a) Estimated from data on waste packages given in Lindgren *et al.* (1998).

Table 2 Compilation of modelled volume [m^3] of different materials in SFL 5.

Material	Modelled volume
Waste	6,087
Structural concrete	3,161
Concrete in walls of packaging	3,103
Porous concrete	789
Gravel	18,143

5 Water flow through the system

The specific ground water flow in the near-field rock is obtained from the regional hydrology modelling (Svensson, 1997 and Hartley and Lindgren, 1997). Combining this with the results from the near-field hydrology modelling (Holmén, 1997) gives the specific flow of water in the SFL 5 tunnel.

The specific flow and the cross sectional area of the different barriers (structure and gravel outside the structure) used in this model give the total flow. The total flow through the tunnel is divided between the concrete structure including its interior and the flow barrier surrounding it. However, since the concrete structure is assumed to have a hydraulic conductivity which is 10^4 times lower than that in the flow barrier (Holmén, 1997), less than 0.03 % of the water flows through the structure.

In the model, there is no water flow through the waste. Instead all water flowing inside the concrete structure flows in the porous concrete surrounding the waste. The hydraulic conductivity used for structural concrete in this work (10^{-8} m/s, Skagius *et al.,* 1999) is expected to be about one to two orders of magnitude lower than for porous concrete. However, the total water flow through the encapsulation is very small why the assumption made is insignificant for the nuclides release rate.

The total flow through the barrier is divided between gravel beneath the structure, backfill material above the structure, and backfill material on the two sides of the structure. The magnitude of water flow through them is determined by their relationship in cross sectional area perpendicular to main flow direction through the tunnel. The cross sectional areas are approximately 7 m^2 for the gravel, 34 m^2 for the backfill material on sides and 95 m^2 for the backfill material above of the structure. Accordingly, 70 % of the water flowing in the barrier flows through the backfill material above the waste, 25 % on the sides of the waste, and the remaining 5 % through the gravel. It is assumed that there is no exchange of water in the vertical direction, but the flow is purely horizontal through the tunnel.

The flow rate of water through each block is presented in Table 3 based on a specific groundwater flow of 0.01 m^3/m^2, year.

Table 3 Flow rate of water [m^3/year] through each block based on a specific ground-water flow of 0.01 m^3/m^2, year

From block	To block	Flow
26	27	0.012
27	28	0.012
28	29	0.012
29	30	0.012
30	46	0.012
31	32	30.5
32	33	30.5
33	34	30.5
34	35	30.5
35	48	30.5
36	37	11.0
37	38	11.0
38	39	11.0
39	40	11.0
40	48	11.0
41	42	2.2
42	43	2.2
43	44	2.2
44	45	2.2
45	48	2.2
46	48	0.012
48	47	43.712
Inflow	26	0.012
Inflow	31	30.5
Inflow	36	11.0
Inflow	41	2.2
47	Outflow	43.712

References

Hartley L and Lindgren M, 1997. Flow and transport parameters for SFL 3-5 – Estimates from regional numerical models for Beberg and Ceberg. Appendix in Skagius *et al.* (1999).

Holmén J, 1997. On the flow of groundwater in closed tunnels. Generic hydrogeological modelling of nuclear waste repository SFL 3-5. SKB Technical Report TR 97-10, Swedish Nuclear Fuel and Waste Management Co., Stockholm.

Lindgren M, Pers K, Skagius K, Wiborgh M, Brodén K, Carlsson J, Riggare P, Skogsberg M, 1998. Low and intermediate level waste in SFL 3-5: Reference inventory. Reg. No: 19.41/DL31. Swedish Nuclear Fuel and Waste Management Co., Stockholm

Skagius K, Pettersson M, Wiborgh M, Albinsson Y, Holgersson S, 1999. Compilation of data for the analysis of radionuclide migration from SFL 3-5. SKB Report R-99-13, Swedish Nuclear Fuel and Waste Management Co., Stockholm.

Svensson U, 1997. Flow and transport from SFL 3-5 – Estimates from regional numerical model. Appendix in Skagius *et al.* (1999).

Appendix D: Corrosion rate limited release of radionuclides in SFL 3-5

Michael Pettersson [a]

Luis Moreno [b]

[a] Kemakta Konsult AB

[b] Dept. Chem. Eng. and Technol., Royal Inst. of Technology

1 Introduction

The waste in SFL 5 originates from the central part of the reactor, and thus the total activity in SFL 5 is dominated by induced activity (Lindgren *et al.,* 1998). The waste in SFL 3 also contains some induced activity. While surface contamination to a large extent can be assumed to be instantaneously available for dissolution in water in contact with the waste, a metal component has to corrode before induced activity is released. Consequently, it is realistic to assume that the release rate of induced activity is reduced in comparison to that of surface contamination. This appendix describes how corrosion rate limited release of radionuclides is modelled using COMP24.

2 Modelling of corrosion rate limited release using COMP24

COMP24 can only handle water streams that do not contain any nuclides when entering the model system. Accordingly it is not possible to simulate a continuous release of radionuclides due to corrosion. However, this can be circumvented by introducing blocks representing fictitious sources (blocks 6-10 in Figure 1) in the model. The initial activity of the nuclide is confined to the fictitious sources only and the initial activity in the true sources (blocks 1-5) is set equal to zero. A very small fictitious water flows through each fictitious source, through the blocks representing the true sources and into the porous concrete surrounding the waste (blocks 26-30). Part of the water flowing through the SFL 3 and SFL 5 tunnels (true water flow) is modelled as flowing through the porous concrete, as indicated in Figure 1.

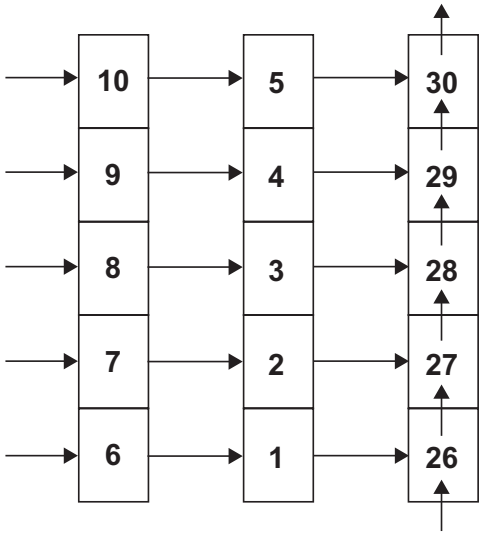

Figure 1 Schematic picture of fictitious and true water flow.

The release rate due to corrosion is approximated with:

$$g_{corr}^{i} = \frac{n_{tot}^{i} \cdot r}{(L/2)} = \frac{n_{tot}^{i}}{t_{corr}} \qquad (1)$$

where g^{i}_{corr} = release rate due to corrosion (mole/yr)

n^{i}_{tot} = total amount of nuclide "i" in the sources (mole)

r = corrosion rate (m/yr)

L = thickness of the metal plate[1] (m)t_{corr} = time to corrode the metal (yr)

Inherent in this equation is the assumption that the induced activity is homogeneously distributed in the metal. The amount of nuclide being transported between the fictitious and the true source per unit time should be equal to the release rate due to corrosion, and is given by:

$$g_{corr}^{i} = Q \cdot c_i \qquad (2)$$

where Q = fictitious flow rate of water through the fictitious source (m^3/yr)

c_i = concentration of nuclide "i" in the fictitious source (mole/m^3)

The values of Q and c_i can be chosen arbitrarily as long as Equation (2) is fulfilled and the fictitious flow rate is negligible in comparison to the true flow rate through the porous concrete.

The block representing a source is thought to consist of two parts; a solid inventory and one containing the species dissolved in the water and sorbed in the solid material. Equilibrium between the species dissolved and the solid inventory is assumed. If the nuclide solubility is small in comparison to the nuclide inventory, the concentration in a source is equal to the value of the nuclide solubility specified by the user. On the other hand, if the nuclide solubility is large in comparison to the inventory, the whole inventory is dissolved in the water and is sorbed in the solid material and the concentration in the source equals the inventory divided by the capacity of the source. Thus the nuclide solubility specified by the user can be used to obtain the concentration c_i in the fictitious source. To prevent that the concentration in the fictitious source exceeds c_i, the solubility of the nuclide is set to the same value as c_i. Note that the solubility of a nuclide is the same for all blocks. Therefore, the solubility c_i obtained from Equation (2) must be sufficiently large that the nuclide concentration obtained in any blocks in the model does not exceed the chosen solubility.

One also has to force COMP24 to dissolve the initial inventory within the same time as the time needed to corrode the waste. This is obtained by assigning an appropriate value to the volume of the fictitious sources (V_{fict}). The value that is assigned to a fictitious source is:

---

[1] It is assumed that the metal has the shape of a plane plate.

$$V_{fict} = \frac{g^{i}_{corr} \cdot t}{c_i} \tag{3}$$

where t is time (equal to 1 year), i.e. the volume is identical to the annual flow through the block.

To avoid that nuclides are transported from the fictitious source to the true one by diffusion, a large diffusive resistance is set between these sources. The convective and the diffusive mass transfer is given by:

$$N_{A,konv} = u \cdot A \cdot c = Q \cdot c \tag{4}$$

and

$$N_{A,diff} = \frac{D_p \cdot A \cdot c \cdot \varepsilon}{L} \tag{5}$$

where u = the velocity through the porous media (Darcy velocity) (m^3/m^2, yr)

Q = the volumetric flow (m^3/yr)

A = the cross sectional area of the porous media (m^2)

c = the concentration in the porous media (mole/m^3)

ε = the porosity of the porous media (-)

D_p = the pore diffusivity (m^2/yr)

L = the diffusion length (m)

Peclets number Pe is defined as the ratio of the convective and the diffusive transport i.e.:

$$Pe = Q \cdot c \cdot \frac{L}{D_p \cdot A \cdot c \cdot \varepsilon} = \frac{Q \cdot L}{\varepsilon \cdot D_p \cdot A} = \frac{Q \cdot L}{D_e \cdot A} \tag{6}$$

The diffusive transfer is negligible in comparison to the convective transfer when Pe >> 1. The diffusive transport between two sources is in COMP24 given by the parameter XRADD, which is defined as:

$$XRADD = \frac{L}{D_e \cdot A} \tag{7}$$

Thus, XRADD should be set to a sufficiently high value that Pe >> 1 using the fictitious flow rate of water through the fictitious source as Q.

In the present model, there is no water flowing through the true sources but through porous concrete surrounding the waste (Figure 1). The nuclides are then transported between the true sources and the porous concrete through diffusion. It is then important

to choose a fictitious flow rate of water which together with the parameters specified for the diffusive transport (L, D_e and A) between the true sources and the blocks representing the porous concrete results in Pe << 1.

3 Estimation of release rate due to corrosion

3.1 Introduction

As shown in Equation (1) the release rate due to corrosion depends on the corrosion rate of the material and of the thickness of the material. The waste to be deposited in SFL 3 and in SFL 5 arise both during maintenance and decommissioning of the nuclear power plants, and part of the waste originates from research, medicine, and industry. Thus, the waste is heterogeneous, both in terms of material and dimensions but also in activity content. This implies that the release rate of nuclides due to corrosion also varies between different types of waste. To model the release due to corrosion in COMP24, the release rate must be constant in time. It is therefore necessary to estimate a representative mean value of the nuclide release rate. It is possible to assign different values of the release rate for different nuclides in COMP24, why the estimated mean release rate can be nuclide specific. To estimate a nuclide specific release rate due to corrosion, a reference waste has to be defined.

3.2 Reference waste

Based on available documentation about the waste, it has been divided into different waste categories (Lindgren *et al.,* 1998). The waste categories for SFL 5 are shown in Table 1. To estimate a nuclide specific release rate due to corrosion, the first step is to determine which waste categories that dominate the total amount of induced activity for that specific nuclide. Each category consists of a waste component made of a certain material (e.g. stainless steel) with an average thickness in which the induced activity of the nuclide is contained. Sometimes a category consists of waste made of different materials or different components made of the same material but with different average thickness, see for example "Used parts" in Table 1. In general the material/component that contains the main part of the induced activity for the specific nuclide in that category is in this work defined to represent the category. This means that for one nuclide a category can be represented by one material/component, but for another nuclide the same category may be represented by another material/component. For example, in the category "Fuel boxes and SRM/IRM detectors" in SFL 5 ^{93}Zr is represented by 2.5 mm thick Zircalloy but ^{36}Cl is represented by stainless steel with a thickness of 6 mm.

Table 1 **Summary of materials and material thickness in different waste categories in SFL 5. SS = stainless steel, BS = boron steel, CS = carbon steel, B_4C = boron carbide. (Lindgren *et al.*, 1998).**

Waste category	Material (mean thickness in mm)
Core grid	SS (9)
Moderator tank	SS (40)
Moderator tank cover	SS (28)
Core spray	SS (6)
Guide tubes	SS (31)
Instrumental tubes	SS (3)
Boron plates	BS (4), SS (-)
Control rods	SS (7.5), Inconel (-), B_4C (-)
Used parts	SS (6), SS (7.5), Zircalloy (2.5), Inconel (-), B_4C (-), hafnium (-)
Fuel channels	Zircalloy (2.5)
Transition pieces	SS (6)
Fuel boxes and SRM/IRM detectors	SS (6), SS (-), Zircalloy (2.5)
Fuel boxes and PRM detectors	SS (6), SS (2), Zircalloy (2.5)
PRM detectors and tubes	SS (2)
TIP detectors	CS (2.2), SS (-), MgO (-)
PWR reactor tank	CS (200)
Burnable absorbers	SS (3), boron glass (-)
Internal parts	SS (14), chromium (-)
Decommissioning waste from Studsvik	SS (50), beryllium (10)

3.3 Nuclide specific mean release rate due to corrosion

The second step is to estimate a representative mean value of the nuclide release rate for each nuclide. This is obtained by assuming that the material/component has the shape of a plane plate with thickness L that corrodes on both sides. First, for each nuclide, a category specific corrosion time is estimated as:

$$t^i_{corr,j} = \frac{(L^i_j / 2)}{r^i_j} \tag{8}$$

where r is the corrosion rate of the material defined for waste category "j" and nuclide "i". Second, based on the waste categories that dominate the content of induced activity for a specific nuclide, called primary categories, an average corrosion time is estimated:

$$\overline{t^i_{corr}} = \frac{\sum_{j=1}^{N} t^i_{corr,j}}{N} \tag{9}$$

The nuclide specific mean release rate is finally obtained by dividing the nuclide activity with the mean corrosion time:

$$\overline{g_{corr}^{i}} = \frac{n_{tot}^{i}}{\overline{t_{corr}^{i}}} \tag{10}$$

4 Application to SFL 3-5

4.1 SFL 5

4.1.1 Nuclides modelled as corrosion rate limited

The waste foreseen to be deposited in SFL 5 is divided into 19 different waste categories, e.g. core grid and control rods (Table 1). The waste contains a considerable amount of metallic components. The main material in the waste to be deposited in SFL 5 is stainless steel, but there are also other steel grades (carbon steel and boron steel), Zircalloy, and boron carbide (B_4C).

Of the nuclides modelled in SFL 5 (see Section 6.3 in main report), the activity of ^{79}Se, ^{90}Sr, ^{129}I, ^{210}Pb, ^{226}Ra, ^{230}Th, ^{234}U, and ^{238}U is entirely due to surface contamination. The release of these nuclides is therefore not modelled as corrosion rate limited. Conservatively ^{99}Tc is not considered to be a corrosion rate limited nuclide, even though approximately 83 % of its activity is induced activity. For ^{3}H, ^{10}Be, ^{14}C, ^{36}Cl, ^{59}Ni, ^{93}Zr, and ^{93}Mo the total activity is dominated by induced activity (0.1 % of the total activity or less is surface contamination). The release rate of these nuclides can therefore be modelled as corrosion rate limited.

Almost the whole inventory of ^{3}H and ^{10}Be is within boron carbide in control rods. No reasonable explanation to why ^{3}H or ^{10}Be should be chemically bonded to boron carbide has been found. It is therefore not reasonable to take any delay in release from the material into account. On the other hand, the boron carbide is contained in drilled holes in the absorber plates of the control rods. These holes are sealed welded. Thickness of material of the "lid" is at least 1 mm (Carlsson, 1999). Assuming a corrosion rate of 1 μm/year, which locally can be a factor of ten higher, it will take at least 100 years before the inventory in boron carbide can be transported away from the waste. From experience it is known that there are fractures in some rods. A reasonable assumption is that there are fractures in 20 % of the rods. Each rod consists of four separate chambers, why 5 % of the initial inventory can be released instantaneously through such fractures (Carlsson, 1999).

4.2 Estimation of mean corrosion time

For ^{14}C, ^{36}Cl, ^{59}Ni, and ^{93}Mo the major part of the induced activity is within steel and for ^{93}Zr within Zircalloy (Lindgren *et al.,* 1998). In this work a corrosion rate of 1 μm/year is used for all steel grades (stainless, carbon and boron) and of 0.01 μm/year for Zircalloy (Wiborgh, 1995). The primary waste categories on which the average

corrosion time is estimated are shown in Table 2. Included in this table is the material defined to represent the category and the mean thickness of the material, L_j^i. The estimated mean corrosion time based on primary waste categories is presented in Table 3.

Table 2 Waste categories on which the calculated mean corrosion time is based upon. P = primary category, S = secondary category. Type of material and mean thickness of material within brackets. SS = stainless steel, BS = boron steel, CS = carbon steel, Zirc = Zircalloy.

Waste category	^{14}C	^{36}Cl	^{59}Ni	^{93}Zr	^{93}Mo
Core grid	P (SS 9 mm)	P (SS 9 mm)	P (SS 9 mm)		P (SS 9 mm)
Moderator tank	P (SS 40 mm)	P (SS 40 mm)	P (SS 40 mm)		P (SS 40 mm)
Moderator tank cover		S (SS 28 mm)			
Core spray		S (SS 6 mm)			S (SS 6 mm)
Boron plates	S (BS 4 mm)	S (BS 4 mm)			S (BS 4 mm)
Control rods	P (SS 7.5 mm)	P (SS 7.5 mm)	P (SS 7.5 mm)		P (SS 7.5 mm)
Used parts				P (Zirc 2.5 mm)	
Fuel channels	S (Zirc 2.5 mm)	S (Zirc 2.5 mm)		P (Zirc 2.5 mm)	S (Zirc 2.5 mm)
Transition pieces		S (SS 6 mm)			S (SS 6 mm)
Fuel boxes and SRM/IRM detectors	S (Zirc 2.5 mm)	S (SS 6 mm)		P (Zirc 2.5 mm)	S (SS 6 mm)
Fuel boxes and PRM detectors	S (SS 2 mm)	P (SS 2 mm)	S (SS 2 mm)	P (Zirc 2.5 mm)	P (SS 2 mm)
PRM detectors and tubes	S (SS 2 mm)	P (SS 2 mm)	P (SS 2 mm)		P (SS 2 mm)
PWR reactor tank	P (CS 200 mm)	P (CS 200 mm)	P (CS 200 mm)		P (CS 200 mm)
Burnable absorbers		P (SS 3 mm)			P (SS 3 mm)
Internal parts	P (SS 14 mm)	P (SS 14 mm)	P (SS 14 mm)		P (SS 14 mm)
Decommisioning waste from Studsvik	S (SS 50 mm)	S (SS 50 mm)	S (SS 50 mm)		S (SS 50 mm)

The waste in SFL 5 contains the PWR reactor tank that is made of exceptional thick material (200 mm). Some other categories contain material which is a few cm thick but most of them material of some millimetre. Categories that contain material/components that are thick have a significant influence of the estimated mean value. If the PWR reactor tank is omitted, the calculated mean corrosion time is reduced for all nuclides for which the PWR reactor tank make a major contribution to the total activity, Table 3.

Table 3 Estimated mean corrosion time in SFL 5.

Nuclide	Half-life	Mean corrosion time based on primary categories	Mean corrosion time based on primary categories excl. category "PWR reactor tank"	Mean corrosion time based on primary and secondary categories	Mean corrosion time based on primary and secondary categories excl. category "PWR reactor tank"
	[year]	[year]	[year]	[year]	[year]
^{14}C	$5.7 \cdot 10^3$	27,000	8,800	38,000	31,000
^{36}Cl	$3.0 \cdot 10^5$	17,000	5,500	21,000	15,000
^{59}Ni	$7.6 \cdot 10^4$	23,000	7,200	20,000	8,900
^{93}Zr	$1.5 \cdot 10^6$	125,000	125,000	–	–
^{93}Mo	$4.0 \cdot 10^3$	17,000	5,500	21,000	15,000

The induced activity in the reactor tank comprises (depending on nuclide) up to 20 % of the total nuclide activity in SFL 5. In practice this activity will be released during a very long period of time in comparison to the rest of the inventory. Two test cases have been modelled for comparison. In the first case (PWR), the transport of induced activity in the reactor tank is modelled assuming that the activity is constantly released from the tank during a period of 100,000 years. This corresponds to a corrosion rate of 1 μm/year and a material thickness of 200 mm. In the second case (excl. PWR), the remaining nuclide activity (i.e. both induced activity and surface contamination) is modelled. The amount of nuclides being available for transport from the waste containers is in this case determined by the release rate corresponding to the mean corrosion time based on primary categories excluding the PWR reactor tank given in Table 3. It is found that the release rate from the far field in Aberg for the first test case is always lower than or equal to the release rate for the second test case (Figure 2). The maximum release rate from the far field in Aberg for the first test case is at least one order of magnitude lower than for the second case. Included in Figure 2 is the release rate obtained if the activity in the PWR is included in the modelled inventory, but the corrosion rate is based on primary categories excluding the PWR.

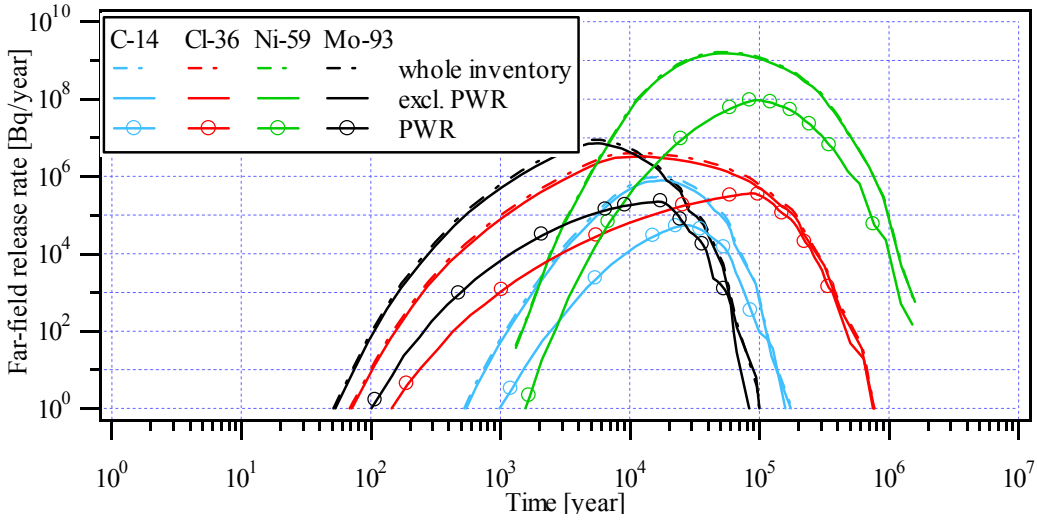

Figure 2 *Comparison of far-field release rate based on a) corrosion of PWR tank, b) corrosion of waste excluding the PWR tank and c) as b) but including the activity in the PWR tank.*

The results presented so far are based on primary waste categories. The induced activity in the primary categories include between 90 % and 97 % of the total nuclide activity in SFL 5. Including secondary categories (see Table 2) with somewhat less (but still not negligible) induced activity, the included induced activity increases to more than 98 % of the total nuclide activity. Taking both primary and secondary categories into account the estimated mean corrosion time normally increases (Table 3).

4.3 Estimation of input data to COMP24

In the model for SFL 5, the waste is divided into five different sources (blocks 1-5 in Figure 1). Each source contains 20 % of the total activity. Five fictitious sources (blocks 6-10) are connected to blocks 1-5.

The mean corrosion time estimated in the previous section and the inventory modelled are summarised in Table 4. As the fictitious water flows from a fictitious source to a true source (e.g. from 6 to 1 in Figure 1) it transfers the same amount of nuclides as that being released due to corrosion of the waste. For ^{36}Cl for example, the release rate in each fictitious source due to corrosion is:

$$g_{corr,6-10}^{Cl-36} = \frac{0.20 \cdot 4.57}{5500} = 1.66 \cdot 10^{-4}\ moles / year \qquad (11)$$

The estimated release rates are included in Table 4.

Table 4 Summary of input data modelling of corrosion rate limited release of nuclides in SFL 5.

Nuclide	Half-life [year]	Modelled inventory [2] [mole]	Mean corrosion time [year]	Mean release rate [mole/year]
^{14}C	$5.7 \cdot 10^{3}$	57.1	8,800	$1.30 \cdot 10^{-3}$
^{36}Cl	$3.0 \cdot 10^{5}$	4.57	5,500	$1.66 \cdot 10^{-4}$
^{59}Ni	$7.6 \cdot 10^{4}$	7,100	7,200	$1.97 \cdot 10^{-1}$
^{93}Zr	$1.5 \cdot 10^{6}$	259	125,000	$4.15 \cdot 10^{-4}$
^{93}Mo	$4.0 \cdot 10^{3}$	0.428	5,500	$1.56 \cdot 10^{-5}$

The true water flow through the porous concrete (blocks 31-35) is shown in Table 5. The fictitious flow rate should be negligible in comparison to the true flow rate of water. The total fictitious flow rate is arbitrarily set to 0.1 % of the true water flow rate through the porous concrete. Since there are five fictitious sources, the fictitious water flow rate through each fictitious source is 1/5 of the total fictitious flow rate. According to Equation (2), for Aberg the concentration of ^{36}Cl in the fictitious source is:

$$c_{Cl-36} = \frac{1.66 \cdot 10^{-4}}{2.4 \cdot 10^{-6}} = 69.2 \text{ mol/m}^3 \tag{12}$$

This is the value specified in the input data file as the solubility of ^{36}Cl. The corresponding values for Beberg and Ceberg are given in Table 5

Table 5 Summary of estimated data for modelling of corrosion rate limited release in SFL 5.

Material	Aberg	Beberg	Ceberg
True water flow rate [m^3/yr]	$1.2 \cdot 10^{-2}$	$1.2 \cdot 10^{-3}$	$1.2 \cdot 10^{-4}$
Fictitious water flow rate [m^3/yr]			
- Total	$1.2 \cdot 10^{-5}$	$1.2 \cdot 10^{-6}$	$1.2 \cdot 10^{-7}$
- Per fictitious source	$2.4 \cdot 10^{-6}$	$2.4 \cdot 10^{-7}$	$2.4 \cdot 10^{-8}$
Nuclide concentration per fictitious source [moles/m^3]			
- ^{14}C	540	5,400	54,000
- ^{36}Cl	69.2	692	6,920
- ^{59}Ni	$8.2 \cdot 10^{4}$	$8.2 \cdot 10^{5}$	$8.2 \cdot 10^{6}$
- ^{93}Zr	173	1,730	17,300
- ^{93}Mo	6.48	64.8	648
Volume of fictitious source [m^3]			
- Per source	$2.4 \cdot 10^{-6}$	$2.4 \cdot 10^{-7}$	$2.4 \cdot 10^{-8}$

[2] Includes the whole inventory in SFL 5 (both induced activity and CRUD) except for induced activity in PWR reactor tank.

According to Equation (3), for Aberg the volume of the fictitious blocks is set to:

$$V_{fict,Cl-36} = \frac{1.66 \cdot 10^{-4} \cdot 1}{69.2} = 2.4 \cdot 10^{-6} \text{ m}^3 \qquad (13)$$

The corresponding values for Beberg and Ceberg are given in Table 5.

To avoid that nuclides are transported from the fictitious source to the true one by diffusion, a large diffusive resistance is set between the sources. In this work XRADD, defined in equation (7), is set to 10^{12} yr/m^3 for the transport between a fictitious source and a true source in Aberg, Beberg as well as Ceberg. This corresponds to $2.4 \cdot 10^4 \leq Pe \leq 2.4 \cdot 10^6$.

Using the data given in Table 5, the estimated mean release rate of ^{59}Ni due to corrosion leads to a nuclide concentration in the true sources that exceeds the solubility of nickel in concrete water (10^{-7} mole/litre). The migration ^{59}Ni is therefore modelled as being limited by solubility instead of the corrosion rate of waste.

The corrosion rate for steel in anaerobic conditions is usually reported to be in the range 10^{-7} – 10^{-5} m/year (Höglund and Bengtsson, 1991), why 10^{-6} m/year used in this work is considered to be a reasonable value. The influence of corrosion rate for steel on the near-field release rate in Aberg is shown in Figure 3. Changing the corrosion rate from 10^{-5} to 10^{-6} m/year has a limited influence on the maximum far-field release rate. For a corrosion rate of 10^{-7} m/year, the maximum release rate of ^{14}C and of ^{93}Mo is reduced approximately by a factor 4 in comparison to that for a corrosion rate of 10^{-6} m/year. For ^{36}Cl on the other hand, there is only a minor difference. Included in this figure is the release rate assuming that the whole inventory of a nuclide is instantaneously available for dissolution in water in contact with the waste.

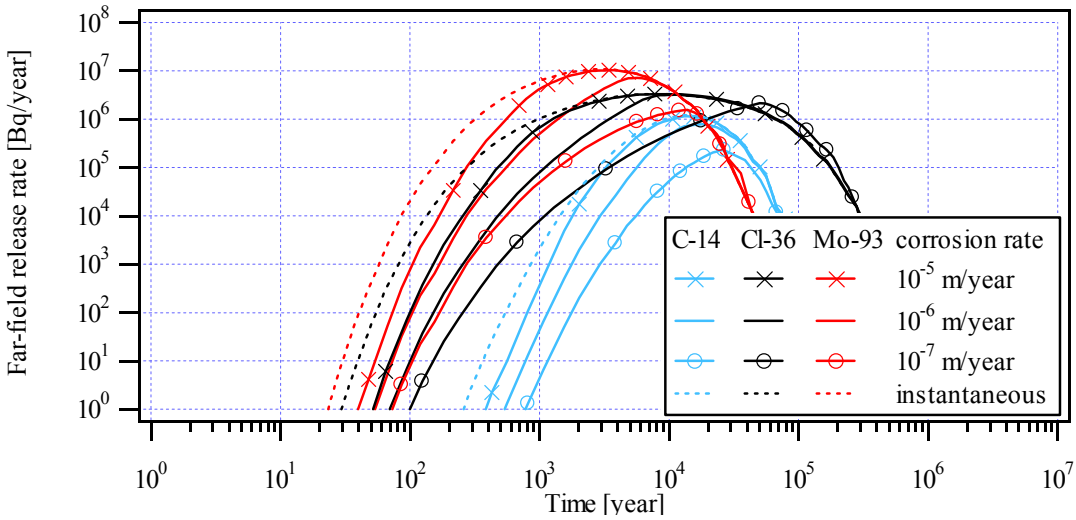

Figure 3 Influence of steel corrosion rate on far-field release rate in Aberg.

To summarise, corrosion rate limited release is taken into account for the inventory of ^{14}C, ^{36}Cl, ^{93}Zr, and ^{93}Mo in SFL 5. The estimated mean corrosion times are based on primary categories, but the reactor tank is neglected. Conservatively, secondary categories are also neglected. The inventory for ^{14}C, ^{36}Cl, ^{93}Zr, and ^{93}Mo on which the estimated mean release rates (Table 4) are based upon is the total inventory in SFL 5 excluding the induced activity in the PWR reactor tank. For ^{59}Ni it is found that modelling the release of the nuclide as corrosion rate limited as described here, results in a pore water concentration in the waste exceeding its solubility. The transport of ^{59}Ni is therefore modelled as being solubility-limited instead. For ^{3}H and ^{10}Be it is assumed that 5 % of the initial inventory (corresponding to fractures in 20 % of the rods) is instantaneously available for dissolution in water. Remaining 95 % is allowed to decay for 100 years, after which the inventory is available for dissolution in water.

5 SFL 4

Of the total activity in waste to be deposited in SFL 4 is only about 0.1 % due to induced activity. For all nuclides except ^{3}H, the induced activity constitutes to less than 1 % of the total nuclide specific activity. For ^{3}H approximately 40 % of the total activity is induced activity. Conservatively, ^{3}H is not modelled as being corrosion rate limited in its release.

6 SFL 3

In contradiction to what was stated in Section 4.1 about the waste in SFL 5, the waste to be deposited in SFL 3 contains only a minor part of metallic waste (Lindgren *et al.,* 1998). For the majority of the nuclides modelled in SFL 3 (see Section 6.3 in main report), the activity is dominated by surface contamination. The exceptions are ^{3}H, inorganic ^{14}C, ^{36}Cl, ^{59}Ni, and ^{93}Mo.

The majority (approximately 90 %) of the activity of ^{36}Cl and ^{59}Ni is induced activity within the waste category “Concrete containers with intermediate level waste”. The waste consists to a large extent of steel and aluminium components with a mean thickness of 5 mm and 10 mm respectively (Lindgren *et al.,* 1998). Assuming a corrosion rate of 1 μm/year for steel it would take 2,500 years to corrode the waste made of steel, which is one to two order of magnitudes faster than the nuclides half-life. Assuming that the whole inventory of these nuclides is instantaneously available for dissolution in water in contact with the waste, the maximum release rate of ^{36}Cl from the far field is obtained after 6,000 to 9,000 years in Aberg and after approximately 30,000 years in Ceberg. Modelling the release of the inventory of ^{36}Cl as being limited by the corrosion rate of steel would reduce the release rate from the far field for short times after repository closure, but the effect on the maximum release rate would be limited. This is shown in Figure 3 for corrosion rate limited release from SFL 5. The models for SFL 3 and SFL 5 are with a few exceptions identical why the results are applicable to SFL 3 as well. ^{59}Ni is released from the far field after much longer times than ^{36}Cl why the effect of corrosion on the release rate will be even smaller. The corrosion rate of aluminium is higher than for steel. Corrosion rates of between a few mm/year up to 40 mm/year are reported (Wiborgh *et al.,* 1986). Thus the release rate from aluminium would be even faster than from steel.

Roughly half of the inventory of inorganic ^{14}C and ^{93}Mo is induced activity. As for ^{36}Cl and ^{59}Ni, the dominating waste category for induced activity is " Concrete containers with intermediate level waste". If the whole inventory of inorganic ^{14}C and ^{93}Mo is instantaneously available for dissolution in water, the maximum release rate from the far field in Aberg is obtained 9,000 years and 2,500 years after repository closure respectively. Taking the corrosion rate of steel into account will have approximately the same effect as for ^{36}Cl, i.e. the reduction in maximum release rate is limited (see Figure 3).

Approximately 90 % of the inventory of ^{3}H is induced activity. This is contained in material made of titanium hydride. The activity content in this material should be available in for release in a way that is similar to activity contained in steel and Zircalloy. Conservatively, it is assumed that the whole inventory of ^{3}H is instantaneously dissolved in water in contact with the waste.

To summarise, there are a few nuclides modelled in SFL 3 whose activity is dominated by induced activity. With the exception of ^{3}H, the main part of the induced activity is contained in a waste category that consists of waste made of both steel and aluminium. Assuming that all induced activity is contained in steel components and that the release rate is determined by the corrosion rate of steel instead of having the whole inventory instantaneously available for dissolution in water, has a limited effect on the maximum release rate from the far field. Furthermore, there is no evidence of that the main part of the induced activity should be in steel and not in aluminium. Since the corrosion rate of aluminium is higher than for steel the effect of corrosion rate limited release should be even less than what is shown for corrosion rate limited release for steel.

References

Carlsson, J, 1999. Personal communication, Swedish Nuclear Fuel and Waste Management Co, Stockholm.

Höglund L O and Bengtsson A, 1991. Some chemical and physical processes related to the long-term performance of the SFR repository, SKB SFR 91-06, Swedish Nuclear Fuel and Waste Management Co, Stockholm.

Lindgren M, Pers K, Skagius K, Wiborgh M, Brodén K, Carlsson J, Riggare P och Skogsberg M, 1998. Low and Intermediate Level Waste in SFL 3-5: Refrence Inventory, Reg. No: 19.41/DL 31, Swedish Nuclear Fuel and Waste Management Co, Stockholm.

Wiborgh M, 1995. Prestudy of final disposal of long-lived low and intermediate level waste, SKB Technical Report TR 95-03, Swedish Nuclear Fuel and Waste Management Co., Stockholm.

Wiborgh M, Höglund L O and Pers K, 1986. Gas Formation in a L/ILW Repository and Gas Transport in the Host Rock, Technical Report 85-17, Nagra, Baden Switzerland.

Appendix E: Screening calculations

Michael Pettersson

Kemakta Konsult AB

1 Description of screening calculations

The radionuclides reported for the waste in SFL 3-5 are summarised in Table 2.1 in main report. However, the estimated activity of many of them is low and/or the nuclides have a half-life that is short in comparison to the time scales for their migration to the biosphere. To reduce the calculation time, and the amount of nuclide specific input data needed for modelling the geosphere migration, screening calculations have been performed. This procedure is described below.

The screening is made independently for the three repository parts (SFL 3, SFL 4 and SFL 5). For each repository part four different screening calculations are performed, using site specific input data regarding water flow rate and type of water (saline or non-saline). The calculations for SFL 3 are based on the assumption that ISA does not influence the transport of radionuclides, and the calculations for SFL 4 does not include the CRUD inventory.

First, the near-field transport of all reported radionuclides (Table 2.1 in main report) except ^{40}K, which is only estimated for SFL 3, and organic ^{14}C is modelled. The physical and chemical data used for the near field are given in Chapter 5 in main report. Chain decay of nuclides in the chains 4N, 4N+1, 4N+2 and 4N+3 has been accounted for as shown in Figure 1. ^{228}Th has not been included in the radionuclide inventory for SFL 3-5 (Lindgren *et al.,* 1998), and is therefore not included in chain 4N in the migration calculations either. ^{232}U is therefore modelled as a single nuclide in the screening calculations. Only 18 % of ^{242m}Am decays to ^{242}Pu, why the formation of ^{242}Pu from ^{242m}Am is neglected. Chain decay of other nuclides than those shown in Figure 1 has not been accounted for. The nuclides thereby neglected are mainly nuclides with a half-life of less than one year. Exceptions are ^{93m}Nb ($t_{1/2}$ = 13.6 years), ^{147}Sm ($1.1 \cdot 10^{11}$years) and ^{152}Gd ($1.1 \cdot 10^{14}$years).

Then the release rate from the near field is recalculated into an intermediate dose using committed effective doses from intake of radionuclides by adults (IAEA, 1996). Based on these results, radionuclides giving a low or a negligible contribution to the total dose from the release from the repository part is excluded from the inventory.

2 Results

The release rate from the near field recalculated into an intermediate dose for the screening calculations are shown in Figures 2 – 13. The nuclides being neglected in the work on migration of radionuclides from SFL 3-5 are given in Tables 1-3. The term "Low" in these tables indicates that the intermediate dose is low in comparison to other nuclides at corresponding times, and the term "Negligible" means that the maximum intermediate dose does not exceed 10^{-10} Sv/year for times up to 10^7 years from repository closure. The radionuclides remaining after the screening and their activity are given in Table 4.

^{244}Pu gives a negligible intermediate dose and is therefore neglected after the screening calculations. Unlike some other nuclides in the modelled chains (discussed in Chapter 6 in main report), the inventory of ^{244}Pu is not transferred to a nuclide later in the chain

(4N). The inventory of ^{244}Pu (in mole) in SFL 3-5 is negligible in comparison to that of ^{240}Pu and ^{236}U. Furthermore, the half-life of ^{244}Pu is of the same order of magnitude as ^{236}U. That the inventory of ^{244}Pu has been neglected has therefore no influence on the dose from nuclides in chain 4N released to recipient in Aberg, Beberg or Ceberg.

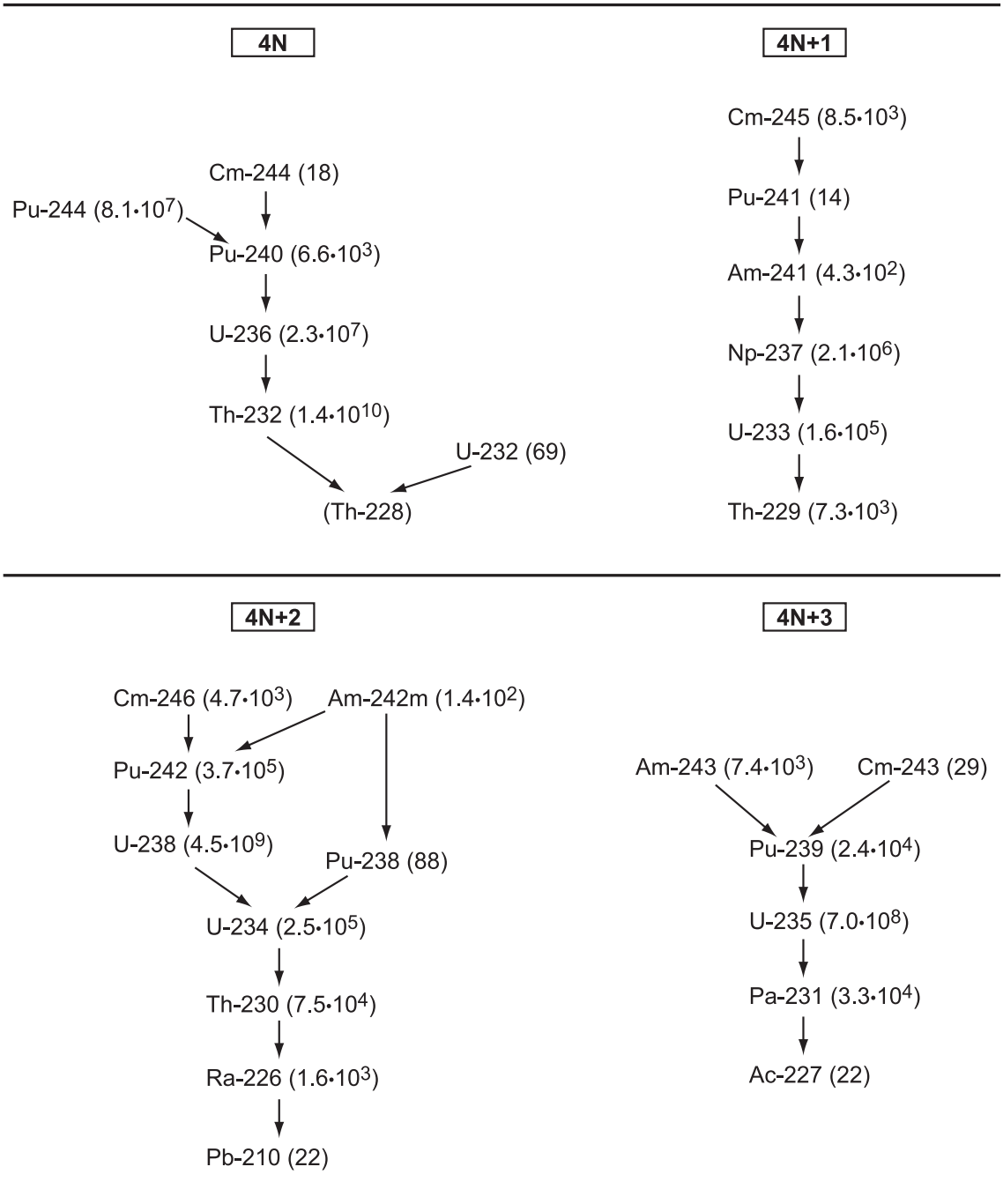

Figure 1 Radionuclides in the natural decay chains.

Table 1 Nuclides being neglected in the calculations for SFL 3.

Nuclide	Comment
^{10}Be	Low intermediate dose from the near-field in comparison to that of ^{59}Ni, ^{135}Cs, ^{210}Pb and ^{226}Ra
^{55}Fe	Negligible intermediate dose from the near-field
^{60}Co	Negligible intermediate dose from the near-field
^{63}Ni	Low to negligible intermediate dose from the near-field in comparison to that of ^{93}Mo
^{93m}Nb	Negligible intermediate dose from the near-field
^{94}Nb	Low to negligible intermediate dose from the near-field in comparison to that of ^{59}Ni and ^{99}Tc
^{107}Pd	Low intermediate dose from the near-field in comparison to that of ^{59}Ni and ^{99}Tc
^{108m}Ag	Low to negligible intermediate dose from the near-field in comparison to that of ^{36}Cl, ^{59}Ni and ^{93}Mo
^{113m}Cd	Negligible intermediate dose from the near-field
^{126}Sn	Low intermediate dose from the near-field in comparison to that of ^{59}Ni, ^{79}Se and ^{99}Tc
^{125}Sb	Negligible intermediate dose from the near-field
^{134}Cs	Negligible intermediate dose from the near-field
^{137}Cs	Negligible intermediate dose from the near-field
^{133}Ba	Negligible intermediate dose from the near-field
^{147}Pm	Negligible intermediate dose from the near-field
^{151}Sm	Negligible intermediate dose from the near-field
^{152}Eu	Negligible intermediate dose from the near-field
^{154}Eu	Negligible intermediate dose from the near-field
^{155}Eu	Negligible intermediate dose from the near-field
^{166m}Ho	Negligible intermediate dose from the near-field
^{227}Ac	Low intermediate dose from the near field in comparison to that of ^{210}Pb and ^{226}Ra.
^{231}Pa	Low intermediate dose from the near-field in comparison to that of ^{210}Pb and ^{226}Ra
^{232}U	Negligible intermediate dose from the near-field
^{235}U	Low intermediate dose from the near field in comparison to that of ^{210}Pb and ^{226}Ra.
^{239}Pu	Low intermediate dose from the near field in comparison to that of ^{210}Pb and ^{226}Ra.
^{244}Pu	Negligible intermediate dose from the near-field
^{243}Am	Negligible intermediate dose from the near-field
^{243}Cm	Negligible intermediate dose from the near-field

Table 2 Nuclides being neglected in the calculations for SFL 4.

Nuclide	Comment
^{10}Be	Negligible intermediate dose from the near-field
^{55}Fe	Low to negligible intermediate dose from the near field in comparison to that of ^{90}Sr and ^{137}Cs.
^{93}Zr	Low to negligible intermediate dose from the near-field in comparison to that of ^{94}Nb and ^{99}Tc.
^{93m}Nb	Negligible intermediate dose from the near-field
^{107}Pd	Negligible intermediate dose from the near-field
^{108m}Ag	Low to negligible intermediate dose from the near-field in comparison to that of ^{59}Ni, ^{63}Ni, and ^{137}Cs
^{113m}Cd	Low to negligible intermediate dose from the near field in comparison to that of ^{63}Ni and ^{137}Cs.
^{126}Sn	Negligible intermediate dose from the near-field
^{125}Sb	Negligible intermediate dose from the near-field
^{134}Cs	Low to negligible intermediate dose from the near-field in comparison to that of ^{137}Cs
^{135}Cs	Low to negligible intermediate dose from the near-field in comparison to that of ^{59}Ni and ^{137}Cs
^{133}Ba	Low to negligible intermediate dose from the near-field in comparison to that of ^{137}Cs
^{147}Pm	Negligible intermediate dose from the near-field
^{151}Sm	Negligible intermediate dose from the near-field
^{152}Eu	Negligible intermediate dose from the near-field
^{154}Eu	Negligible intermediate dose from the near-field
^{155}Eu	Negligible intermediate dose from the near-field
^{166m}Ho	Negligible intermediate dose from the near-field
^{227}Ac	Negligible intermediate dose from the near-field
^{229}Th	Negligible intermediate dose from the near-field
^{232}Th	Negligible intermediate dose from the near-field
^{231}Pa	Negligible intermediate dose from the near-field
^{232}U	Negligible intermediate dose from the near-field
^{233}U	Negligible intermediate dose from the near-field
^{235}U	Negligible intermediate dose from the near-field
^{236}U	Negligible intermediate dose from the near-field
^{237}Np	Negligible intermediate dose from the near-field
^{239}Pu	Low to negligible intermediate dose from the near field in comparison to that of ^{99}Tc.
^{240}Pu	Low to negligible intermediate dose from the near field in comparison to that of ^{99}Tc.
^{241}Pu	Negligible intermediate dose from the near-field
^{244}Pu	Negligible intermediate dose from the near-field
^{241}Am	Negligible intermediate dose from the near-field
^{243}Am	Low to negligible intermediate dose from the near-field in comparison to that of ^{99}Tc
^{243}Cm	Negligible intermediate dose from the near-field
^{244}Cm	Negligible intermediate dose from the near-field
^{245}Cm	Negligible intermediate dose from the near-field

Table 3 Nuclides being neglected in the calculations for SFL 5.

Nuclide	Comment
^{55}Fe	Negligible intermediate dose from the near-field
^{60}Co	Negligible intermediate dose from the near-field
^{63}Ni	Low to negligible intermediate dose from the near-field in comparison to that of ^{93}Mo
^{93m}Nb	Negligible intermediate dose from the near-field
^{94}Nb	Low to negligible intermediate dose from the near-field in comparison to that of ^{59}Ni and ^{99}Tc
^{107}Pd	Low to negligible intermediate dose from the near-field in comparison to that of ^{59}Ni and ^{99}Tc
^{108m}Ag	Low to negligible intermediate dose from the near-field in comparison to that of ^{36}Cl, ^{59}Ni and ^{93}Mo
^{113m}Cd	Negligible intermediate dose from the near-field
^{126}Sn	Low to negligible intermediate dose from the near-field in comparison to that of ^{59}Ni, ^{79}Se and ^{99}Tc
^{125}Sb	Negligible intermediate dose from the near-field
^{134}Cs	Negligible intermediate dose from the near-field
^{135}Cs	Low intermediate dose from the near-field in comparison to that of ^{10}Be, ^{59}Ni and ^{93}Zr
^{137}Cs	Negligible intermediate dose from the near-field
^{133}Ba	Negligible intermediate dose from the near-field
^{147}Pm	Negligible intermediate dose from the near-field
^{151}Sm	Negligible intermediate dose from the near-field
^{152}Eu	Negligible intermediate dose from the near-field
^{154}Eu	Negligible intermediate dose from the near-field
^{155}Eu	Negligible intermediate dose from the near-field
^{166m}Ho	Negligible intermediate dose from the near-field
^{227}Ac	Low to negligible intermediate dose from the near field in comparison to that of ^{210}Pb and ^{226}Ra.
^{229}Th	Low to negligible intermediate dose from the near field in comparison to that of ^{210}Pb and ^{226}Ra.
^{232}Th	Negligible intermediate dose from the near-field
^{231}Pa	Low to negligible intermediate dose from the near-field in comparison to that of ^{210}Pb and ^{226}Ra
^{232}U	Negligible intermediate dose from the near-field
^{233}U	Negligible intermediate dose from the near-field
^{235}U	Negligible intermediate dose from the near-field
^{236}U	Negligible intermediate dose from the near-field
^{237}Np	Negligible intermediate dose from the near-field
^{239}Pu	Negligible intermediate dose from the near-field
^{240}Pu	Negligible intermediate dose from the near-field
^{241}Pu	Negligible intermediate dose from the near-field
^{244}Pu	Negligible intermediate dose from the near-field
^{241}Am	Negligible intermediate dose from the near-field
^{243}Am	Negligible intermediate dose from the near-field
^{243}Cm	Negligible intermediate dose from the near-field
^{244}Cm	Negligible intermediate dose from the near-field
^{245}Cm	Negligible intermediate dose from the near-field

Table 4 Nuclides remaining after screening calculations and their initial activity [Bq] year 2040.

Radionuclide	Half-life [year] [a]	SFL 3	SFL 4 w/o CRUD	SFL 5
^{3}H	12	$3.2 \cdot 10^{12}$	$1.6 \cdot 10^{9}$	$2.5 \cdot 10^{15}$
^{10}Be	$1.5 \cdot 10^{6}$	– [b]	– [b]	$1.4 \cdot 10^{11}$
$^{14}C_{inorganic}$	$5.7 \cdot 10^{3}$	$3.5 \cdot 10^{13}$	$3.1 \cdot 10^{7}$	$1.7 \cdot 10^{14}$
$^{14}C_{organic}$	$5.7 \cdot 10^{3}$	$8.2 \cdot 10^{4}$	–	–
^{36}Cl	$3.0 \cdot 10^{5}$	$2.1 \cdot 10^{10}$	$2.6 \cdot 10^{4}$	$2.5 \cdot 10^{11}$
^{60}Co	5.3	– [b]	$4.1 \cdot 10^{10}$	– [b]
^{59}Ni	$7.6 \cdot 10^{4}$	$1.6 \cdot 10^{14}$	$1.2 \cdot 10^{8}$	$1.4 \cdot 10^{15}$
^{63}Ni	$1.0 \cdot 10^{2}$	– [b]	$1.7 \cdot 10^{10}$	– [b]
^{79}Se	$1.1 \cdot 10^{6}$	$4.6 \cdot 10^{8}$	$5.0 \cdot 10^{3}$	$4.5 \cdot 10^{7}$
^{90}Sr	29	$2.3 \cdot 10^{12}$	$1.6 \cdot 10^{8}$	$5.6 \cdot 10^{11}$
^{93}Zr	$1.5 \cdot 10^{6}$	$2.1 \cdot 10^{10}$	– [b]	$2.2 \cdot 10^{12}$
^{94}Nb	$2.0 \cdot 10^{4}$	– [b]	$6.6 \cdot 10^{6}$	– [b]
^{93}Mo	$4.0 \cdot 10^{3}$	$2.4 \cdot 10^{11}$	$2.0 \cdot 10^{5}$	$1.8 \cdot 10^{12}$
^{99}Tc	$2.1 \cdot 10^{5}$	$5.8 \cdot 10^{11}$	$6.2 \cdot 10^{6}$	$3.2 \cdot 10^{11}$
^{129}I	$1.6 \cdot 10^{7}$	$3.4 \cdot 10^{7}$	$3.7 \cdot 10^{2}$	$3.4 \cdot 10^{6}$
^{135}Cs	$2.3 \cdot 10^{6}$	$5.7 \cdot 10^{8}$	– [b]	– [b]
^{137}Cs	30	– [b]	$1.2 \cdot 10^{9}$	– [b]
^{210}Pb	22	$2.7 \cdot 10^{11}$	< 1	< 1
^{226}Ra	$1.6 \cdot 10^{3}$	$3.8 \cdot 10^{11}$	< 1	< 1
^{229}Th	$7.3 \cdot 10^{3}$	$1.4 \cdot 10^{2}$	– [b]	– [b]
^{230}Th	$7.5 \cdot 10^{4}$	$1.8 \cdot 10^{5}$	< 1	73
^{232}Th	$1.4 \cdot 10^{10}$	$1.1 \cdot 10^{10}$	– [b]	– [b]
^{233}U	$1.6 \cdot 10^{5}$	$3.1 \cdot 10^{4}$	– [b]	– [b]
^{234}U	$2.5 \cdot 10^{5}$	$7.8 \cdot 10^{8}$	24	$2.4 \cdot 10^{5}$
^{236}U	$2.3 \cdot 10^{7}$	$8.1 \cdot 10^{7}$	– [b]	– [b]
^{238}U	$4.5 \cdot 10^{9}$	$4.6 \cdot 10^{10}$	9.6	$7.5 \cdot 10^{4}$
^{237}Np	$2.1 \cdot 10^{6}$	$1.8 \cdot 10^{8}$	– [b]	– [b]
^{238}Pu	88	$3.7 \cdot 10^{11}$	$8.9 \cdot 10^{4}$	$5.9 \cdot 10^{8}$
^{240}Pu	$6.6 \cdot 10^{3}$	$1.8 \cdot 10^{12}$	– [b]	– [b]
^{241}Pu	14	$4.4 \cdot 10^{12}$	– [b]	– [b]
^{242}Pu	$3.7 \cdot 10^{5}$	$1.2 \cdot 10^{9}$	72	$5.6 \cdot 10^{5}$
^{241}Am	$4.3 \cdot 10^{2}$	$5.0 \cdot 10^{12}$	– [b]	– [b]
^{242m}Am	$1.4 \cdot 10^{2}$	$2.0 \cdot 10^{9}$	$2.4 \cdot 10^{2}$	$1.6 \cdot 10^{6}$
^{244}Cm	18	$4.4 \cdot 10^{10}$	– [b]	– [b]
^{245}Cm	$8.5 \cdot 10^{3}$	$7.7 \cdot 10^{7}$	– [b]	– [b]
^{246}Cm	$4.7 \cdot 10^{3}$	$2.1 \cdot 10^{7}$	1.9	$1.5 \cdot 10^{4}$

a) Firestone (1998)
b) Screened out

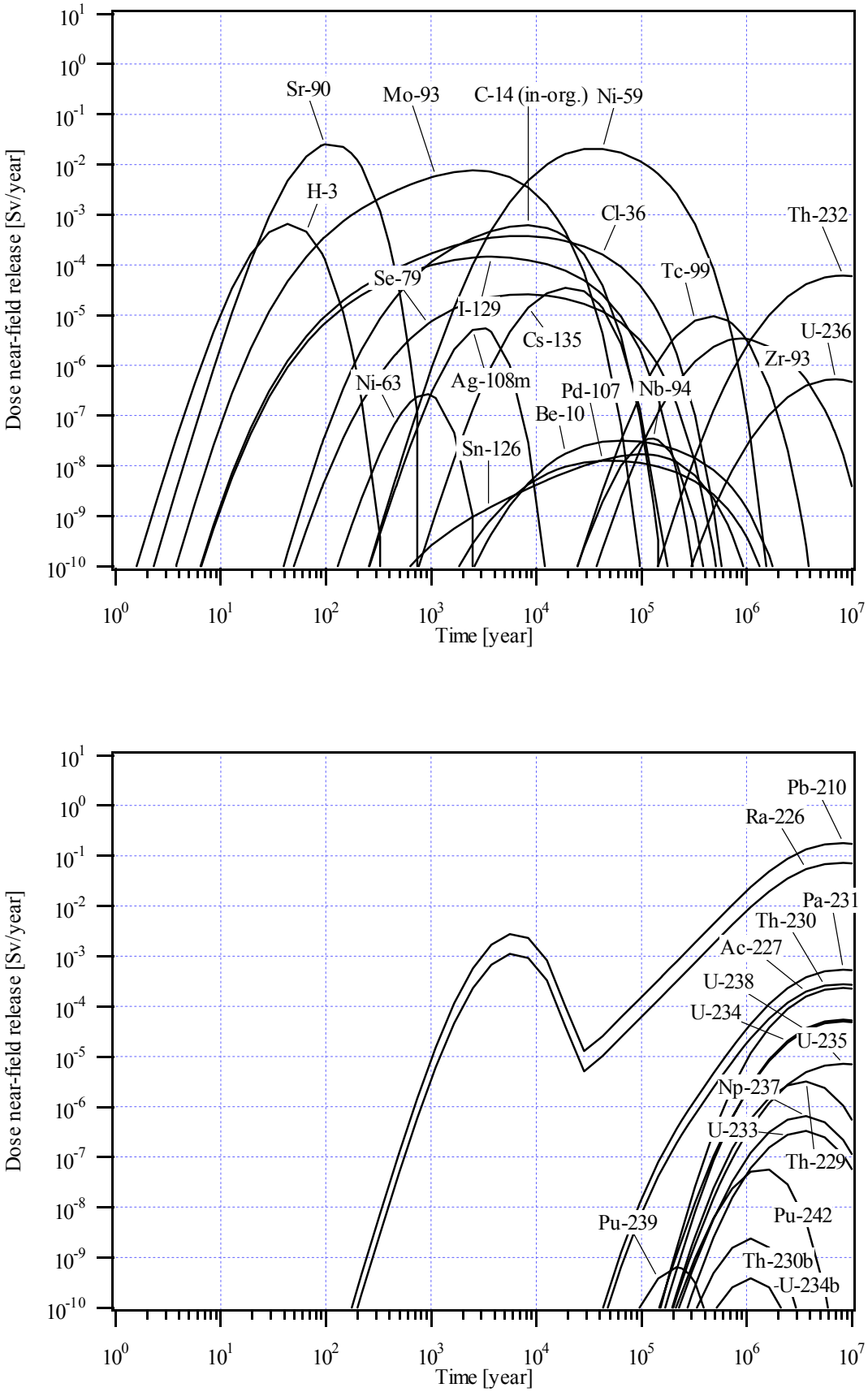

Figure 2 Intermediate dose for release from SFL 3 in Aberg.

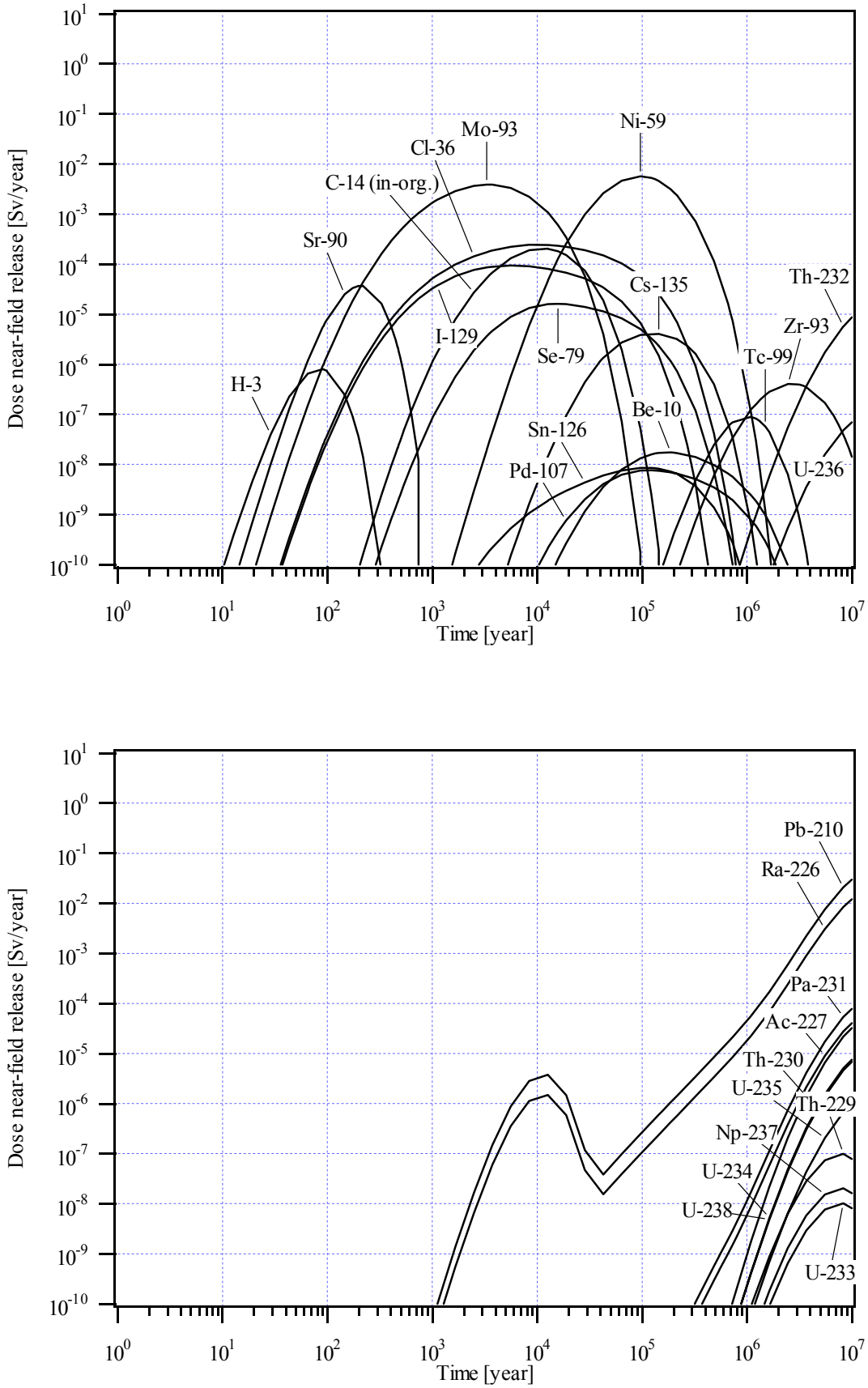

Figure 3 Intermediate dose for release from SFL 3 in Beberg (saline).

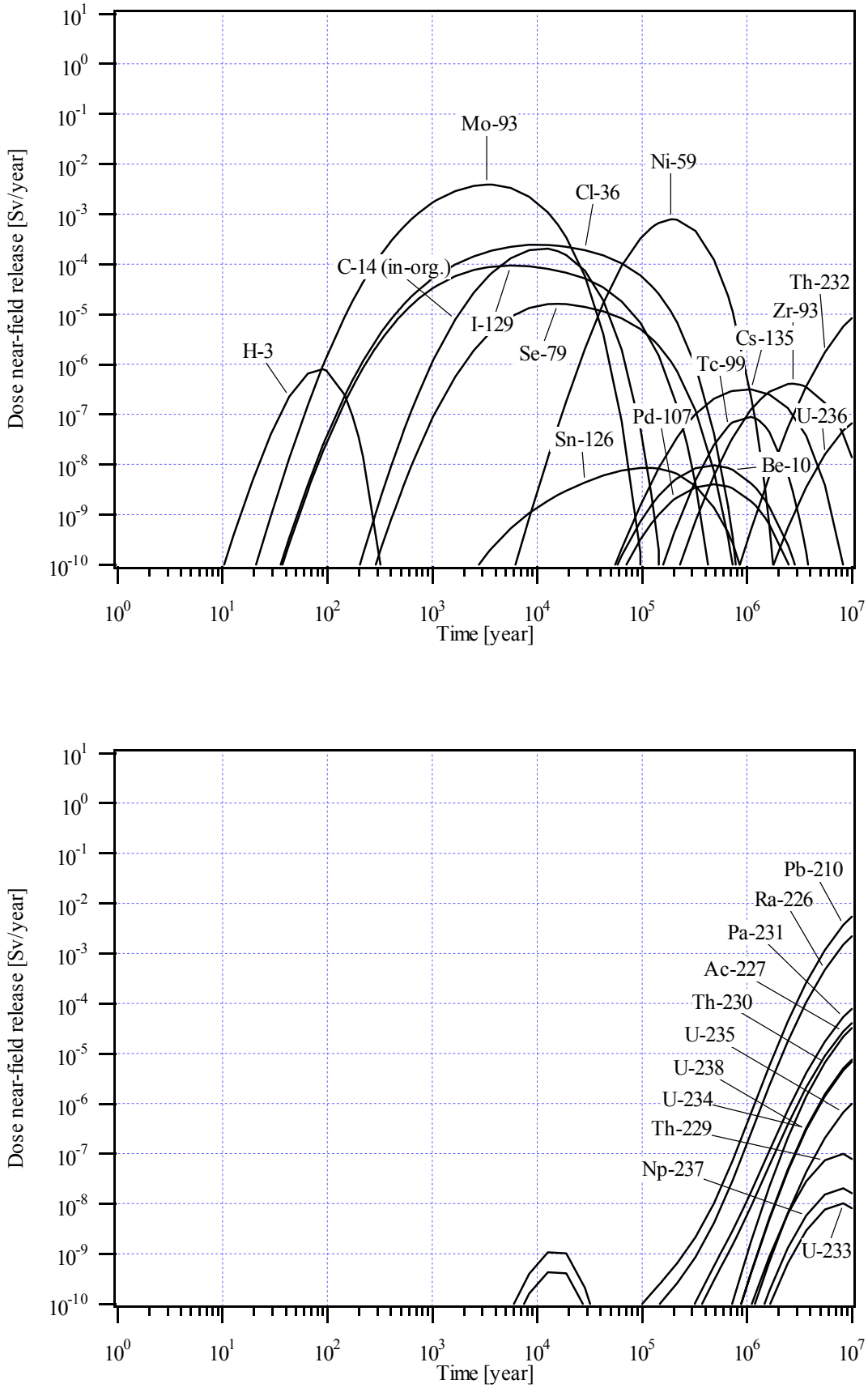

Figure 4 Intermediate dose for release from SFL 3 in Beberg (non-saline).

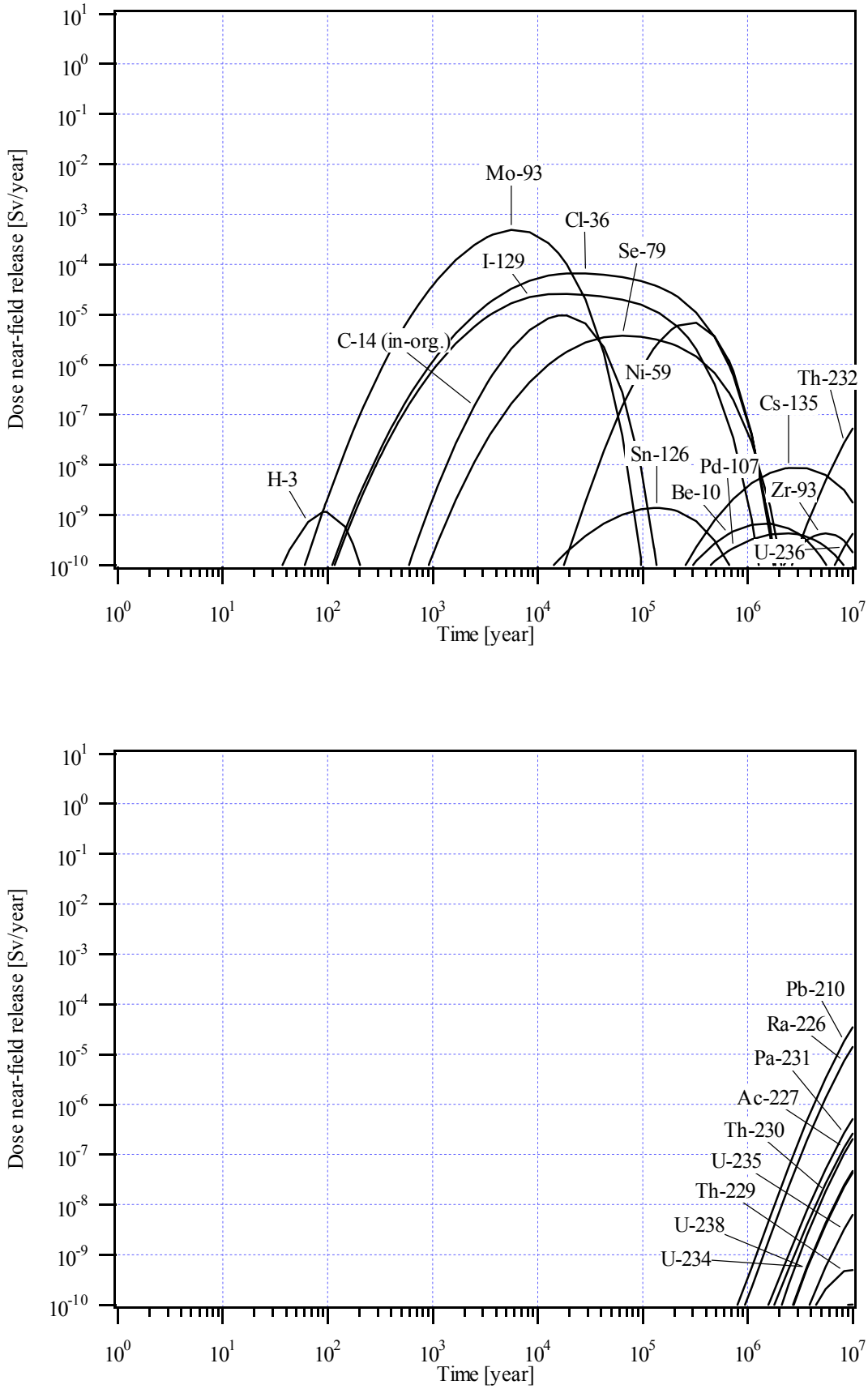

Figure 5 Intermediate dose for release from SFL 3 in Ceberg.

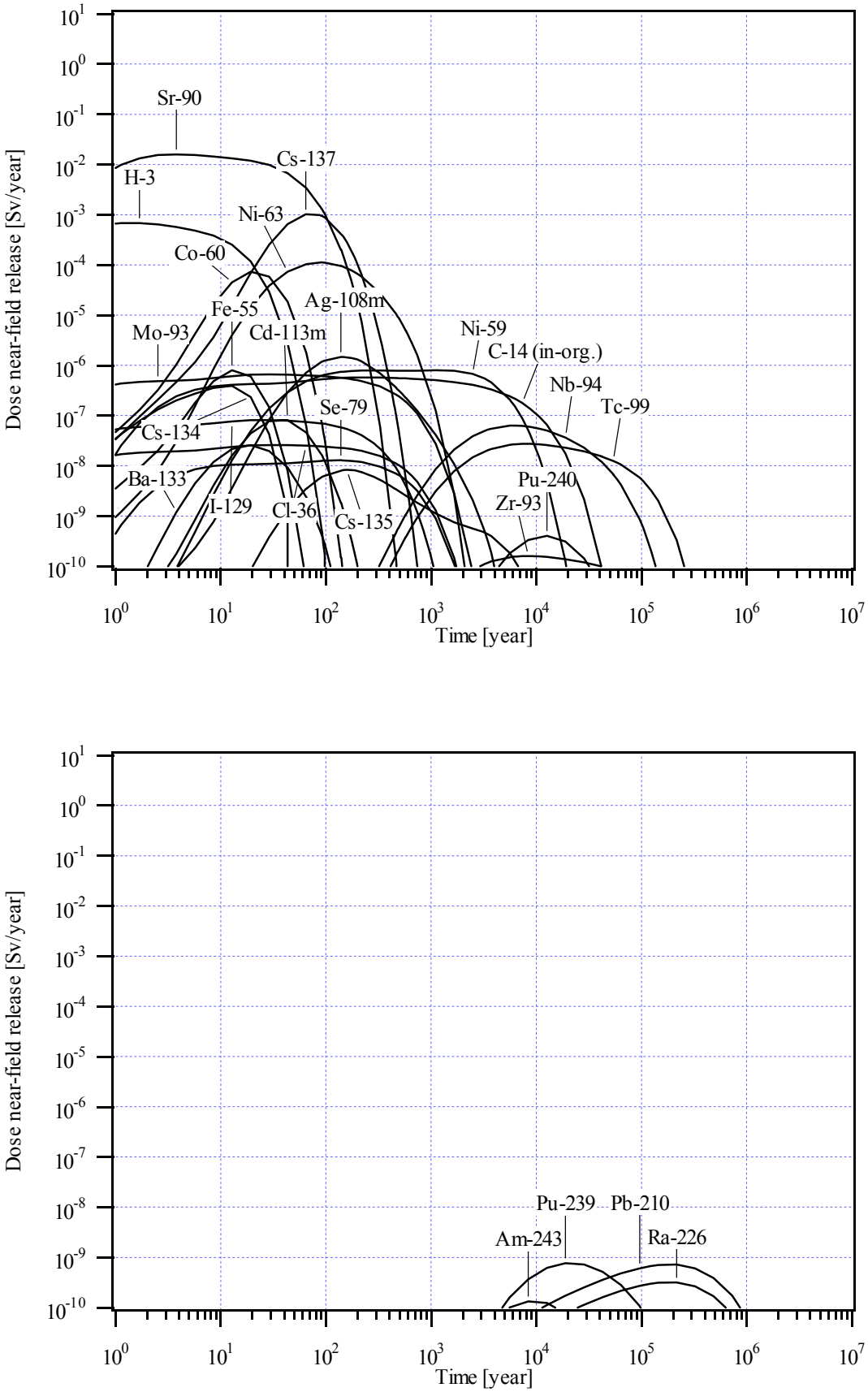

Figure 6 Intermediate dose for release from SFL 4 in Aberg.

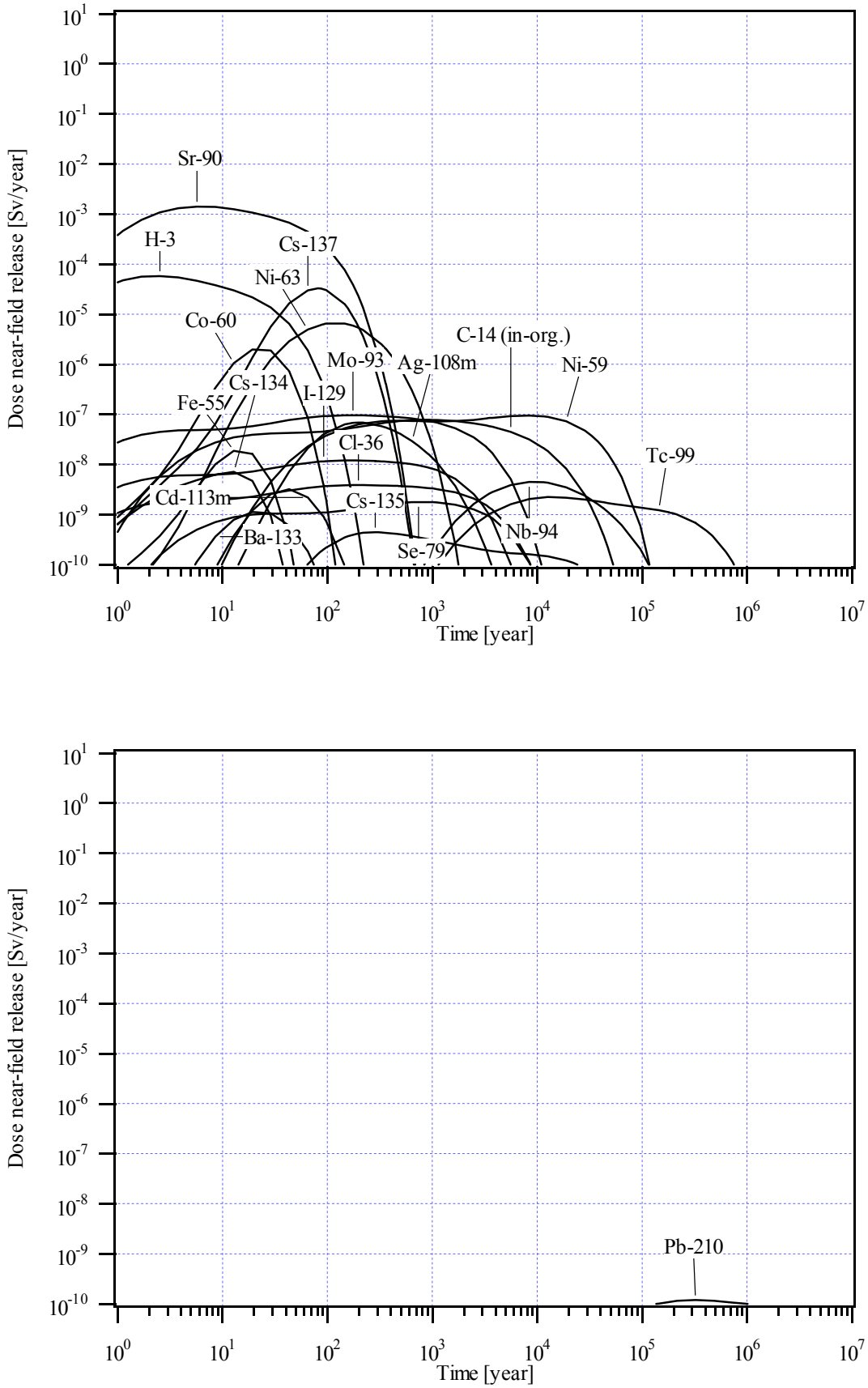

Figure 7 Intermediate dose for release from SFL 4 in Beberg (saline).

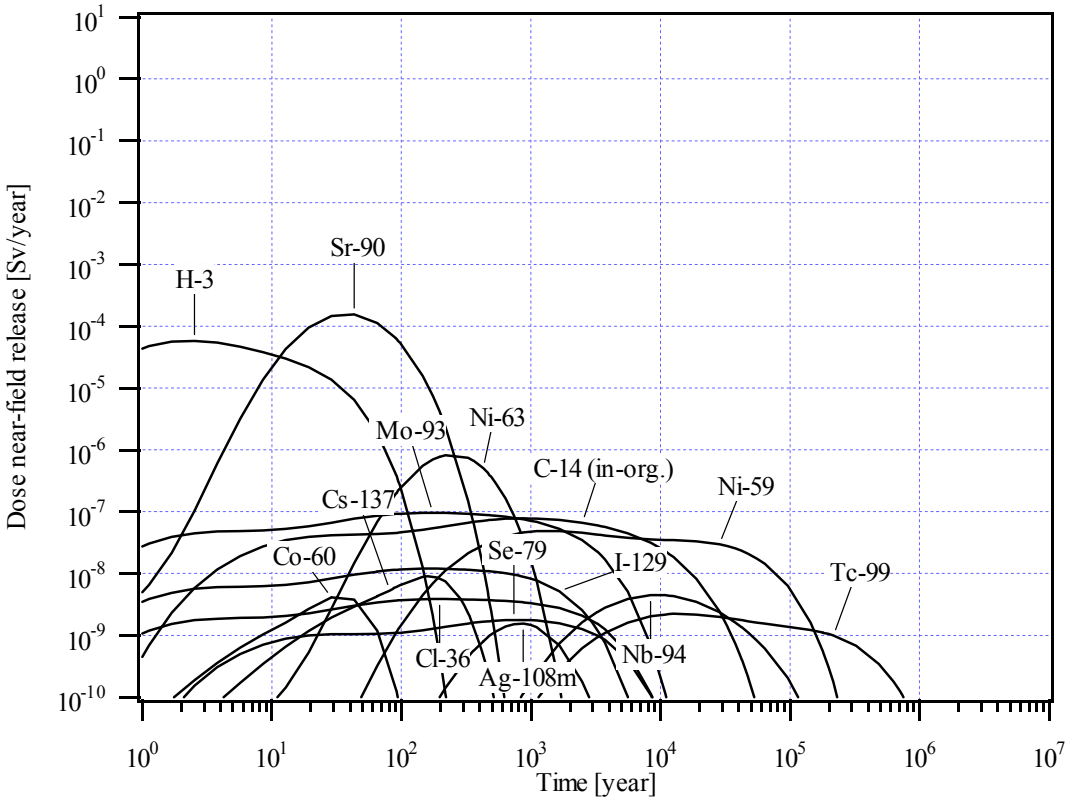

Figure 8 Intermediate dose for release from SFL 4 in Beberg (non-saline).

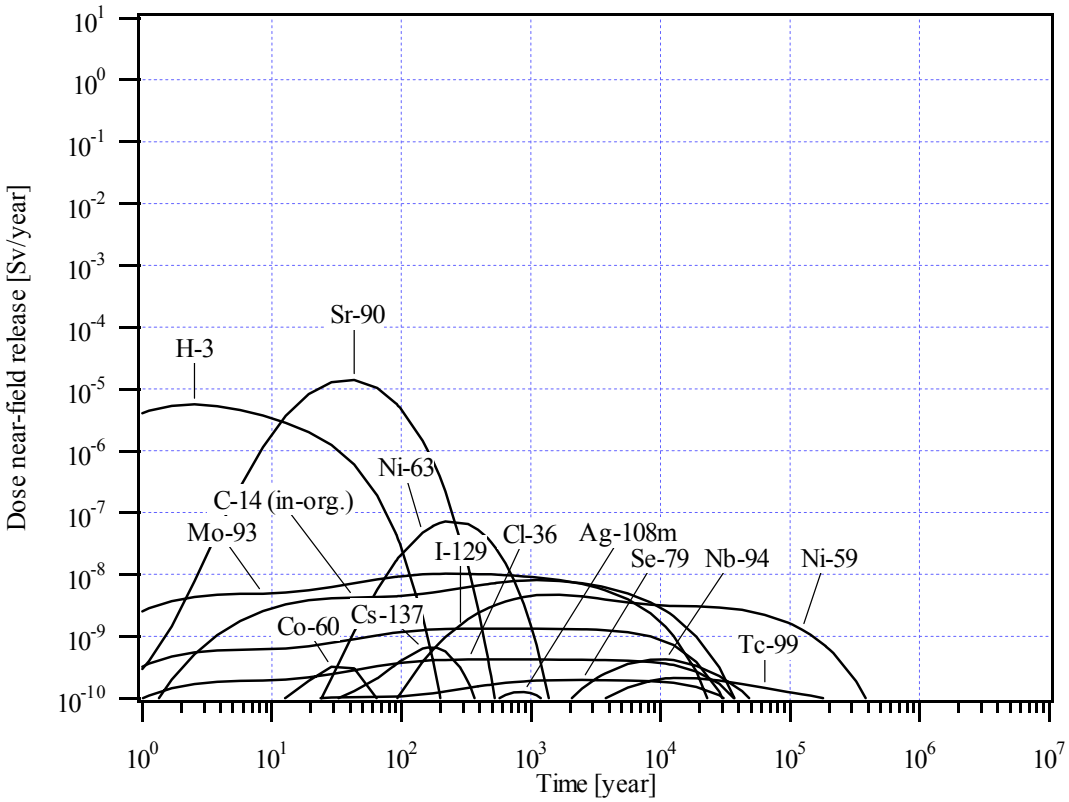

Figure 9 Intermediate dose for release from SFL 4 in Ceberg.

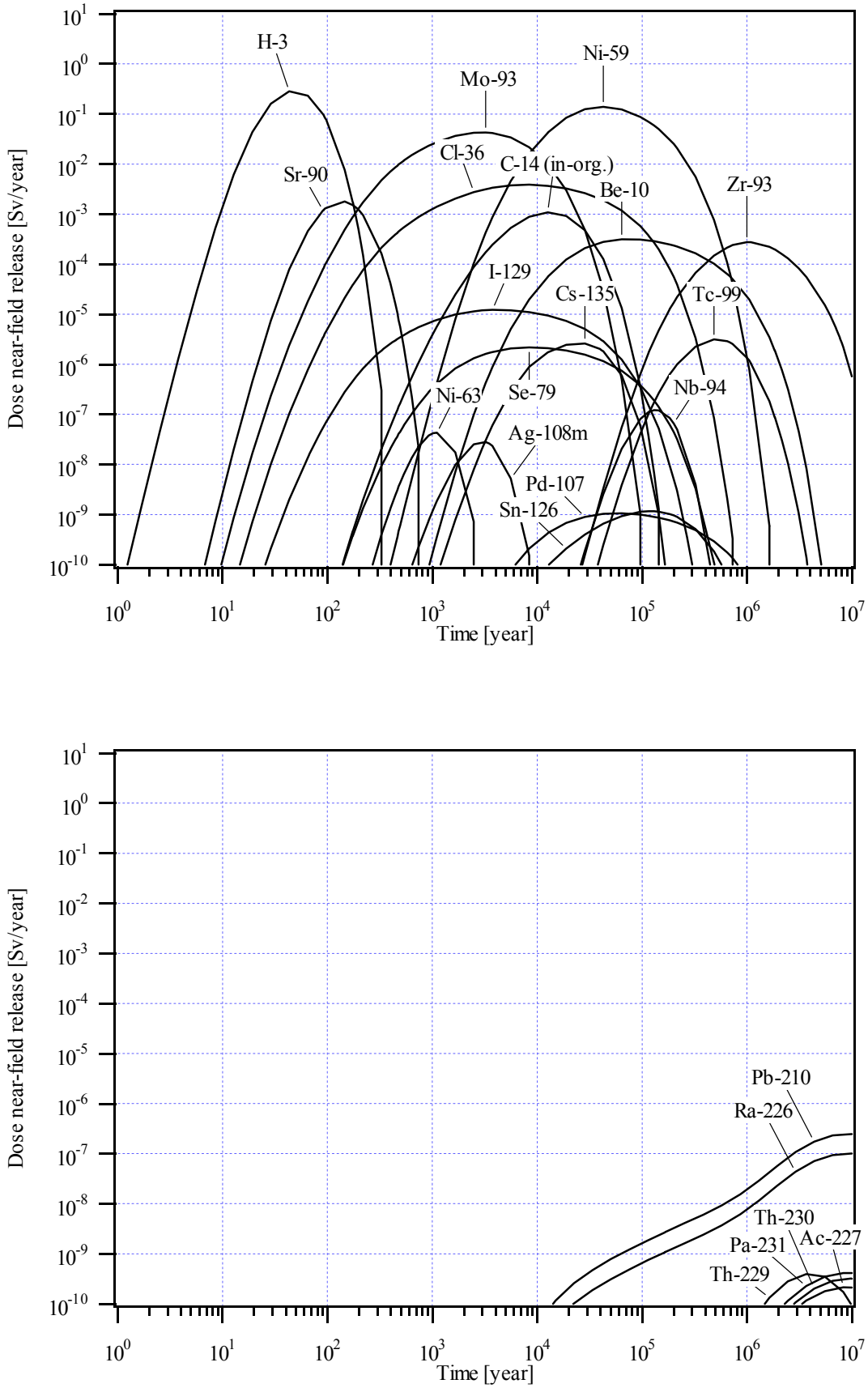

Figure 10 Intermediate dose for release from SFL 5 in Aberg.

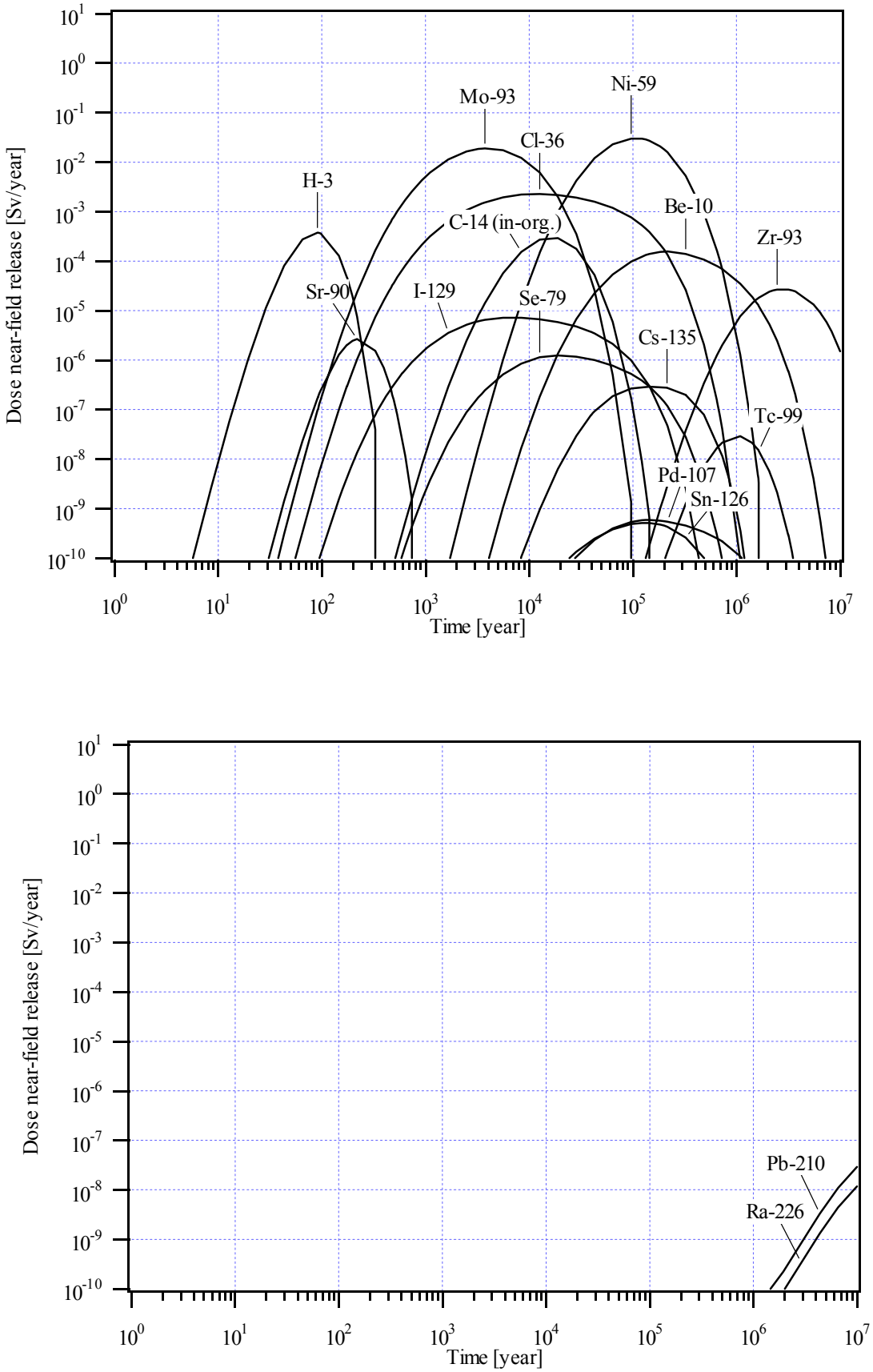

Figure 11 Intermediate dose for release from SFL 5 in Beberg (saline).

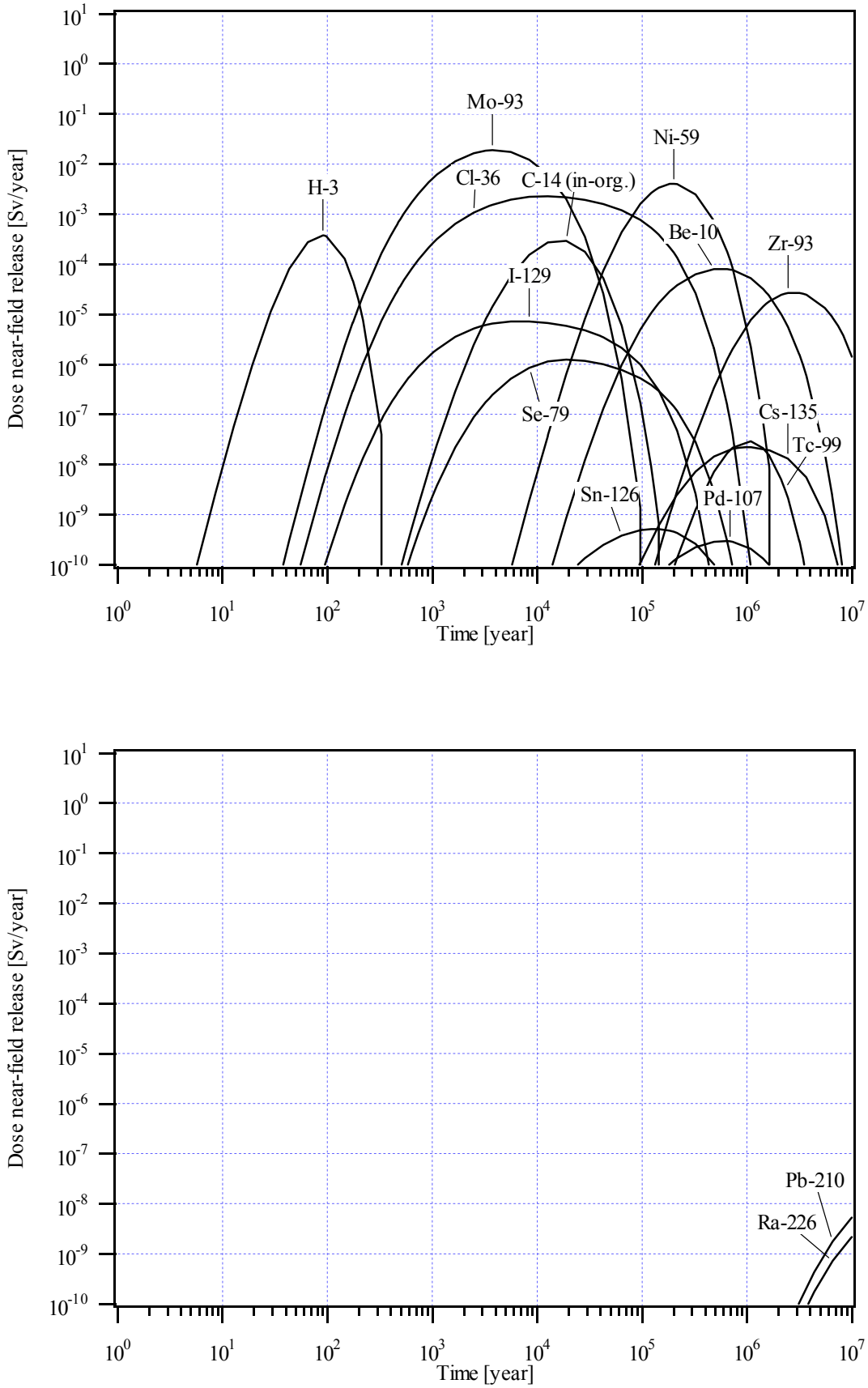

Figure 12 Intermediate dose for release from SFL 5 in Beberg (non-saline).

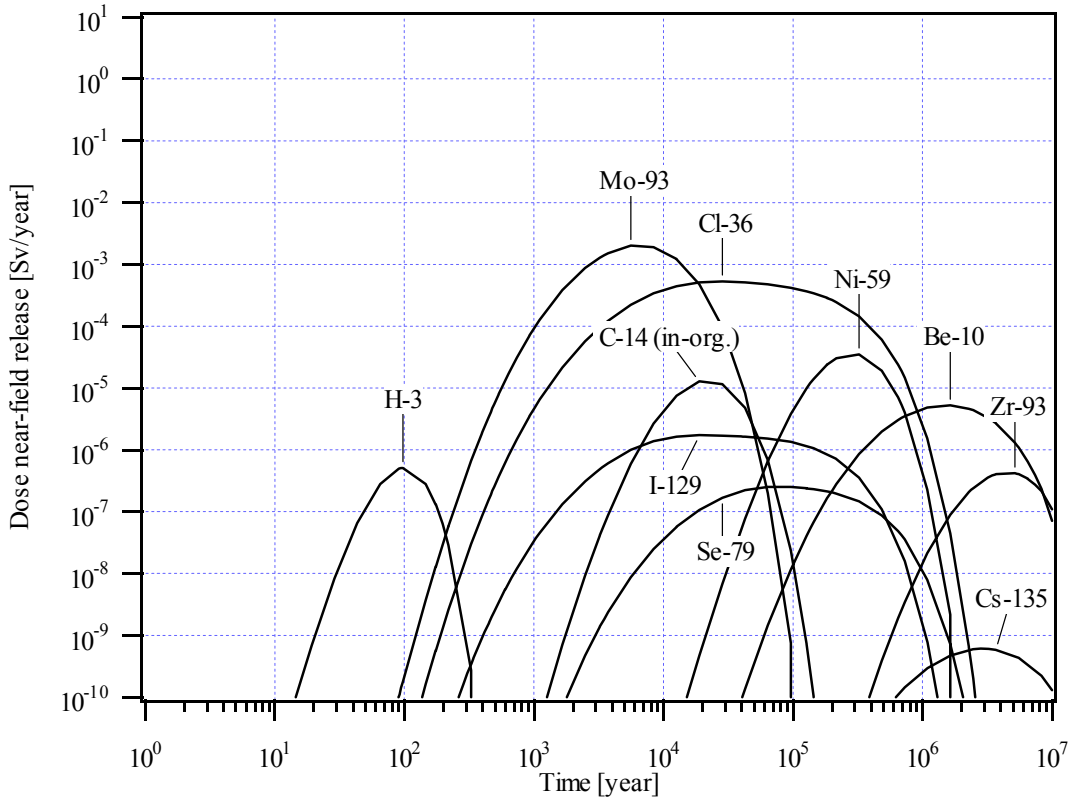

Figure 13 Intermediate dose for release from SFL 5 in Ceberg.

References

Firestone R B, 1998. Table of Isotopes, 8th ed., 1998 Update, Ed. C M Baglin, John Wiley & Sons, Inc., New York.

IAEA, 1996. International Basic Safety Standards for Protection against Ionizing Radiation and for the Safety of Radiation Sources. Safety Series No. 115, International Atominc Energy Agency, Vienna.

Lindgren M, Pers K, Skagius K, Wiborgh M, Brodén K, Carlsson J, Riggare P, Skogsberg M, 1998. Low and intermediate level waste in SFL 3-5: Reference inventory. Reg. No: 19.41/DL31. Swedish Nuclear Fuel and Waste Management Co., Stockholm.

Appendix F: Transport of radionuclides at the outlet of the repository

Luis Moreno

Dept. of Chemical Engineering and Technology,

Royal Institute of Technology

1 Introduction

In the model, it is considered that the transport of radionuclides takes place both by advection and by diffusion, except for at the outlet of the tunnel where only the transport by advection is modelled. The transport by diffusion is assumed to be insignificant. In this appendix, the contribution of the diffusion to the transport of radionuclides from the tunnel into the rock is studied.

2 Results

When the groundwater that flows along the tunnel reaches the tunnel end, it flows from the tunnel through the rock surrounding the tunnel. The flow through the plug located at the end of the SFL 3 and SFL 5 is expected to be small, due to the lower hydraulic conductivity of the concrete used in the plug construction in comparison to the hydraulic conductivity of the rock. However, for Ceberg, where the conductivity of the rock is expected to be low the importance of the water flow through the plug may be more significant.

When groundwater flow out from the tunnel into fractures in the rock, the radionuclides are transported by advection with the flowing water and also by diffusion. In order to determine the relative contribution of these two mechanisms to the radionuclide transport the Peclet number may be used. The Peclet number indicates the relative importance of the transport by advection compared with the transport by diffusion and is defined as:

$$Pe = \frac{u \cdot L}{D} = \frac{u_o \cdot L}{\phi_f \cdot D} \qquad (1)$$

where u (m/year) is the water velocity, which is calculated from the Darcy's velocity, u_o (m^3/m^2 year), and flow porosity, ϕ_f. L (m) is the transport length and D (m^2/year) is the diffusion coefficient in the fracture.

In order to determine the Darcy's velocity, it is assumed that the groundwater flows out from SFL 3 and SFL 5 through the rock walls surrounding the 20-m tunnel close to the plug. Since the perimeter of the tunnel is about 60 m, the total surface is 1,200 m^2. Flow porosity for Aberg and Beberg is assumed to be 0.001 based in the rather high average hydraulic conductivity of the rock. This value of flow porosity means a fracture aperture of 1.0 mm per metre, which is a large value. For Ceberg a value of 0.0001 is used because the average hydraulic conductivity of the rock is very low in Ceberg. The Peclet number is calculated for a transport distance of 1.0 m. Values used in these calculations are shown in Table 1. The results show that for the three cases the radionuclide transport out from the tunnel is determined by the advection, large Peclet number. Transport by diffusion is negligible in these cases.

Table 1 Data used for estimating Peclet number.

	Aberg	Beberg	Ceberg
Specific groundwater flow [m^3/m^2 year]	10^{-2}	10^{-3}	10^{-4}
Average hydraulic conductivity [m/s]	10^{-7}	10^{-8}	10^{-10}
Total flow rate in the tunnel [m^3/year]	40	4	0.4
Cross section for flow into the rock [m^2]	1,200	1,200	1,200
Flow porosity [–]	10^{-3}	10^{-3}	10^{-4}
Transport length [m]	1.0	1.0	1.0
Diffusion coefficient in fractures [m^2/year]	0.063	0.063	0.063
Peclet number	500	50	50

For Ceberg a part of the groundwater flow in the tunnel can flow through the plug located at the ends of the tunnel due to the small hydraulic conductivity of the rock. For the hydraulic conductivity used in the calculations (10^{-10} m/s for the rock and 10^{-8} m/s the concrete) about 90 % of the water flow may take place through the plug . Assuming a porosity of 0.15, a plug thickness of 2 m, and a diffusion coefficient of 0.0003 m^2/year, a Peclet number of 100 is obtained. This means that most of the radionuclide the transport through the plug occurs also by advection.